

RESILIENCE-DRIVEN MANAGEMENT OF WATER DISTRIBUTION NETWORKS

Ahmed Assad

A Thesis

In the department

Of

Building, Building Civil, and Environmental Engineering

Presented in Partial Fulfillment of the Requirements

For the Degree of

Doctor of Philosophy (Civil Engineering) at

Concordia University

Montreal, Quebec, Canada

September 2020

© Ahmed Assad, 2020

**CONCORDIA UNIVERSITY
SCHOOL OF GRADUATE STUDIES**

This is to certify that the thesis prepared

By: **Ahmed Assad**

Entitled: **Resilience-Driven Management of Water Distribution Networks**

and submitted in partial fulfillment of the requirements for the degree of

DOCTOR OF PHILOSOPHY (Civil Engineering)

complies with the regulations of the University and meets the accepted standards with respect to originality and quality.

Signed by the final examining committee:

_____	Chair
Dr. A. Mohammadi	
_____	External Examiner
Dr. A. Bouferguene	
_____	External to program
Dr. K. Schmitt	
_____	Examiner
Dr. F. Nasiri	
_____	Examiner
Dr. Z. Chen	
_____	Thesis Co-Supervisor
Dr. O. Moselhi	
_____	Thesis Co-Supervisor
Dr. T. Zayed	

Approved by: _____
Dr. M. Nokken, Graduate Program Director

Nov. 1, 2020 _____
Dr. M. Debbabi
Interim Dean of Gina Cody School of Engineering and Computer Science

ABSTRACT

Resilience-Driven Management of Water Distribution Networks

Ahmed Assad, Ph.D.

Concordia University 2020.

Water distribution networks (WDNs) are critical infrastructure systems that secure needed supply of potable water to the public. Efficient management of WDNs has always been a primary concern for decision-makers, particularly in events of natural disasters, deliberate attacks, human-made accidents and/or sudden failures. Aging and deterioration of WDNs further exacerbate their vulnerability and likelihood of service disruption. Previous hazards reveal that classical risk-based approaches are not sufficient to prevent disruptions of WDNs. As a result, the concept of resilient WDNs has emerged to cope up with inevitable disruptions that are becoming more frequent.

The objective of this research is to develop a holistic resilience-based management model for WDNs. In this context, WDNs is sought to be strong enough to withstand unforeseen disruptions with a minimum performance impact and to recover rapidly after a service interruption. Firstly, a multi-attribute metric is developed for assessing resilience of WDNs based on robustness and redundancy. Attributes from graph theory are employed to quantify the network redundancy. Robustness is measured by integrating the reliability and criticality of pipe segments of the network. Multi-attribute utility theory and Fuzzy analytical network process are exploited to estimate the criticality of water segments based on a set of economic, social, and environmental factors. Survival analysis and maximum likelihood estimate are employed to dynamically determine reliability of pipe segments. Censored inter-failure time data are leveraged to model the deterioration behavior of homogenous cohorts of pipe. The developed metric was used to measure

the resilience of a real-life WDN in the City of London, Ontario. The results obtained showed an average of 5% variation when compared to previously developed flow-based and topology-based metrics.

In the second step, rapidity and resourcefulness qualities are considered to develop a resilience-based restoration model. A failure scenario causing multiple simultaneous breaks across the network is simulated to investigate the recovery process. A stochastic multi-objective optimization model that maximizes resilience while minimizing the total time and cost of the recovery process is then formulated. This model accounts for different restoration methods, relocation time and cost of restoration crews, and uncertainties in recovery estimates. The optimum restoration plan encompasses a sequence of failed segments restorations along with the restoration method. This plan achieved 4% cost saving, 48% duration reduction, and 4% resilience improvement when compared to current planning practices.

The last step involves developing a multi-objective resilience enhancement model so that WDNs can be better prepared for future disruptions. The aim is to maximize resilience of WDNs while minimizing the life cycle cost and carbon emissions of enhancement actions. Optimum enhancement interventions are firstly determined and clustered into work packages before an optimized schedule is generated considering various operational and managerial factors. Applied to a section of an actual WDN of 34 km in a length and average age of 40 years, resilience was increased by 20% with CAD 1.65 million of current investment. The study of that network indicates that a cost-saving of 32% could be attained when adopting the developed model over ongoing portfolio management practices.

The novel resilience-driven management model introduced in this research is expected to assist decision-makers better assess and enhance resilience of WDNs and improve restoration planning. The developed model can assist city managers in allocation and utilization of resources more effectively in development of optimized plans for resilient and sustainable WDNs.

بِسْمِ اللّٰهِ الرَّحْمٰنِ الرَّحِیْمِ

Dedicated To

*My beloved mother “Dawlat Sha'aban” and my inspiring
father “Ibrahim Assad”*

My dear brother and sisters and their families

Acknowledgment

All gratitude and praise are due to ALLAH almighty who guided me to bring this dissertation to light.

No words could ever express my deepest love and gratitude to my mother “Dawlat Sha'aban” and father “Ibrahim Assad” for sacrificing a lot to make me, my brother, and sisters what we are today. Their endless love, encouragement, and enthusiasm to see the completion of this work was above all a significant motivator.

Much gratitude is also due to my brother “Mohammed” and sisters “Hala”, “Shatha”, and their families for their continuous encouragements and for putting a smile on my face when I needed it most. My lovely nephew and niece "Ibrahim " & "Lujain" were always my source of joy in times of hardships!

I am thankful to my advisors, “Prof. Osama Moselhi” and “Prof. Tarek Zayed” for their mentorship and valuable advises throughout my studies. I have learned a lot from them, and it was a great honor to work under their supervision. Your continuous help and support will always be appreciated.

I would like to thank Dr. Khaled Shahata for securing the data needed for the development and validation purposes. I am grateful for Dr. Shahata and Dr. Mohamed Elmasry for their valuable insights and feedback. I am also thankful to my brother-in-law, Ahmed Zeidan, and My cousin, Farah AlHourani for lending a hand whenever programming assistant was needed.

I am deeply grateful for many true friends that I was horned to know during the course of my PhD, here in Montreal and across Canada from Coast to Coast! I am also thankful for my friends and big family back in Kuwait, Jordan, and Palestine for their continuous support and motivation.

Table of Contents

List of Figures.....	xii
List of Tables	xvi
List of Acronyms.....	xix
1 Chapter 1: Introduction	1
1.1 Overview	1
1.2 Problem statement.....	2
1.3 Research Objectives	3
1.4 Methodology Overview.....	4
1.5 Dissertation Outline.....	4
2 Chapter 2: Literature Review.....	6
2.1 Overview	6
2.2 Resilience of Water Distribution Networks	7
2.3 Resilience Assessment Models of WDNs.....	10
2.4 Resilience-based Restoration Models of WDNs.....	22
2.5 Resilience Enhancement Models of WDNs.....	26
2.6 Rehabilitation Techniques.....	29
2.7 Research Methods	31

2.7.1	Fuzzy analytical network process (FANP)	31
2.7.2	Preference Ranking Organization Method for Enrichment of Evaluations (PROMETHEE).....	34
2.7.3	Survival Analysis	36
2.7.4	K-means Clustering	39
2.7.5	Shannon entropy	41
2.8	Optimization algorithms.....	42
2.9	Gaps in Literature.....	46
3	Chapter 3: Developed models for Resilience-Based Management of WDN	50
3.1	Overview	50
3.2	Resilience Assessment Model.....	53
3.2.1	Robustness	54
3.2.2	Redundancy.....	73
3.2.3	Resilience Metric	74
3.3	Resilience-based Restoration Model.....	79
3.3.1	Crew Relocation Sub-model.....	81
3.3.2	Restoration Sub-model.....	82
3.3.3	Optimization Framework	83
3.3.4	Deterministic Versus Stochastic optimization	87
3.4	Resilience Enhancement Model.....	90

3.4.1	Enhancement Sub-model	92
3.4.2	Optimization Framework	93
3.4.3	Packaging and Scheduling Sub-model.....	95
3.4.4	Multi-objective Optimization.....	98
3.4.5	Redundancy Enhancement Strategy	100
3.5	Research Limitations.....	102
3.6	Summary	103
4	Chapter 4: Developed Automated Computer Application.....	105
4.1	Overview	105
4.2	Resilience Assessment Module.....	108
4.2.1	Criticality computations.....	108
4.2.2	Reliability computations	112
4.2.3	Resilience computations	115
4.3	Resilience Restoration Module	116
4.4	Resilience Enhancement Module.....	119
4.5	Dashboard.....	124
4.6	Summary	131
5	Chapter 5: Testing and Validation.....	132
5.1	Overview	132

5.2	Resilience Assessment Model.....	137
5.3	Resilience-Based Restoration Model.....	241
5.4	Resilience Enhancement Model.....	253
5.5	Summary.....	266
6	Chapter 6: Conclusions and Recommendations.....	267
6.1	Summary.....	267
6.2	Recommendation and Future Work.....	269
7	References.....	270

List of Figures

Figure 1-1: Methodology Overview	5
Figure 2-1: Resilience-based Management Models of WDNs	6
Figure 2-2: Components of Water Supply System (Klise et al. 2015)	7
Figure 2-3: Continuous Cycle of Building Resilience to Hazards (Klise et al. 2015).....	9
Figure 2-4: Resilience Loss Measurement (Bruneau et al. 2003).....	12
Figure 2-5: System State and Delivery Function Transition in Resilience (Henry and Ramirez-Marquez 2012).....	13
Figure 2-6: Five States Engineering Resilience Curve (Dessavre et al. 2016).....	14
Figure 2-7: Rehabilitation Techniques of Water Pipe Segments.....	29
Figure 2-8: Triangular fuzzy number (Wei et al. 2010).....	33
Figure 2-9: Bathtub Failure Rate Function (Murthy et al. 2008).....	37
Figure 2-10: Optimization Solving Techniques.....	43
Figure 3-1: Research Methodology	52
Figure 3-2: Resilience Metric Methodology (Assad et al. 2019).....	54
Figure 3-3: Flow Diagram of Criticality Estimation Process (Assad et al. 2019).....	57
Figure 3-4: Criticality Factors and Sub-factors (Assad et al. 2019)	58
Figure 3-5: Distribution of Respondents' Experience	60
Figure 4-6: Sample of Criticality Sub-factors' Relative Importance Questions.....	61
Figure 3-7: Sample of Criticality Main Factors' Relative Importance Questions	62
Figure 3-8: Sample of Criticality Factors' Effect Values Questions	62
Figure 3-9: Flow Diagram of Reliability and Deterioration Estimation (Assad et al. 2019).....	68
Figure 3-10: GIS Shapefiles for Water Pipe segments and Previous Breaks (London, Ontario).	69

Figure 3-11: Simulation Approach for the Impact of Pipe Damages	78
Figure 3-12: Restoration Model Methodology framework (Assad et al. 2020)	81
Figure 3-13: Procedure for stochastic optimization.....	89
Figure 3-14: Resilience Enhancement Model Methodology framework.....	91
Figure 4-1: Input and Output of RSWDN.....	107
Figure 4-2: Homepage of the developed tool, RSWDN.....	108
Figure 4-3: Inputs and Outputs of Criticality Computation.....	109
Figure 4-4: Input Sheets for Criticality Computations	110
Figure 4-5: Sample of Automatically Formulated Lower, Upper and Most Probable Matrices	110
Figure 4-6: A Matlab Interface Asking the User to Specify a Sheet Contacting a Respondent's Answerers	111
Figure 4-7: Automatically Formulated Matrices for Criticality Computations	112
Figure 4-8: Inputs and Outputs of Reliability Computations	113
Figure 4-9: Sample of Breakage Input Data	113
Figure 4-10: Output Sample of Breaks Counting and Connecting to Pipe Segments	114
Figure 4-11: Output Sample of Inter-failure Time Fitting.....	115
Figure 4-12: Resilience Assessment Input Window	116
Figure 4-13: Inputs and Outputs of Resilience Restoration Module	116
Figure 4-14: Restoration Methods Input Window	117
Figure 4-15: Sample of Relocation Time Results.....	118
Figure 4-16: Resilience Restoration Input Window	118
Figure 4-17: Sample of Resilience Restoration Module Output.....	119
Figure 4-18: Inputs and Outputs of Resilience Restoration Module	120

Figure 4-19: Enhancement Methods Input Window.....	120
Figure 4-20: Resilience Enhancement Input Window	121
Figure 4-21: Resilience Enhancement Constraints Input Window.....	122
Figure 4-22: Sample of Resilience Enhancement Output - Phase I.....	123
Figure 4-23: Sample of Inputs to the Packaging and Scheduling Step.....	123
Figure 4-24: Packaging Constraints Input Window.....	124
Figure 4-25: Dashboard Components	126
Figure 4-26: Homepage View of London WDN Dashboard.....	126
Figure 4-27: Sub-network 2 View of London WDN Dashboard.....	128
Figure 4-28: Segments in Poor Condition View of London WDN Dashboard	129
Figure 4-29: Segments in Good Condition View of London WDN Dashboard.....	129
Figure 4-30: Breaks Heat Map of London WDN	130
Figure 4-31: Breaks Timeline of London WDN.....	131
Figure 5-1: Developed Models' Application and Validation	133
Figure 5-2: Distribution of Pipes' Material in Collected Data	134
Figure 5-3: Distribution of Pipes' Diameters in Collected Data.....	135
Figure 5-4: Water Distribution Network (London, Ontario)	137
Figure 5-5: A layout of London Water Distribution Network, LWDN (Assad et al. 2019).....	139
Figure 5-6: Characterization through Distribution of Pipe: (a) Material; (b) Diameter (mm) of the Selected Network for Resilience Assessment Model (Assad et al. 2019)	139
Figure 5-7. Reliability, Survival, Behavior for the Cohort (CI <150mm) (Assad et al. 2019)	227
Figure 5-8: Effect of Changing Robustness's Weight on Resilience (Assad et al. 2019)	231
Figure 5-9: Convergence of the Genetic Algorithm Optimization Model (Assad et al. 2019) ..	233

Figure 5-10: Resilience Versus Cost Trade-Off for LWDN (Assad et al. 2019)	234
Figure 5-11: Comparison of Three Resilience Restoring Strategies Based on the Proposed Metric (Assad et al. 2019)	237
Figure 5-12: Comparison of Three Resilience Restoring Strategies Based on Serviceability (Assad et al. 2019)	240
Figure 5-13: Optimal Solution Sets Generated from Running Optimization Model.....	246
Figure 5-14: Restoration Schedule Based on a Sample Output of the Restoration Model.....	247
Figure 5-15: Sample of Input Probability Distributions (a) Cost (b) Time	249
Figure 5-16: Distributions of the Optimal Solution Resulting from Stochastic Optimization (a) Cost (b) Time (c) Resilience Improvement (Assad et al. 2020)	251
Figure 5-17: Tornado Graph Ranking Inputs by Effect on the Mean of the Restoration Cost (Assad et al. 2020)	253
Figure 5-18: Layout of the Water Network in the City of London, Ontario	255
Figure 5-19: Layout of the Selected Sub-networks	255
Figure 5-20: Variation of Carbon Emissions Associated with Various Rehabilitation Techniques	257
Figure 5-21. Pareto Frontier Points of the Modified ACO Algorithm	260
Figure 5-22: Distribution of Rehabilitated Segments Based On a) sub-network; b) age; and c) size.	262
Figure 5-23: Interface of the Clustering Algorithms Utilizing RapidMiner Platform.....	263
Figure 5-24: Optimum Scheduling Results.....	264

List of Tables

Table 2-1: Structural Network Indicators Commonly Used for Resilience Evaluation (Yazdani et al. 2011; Archetti et al. 2015)	21
Table 2-2: Cheng, Kahraman and Saaty Scale (Etaati et al. 2011).....	32
Table 2-3: Comparison between Reviewed Resilience Metric.....	48
Table 3-1: Effect Values of Criticality Factors.....	63
Table 3-2: Cheng’s Fuzzy Linguistic Scale for Importance and the Corresponding Triangular Fuzzy Numbers (Wei et al. 2010).....	64
Table 3-3: Sample of Water Pipe Segment’s Failure History.....	70
Table 3-4: Sample of Water Pipe Segment’s Intervention Actions History.....	73
Table 5-1: Sample Pipelines Characteristics in GIS Shapefiles (London, Ontario).....	134
Table 5-2: Sample Pipelines Surrounding Conditions in GIS Shapefiles (London, Ontario)	136
Table 5-3: Main Factors Pairwise Comparison With respect to Main Goal for (Lower, Most Probable, Upper).....	140
Table 5-4: Financial Sub-Factors Pairwise Comparison (Lower, Most Probable, Upper).....	140
Table 5-5: Environmental Sub-Factors Pairwise Comparison (Lower, Most Probable, Upper)	140
Table 5-6: Social Sub-Factors Pairwise Comparison (Lower, Most Probable, Upper).....	141
Table 5-7: Pairwise Comparison between Environmental and Social (Lower, Most Probable, Upper)	141
Table 5-8: Pairwise Comparison between Financial and Social (Lower, Most Probable, Upper)	141
Table 5-9: Pairwise Comparison between Financial and Environmental (Lower, Most Probable, Upper)	141

Table 5-10: Unweighted Super Matrix (Assad et al. 2019).....	142
Table 5-11: Weighted Super Matrix (Assad et al. 2019).....	143
Table 5-12: Limited Matrix (Assad et al. 2019).....	144
Table 5-13: Global Weights of Criticality Factors (Assad et al. 2019).....	225
Table 5-14: Criticality Computation for a Pipe Segment in LWDN (Assad et al. 2019).....	226
Table 5-15: Parameters of the Weibull Fitting for Each State (CI<150mm) (Assad et al. 2019)	226
Table 5-16: Goodness of Fitting the Time to 1 st Failure Data (CI<150mm).....	227
Table 5-17: Reliability Computations for a Pipe Segment in LWDN (Assad et al. 2019).....	228
Table 5-18: Resilience of LWDN along the Next Five Years (Assad et al. 2019).....	230
Table 5-19: LWDN Behavior Following Restoration Strategy 1 (Assad et al. 2019).....	235
Table 5-20: Resilience Computations for Strategy 1 (Assad et al. 2019).....	236
Table 5-21: Sample of Hydraulic Simulation Results both before and after Disruption.....	239
Table 5-22: Sample of Input Data Used in the Restoration Optimization Model (Assad et al. 2020)	242
Table 5-23: Summary of Rehabilitation Methods	243
Table 5-24: Comparison of Optimization Results Using GA, ACO, and TS (Assad et al. 2020)	244
Table 5-25: Different Optimal Solution Sets Resulting from Different Iterations (Assad et al. 2020)	244
Table 5-26: Restoration Schedule Based on a Sample Output of the Restoration Model (Assad et al. 2020)	248

Table 5-27: Comparison between Deterministic and Stochastic Solutions of the Restoration Optimization Model (Assad et al. 2020).....	251
Table 5-28: Comparison between City’s Approach and Suggested Optimization Model (Assad et al. 2020)	252
Table 5-29: Comparison between Results of the Modified ACO and GA	258
Table 5-30: Calculation of Objectives’ Weights based on Shannon Entropy	259
Table 5-31: Different Optimal Solution Resulting from the Modified ACO	260
Table 5-32: Packaging and Scheduling of Enhancement Actions of Year 1	263
Table 5-33: Results of Resilience Enhancement due to Redundancy Improvement	265
Table 5-34: Comparison between City’s Approach and Suggested Optimization Model.....	265

List of Acronyms

WDN Water Distribution Network

NRI Network Resilience Index

PDA Pressure Driven Analysis

HOR Head Outflow Relationship

PROMETHEE Preference Ranking Organization Method for Enrichment of Evaluations

FANP Fuzzy Analytical Network Process

GA Genetic Algorithm

ACO Ant Colony Optimization

SP Stochastic Optimization

MILP Mixed Integer Linear Programming

GUI Graphical User Interface

GIS Geographical Information System

EL Epoxy lining

CIIP cured in place pipe

PB Pipe Bursting

OCM Open Cur Method

NASTT North American Society of Trenchless Technology

MLE Maximum Likelihood Estimate

DBI Davies and Bouldin

WDF Weibull Distribution Function

NOPB Number of Previous Breaks

Chapter 1: Introduction

1.1 Overview

Critical infrastructure systems are those whose continuous function must be secured and quickly restored following to any disruption. They include systems that transport people and goods, deliver drinking water, handle waste, and protect cities against natural hazards. Water supply networks are civil infrastructure systems that are responsible for securing adequate quantities of safe high-quality water to the public. Ensuring a proper function of water systems has always been a major concern for utilities and municipalities because of their direct impact on public health and safety. Water is delivered to the users via millions of pipes that extend over thousands of miles across any country. In North America, many of those pipes were installed back in the early to mid of the twentieth century with lifespans extended in some cases to more than 100 years (ASCE 2017). According to the Canadian Infrastructure Report Card (CIRC 2019), one-fourth of potable water infrastructures are in fair, poor, and very poor condition. The Canadian Infrastructure Report Card indicates that rehabilitation or replacement of these assets is required within the next 5-10 years to ensure continuous provision of accepted levels of service (CIRC 2019). The situation is not quite different in the United States, where the general grade of the water network on the national level is D, (ASCE 2017).

Aging is not the sole challenge that threatens the continuous function of water infrastructure systems. In fact, the ubiquitous nature and extended service life of water distribution networks (WDNs) have made them highly vulnerable to a wide spectrum of disruptions, whether natural or anthropogenic. Earthquakes, hurricanes, extreme temperatures, and climate change are examples of such natural hazards. Human-made threats include terrorist and cyber-attacks, overloading, and vandalism. The aforementioned hazards might cause adverse impacts on water supply networks,

including hydraulic failure, mechanical failures, and failures related to water quality requirements. Pipe breaks, leaks, loss of pressure, and contaminants entering the network are all instances of such potential failures (Klise et al. 2015). After hazardous events, water networks play a central role in firefighting and other rescue activities. Thus, sustaining functionality of such networks is more crucial during and after such undesirable events (Farahmandfar et al. 2016). Traditional approaches of managing WDNs were emphasized on physical protection to maintain functionality of these systems by either avoiding the likelihood of failure or mitigating the adverse expected consequences. Nonetheless, due to the stochastic nature of hazard events and failures, classical risk-based strategies fall short of protecting water networks from all hazards.

In light of these issues, a new concept of infrastructure resilience is recently emerging as an important consideration in both planning and management of WDNs. Increasing efforts both in practice and academia are being directed towards defining resilience of water networks and to deriving quantifiable resilience metrics. In this context, WDNs are sought to be strong enough to withstand disruptions with minimum degradation and to rapidly recover in case of service interruptions (Assad et al. 2019). To ensure this, a multi-attribute resilience index shall be formulated to provide an eloquent valuation of WDNs resilience. In addition, reliable prioritization tools shall be developed that can help in establishing better enhancement programs and optimal restoration schedules.

1.2 Problem statement

Water distribution networks (WDNs) confront momentous challenges that disrupt their sustainable functionality. Classical approaches of physical protection are not sufficient to sustain the functionality of WDNs, which necessitates the inclusion of resilience WDNs management.

Several models have been developed to incorporate resilience in the design of new WDNs, however, there are fewer models that integrate resilience in operation and management of current WDNs. Many of these models involve exhaustive hydraulic simulation, which makes them infeasible in view of the expansive size and complexity of networks parameters. Other models require calibrating numerous parameters leading to impractical metrics that cannot be utilized in real-life applications to assess and enhance resilience of WDNs. Most of the previous efforts addressed the technical component of resilience disregarding other vital social, and economic aspects. In addition, these models did not holistically address the four qualities of resilience: robustness, redundancy, available resources, and rapidity of restoration.

Most resilience enhancement and service restoration models after disruptions have focused solely on cost minimization, disregarding other significant objectives. Time of service disruption, criticality of segments, and the compelling need to cut down carbon emissions are examples of such overlooked issues. Enhancement and restoration models shall assess the suitability of various intervention actions for different segments and failures characteristics. Given the ubiquitous nature of WDNs, optimization models shall aim at minimizing the relocation time and cost between failed segments' locations. In addition, work packaging and scheduling tools are required to cope up with the limited resources and tight budgets, and to assure fair business practices.

1.3 Research Objectives

The main objective of this research is to develop a holistic resilience-driven management model for water distribution networks. This model intends to facilitate decisions aiming at maximizing both the absorptive and restorative capacities of WDNs. The former maximizes the network's ability to withstand disruptions with minimum service interruption. The latter utilizes available funds and resources to determine the optimal strategy for putting the system back into

service after an interruption. To achieve the main objective, the following sub-objectives are defined:

1. Identify and study existing resilience assessment models of WDNs to highlight their advantages and limitations.
2. Develop a multi-attribute metric for assessing resilience levels of WDNs.
3. Develop a recovery optimization model for minimizing time and cost of restoration and maximizing resilience improvement.
4. Develop an optimization model for forming work packages and scheduling optimized resilience enhancement actions.
5. Automate the developed models in a user-friendly computer application tool.

1.4 Methodology Overview

A detailed methodology of this research is described in Chapter 3. Figure 1-1 illustrates its main components. It encompasses review of related literature and development of three models for assessment of resilience levels, optimized restoration and optimized enhancement plans.

1.5 Dissertation Outline

Chapter 2 provides a comprehensive literature review of previous research efforts related to resilience WDNs. The review includes an illustration of the previously developed metrics and formworks for resilience assessment of WDNs. In addition, resilience enhancement and resilience-based restoration models are discussed to complete building the theoretical background for this research. A brief explanation of the techniques and tools utilized in this research is included in this chapter. The chapter concludes by identifying the gaps and limitations of existing methods.

Chapter 3 details the methodology adopted in this research. It starts with general overview and proceeds by describing the models developed in this research.

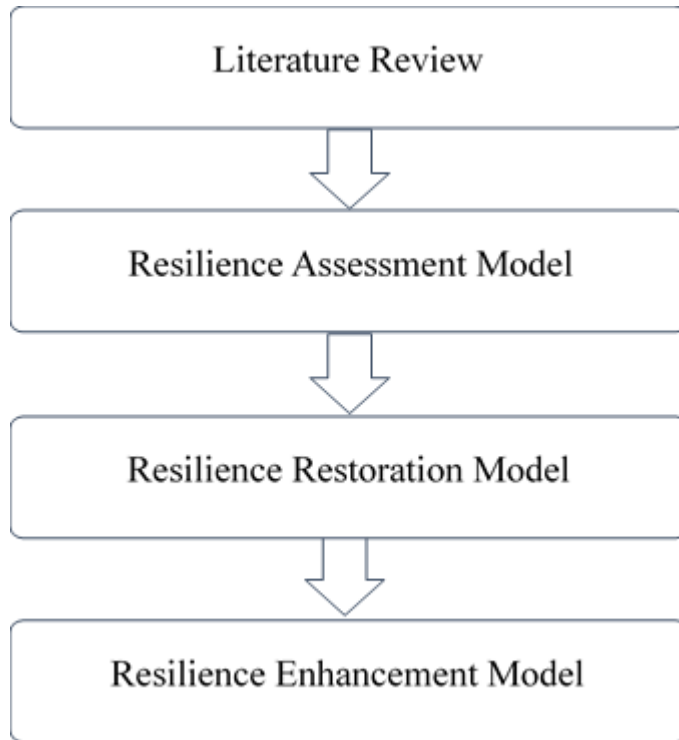


Figure 1-1: Methodology Overview

It then proceeds by describing the resilience-based restoration and enhancement optimization models. Underlying concepts, data gathered, and mathematical formulations of each model are presented in detail in this chapter.

Chapter 4 illustrates the development of an automated tool and a dashboard to integrate the developed models and visualize the obtained results.

Chapter 5 demonstrates the practicality of the developed model by an application on a real case study from the City London, Ontario. It also includes the evaluation and validation results of the developed models.

Chapter 6 draws a summary of this dissertation, highlighting the research contributions and limitations. Recommendations for future work and enhancements are finally presented in this chapter.

Chapter 2: Literature Review

2.1 Overview

This chapter presents an overview of previous research efforts in the field of resilience management of water distribution networks (WDNs). The review starts by defining the nature and some features WDNs as vital critical infrastructure systems. Next, the concept of resilience and characteristics of resilient WDNs are discussed. This review proceeds by detailing an illustration of previously developed resilience assessment metrics and frameworks. An overview of resilience-based restoration models is then included. Various deterministic and stochastic restoration models are discussed along with the role of criticality in the efficient restoration of WDNs. Previous research attempts to enhance resilience of WDNs are then illustrated. This section sheds light on the role of resilience in the rehabilitation planning of WDNs. Figure 2-1 depicts three types of resilience-based applications of WDNs that are discussed in this chapter. Subsequently, the techniques and algorithms utilized in this research are introduced. Finally, a summary highlighting some of the limitations in existing models and gaps identified in this field are included.

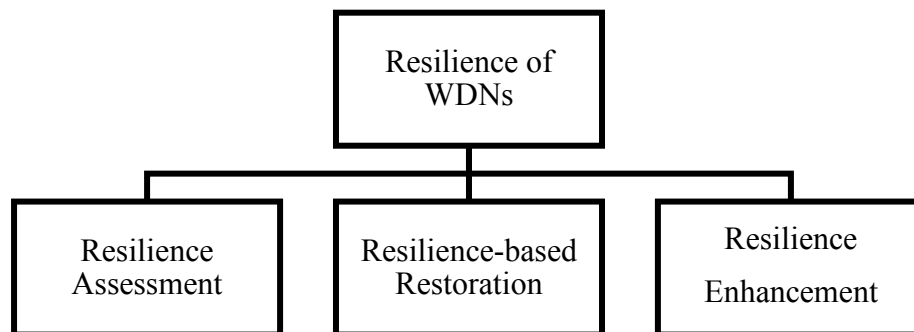


Figure 2-1: Resilience-based Management Models of WDNs

2.2 Resilience of Water Distribution Networks

In a broader sense, water supply systems consist of physical infrastructure components, service provided, organizations that regulate and maintain the provision of this service, and customers who use this service as depicted in Figure 2-2 (Klise et al. 2015). Hence, water distribution network is a component of water supply systems that represents the physical infrastructure. It consists of several subcomponents such as pipes, pumps, tanks, valves, and others.

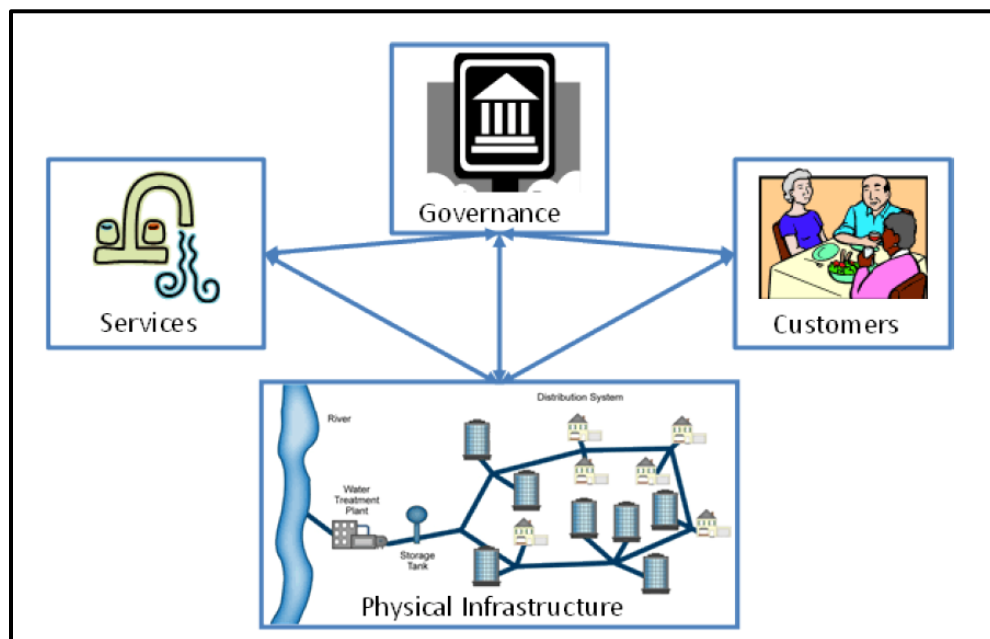


Figure 2-2: Components of Water Supply System (Klise et al. 2015)

Water distribution network is the backbone and water supply systems that dictates the status and level of service of the entire system. Consequently, tremendous endeavors both in practice and academia have been directed to sustain and maximize the performance of WDNs, as will be reported in subsequent sections.

The root of the word resilience is found in the Latin language, *resilio*. It consists of two parts, *re* (again) and *silio* (jump), which means to bounce back. Resilience of an entity is characterized by its ability to return to the normal state after being disrupted. Individuals who

overcome a severe shock, sports teams who get back to win after a series of losses, markets that recover from a fiscal crisis, and troops winning a battle from a losing start are all examples of resilient entities (Henry and Ramirez-Marquez 2012). In disaster management, resilient cities and communities are those who return back to original conditions after catastrophic events. Cities that return, recover, faster to normalcy are recognized to be more resilient (Ayyub 2014).

In the past few years, the concept of resilience has gained much interest in engineering infrastructure systems. Scholars elicited several frameworks to incorporate the concept of resilience in design, operation, and management of infrastructure systems. The American Society of Civil Engineers defines resilience of infrastructure systems as the ability to mitigate hazards and rapidly restore critical services with least harm to the public health, safety, economy and national security (Ayyub 2014). The US Department of Homeland Security outlined that resilient systems are those that can resist, absorb, recover from, and prepare to or adapt to a destruction or a loss (Collins and Baggett 2009).

These definitions proclaim resilience of infrastructure systems as a process that encompasses four phases, as illustrated in Figure 2-3. The process starts with some preparedness measures to mitigate the impacts of expected hazards. After a hazard occurrence, recovery actions are taken to restore the service. Afterward, policies and procedures are revised based on lessons learned to be better prepared for next disruptions. Resilience is not only about rapid recovery, but it is also about having some preparedness measures to reduce the vulnerability, potential performance loss, of this system.



Figure 2-3: Continuous Cycle of Building Resilience to Hazards (Klise et al. 2015)

In actual fact, resilience of infrastructure systems are usually characterized by three main capacities, namely: absorptive, adaptive, and restorative capacities (Vugrin et al. 2011). Absorptive capacity measures the ability of an infrastructure system to withstand impacts of hazards with minimum interruption in services provided. Adaptive capacity measures the system's capability to continue functioning by adjusting itself under a new disrupted state. Restorative capacity measures the efficiency of an infrastructure system's recovery (Assad et al. 2019).

The concept of infrastructure resilience is still an evolving topic as evidenced by the different definitions and frameworks proposed to quantify it. Resilience may also share some similarities with other existing concepts such as vulnerability and disaster risk. Vulnerability is the degree to which a structure is likely to undergo a performance loss as a result of a specific hazard. On the other hand, the National Academic Science defines disaster risk as: "the potential adverse effects from the occurrence of a particular hazardous event, which is derived from the combination of physical hazards, exposure levels, and vulnerabilities" (Cutter et al. 2013). The main difference between these concepts and resilience is that the latter investigates both the performance loss and recovery efforts. As such, the focus is not only directed towards estimating the potential damage

as in vulnerability assessment or on anticipating the potential consequences resulting from an asset failure as in disaster risk assessment. Restorative capacity is a vital quality of resilience that makes it more than just the inverse of vulnerability. Resilience explains why two different systems of the same vulnerabilities may undergo different restoring behaviors in terms of rapidness and final level of service. It is worth mentioning that despite such differences, these concepts might still be highly related. Measures that aim at reducing a system's vulnerability and risk of failure are simultaneously contributing to increasing the system's resilience (Brashear and Jones 2008). For example, the location of specific components of a water system in flood plain makes them highly vulnerable to flooding. Measures aiming to change their location will decrease their vulnerability. At the same time, these measures increase the water system's resilience because the level of disruption will be reduced, and the service will be restored more rapidly.

2.3 Resilience Assessment Models of WDNs

The literature includes several models and approaches for assessing and evaluating resilience of WDNs. These approaches are generally classified as either qualitative approaches or quantitative approaches (Klise et al. 2015).

Qualitative approaches include research efforts that introduce conceptual frameworks or semi-quantitative indices for resilience assessment (Hosseini et al. 2016). Tierney and Bruneau (2007) introduced a widely accepted framework, the 4R's framework, for resilience assessment. 4R stands for robustness, redundancy, resourcefulness, and rapidity, four main aspects of resilient systems. In this framework, the ability to cope with a disruption without substantial performance loss is denoted as robustness. Redundancy is the availability of alternative paths to substitute the unviable damaged components. Resourcefulness is the accessibility to a wide range of suppliers and materials needed for restoration activities. Rapidity measures the extent to which a disrupted

system can be restored swiftly (Tierney and Bruneau 2007). Fiksel et al. (2014) developed another example of conceptual frameworks for evaluating resilience of WDNs. In this model, several factors are included to assess resilience such as vulnerability, adaption, resource productivity, cohesion, diversity, and recoverability.

On the other hand, semi-quantitative indices are generated by aggregating specific weighted resilience indicators. Fisher et al. (2010) proposed a resilience assessment index based on an extensive data collection of about 1,500 variables related to robustness, recovery, and resourcefulness. Weights of these variables are then estimated, and weighted factors summed to produce a single global index. This index can be utilized to compare resilience levels of different infrastructure systems (Fisher et al. 2010). The main drawback of qualitative approaches is that they are subjective by nature, and detailed technical results cannot be generalized on a large scale due to the variations in the operational requirements of each network.

Quantitative approaches for resilience assessment aim at identifying some quantifiable performance functions or systems' outcomes that can be observed before and after hazard occurrence. These approaches can be either probabilistic or deterministic based on whether the stochastic nature of system function during different phases is considered. In addition, some of these approaches are dynamic as they consider time-dependent system performance functions or outputs. Others are static approaches since they provide an estimation of resilience as a snap-shot of time. Bruneau et al. (2003) developed one of the most commonly utilized metrics for resilience assessment. Resilience loss, Equation 2.1, is a deterministic dynamic metric that quantifies the degradation of a system following a hazard event.

$$RL = \int_{t_0}^{t_1} [100 - Q(t)] dt \quad (2.1)$$

Where RL is the resilience loss, $Q(t)$ is a function that measures the system performance as a percentage, t_0 is the time of disruption occurrence, and t_1 the time at which the resilience is calculated. The performance function $Q(t)$ can be any performance indicator of the system such as structural connectivity, hydraulic performance, or concentration of contaminants. Figure 2-4 provides a graphical illustration of resilience loss calculation based on the resilience triangle method. In this method, quality-based method, the initial system performance is assumed to be 100, and the shaded area represents the resilience loss (Bruneau et al. 2003; Nicholson et al. 2015; Adams et al. 2012; Sahebjamnia et al. 2015). Equations 2.2 and 3.3 are used to calculate the average values of resilience loss and retained resilience, respectively (Bruneau et al. 2003).

$$ARL = \frac{RL}{t_1 - t_0} \quad (2.2)$$

$$ARR = 100 - \frac{RL}{t_1 - t_0} \quad (2.3)$$

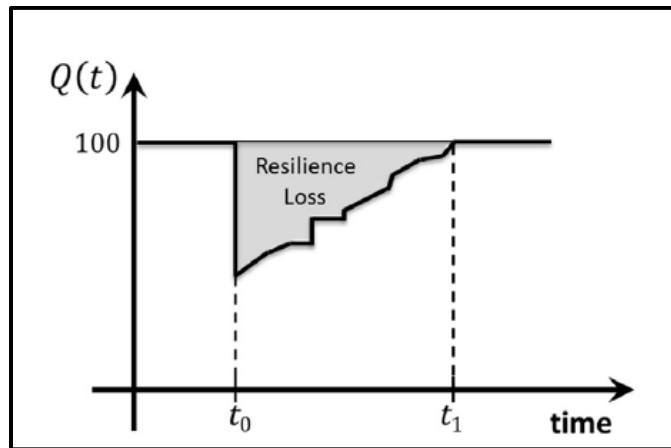


Figure 2-4: Resilience Loss Measurement (Bruneau et al. 2003)

Henry and Ramirez-Marquez (2012) proposed an extension to this method by considering the system's status before, during, and after disruptions. Three distinct states were defined in this model: original stable (S_0), disrupted (S_d), and stable recovered (S_f). Figure 2-5 shows these states along with two transition periods: system disruption and system recovery. Function $F(\bullet)$ in Figure

2-5 represents the system delivery function, which is equivalent to the system quality function in quality-based methods. For each system state, there exists a value for the figure of merit function $F(\bullet)$. Equation 2.4 was formulated to calculate resilience as a ratio between the recovery level at any instant and the initial loss in the performance function (Cutter et al. 2008; Henry and Ramirez-Marquez 2012; Pant et al. 2014; Dessavre et al. 2016).

$$\mathcal{R}_F(t_r|e_j) = \frac{[F(t_r|e_j) - F(t_d|e_j)]}{[F(t_0) - F(t_d|e_j)]} \quad (2.4)$$

Where $\mathcal{R}_F(t_r|e_j)$ is the proportion of delivery function recovered from the disrupted state under event e_j , $F(t_r|e_j)$ is the figure-of-merit of the system at the recovered state t_r , $F(t_d|e_j)$ is the figure-of-merit of the system at the disrupted state t_d under the event e_j .

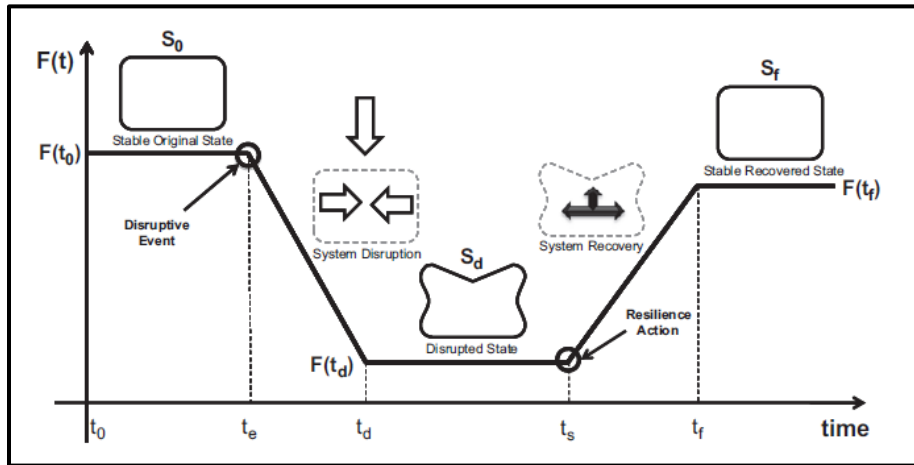


Figure 2-5: System State and Delivery Function Transition in Resilience (Henry and Ramirez-Marquez 2012)

A more recent extension was suggested by Dessavre et al. (2016), who formulated a five-state resilience framework urban infrastructure resilience assessment. Figure 2-6 illustrates the model, which starts at some steady reliability condition as the system usually functions before disruptions. When a disruptive event occurs, the system undergoes some transition states starting with a gradual reduction in its performance, followed by idle time for damage estimation and restoration planning. Finally, a course of recovery actions is taken to restore services. The final

recovered state may be either the same, less, or even more of than the initial state. Some conceptual attributes can be drawn from this illustration such as vulnerability, which is the difference between the initial performance, P_o , in the reliability state and the vulnerable performance, P_v , in the unreliability state (Dessavre et al. 2016).

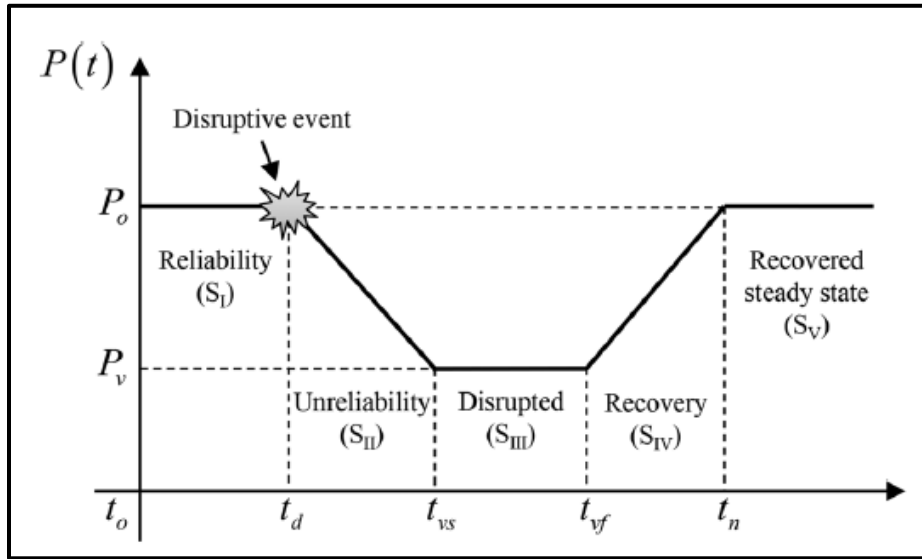


Figure 2-6: Five States Engineering Resilience Curve (Dessavre et al. 2016)

Ouyang et al. (2012) advanced previous models to present a stochastic time-dependent resilience assessment metric. Annual resilience metric, AR , given in Equation 2.5 measures resilience as the expected ratio between the actual performance curve, $P(t)$, and the target performance curve, $TP(t)$, over a time period T , equals one year in this model.

$$AR = E \left[\frac{\int_0^T P(t) dt}{\int_0^T TP(t) dt} \right] \quad (2.5)$$

In a different effort, Rose (2007) introduced the concept of economic resilience as "the ability of an entity or system to maintain system functionally when a disruption occurs." Economic resilience is measured as a ratio between avoided drops in infrastructure performance to the maximum potential drop, as shown in Equation 2.6.

$$R = \frac{\Delta Y^{max} - \Delta Y}{\Delta Y^{max}} \quad (2.6)$$

Where ΔY_{\max} is the difference between undisrupted and worst disrupted system outputs, and ΔY is the difference between undisrupted and expected disrupted system outputs.

Some researchers utilized hydraulic performance indicators as the system performance function to assess resilience of WDNs. Metrics that assess resilience based on these approaches are usually referred to as flow-based metrics. They require running hydraulic simulation models to find the flow and pressure conditions at different points throughout the network. Todini (2000) introduced one of the early and widely cited flow-based resilience metrics. In this approach, resilience is measured as the excess energy available in WDNs. Todini (2000) demonstrated the applicability of his metric in the design of WDNs by measuring the surplus power that could be dissipated due to physical failures or increased demand. He perceived resilient networks as those who have sufficient energy to be dissipated when failures occur. Todini's resilience metric, Equation 2.7, is a ratio between the available energy surpluses at the nodes over the maximum energy surplus in the network.

$$R = \frac{\sum_{i=1}^n q_i^*(h_i - h_i^*)}{\sum_{j=1}^r Q_j H_j + \sum_{k=1}^p \left(\frac{P_k}{\gamma}\right) - \sum_{i=1}^n q_i^* h_i^*} \quad (2.7)$$

Where q_i^* and h_i^* are design demand and required head at node i ; h_i is the head available at node i ; Q_j is the flow from reservoir j ; H_j is the total head at reservoir j ; P_k is the energy supplied to the network from pump k , γ is the water specific weight; and n ; r ; and p are the number of nodes, reservoirs, and pumps, in the network respectively. Values of these parameters depend on the size of the analyzed network. In his application, the author utilized the metric in resilience assessment of a small sub-network that consists of seven nodes and one reservoir. Prasad and Park (2004) built on Todini's work to investigate the effect of redundancy on WDNs resilience by incorporating loops and surplus power in calculating the resilience index. Their index called, network resilience index, assigns more weights to energy surplus at nodes where connected pipes have less diameters

variation since these loops are sought to be more reliable. The weighting factor, node's uniformity, is given in Equation 2.8, Prasad and Park (2004):

$$C_i = \frac{\sum_{j=1}^{N_{p,i}} D_{j,i}}{N_{p,i} \times \max \{D_{j,i}\}} \quad (2.8)$$

Where C_i is the uniformity of node i ; $D_{j,i}$ is the diameter of j^{th} pipe connected to node i ; and $N_{p,i}$ is the number of pipes connected to node i . Similarly, Jayaram and Srinivasan (2008) extended the original Todini's metric to formulate a modified resilience that accounts for multiple sources in resilience quantification. The proposed modified resilience index is a ratio of surplus energy to the demand energy, Equation 2.9.

$$MRI = \frac{\sum_{i=1}^n q_i^* (h_i - h_i^*)}{\sum_{i=1}^n q_i^* h_i^*} \quad (2.9)$$

Suribabu (2017) utilized Todini's index and the modified resilience index to optimize the design of WDNs. In this work, the authors considered minimizing the cost of the network subject to specific pipe diameters and pressure head constraints. The optimization suggested configuring the network such that the pipe sizes are decreasing along the shortest path (Assad et al. 2019). Another variation of Todini's resilience index was proposed by Liu et al. (2017). Liu et al. (2017) utilized hydraulic head surplus instead of hydraulic energy surplus. In this analysis, the available hydraulic head surplus is compared to the head surplus at previous nodes in estimating resilience of WDNs. In a different study that aims to optimize the design of WDNs, Choi and Kim (2019) formulated a multi-objective model that accounts for mechanical redundancy under multiple pipe failures of different states. The study established a relationship between pipe failure states and mechanical redundancy. Through simulation, the authors were able to analyze the demand levels of abnormal situations based on a defined extreme demand. In this study, hydraulic reliability was used as an indication of the system's redundancy instead of structural redundancy. Creaco et al.

(2016) presented a flow-based resilience index based on Todini's work. In this research effort, the authors extended the original resilience index by utilizing pressure-driven modeling and accounting for the energy dissipated through pipes and leaks, Equation 2.10:

$$I_r = \frac{\max(\sum_{i=1}^{N_s} Q_i^s H_i^s + \sum_{j=1}^{N_p} Q_j^p H_j^p - \sum_{k=1}^{N_d} Q_k H_{k,0})}{\sum_{i=1}^{N_s} Q_i^s H_i^s + \sum_{j=1}^{N_p} Q_j^p H_j^p - \sum_{k=1}^{N_d} Q_k H_{min,k}} \quad (2.10)$$

Where Q_i^s and H_i^s are the flow and total head at source i , respectively; Q_j^p and H_j^p are the flow and total head at pump j , respectively; Q_k and $H_{min,k}$ are nodal demand and minimum nodal head required by users at node k , respectively; N_s ; N_p ; and N_d are the number of sources; pumps; and demand nodes, respectively. The maximum function in Equation 2.10 was used to set the resilience index value equal to 0 in networks that feature a power deficit rather than a power surplus. Raúl Baños et al. (2011) compared the performance of the Todini's *RI*, Prasad's *NRI*, and Jayaram's *MRI* in the problem of resilient WDNs design. Through multi-objective optimization and simulation of over-demand scenarios, the authors analyzed the advantages and disadvantages of each metric. The authors concluded that none of those metrics could accurately determine the network's capability to provide sufficient supply under demand uncertainty. Those metrics considered the global excess of network pressure rather than where over-demand is applied. As such, the authors suggested that topology of the network be considered to determine the most critical points.

Chang and Shinozuka (2004) proposed a probabilistic method, acceptance method, for resilience quantification based on performance loss and recovery period. Resilience is calculated as the probability that a system's performance loss, r_o , is less than a maximum acceptable performance loss, r^* , and that the time to full recovery, t_l , is less than some maximum allowable disruption time, t^* , Equation 2.11. The authors demonstrated the practicality of this metric in mitigating seismic consequences on a WDN in Memphis, TN, USA (Chang and Shinozuka 2004).

$$R = P(r_0 < r^* \text{ and } t_1 < t^*) \quad (2.11)$$

Gay Alanis (2013) employed the acceptance method along with hydraulic simulations to assess resilience of water systems. The authors utilized both Matlab and EPANET software packages to investigate system performance under several disruptive scenarios. Resilience was then calculated by comparing the system performance to some previously defined resilience thresholds. Zhuang et al. (2013) employed the concept of availability in resilience evaluation of WDNs. Resilience in this model was captured as the ratio between the flow supplied to demand nodes to the required demand during disrupted conditions. The authors utilized Monte Carlo simulation to model various failure scenarios and calculate the resultant resilience accordingly. Cimellaro et al. (2015) proposed a more general metric for assessing resilience of WDNs based on technical, social, and environmental performance functions. The authors defined the ratio of water level in the tank to the tank capacity as the technical performance, the ratio of households with satisfying water demand to the total number of households as the social performance, and the ratio of water quality before and after disruption as the environmental performance. Resilience related to each system performance function is given by Equation 2.12:

$$R_i = \int_0^{T_C} \frac{F_i(t)}{T_C} dt \quad (2.12)$$

Where R_i and F_i are the resilience and the system performance functions related to the i^{th} domain, respectively (i.e. social, technical, environmental). T_C is the control time, which is the time from disruption until full restoration. The authors formulated a weighted multiplication model to aggregate the metric into a single general resilience index.

Besides energy perspective, resilience of WDNs was also assessed utilizing graph-based methods. In these approaches, researchers leverage the concepts of structural connectivity and redundancy as the system performance function. WDNs are expressed as networks of nodes and

links. Indicators from graph theory are utilized to assess the topological performance of WDNs. (Meng et al. 2018; Shuang et al. 2019).

Table 2-1 illustrates some of the topological metrics that were used in resilience evaluation of WDNs. Yazdani et al. (2011) analyzed the suitability of structure metrics such as link density, meshed-ness, nodal degree, clustering coefficient and spectral gap, and spectral metrics such as spectral gap and algebraic connectivity in assessing resilience of WDNs. In a later effort, Yazdani and Jerey (2012) exploited the flow passing through pipe segments and the connectivity information to propose a new entropic degree metric of resilience assessment. Zarghami et al. (2018) proposed a two-stage method to assess redundancy of WDNs. Local redundancies of pipes were first quantified utilizing the cospanning tree technique. Entropy theory was then employed to aggregate these redundancies and compute a global network redundancy index. Farahmandfar et al. (2016) proposed a new topology-based metric for assessing the seismic resilience of WDNs. In their model, the authors integrated robustness and redundancy in resilience evaluation for water segments. The authors employed a variation of the nodal degree to measure network redundancy and reliability to estimate the robustness. The metric was then utilized in formulating a resilience enhancement optimization problem. The authors reported a resilience enhancement by 8% with a \$10 million investment in replacement and new installation interventions.

Other authors attempted to integrate both flow-based and topological-based approaches in assessing resilience of WDNs. For example, Di Nardo et al. (2018) introduced a two-stage model for assessing resilience of WDNs. The model starts by evaluating the network topology and then proceeds in resilience quantification based on flow-based indices. The authors showed that topological features provide useful knowledge about resilience assessment of WDNs even in cases when partial hydraulic information is not available.

Table 2-1: Structural Network Indicators Commonly Used for Resilience Evaluation (Yazdani et al. 2011; Archetti et al. 2015)

Metric	Definition
Link density	The ratio between the total and the maximum possible number of links
Average nodal degree	The average value of the nodal degrees in a graph
Meshed-ness	The ratio between the total and the maximum number of independent loops in planar graphs
Diameter	The maximum geodesic length of the shortest path between possible pairs of nodes
Average path length	The average geodesic distance of the shortest paths between all possible pairs of nodes
Clustering coefficient	The ratio between the total triangles and the total connected triples
Betweenness centrality	The number of all the shortest paths passing through a node
Closeness centrality	The inverse average distance of the shortest paths between a node and other nodes
Central-point dominance	The average difference between maximum betweenness centrality and betweenness centrality of all other nodes
Spectral gap	Difference between the first and the second eigenvalues of the graph's adjacency matrix
Algebraic connectivity	The second smallest eigenvalue of the Laplacian matrix of the graph

Similarly, Herrera et al. (2016) employed K- shortest paths and closeness centrality to evaluate resilience of WDNS. In his work, Herrera et al. (2016) combined the topological computation with a hydraulic simulation model to calculate the head losses. A water network including many nodes with a low value of flow closeness and K-shortest path is considered as a low resilient system. That is because more energy is required, and dissipated, to supply water for such nodes that also have poor connectivity to water sources. Soldi et al. (2015) provided a similar study that integrated the flow-based and topology-based approaches for assessing resilience and vulnerability of an actual WDNs in Milan. In their work, the authors utilized connectivity metrics for resilience and vulnerability evaluation and hydraulic simulation for pipes' potential failures

estimation. Results about components connectivity and potential failure have been integrated into an asset management plan to suggest the most suitable intervention.

2.4 Resilience-based Restoration Models of WDNs

As previously mentioned, restoration capacity is one of the main aspects of resilient infrastructure systems. Restorative capacity can be conceptualized by two main attributes: the degree of recovery and recovery time (Assad et al. 2020). The recovery degree measures the level of the system performance function after accomplishing all recovery actions. This is usually controlled by funds allocated for recovery actions and availability of required material and skilled personal (Zhao et al. 2016). The recovery time refers to the total time elapsed since the service was interrupted until it was restored to normal conditions. It depends on the recovery strategy, recovery schedule, and available resources Cimellaro et al. (2015).

Several researchers focused their research on the recovery efforts of WDNs following hazardous events. Many of these efforts attempted to determine the most efficient recovery strategies to minimize the time of service disruption. For example, Luna et al. (2011) developed a discrete event simulation model to improve the restoration process of WDNS after a rare disastrous event. Through colored Petri nets, the authors modeled the system behavior leveraging a real network, trunk network, in Tokyo, Japan. The authors simulated various recovery strategies; each represents a distinct resource allocation and restoration time management plan. The model determined the earliest expected recovery time at a specific location following an earthquake event of a specific magnitude. Zhao et al. (2015) provided another model for WDNs restoration after seismic hazards. Zhao et al. (2015) employed the stochastic time-dependent resilience metric introduced by Ouyang et al. (2012), Equation 2.5, to compare the technical and organizational effects of two restoration strategies on improving the seismic resilience of WDNs. The authors

analyzed the effects of ductile retrofitting strategy and meshed expansion strategy on seismic resilience of an actual WDN in China. They concluded that ductile retrofitting was a more effective strategy for resilience improvement of WDN in cases of limited resource and fund scarcity. Mahmoud et al. (2018) developed an optimization model to minimize the adverse impacts of sudden failures on WDNs performance and the costs associated with intervention actions. The authors employed GA and pressure-driven hydraulic simulation to select the optimal set of operational interventions such as resetting pressure reducing valves and installing temporary bypasses to respond to several sudden failures.

In a different effort, Balut et al. (2019) applied the preference ranking organization method for enrichment evaluation (PROMETHEE) technique and hydraulic simulation to rank the set of failed segments restoration and to select the best ranking strategy. In this analysis, five disputing scenarios were simulated, and several performance indicators were measured such as rapidity of recovery and volume of water loss (Balut et al. 2019). Liu et al. (2020) provided a framework for resilience-based restoration of WDNs considering different types of accidents such as leakages and bursts. The authors considered two repair methods, plugging and replacement, to test and compare various combinations of resilience restoration strategies. Replacing all the cast iron pipes with new ductile iron pipes after failure was found to be the best restoration strategy of a disrupted water network in Mianzhu city, China. Besides, some scholars studied the role of interdependency in selecting the best restoration strategy. For example, Almoghathawi et al. (2019) developed an optimization model to minimize the cost of restoring fictitious interdependent water and power networks. In this resilience restoration application, the authors focused on retaining the performance of the interdependent networks to the same level before the disruption. This approach, however, might lead to some of the disrupted components being unrestored.

Once a hazard event occurs, it can result in multiple simultaneous failures along the WDNs. This is different from the case of random failures that occur individually in pipe segments at different time periods. In the first case, water service providers shall prioritize their response plan and recovery efforts to restore the most critical segments first. In this regard, there is a need to quantify the criticality of pipe segments in WDNs to prioritize the sequence of restoration actions. Asset Criticality is a measure of the associated consequences with the failure of this asset to perform its intended function (Cromwell 2002; InfraGuide 2004). Critical Assets are those whose failure is accompanied by significant economic, social, and environmental consequences. Continuous monitoring, regular maintenance, and rapid restoration of these assets are of paramount importance to minimize the overall system degradation.

Many authors attempted to develop models and metrics for assessing the criticality of infrastructure components and WDNs segments. For example, Salman (2011) provided one of the earliest and practical criticality estimation metrics. Criticality index of each segment was calculated based on a set of economic, operational, social, and environmental factors. To ensure consistency in relative weights assigning, the Analytical Hierarchy Process (AHP) was utilized. This index was computed considering the land use to assist in resource allocations purposes. For each distinct land zone, the weights of critical factors would assume different values (Salam 2011). The model was incorporated in the WDN management plan for the City of Hamilton, ON. Wang et al. (2012) developed another metric to identify the criticality of infrastructure components based on their physical interdependency with other infrastructure networks. The importance of a component is determined by estimating the drop in network performance when this specific component is disrupted. Accordingly, components are ranked based on their contribution to the

overall network performance degradation when all segments are disrupted; a higher degradation share indicates a more vulnerable, critical, component.

Baroud et al. (2014) and Barker et al. (2013) introduced two component importance measures to rank the most critical links in infrastructure networks. The authors formulated these two metrics to rank segments based on their contribution to network resilience as a function of vulnerability and recoverability. The first metric estimates the system performance loss when a disruption impacts a particular link. The second metric quantifies the potential positive impacts on system performance when measures are taken to avoid the failure of particular links. The authors utilized a stochastic ranking technique, Copeland Score method, to order the components according to those metrics. Similarly, Laucelli and Giustolisi (2015) proposed a risk-based methodology to specify the most critical segments in WDNs whose failure due to seismic hazard would result in the most degradation of system performance. The authors formulated a multi-objective optimization model to determine the most critical scenario, a set of links disruption that would lead to the most amount of unsatisfied water supply demands. The scope was limited to a single hazard and a single damage indicator without considering other factors such as the characteristics of the pipe segment or the time of restoration.

In a different effort, Moursi (2016) introduced a model for estimating the criticality of water mains using Paprika and Swing techniques. While maintaining the same categorization as in Salman's work (Salman 2011), Moursi (2016) included more factors in each category of his model. Opinions from experts in North America, Europe, and Qatar were sought to rank the relative importance of those factors. Subsequently, Moursi established a criticality index scale that reflects the level of criticality along with linguistic descriptions (Moursi 2016). More recently, He and Yuan (2019) developed a framework for identifying critical pipeline from a restorative resilience

perspective. The authors proposed a WDN recovery optimization model that aims at minimizing network service loss. In this model, the authors utilized two metrics to quantify the criticality of water segments. The first metric, optimal repair priority, represents the priority at which a pipeline shall be repaired to minimize the system's service loss. The second metric is recovery reduction worth, which measures the increase in service loss due to delaying the optimal repair priority of a pipeline. The model was applied on a WDN with an assumed number of pipelines failures. A high positive correlation between the two metrics was reported suggesting that pipelines with high repair priority are those whose delay results in the most unfavorable impact on service recovery.

2.5 Resilience Enhancement Models of WDNs

Resilience absorptive capacity is another essential quality of resilience WDNs. In this regard, measures to increase the strength of WDNs such that it can withstand future disruptions with minimum performance loss are taken. Such measures include developing optimal rehabilitation programs for aging components or actions that increase the level of network redundancy such that alternative paths are available, especially around critical components.

Jayaram and Srinivasan (2008) utilized their proposed modified resilience index, Equation 2.9, to develop one of the very first resilience enhancement models of WDNs. In this study, a multi-objective optimization model was developed to obtain a trade-off analysis between the modified resilience index and life-cycle cost. The authors modeled the deterioration of pipe segments by simulating a fictitious network with an increasing roughness coefficient over an extended period. The main finding was a significant cost saving when considering design and rehabilitation in one single analysis rather than solely focusing on network overdesigning. It is worth mentioning that the roughness increase rate was arbitrarily assumed without considering an accurate deterioration estimation. Yazdani et al. (2011) employed some metrics from graph theory to model and compare

different resilience enhancement actions. The rationale of this study is an interplay between WDNs structural connectivity and resilience. The authors investigated the effect of four different expansion strategies in improving the resilience of a WDN in a developing country, Ghana. The objective was to determine an invulnerable expansion strategy of the network subjected to a set of budget and design constraints. Utilizing statistical and spectral metrics shown in Table 2-1, the authors were able to objectively quantify the network structural robustness, optimal connectivity, and path redundancy.

Yoo et al. (2014) introduced a multi-criteria methodology for determining the rehabilitation priority of pipe segments subjected to a seismic hazard. The authors ranked the needs for rehabilitation based on the importance of each segment. However, they did not investigate different types of rehabilitation actions and their impact on the overall network robustness. In a different effort, Suribabu et al. (2016) proposed a model to enhance resilience of WDNs considering pipe diameter increase and parallel piping. The authors modeled two benchmark networks and iteratively increased the diameter of the pipe segment that has the maximum flow velocity to the next available commercial size. Similarly, pipes were added parallel to those through which water flows with maximum velocity. Such a simplified approach is, however, not feasible for large-sized networks. Similarly, Creaco et al. (2016) utilized a generalized form of Todini's index, Equation 2.10, to analyze a time variation of resilience resulting from changing pipe leakage and roughness coefficients while investigating the cost of the network. The results of the optimization showed that cost and delivered power of configuration obtained by the proposed index outperform the original ones suggested by Todini (2000). In this analysis, leakage and roughness coefficients were randomly increased to capture the network deterioration.

Farahmandfar and Piratla (2017a) introduced a resilience-based rehabilitation plan utilizing different resilience metrics. The authors compared the effectiveness of topology-based and flow-based methods in selecting optimal rehabilitation strategies of a WDN located in a seismic prone location. The model considered a single objective of maximizing resilience enhancement subject to a budgetary constraint. Resilience could be enhanced via two distinct methods: pipeline replacements and new pipeline installations. They found that the flow-based metric yielded relatively accurate results. However, the computational time of the simulation was significantly increased compared to the case of the topology-based metric. In a different effort, Farahmandfar and Piratla (2017b) considered two main rehabilitation actions, relining and replacement, to enhance resilience of WDNs against seismic hazards. GA was employed to determine which pipe segments to be rehabilitated considering their current condition and an expected earthquake scenario. However, this analysis was limited to one year, a snap-shot in time, without considering the effect of deterioration and life cycle cost on the rehabilitation planning decisions.

Cimorelli et al. (2018) developed a rehabilitation methodology to improve resilience of WDNs subject to a limited budget. The authors utilized genetic algorithm, GA, and pressure-driven hydraulic simulation to investigate the practicality of Creaco's resilience index and flow entropy in rehabilitation planning. The study concluded that the resilience index is more accurate in reliability estimations and, thus, resilience enhancements than flow entropy. Demand satisfaction was suggested to be considered as an auxiliary factor if flow entropy is to be considered in the rehabilitation planning of WDNs. However, only one rehabilitation method, replacement, was considered, and a single failure was studied in this work. Meirelles et al. (2018) suggested considering the energy generated and resilience improvement to justify the costs encountered in pipe rehabilitation. It was found that increasing the size of 20% of the pipes would result in both

significant resilience improvement and considerable energy recovery benefits that even surpasses additional needed investment in this regard. This approach asserts the economic and technical added values of WDNs rehabilitation, as evidenced by improved resilience and energy recovery benefits, respectively.

2.6 Rehabilitation Techniques

For resilience enhancement and service restoration purposes of WDNs, various rehabilitation intervention actions shall be carried out as deemed necessary. These interventions can be divided into several activities based on the rehabilitation type. Figure 2-7 shows the different water segments rehabilitation methods that include repair, renovation, and replacement.

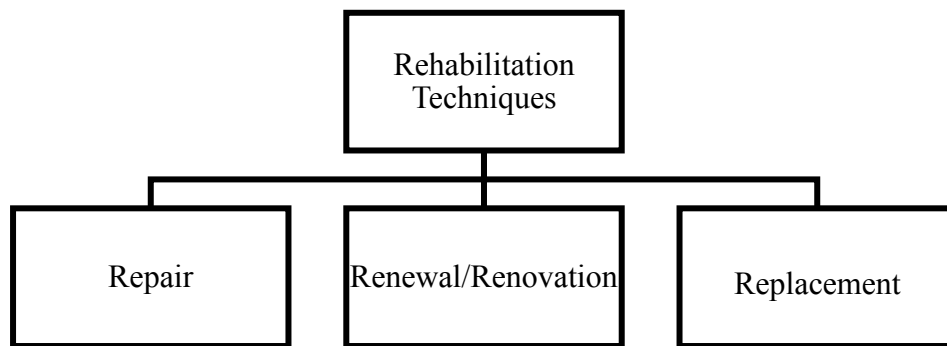


Figure 2-7: Rehabilitation Techniques of Water Pipe Segments

Repairs are utilized to fix leakages and small breaks on water pipes. Typically, a repair option would be sought if in structural condition of the pipe segment is not compromised. In addition, some municipalities set a certain threshold for the number of breaks, after which the pipe segment shall be replaced. Mechanical clamps and couplings are the main types of repair techniques that are used to fix small breaks, leaks, and circumferential cracks. Clamps, in

particular, facilitates the execution of repair actions without the need for full depressurization of water pipe segments (Weaver and Woodcock 2014).

When a water pipe segment deteriorates such that its structural condition is debilitated, employing some renovation or renewal actions becomes mandatory. Pipe renovation encompasses applying either a coating or a lining to the aged pipe segment. Epoxy lining (EL) and cured in place pipe (CIPP) are two of the widely applied minor and major renewal actions, respectively. In epoxy lining (EL), a thin coating of liquid epoxy is sprayed on the internal wall of aging yet structurally sound pipe segments. Some advantages of EL over regular cement mortar lining are the provision of a smoother surface that is easier to be maintained, being faster to be cured, and more flexible to even smaller pipes segments (Yazdekhashti et al. 2014). Cured in Place Pipe (CIPP) is a major rehabilitation method in which a resin-coated fiber tube, liner, is inserted into a structurally deteriorated host pipe. This method results in the least diameter reduction with a significantly smoother surface among other structural rehabilitation techniques (Yazdekhashti et al. 2014).

Replacement is a conventional technique for water pipe rehabilitation. Open cut method (OCM) is the most commonly used method for water pipes replacement with no restrictions on the size or material type of pipes that can be replaced. In this type of rehabilitation, a new pipe segment is installed instead of a severely deteriorated one. Despite being the most trivial rehabilitation technique, it is usually accompanied by significant disruption to users and other infrastructure systems such as the transportation network. Accordingly, various trench-less technologies have been developed to decrease the time, cost, and efforts associated with this lengthy and tedious process (Yazdekhashti et al. 2014).

Pipe Bursting (PB) is the most common trenchless technology that has been widely utilized to replace deteriorated pipe segments. In this method, a bursting head is inserted to break a host pipe and pull along a new pipe of the same or larger diameter. PB has been applied to replace water pipes of various sizes, material types, and surrounding conditions. However, rocks and densely compacted soils are not favorable conditions for this method. (Yazdekhashti et al. 2014). Pipe Splitting (PS) is a method for replacing an existing deteriorated pipe segment by longitudinal splitting and drawing in a new pipe. Similar to PB, this method allows for installing new pipes of the same or even larger diameters. PS is considered a special variant of PB to replace water pipes segments that do not fracture using regular PB, such as ductile iron pipes (Alan Atalah 2009).

2.7 Research Methods

In this research, multiple techniques were utilized to achieve its ultimate objectives. Such techniques include but are not limited to; fuzzy analytical network process (FANP), PROMETTE, survival analysis, k-means clustering, Shannon entropy, and optimization algorithms. Below is a brief description of each.

2.7.1 Fuzzy analytical network process (FANP)

Fuzzy analytical network process (FANP) belongs to the family of multi-criteria decision making (MCDM) techniques. MCDM tools are employed to obtain the best alternative among a set of feasible alternatives based on multiple decision criteria (Işıklar and Büyüközkan 2007). There are different techniques to solve MCDM problems such as Analytic Hierarchy Process (AHP), Fuzzy AHP, Technique for Order Preference by Similarity to Ideal Solution (TOPSIS), Preference Ranking Organization Method for Enrichment of Evaluations (PROMETHEE), ANP, and FANP.

AHP has gained wide acceptance as a powerful and flexible method for ranking decision alternatives and selecting the best solution based on multiple criteria. It has many advantages, such as ease of application and effectively handling both qualitative and quantitative criteria. However, one of the main drawbacks of AHP is the inability to deal with the imprecise or vague nature of linguistic assessment (Srichetta and Thurachon 2012). FAHP has been developed to overcome this limitation by using common sense linguistic statements in the pairwise comparison. Table 2-2 shows three of the most used linguistic scales in FAHP and FANP calculations (Etaati et al. 2011). In addition, Saaty (2007) developed ANP as an extension to AHP to account for the interdependencies and feedback among the assessment criteria. Since then, ANP has been the most inclusive approach for the analysis of societal, governmental, and corporate decisions. This is mainly because of its nature as a comprehensive approach that handles all tangible and intangible assessment criteria as well as allowing both interaction and feedback within elements of clusters, inner dependence, and between clusters, outer dependence (Wei et al. 2010).

Table 2-2: Cheng, Kahraman and Saaty Scale (Etaati et al. 2011)

Scale	Fuzzy Linguistic Scale
Cheng	$\{(0,0,0.25); (0,0.25,0.5); (0.25,0.5,0.75); (0.5,0.75,1); (0.75,1,1);\}$
Kahraman	$\{(1,1,1); (0.5,1,1.5); (1,1.5,2); (1.5,2,1.5); (2,2.5,3); (2.5,3,3.5)\}$
Saaty	$\{(1,1,1); (2,3,4); (4,5,6); (6,7,8); (8,9,10)\}$

Fuzzy set theory was introduced by Zadeh (1965) to deal with uncertainty due to imprecision and vagueness. Typically, a fuzzy set is defined by a membership function that represents the grade of any element x of X that has the partial membership to M . Triangular membership function is one, and the most common, fuzzy membership functions that have been reported in the literature. A triangular fuzzy number is defined as (l, m, u) , where the parameters l , m , and u denote the

smallest possible value, the most promising value, and the largest possible value that describe a fuzzy event respectively. **Figure 2-8** shows a triangular fuzzy number.

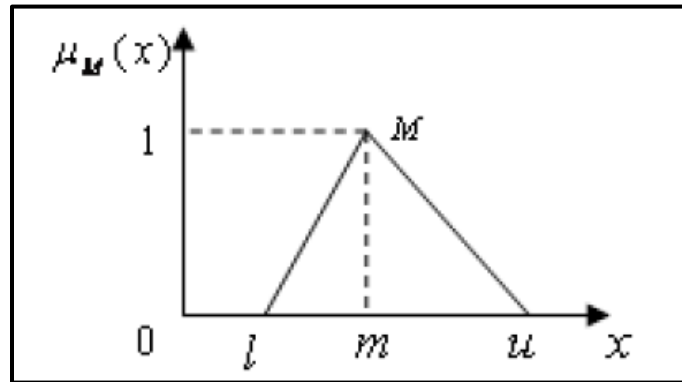


Figure 2-8: Triangular fuzzy number (Wei et al. 2010)

Fuzzy ANP is a technique that combines the capabilities of ANP, fuzzy theory, and fuzzy AHP to account for both inner and outer interdependence as well as the uncertainty and imprecision in decision making. Application of FANP involves computing three relevant matrices known as supermatrix, weighted supermatrix, and limited matrix. Supermatrix is firstly constructed after specifying the system's objective and criteria hierarchy. Pairwise comparison is usually made by seeking expert's opinions about the relative importance of one criterion when compared to another with respect to the problem's preference. Generally, a scale 1-9 is used to evaluate this comparison where 1 and 9 stand for equal importance and extreme importance, respectively. Weighted supermatrix is then readily calculated by dividing each cell in the supermatrix by the sum of the column in which it lies, Equation 2.12 (Etaati et al. 2011)

$$A_{ij} = \frac{a_{ij}}{\sum_{i=1}^n a_{ij}} \quad (2.12)$$

Where A_{ij} is the value in the weighted supermatrix; a_{ij} is the corresponding value in the unweighted supermatrix; and n is the number of cells in column j . Finally, the limited matrix is

found by raising the weighted supermatrix to limiting powers to get the global priority vector, global weights column, Equation 2.13, (Etaati et al. 2011).

$$\bar{W}^{\infty} = \lim_{k \rightarrow \infty} \bar{W}^k \quad (2.13)$$

Where \bar{W} is weighted supermatrix.

The weighted supermatrix is raised to many powers unit convergence is achieved, i.e., the resulted matrix is the same as the one before it (Wei et al. 2010). Examples of using FANP in asset management of water systems can be found in El Chanati (2014) and El-Abbasy (2016). In these models, FANP was utilized to establish indices for assessing the performance of water pipelines and accessories. These indices are then aggregated to generate an integrated performance assessment model for WDNs (El Chanati 2014; El-Abbasy et al. 2016).

2.7.2 Preference Ranking Organization Method for Enrichment of Evaluations (PROMETHEE)

Preference Ranking Organization Method for Enrichment of Evaluations (PROMETHEE) is multi-criterion decision-making (MCDM) technique that assists in selecting the most appropriate solution among a set of alternatives. In this research study, PROMETHEE II is utilized to determine the best solution of the Pareto frontier points resulted from a multi-objective optimization model. The PROMETHEE method is an interactive MCDM technique that can handle quantitative as well as qualitative criteria with discrete alternatives (Brans et al. 1986). Recently, the PROMETHEE method has been successfully applied to real-life planning problems to rank alternatives which are difficult to be compared because of the conflicting trade-off relation between the evaluation criteria. (Abdullah et al. 2019). In this method, a preference function for each criterion is selected. Based on this function, a preference index for alternative "a" over "b" is

computed. This index represents a measure to support the hypothesis that alternative "a" is preferred to "b". The steps of applying the PROMETHEE II method are detailed below based on and (Brans et al. 1986; Polat 2016)

1. Determine the criteria, along with their relative weights of importance, and the set of possible alternatives for the considered problem. In this study, the criteria are the objective functions: cost, resilience, and emissions. Shannon entropy was employed to determine the weights of the criteria. The set of alternatives is the set of Pareto optimal points.
2. Normalize the decision matrix using Equations 2.14 or 2.15 in case of beneficial or non-beneficial criteria, respectively:

$$R_{ij} = \frac{[X_{ij} - \min(X_{ij})]}{[\max(X_{ij}) - \min(X_{ij})]} \quad (2.14)$$

$$R_{ij} = \frac{[\max(X_{ij}) - X_{ij}]}{[\max(X_{ij}) - \min(X_{ij})]}, \quad i = 1, 2, \dots, n \text{ and } j = 1, 2, \dots, m \quad (2.15)$$

Where X_{ij} is the performance measure of i^{th} alternative with respect to j^{th} criteria.

3. Determine the differences in criteria values for each alternative by pairwise comparison with respect to other alternatives.
4. Define the preference function $P_j(a, b)$. In this study, a linear preference function is assumed for the criteria, as shown in Equation 2.16:

$$P(x) = \begin{cases} 0, & x < 0 \\ \frac{x}{m}, & 0 \leq x \leq m \\ 1, & x > m \end{cases} \quad (2.16)$$

Where m is an arbitrary parameter called the preference threshold, it represents the smallest deviation that is considered sufficient to generate a full preference.

5. Calculate the aggregated preference index using Equation 2.17:

$$\pi(a, b) = \sum_{j=1}^m P_j(a, b)w_j \quad (2.17)$$

Where $w_j > 0$ is the weight of the j^{th} criterion. $0 \leq \pi(a, b) \leq 1$ indicates the degree that alternative a is preferred to alternative b overall criteria.

6. Calculate the leaving (positive) and entering (negative) outranking flows as follows:

$$\phi^+(a) = \frac{1}{n-1} \sum_{x \in A \setminus \{a\}} \pi(a, x) \quad (2.18)$$

$$\phi^-(a) = \frac{1}{n-1} \sum_{x \in A \setminus \{a\}} \pi(x, a) \quad (2.19)$$

Where ϕ^+ is the leaving outranking flow and it represents how "a" dominates all other alternatives, and ϕ^- is the entering outranking flow, and it represents how "a" is dominated by all other alternatives, and A is the set of alternatives.

7. Determine the ranking of the considered alternatives based on the net outranking flow which is given by Equation 2.20:

$$\phi(a) = \phi^+(a) - \phi^-(a) \quad (2.20)$$

Where $\phi(a)$ is the net outranking flow for alternative "a". The most preferred alternative is donated by the highest value of $\phi(a)$.

2.7.3 Survival Analysis

Survival analysis is the set of methods used for data analysis where the outcome is the time until the occurrence of an event of interest (Kleinbaum and Klein 2010). In this analysis, subjects are monitored for a specific period, and times at which certain events occur are recorded. Objects whose survival time information is not complete by the end of the observation process are called censored observations. Classical linear regression cannot sufficiently handle censored observations. On the other hand, survival analysis can accommodate both censored and uncensored observations in estimating the parameters of interest. Once the time to events and events status is

known, hazard function and survival function can be ascertained. The most common approach for fitting survival models is the parametric approach. In this approach, the underlying distribution of survival times is assumed to follow a known distribution such as Weibull and exponential models. Model parameters are then estimated utilizing the maximum likelihood method. In this study, several probability distributions were tested to fit the inter-failure time of water pipe segments. The most common type of these approaches, Weibull Distribution, is explained in the remainder of this subsection.

In 1939 Waloddi Weibull developed a failure distribution function that is presented by a bathtub curve, Figure 2-9, to describe the deterioration phenomenon (Weibull 1939). Since then, this formulation has been accepted as the most popular model to assess and predict failures and malfunctions across several fields (Jardine and Tsang 2013). The probability density function for a 3-parameter Weibull distribution is given by Equation 2.21, (Jardine and Tsang 2013):

$$f(T, \beta, \eta, \gamma) = \frac{\beta}{\eta} \left(\frac{T-\gamma}{\eta} \right)^{\beta-1} e^{-\left(\frac{T-\gamma}{\eta} \right)^\beta} \quad (2.21)$$

Where: $T \geq 0$, $\beta > 0$, $\eta > 0$, $-\infty \leq \gamma \leq \infty$, β is the shape parameter, η is the scale parameter, and γ is the location parameter.

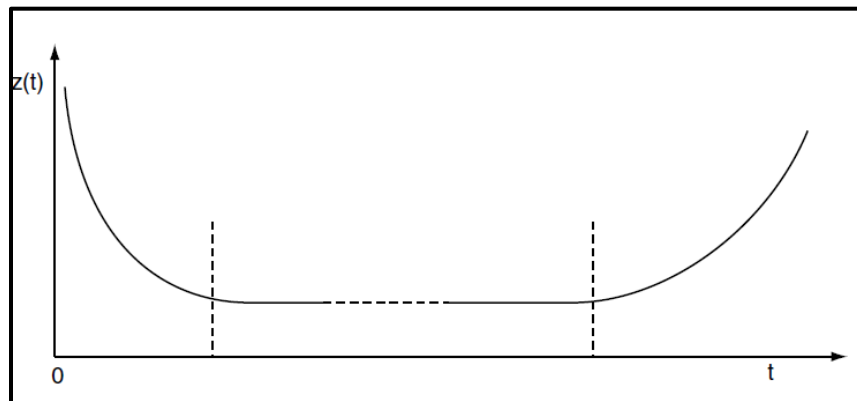


Figure 2-9: Bathtub Failure Rate Function (Murthy et al. 2008)

A Weibull distribution with a shape factor β less than one corresponds to a decreasing failure rate over time, improving reliability. This phase is known as the infant mortality phase or early-life failures. On the other hand, a Weibull distribution with a shape factor β more than one corresponds to an increasing failure rate over time, deteriorating reliability. This phase is known as the wear-out phase or end-life failures. A Weibull distribution that has a shape parameter β equals exactly one corresponds to a constant failure rate. In such a particular case, the Weibull distribution reduces to an exponential one indicating a Poisson process. The scale parameter η determines the spread of the Weibull distribution. A higher value of η corresponds to a lower failure rate or higher reliability. The location parameter γ describes the shift, time offset, of the distribution. When the value of the location parameter is set to zero, the distribution is reduced to a 2-parameter Weibull distribution. The reliability, survivability, for the 3-parameter Weibull distribution and the failure rate can be given by Equations 2.22 and 2.23, respectively, (Jardine and Tsang 2013):

$$R(T) = e^{-\left(\frac{T-\gamma}{\eta}\right)^\beta} \quad (2.22)$$

$$\lambda(T) = \left(\frac{\beta}{\eta}\right) \left(\frac{T-\gamma}{\eta}\right)^{\beta-1} \quad (2.23)$$

Where $T \geq 0$ is the duration, $\beta > 0$ is the shape parameter, $\eta > 0$ is the scale parameter, and $-\infty \leq \gamma \leq \infty$ is the location parameter.

To calibrate a Weibull distribution, the maximum likelihood method is employed. The first step is to establish the likelihood function, as shown in Equation 2.24 (Kleinbaum and Klein 2010):

$$L = \prod_{i=1}^n L_i = \prod_i \lambda(t_i)^{d_i} R(t_i) \quad (2.24)$$

Where n = the number of pipe segments; t_i is the observation period; and d_i is a failure indicator that takes a value of one when if pipe i failed during period t_i and zero otherwise. Calibrating the model parameters can then be performed by setting the partial derivative of the natural logarithm of L to zero and solving the set of system of equations, Equation 2.25. The parameter values that maximize L are the maximum likelihood estimates (Kleinbaum and Klein 2010).

$$\frac{\partial \Lambda}{\partial \theta_j} = 0 \quad (2.25)$$

Where $\Lambda = \ln L$; θ_j is the distribution parameters vector. In this case $j=3$ and the parameters are β , η , and γ .

2.7.4 K-means Clustering

Clustering is the process of portioning a set of objects into homogenous groups based on shared similarities. In this analysis, clustering techniques are utilized to divide the selected network into a set of clusters based on the geographical location. K-means and K-medoids algorithms are investigated and compared to select the best performing algorithm in clustering the chosen network. K-means clustering algorithm is based on minimizing the squared error between the empirical mean of a cluster, clusters' centroids, and the points in the cluster. In this algorithm, the cluster's centroid can, but does not have to, be one of the data points. This is the main distinction between K-means and K-medoids. In K-medoids, the centroid of a cluster is always one of the points in that cluster. The steps of K-means algorithms are shown below (Jain 2010):

1. Select the desired number of clusters K , and select K random starting points that will serve as the initial clusters' centroids.
2. Calculate the Euclidean distance between each data point and the centroids. Euclidean distance is the square root of the sum of squares of differences between components of two

pattern vectors $X_i = X_{i1}; X_{i2}; \dots, X_{id}$, and $X_j = X_{j1}; X_{j2}; \dots X_{jd}$, as shown in Equation 2.26 (Sawant 2015):

$$d_{ij} = \sqrt{\sum_{k=1}^d (x_{ik} - x_{jk})^2} \quad (2.26)$$

3. Assign data points to clusters based on the minimum distance between the data points and clusters' centroids, and recalculate the clusters' centroids.
4. Repeat steps 2-3 until convergence, centroid and data points do not move anymore.

As clustering is an unsupervised machine learning algorithm, evaluating the quality of the generated clusters may not be trivial. Clustering aims to minimize the intra-cluster distance, distance within the same cluster, and to maximize the inter-cluster distance, the distance between clusters. To attain that, the Davies–Bouldin Index is employed to compare the clustering quality of K-means and K-medoids. Davies–Bouldin Index is a ratio between the sums of intra-cluster scatter and the inter-cluster separation, as shown in Equation 2.27 (Davies and Bouldin 1979):

$$DBI = \frac{1}{N} \sum_{i,j=1}^N \max_{i \neq j} \left(\frac{D_i + D_j}{d_{i,j}} \right) \quad (2.27)$$

Where D and d are the intra-cluster and the inter-cluster distances. The intra-cluster distance is the average distance between the data points and the cluster centroid, Equation 2.28. The inter-cluster distance is the distance between the centroids of the two clusters, Equations 2.26, by replacing X_i and X_j with C_i and C_j .

$$D = \frac{\sum_i \|X_a - C_i\|}{N_i} \quad (2.28)$$

Where X_a is an arbitrary point in cluster i ; C_i and N_i are the centroid and the total number of points in cluster i . A lower value of Davies–Bouldin index denotes compact clusters with centroids far from each other, thus a better cluster (Sahani and Bhuyan 2017).

2.7.5 Shannon entropy

The concept of entropy was presented in the 1940s by Claude Shannon as a mathematical component of the information theory (Shannon 1948). In this mathematical formulation, information entropy refers to the amount of earned information content from observing a specific result. This information portion represents the amount of uncertainty inherited from the information source and the stochastic nature of random events. The concept of information theory had been adopted in a wide range of scientific fields such as physics, engineering, social science, and others. In this research, Shannon entropy was utilized to compute the weights of objectives in multi-objective optimization problems.

As the theory implies, smaller weights are assigned to those attributes that assume similar values across alternatives. When the measures of performance of a specific attribute are close to each other across the studied alternatives, this attribute is considered relatively unimportant by the decision-maker. In this thesis, weights of attributes were calculated based on the degree of index dispersion (Akyene 2012) as detailed below:

1. Calculate the weight of the i^{th} alternative with respect to j^{th} attribute, P_{ij} , as shown in Equation 2.29:

$$P_{ij} = \frac{x_{ij}}{\sum_{i=1}^m x_{ij}} \quad (1 \leq i \leq m, 1 \leq n \leq j) \quad (2.29)$$

Where x_{ij} is the measure of performance of the i^{th} alternative with respect to j^{th} attribute; m and n is the number of alternatives and number of attributes, respectively.

2. Calculate the entropy value of the j^{th} attribute, e_j , as shown in Equation 2.30

$$e_j = -\frac{1}{\ln(m)} \times \sum_{i=1}^m P_{ij} \times \ln P_{ij} \quad (2.30)$$

3. Calculate the variation coefficient of the j^{th} attribute, d_j , as shown in Equation 2.31

$$d_j = 1 - e_j \quad (2.31)$$

4. Calculate the weights of the j^{th} attribute, w_j , as shown in Equation 2.32

$$w_j = \frac{d_j}{\sum_{i=1}^n d_j} \quad (2.32)$$

2.8 Optimization algorithms

As stated earlier, municipalities manage a massive inventory of infrastructure assets that are running over extended life spans. Municipalities are expected to face an increased number of widespread failures due to natural and human-made disruptions. Given fund scarcity and limited resources, maintenance programs are usually postponed for several years. As such, decision-makers need to utilize optimization techniques to solve this performance-cost paradox. Typically, optimization models aim at maximizing performance improvement, both before and after anomalous events, while minimizing associated costs. Optimization techniques are search engines that aim at minimizing a cost function while satisfying a set of constraints. Both cost function(s) and constraints can be mathematically represented as functions of decision variables. The result is an optimization problem that can be solved by a method from those reported in the operational research and optimization field. Appropriate optimization techniques may be selected based on the type and number of decision variables, the form of the objective functions and constraints, and whether a decision must be made in sequence (Shahata 2013). Optimization techniques can be broadly classified into two main categories: classical mathematical programming and evolutionary algorithms, as shown in Figure 2-10.

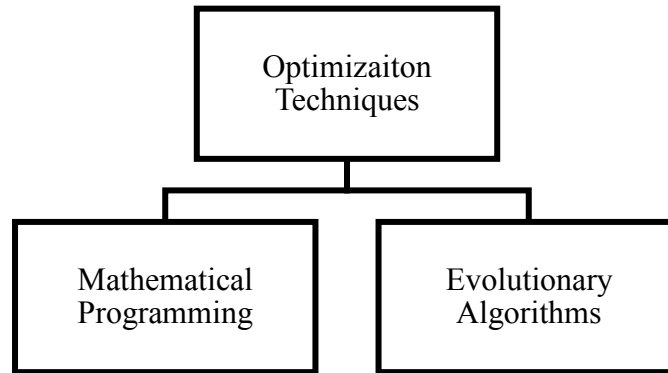


Figure 2-10: Optimization Solving Techniques

Mathematical programming models converge faster and are guaranteed to obtain a global optimum solution in a specific type of problems. Linear Programming (LP), Integer Programming (IP), Dynamic Programming (DP) are examples of mathematical optimization models that had been widely used in the field of infrastructure asset management (Nunoo 2001). Linear Programming is the most straightforward optimization solving method in which both objective functions(s) and constraints are linear functions of the decision variables. However, this method cannot handle a substantial number of decision variables or non-linear formulations. Integer Programming can handle both linear and non-linear formulation of optimization problems. Decision variables are constrained to integer values. In some cases, they can take values of 0's and 1's only, binary integer programming. The issue of significant decision variables cannot be handled using this type of algorithms, either. Mixed Integer Non-Linear Programming represents a combination of both mixed integer programming and non-linear programs. It can handle both linear and non-linear formations of objectives and constraints. In this formulation, some, but not all, of the decision variables must be integers. However, in many cases, it is challenging to be solved.

As the scale and complexity of the optimization problem increase, metaheuristic algorithms emerge as feasible alternatives. These algorithms are usually inspired by biological evolution, social behavior, or human memory. They utilize stochastic approaches in learning, adaptation, and evolution to reach a near-optimum solution (Dorigo and Gambardella 1997). It is worth mentioning that the concept of an optimal solution does not exist in evolutionary algorithms. Hence, users need to define some termination criteria to stop the search process before starting as there is no explicit way to test whether a given solution is optimal (El-Ghandour and Elbeltagi 2017). Below is a brief description of common types of evolutionary algorithms that were utilized, tested, in this research:

- Genetic Algorithm (GA) is a search heuristic that was introduced in the 1970s by John Holland (Holland 1975), inspired by the natural evolution theory. The search process starts by initializing a population, a set of random solutions; each represents a possible combination of the decision variables. The fitness of each solution is then calculated, and solutions are ranked according to their fitness. Best solutions are then selected via a specific selection strategy to reproduce by undergoing further genetic operators of crossover and mutation. In crossover, genes in two parents are exchanged until reaching a randomly selected crossover point. To prevent premature convergence, genes are randomly flipped with a low probability in the mutation step. The process is iteratively repeated until meeting the stopping criteria (Assad et al. 2020).
- Tabu Search is a local-based metaheuristic algorithm that has been used to solve many combinatorial problems such as water network design optimization, traveling salesman problem and routing problems (da Conceicao Cunha and Ribeiro 2004; Brandão 2009; Basu 2012). The search process starts with an initial solution expressed as a combination of the

decision variables. Exploring the possible neighborhood of that solution is then iteratively conducted. A neighborhood to a solution is any other solution that can be obtained by altering the values of the decision variables. To avoid cycling within a small set of the search space, moves that lead to recently visited solutions are temporarily prohibited, stored in the Tabu List. Sporadically, certain Tabu moves are allowed given that they generate better solutions than the best-known solutions so far, aspiration criteria. A diversification procedure is added to minimize the possibility of getting trapped around a local optimum. This is achieved by boosting moves to new regions in the search space that was not previously visited. The algorithm terminates after a pre-specified number of iterations (Glover 1997).

- Ant Colony Optimization (ACO) is an evolutionary algorithm that is inspired by the social behavior of ants trying to reach a source of food. ACO was firstly introduced by Dorigo (1996) and has been widely used since then, especially in scheduling and graph routing optimization problems (Dorigo and Gambardella 1997; Maier et al. 2003; El-Ghandour and Elbeltagi 2017). The algorithm exploits that ants deposit pheromone while traveling as a method of indirect communication. The shortest path is the one with the largest amount of deposited pheromone. The process starts by initiating some randomly generated ants that represent different possible solutions. In this context, ants are expressed by several variables and pheromone concentration. Ants are first evaluated according to the objective function. Next, pheromone concentrations for each possible path are iteratively updated to reinforce good solutions, shorter paths. The variable values of each ant are then changed according to the updated pheromone concentration until meeting the termination criteria (Elbeltagi et al. 2005). To prevent premature convergence, a pheromone evaporation parameter is introduced (Dorigo et al. 2006).

- An extension of the classical ant colony optimization is proposed by (Schlüter et al. 2009). In the original formulation of ACO, Pheromone values, usually within a pheromone table, are continuously updated based on information gained during the search process. Schlüter et al. (2009) exploited an aggregated weighted sum of several Gaussian distribution functions instead of pheromone tables to guide the search process. A discretization of this continuous function is introduced to allow intuitive handling of integer variables. Solution archive, SA, is proposed to continuously store and rank the most promising solutions investigated so far. In this extension, the mean and deviation of the Gaussian PDF are updated based on solutions stored in the SA. Each time a solution is created, its attractiveness is calculated and compared to those in the SA archive. A solution will be placed in the j^{th} position of the SA only if it has a better attractiveness than the existing solution j . This way updating the SA implies updating the characteristics of the PDF, pheromone update, and thus the process of creating new solutions. The algorithm is also fortified with a robust penalty method for constraints handling. A local heuristic, sequential quadratic programming, is also employed to guide searching around the best known solution (Exler and Schittkowski 2007). More details about this modified version of ACO and its implementation on real-world problems can be found at (Schlüter et al. 2009; Schlüter et al. 2012).

2.9 Gaps in Literature

Previous research studies were reviewed to search for suitable resilience assessment models for WDNs. It was found that resilience metrics can be either flow-based or structural-based indexes. The reviewed literature covered different restoration and resilience enhancement frameworks from which system performance can be improved to some accepted thresholds. Several optimization algorithms and multi-criteria decision-making techniques utilized in this research were also discussed in this chapter. Table 2-3 depicts a comparison analysis between the

main resilience metrics and frameworks reviewed in this dissertation. Main findings and limitations of the literature review can be listed in the following points below:

- Considerable efforts have been directed towards developing resilience metrics to help achieve the optimal design of WDNs. Very few studies have incorporated resilience in the rehabilitation-based decision making process.
- Even though several studies attempted to quantify the resilience of WDNs, very few introduced a practically applicable and easy-to-use metrics along with a comprehensive framework that can be used by municipalities in resilience improvement planning.
- Many of the previously developed metrics for resilience assessment of WDNs are flow-based ones necessitating the need to run sophisticated and hard-to-calibrate hydraulic simulations. Such approaches require extensive computational time, that can extend up to several hours especially as the size and complexity of the network increase. Faster models are needed for the restoration planning after each hazardous event.
- Many structural-based metrics are solely based on graph theory indicators and rarely consider other non-topological characteristics of WDNs such as pipe lengths, sizes, aging effects, surrounding conditions.

Table 2-3: Comparison between Reviewed Resilience Metric

Authors (Metric)	Functionality Thresholds	Component Criticality	Components Deterioration	System Redundancy	Resilience Time Variation	Multiple-Hazard	Stochastic Failure Scenarios	Restoration Investigation	Enhancement Planning
Todini (2000)	✓					✓			
Prasad and Park (2004)	✓			✓		✓			
Jayaram and Srinivasan (2008)	✓		✓		✓				✓
Yazdani et al. (2011)				✓		✓			✓
Luna et al. (2011)	✓	✓			✓	✓	✓	✓	
Gay Alanis (2013)	✓		✓		✓		✓	✓	
Cimellaro et al. (2015)	✓				✓			✓	
Soldi et al. (2015)				✓			✓		✓
Zhao et al. (2015)				✓	✓		✓	✓	
Herrera et al. (2016)				✓			✓		
Creaco et al. (2016)	✓		✓		✓	✓			✓
Farahmandfar et al. (2016)	✓		✓	✓	✓				✓
Liu et al. (2017)	✓					✓			
Di Nardo et al. (2018)				✓		✓	✓		
Mahmoud et al. (2018)						✓	✓	✓	
He and Yan (2019)		✓			✓		✓	✓	
Choi and Kim (2019)				✓	✓	✓			
Balut et al. (2019)		✓			✓	✓	✓	✓	
Liu et al. (2020)					✓	✓		✓	

- The majority of previous efforts investigated the resilience of WDNs to a particular specific hazard, such as earthquakes. There is a need for a comprehensive approach that shifts the emphasis from analyzing separate threats to studying the impact of such hazards on WDNs and how they respond to different resorting strategies.
- Models that investigated restoration actions of WDNs following disruptive events overlooked several vital issues such as the need to consider various repair methods along with their suitability to various pipes characteristics and failure types. The impact of such actions of the restoration objectives has been rarely investigated. The time and cost crews spend relocating between failed components location along with uncertainties in estimating the time and cost of restoration activities had received little or no attention in previous research efforts. The relocation time plays a more dominant rule in the case of multiple simultaneous failures across the network.
- A proper framework of resilience-based management of WDNs shall integrate social, economic, and environmental aspects of resilience by including the criticality of different segments in the network. There is no criticality assessment model for WDNs, at least to the knowledge of the author, which captures the interdependency between criticality factors and handle the inherited uncertainty in criticality estimating.
- Most resilience enhancement models lack explicit precise deterioration and improvement estimation models.
- Resilience enhancement planning shall consider distinct resilience targets for different zones in the network. Clustering enhancement actions into work packages based on repair methods and geographical location is another concern that needs to be addressed. Such

clustering and work packing formulating facilitate the scheduling and resource allocation process while complying with fair business practices.

Chapter 3: Developed models for Resilience-Based Management of WDN

3.1 Overview

To meet the ultimate objective of this dissertation, the research process encompasses four main phases: i) conducting a comprehensive literature review of current resilience frameworks and their application on WDNs; ii) proposing a new metric to assess and evaluate resilience of WDNs; iii) developing a restoration model to obtain an optimal recovery strategy that minimizes the time and cost of service interruption; and iv) developing an optimization model to determine the optimum resilience enhancement program. Each of these phases will be further explained in the subsequent sections. Tasks included in each phase, underlying concepts, required assumptions, and mathematical formulations, along with the final expected output of each model, are presented in detail. In this work, resilience is defined as the ability of WDNs to withstand various hazards with minimum physical impacts. Besides, restoring activities shall be prioritized in a way that minimizes the time of service disruption while satisfying a set of operational and managerial constraints. Even though WDNs consist of several components such as water mains, fire hydrants, valves, and other accessories, this study focuses on water pipe segments. This is because water pipe segments constitute the biggest majority of components and play the most significant role in functioning of WDNs.

The general flow chart of this research methodology is depicted in Figure 3-1. The process starts by reviewing existing resilience approaches that aim at evaluating and enhancing resilience of water networks followed by developing comprehensive resilience-based management model that consists of i) a metric to assess the resilience of WDNs; ii) a prioritization model to optimize

the restoration process scheduling; and iii) an optimization model to develop an optimum, or near-optimum, resilience enhancement plans. The work developed in this study is based on a comprehensive framework presented by Bruneau et al. (2003) for analyzing the resilience of urban communities and infrastructure systems. Generally, resilience of infrastructure systems can be conceptualized by four main qualities, namely: robustness, redundancy, rapidity, and resourcefulness (Tierney and Bruneau 2007). The first two properties are integrated to develop a new practical metric for assessing resilience of WDNs. Concepts of rapidity and resourcefulness are then integrated in developing an optimization model that investigates recovery strategies and selects an optimal one that minimizes the time and cost of service interruption following a hazardous event. In addition, a sustainability objective is included in developing a resilience enhancement model that maximizes the strength of WDNs to withstand future expected disruptions.

Data needed to develop, apply, and validate the proposed models was acquired from various sources. Literature review, maintenance reports, and experts' opinions are examples of these sources. Moreover, geographic information systems, GIS, shapefiles represent the main component of gathered information in this research. Data about pipeline characteristics, geographical features, previous failures, are extracted from these files. Another set of GIS files contain information about land use, street types, and distribution of water streams.

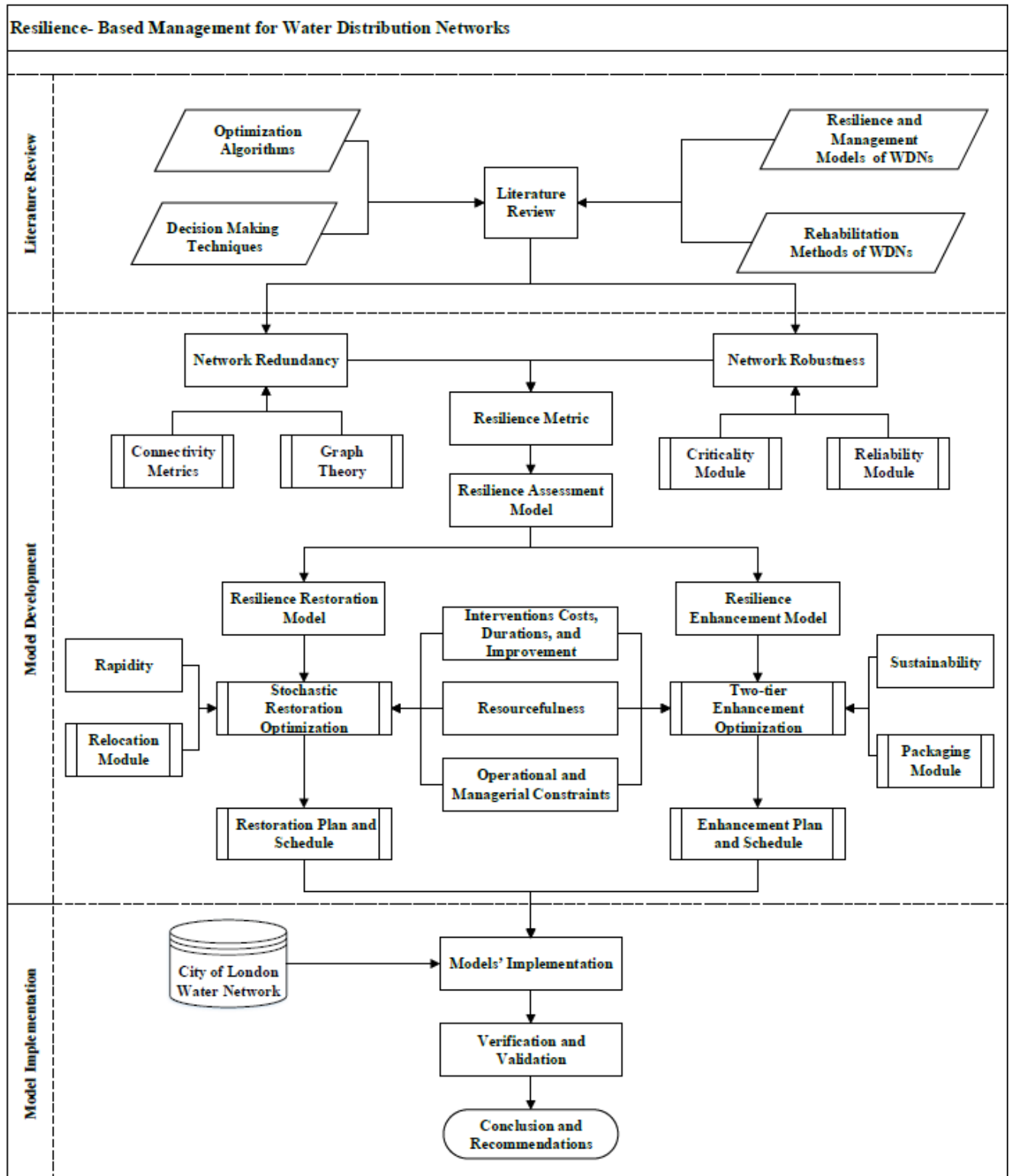


Figure 3-1: Research Methodology

3.2 Resilience Assessment Model

In this section, a metric that can be readily used by utility managers to evaluate resilience of WDNs is introduced. Figure 3-2 illustrates the overall methodology of developing this metric. As shown in Figure 3-2, this metric is based on the robustness and redundancy of WDNs. Robustness is quantified as a function of the reliability and criticality of water mains. Redundancy is computed by utilizing concepts of graph theory. Detailed assumptions and analytical quantifications of each attribute of this metric are presented in the following sub-sections. The metric is then applied on a real WDN that serves a selected area in the City of London, Ontario. After evaluating the current resilience level of the network, the practicality of this model is demonstrated by assuming a specific disruption event and investigating various restoration strategies. Results are then compared with different flow-based and topological-based metrics for verification and validation purposes.

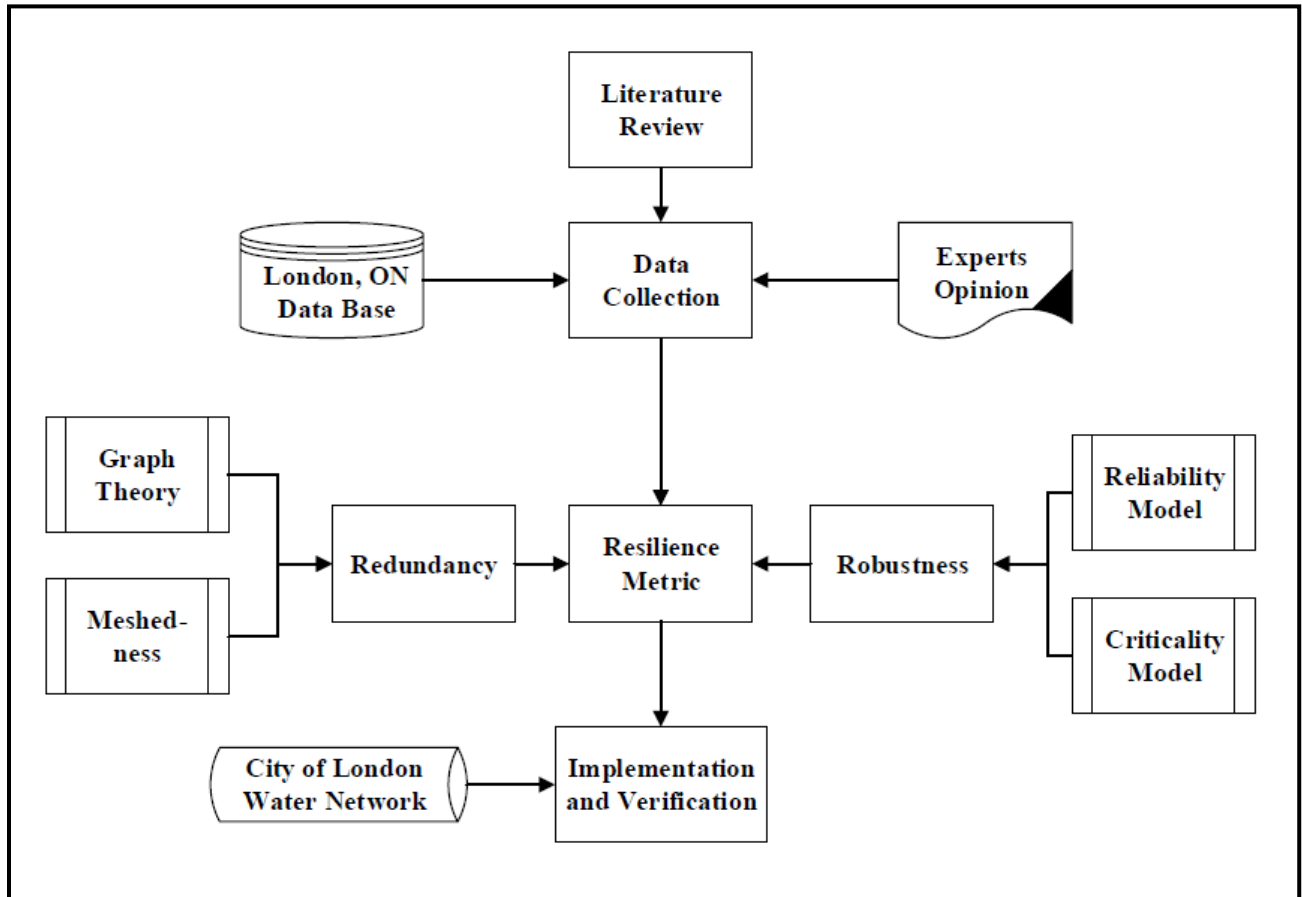


Figure 3-2: Resilience Metric Methodology (Assad et al. 2019)

3.2.1 Robustness

Robustness of a WDN is its ability to withstand destructive forces without significant degradation (Bocchini et al. 2013). Robustness can be viewed as the resistance to unusual external shocks often measured by the residual functionality level, system performance, after a hazard occurrence (Bocchini et al. 2013). In this work, mechanical reliability was chosen as the base for quantifying the robustness of WDNs. Mechanical reliability presents a direct measure of WDNs structural performance. Mechanical reliability can be defined as the “probability that an item can perform its intended function for a specified interval under stated conditions” (Murthy et al. 2008). In this dissertation, mechanical reliability will be referred to as reliability. The structural performance of WDNs is a measure of the condition and strength of its components. A pipe burst

or a pump malfunctioning can compromise the structural performance of a WDN and decrease its reliability (Murthy et al. 2008; Verma et al. 2010). Additionally, a deteriorated pipe segment with long failure history is more fragile, vulnerable, to even light disruptions. Robustness was thus calculated as a function of reliabilities of all connected pipe segments according to the connection type. Criticality of each pipe segment was then added as weights to prioritize critical segments. For a network that consists of several pipe segments, the most important segments in determining its performance are the most critical ones. Critical segments are defined below according to the considered criticality factors. Finally, the weighted formulation was normalized by the sum of the criticalities of all pipe segments. By adding criticalities, the developed metric was extended to account for the socioeconomic dimensions of resilience beside the technical one, which was captured in the reliability estimation. Criticality and reliability calculations are presented in detail below:

3.2.1.1 Criticality

Asset Criticality is a measure of the consequences associated with the failure of an asset to perform its intended function (Cromwell 2002; Vanier and Rahman 2004). Estimating criticality of pipe segments involves identifying some factors, known as criticality factors, that play a dominant role in dictating criticality of water pipe segments. A criticality factor is thus a factor that impacts the consequence of the pipe segment's failure. For example, the size of a pipe segment is an economic criticality factor because it affects the economic consequence associated with this segment's failure. Based on the type of potential consequences, criticality factors can be classified into three main categories: economic, environmental, and social factors. A factor can be assigned to one or more categories if it impacts the type of consequences represented by that category. For example, the size of a pipe segment can be categorized as both economic and environmental factor

because the failure of bigger segments results in more environmental consequences and require more budgets to be repaired. Also, there is a considerable degree of interdependency between the main categories of these factors. Social consequences, for example, may contribute to worsening the economic effects. As illustrated in Chapter 2, despite several previous efforts, estimating water segment's criticality is still subjected to bias and uncertainty. Bias arises from specific previous experience of practitioners participating in estimating the segment's criticality. As a result, a proper criticality estimation of water pipe segments shall account for uncertainties and interdependencies between the criticality factors.

Data needed for developing this model include factors affecting the criticality of water pipe segments, their relative importance, and scores for their measure of performance. Figure 3-3 illustrates a flow diagram that summarizes the criticality estimation steps. A set of criticality factors was first determined, and their ranges of measure were defined. Next, relative weights of importance of these factors were derived. Weighted factors were then aggregated into a single index that represents the criticality of each segment.

Firstly, the available literature was consulted to gather relevant criticality influential factors. As stated previously, three main categories of criticality factors were included in this study, shown in Figure 3-4. Economic factors provide a measure of the monetary losses realized due to a water segment's failure. These losses can be quantified as increased repair costs or loss of revenues. The economic category includes pipeline size, material, installation depth, and accessibility factors. As the size of a water pipe segment increases, the monetary losses associated with its failure increases due to the increased repair costs. Similarly, the repair costs increase with increasing the depth at which a water segment is buried. It was reported that the repair cost

dramatically increases when the failed water segment is buried at a depth exceeding four meters, Salman (2011).

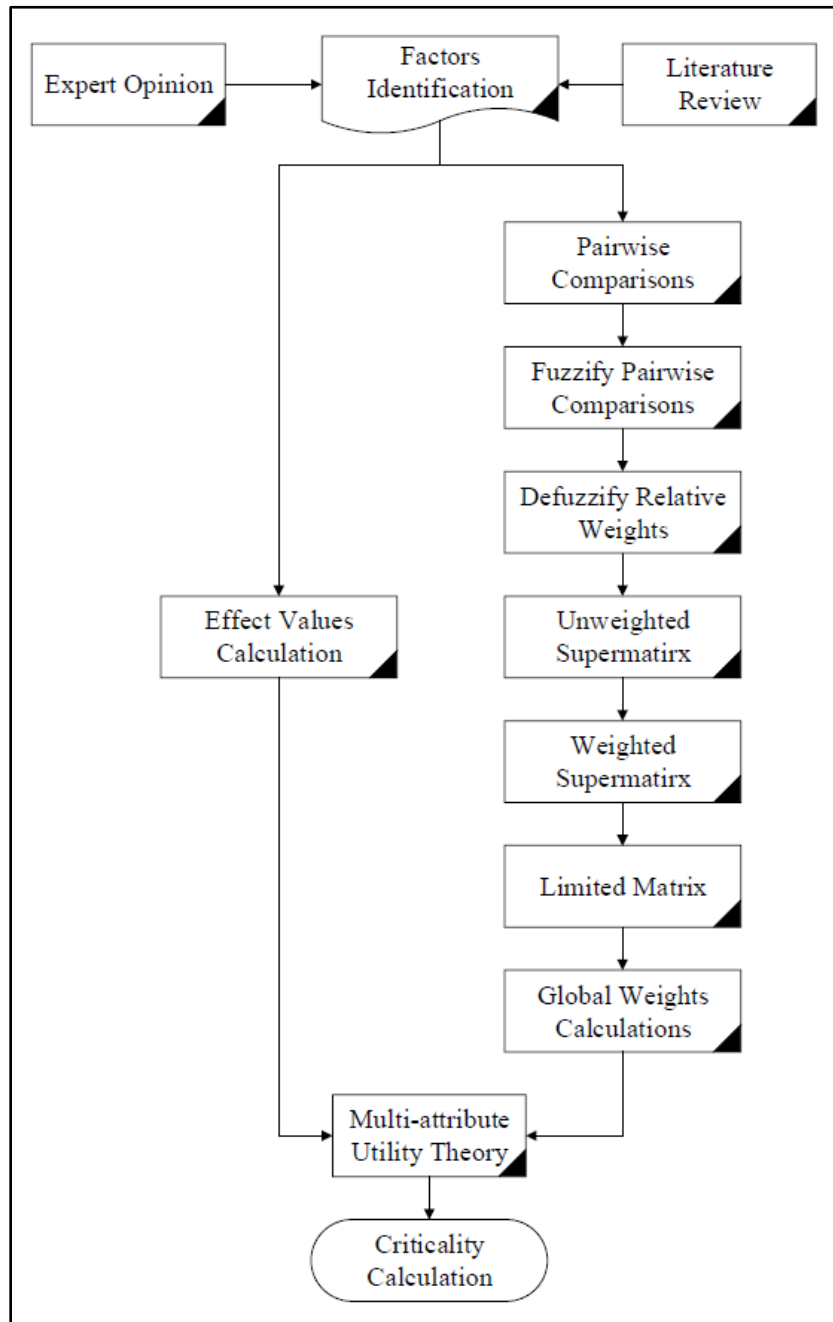


Figure 3-3: Flow Diagram of Criticality Estimation Process (Assad et al. 2019)

Moreover, material type plays a vital role in specifying the repair type and methodology. Hence, it directly affects the cost of failure and repair actions. Concrete pipes usually have more

repair costs than other material types (Salman 2011). Finally, the financial consequences of the water pipe’s failure are more significant when it is difficult to access.

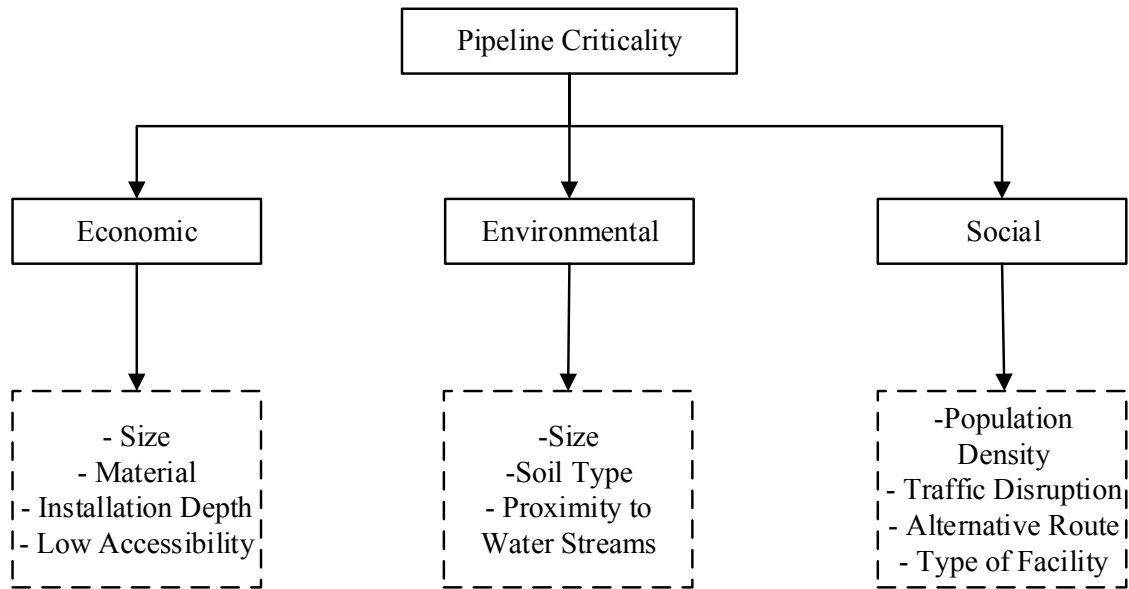


Figure 3-4: Criticality Factors and Sub-factors (Assad et al. 2019)

Environmental factors are those that measure the environmental impacts resulting from a water segment’s failure. These impacts can be in the form of health impacts, contaminations, pollutions, and others. In this category, soil type, proximity to water streams, and pipeline size are the sub-factors considered. It is well-known that water segments closer to water streams such as rivers and lacks are more critical due to the possible contamination that might result from their failure. Additionally, environmental impacts increase gradually with the size increase of the failed segment due to the higher amount of discharged water. Each soil type has its own permeability and density characteristics that control the amount and spread of the consequences resulted from a water main failure. Failures in sandy soil are considered more critical due to the possibility of runoffs and adversely affecting adjacent facilities. Social factors include sub-factors that influence the social disruptions exhibited due to the failure of a water pipe segment. Population density,

traffic disruption, existence of an alternative route, and type of the serviced area are the sub-factors included in this category. Social impacts are increased as the population density increases due to the larger number of affected users as a result of a pipe failure. In addition, the availability of an alternative path to deliver water for end-users reduces the criticality of those pipe segments. A water segment that is under, or close, to a highway is known to be more critical than those buried under small local roads due to a higher volume of disrupted traffic. Similarly, water mains that deliver water to sensitive facilities such as hospitals and power plants are deemed more critical. The consequence of failure of such segments has more adverse impacts on society and may take more extended periods to recover due to the propagated effects resulting from the insufficient water supply to those facilities.

Secondly, structured questionnaires were conducted with experts to collect the rest of the data needed for estimating the criticality of pipe segments. Structured questionnaires were exploited in these interviews to assure the consistency and reliability of the gathered responses. Figure 3-5 depicts a distribution of the respondents according to their years of experience. As observed in Figure 3-5, most of the participated respondents are of 5-15 years of experience, with a percentage of 55%. These experts were reached out via phone calls, e-mails, LinkedIn messages, and other research portals. After filling some personal-related questions, they were asked to 1) answer the pairwise comparison questions regarding the criticality factors, and 2) estimate, propose, effect values for each possible range of criticality factors.

In the criticality factors weights section, experts were asked "How much a certain criticality factor is more important than another one?" (Wei et al. 2010). To ensure the consistency of the collected judgments by the experts, consistency ratio was calculated for each pairwise comparison matrix, as shown in Equations 3.1 and 3.2 (Lee 2010):

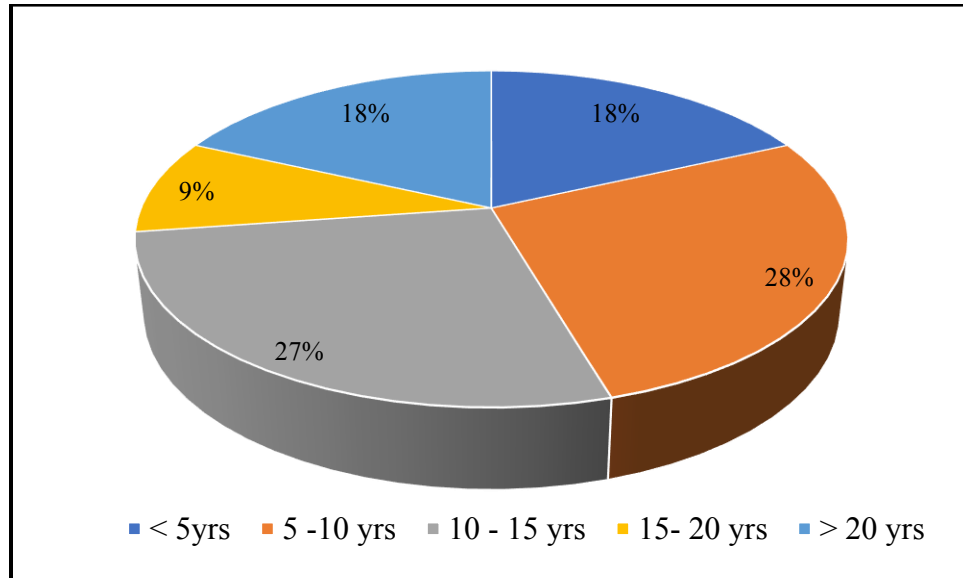


Figure 3-5: Distribution of Respondents' Experience

$$CR = \frac{CI}{RI} \quad (3.1)$$

$$CI = \frac{\lambda_{max} - n}{n-1} \quad (3.2)$$

Where λ_{max} is the biggest eigenvalue of the considered pairwise comparison matrix; n is the number of factors in the considered pairwise comparison matrix; CR is the consistency ratio; CI is the consistency index; and RI is the random index. The value of the RI is determined based on the size of the pairwise comparison matrix. For example, the RI values for (3×3) and (4×4) matrices are 0.58 and 0.90, respectively (Saaty 2007; Lee 2010). The pairwise comparison matrix is considered to achieve satisfactory consistency as the value of CR is less than 0.1.

Figure 3-7 depicts a section of the questionnaire questions in which experts were asked to evaluate the relative importance of economic criticality sub-factors. Similar to Figure 3 6, experts were asked to evaluate the relative importance of social and environmental criticality sub-factors.

Example:

In the table below, consider comparing “Pipeline Size” (Criterion X) with “Pipeline Material” (Criterion Y) with respect to “Physical Factors.”

		PHYSICAL FACTORS										
Criterion (X)	Degree of Importance										Criterion (Y)	
	(9) Absolute	(7) Very Strong	(5) Strong	(3) Moderate	(1) Equal	(3) Moderate	(5) Strong	(7) Very Strong	(9) Absolute			
Pipeline Size												Pipeline Material
												Installation Depth
												Low Accessibility

If you consider that “Pipeline Size” is more important than “Pipeline Material” and the degree of this importance is “Strong” then tick (✓) here

If you consider both “Pipeline Size” and “Pipeline Material” have “Equal” importance; then tick (✓) here.

If you consider the “Pipeline Material” is more important than “Pipeline Size” and the degree of importance is “Absolute” then tick (✓) here

Figure 3-6: Sample of Criticality Sub-factors’ Relative Importance Questions

In addition, experts were asked to evaluate the relative importance of the main factors concerning their effect on each other and on the overall pipeline criticality, as shown in Figure 3-8. In this research, the average values of the collected responses were utilized as the adopted weights.

Criterion (X)	Degree of Importance										Criterion (Y)
	(9) Absolute	(7) Very Strong	(5) Strong	(3) Moderate	(1) Equal	(3) Moderate	(5) Strong	(7) Very Strong	(9) Absolute		
WATER PIPELINES Criticality											
Economic Factors											Environmental Factors
											Social Factors
Environmental Factors											Social Factors
ECONOMIC FACTORS											
Environmental Factors											Social Factors
ENVIRONMENTAL FACTORS											
Economic Factors											Social Factors
SOCIAL FACTORS											
Economic Factors											Environmental Factors

Figure 3-7: Sample of Criticality Main Factors’ Relative Importance Questions

After identifying criticality factors, experts' opinions were sought to derive the relative weight of importance of each sub-factor and to determine their effect values on criticality on a scale from 0-10. This scale is used to provide an adequate range of options for the possible performance measure of each factor, with higher values representing more critical situations. Figure 3-8 illustrates an example of this section. In this example, the experts are asked to set a unique effect value, score, for each possible material type. Similarly, experts were asked to determine a score for each possible value of the economic, social, and environmental criticality factors. Criticality estimation process constitutes integrating a diverse set of factors, not all of which are measured on comparable scales. For example, some criticality factors are measured on a binary scale, while others are measured on a continuous range or a discrete categorical interval. It is thus necessary to define a unified scale, effect value, to facilitate a meaningful combination of the different factors in a multi-attribute utility model.

Example:
 In the table below, consider evaluating the “Pipeline Size” factor.

Main Factor	Sub-factors	Unit Of Measure	Qualitative Description (Parameters)	Effect Value Range On Pipeline Condition (0 – 10)
PHYSICAL	Pipeline Material	-	Type 1	{ 2 5 10
			Type 2	
			Type 3	

The “Effect Value Range” can be one value from “0 to 3”, “4 to 7”, and “8 to 10” for the “small”, “Medium”, and “large” parameters respectively.

Figure 3-8: Sample of Criticality Factors’ Effect Values Questions

Table 3-1 shows the adopted ranges of performance and effect values for each criticality factor. These ranges were sought both from expert opinion and consulting the literature (Salman 2011; Shahata 2013; Moursi 2016). Taking an economic sub-factor in Table 3-1 as an example,

accessibility is measured on a binary scale as either high or low. Thus, only two effect values are considered 1 and 10 representing the least and most critical conditions, respectively, without considering the intermediate conditions. Effect values that represent these intermediate conditions were marked as NA. The same approach was followed for the installation depth criticality factor. Similar values were collected for environmental and social factors as shown in Table 3-1.

Table 3-1: Effect Values of Criticality Factors

Economic Factors				
Effect Value	Pipe Size	Pipe Material	Installation Depth	Accessibility
1	Less or equal 150 mm	PVC, Poly Ethylene	Less than 4.0 m	High
3	150 to 350 mm	NA	NA	NA
5	350 to 700 mm	Steel, Iron	NA	NA
7	NA	Copper	NA	NA
10	Greater or equal 700 mm	Concrete	Greater or equal 4.0 m	Low
Environmental Factors				
Effect Value	Pipe Size	Soil Type	Proximity to rivers and streams	
1	Less or equal 150 mm	Clay	No	
3	150 to 350 mm	NA	NA	
5	350 to 700 mm	Silt	NA	
7	NA	NA	NA	
10	Greater or equal 700 mm	Sand	Yes	
Social Factors				
Effect Value	Population Density	Traffic Disruption	Alternative Route	Type of Facility
1	NA	Low	Yes	Parking/open space
3	Low	NA	NA	Residential
5	Medium	Medium	NA	NA
7	NA	NA	NA	Commercial
10	High	High	No	Industrial and Institutional

The fuzzy analytical network process (FANP) was then employed to determine the global weights of the criticality factors. The process starts by identifying the system objective and sub-

criteria, which has been done in the previous steps. The aim is to calculate the criticality index of water pipe segments, and the criteria are the main factors and sub-factors considered. Subsequently, a comparison between criteria was performed as stated above.

The fuzzy component was implemented by applying a fuzzification scale, shown in Table 3-2 on the gathered responses. Cheng's fuzzy scale was exploited in this study for pairwise comparisons and fuzzified weights computations (Cheng et al. 1999; Kiriş 2013). According to this scale, if a particular expert evaluated factor A to be weekly more important than factor B, then the mean value of the fuzzy membership function associated with this evaluation response would be 3/2. Furthermore, the corresponding lower and upper values associated with this response would be 1 and 2, respectively. This application yields formulation of three matrices, namely: lower, most probably, and upper matrices, which represent the three vertices of a triangle fuzzy number ship function. Triangular fuzzy membership function was utilized in this application since it is the most commonly utilized in literature. Besides, this function fits for the objective of this application, where three points are sufficient to describe the inherited uncertainty. This step was repeated to compare all sub-factors in each category and between the three main considered categories. The output of this step is a set of lower, upper, and most probable matrices for each evaluated comparison.

Table 3-2: Cheng’s Fuzzy Linguistic Scale for Importance and the Corresponding Triangular Fuzzy Numbers (Wei et al. 2010)

Linguistic Scale for Importance	Triangular Fuzzy Scale	Triangular Reciprocal Scale
Equally important (EI)	(1/2,1,3/2)	(2/3,1,2)
Weakly more important (WMI)	(1,3/2,2)	(1/2,2/3,1)
Strongly more important (SMI)	(3/2,2,5/2)	(2/5,1/2,2/3)
Very strongly more important (VSMI)	(2,5/2,3)	(1/3,2/5,1/2)
Absolutely more important (AMI)	(5/2,3,7/2)	(2/7,1/3,2/5)

The fuzzifying scale was applied to account for the vagueness and uncertainty in the collected responses. These matrices are then used as inputs for a specific written Matlab code to obtain the factors' relative weights. The obtained relative weights were used to construct the unweighted supermatrix. The weighted supermatrix was next attained by normalizing each cell in the unweighted supermatrix by dividing over the summation of cells in the column in which it lies. This step is similar to the concept of Markov chains for ensuring the sum of these probabilities of all states is equal to one. The weighted supermatrix was then iteratively multiplied by itself to get the limited matrix, as shown in equation 3.3. This step is essential because the weighted supermatrix will not be in a steady state until the row values converge to the same value for each column of the matrix. The first column in the limited matrix is the global priority vector or weights (Wei et al. 2010). Summing up the weights obtained from the limited matrix yields an exact unity.

$$\bar{W}^{\infty} = \lim_{k \rightarrow \infty} \bar{W}^k \quad (3.3)$$

Multi-attribute utility theory (MAUT) was finally employed to obtain the criticality index of each pipe segment using equation 3.4. A Matlab code that is integrated within an Excel environment was written to automate the criticality computations.

$$C_i = \sum_{j=1}^r W_j \times AV_j \quad (3.4)$$

Where C_i is the criticality index for pipe segment i , W_j is the global weight of criticality sub-factor j , AV_j is the effect value of sub-factor j , and r is the number of criticality sub-factors. This criticality index reflects the significance of failure associated with water segments on a scale from 0-1, where 0 represents the least critical, and 1 represents the most critical pipe segments.

3.2.1.2 Reliability

Reliability is defined as the probability that an infrastructure system, or any of its components, will perform its intended function without failure for a specified period (Verma et al.

2010). A failure in water pipe segments could be either a hydraulic failure, a structural /mechanical failure, or a failure related to water quality issues (Gheisi and Naser 2014; Mohammed 2016). This work focused exclusively on the structural failure of water segments in the form of pipe breaks and leaks. Reliability of an asset can be calculated using equations 3.5 (Murthy et al. 2008):

$$R(T) = P(t > T) = 1 - \int_T^{\infty} f(x)dx \quad (3.5)$$

Where t is the time to failure, T is the failure-free period, and $f(x)$ is the failure probability density function. The overall methodology of reliability and deterioration estimation is illustrated in Figure 3-9.

Data needed for calibration of this model include characteristics, locations, and failure history of water segments. These data were gathered from the City of London, Ontario. The concept of censored data was utilized in this research. The most generic form of censoring is right-censored data. In this case, the failure event starting the inter-failure time series has occurred, but at the time of the last observation, the failure ending this series has not occurred yet. The only thing known for sure is that the failure will happen sometime in the future. The main advantage of employing data censoring is the ability to include the effect of no-failures in addition to the effect of failures. Once the required data were collected, preprocessing steps proceeded as follows:

1. Data cleansing was firstly done to eliminate miscoded and irrational data like those whose installation date, or failure date was sometime in the future.
2. Pipes that had significant time to the first failure were excluded from modeling. This step was essential to avoid the bias resulting from intervention and major rehabilitation works that were carried out but not reported in the database.
3. Pipe material types that do not match construction era were excluded (e.g., PVC pipe with a construction date of 1940).

4. Pipe construction eras do not match urban development patterns were excluded (e.g., new pipe in an old location that did not undergo any pipe replacement projects).
5. Pipe material types do not match diameters were excluded (e.g., 6 in. prestressed concrete pipe).
6. The number of breaks in each pipe segment was counted and linked to that specific pipe. The gathered data included several GIS layers that were not spatially linked to each other. A joining technique was needed to link the breaks to each corresponding pipeline. Hence, a Matlab code was written to count the number the breaks and match them to the appropriate pipe segment utilizing features of Arc-GIS as shown in Figure 3-10.
7. The inter-failure time, the time between successive failures was calculated to get times to the n^{th} failure. These times would be used later to calibrate the model and find the best fit, as will be shown in this section.

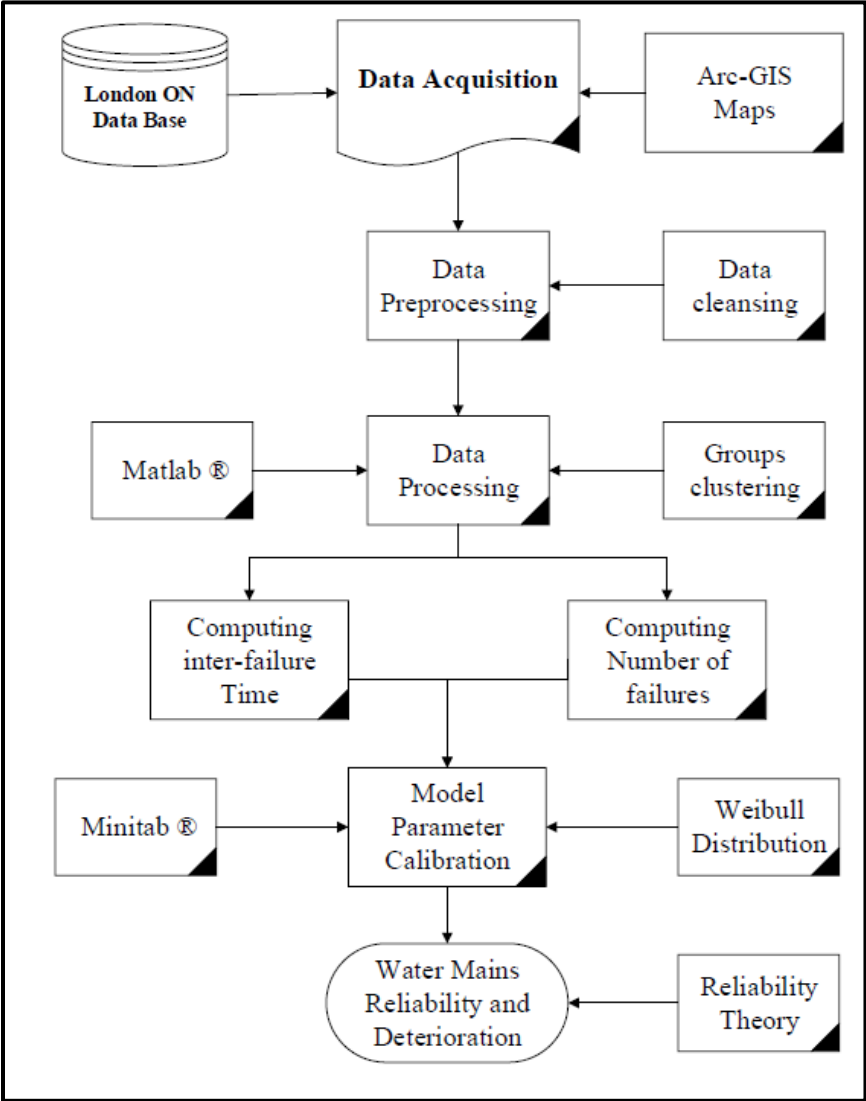


Figure 3-9: Flow Diagram of Reliability and Deterioration Estimation (Assad et al. 2019)

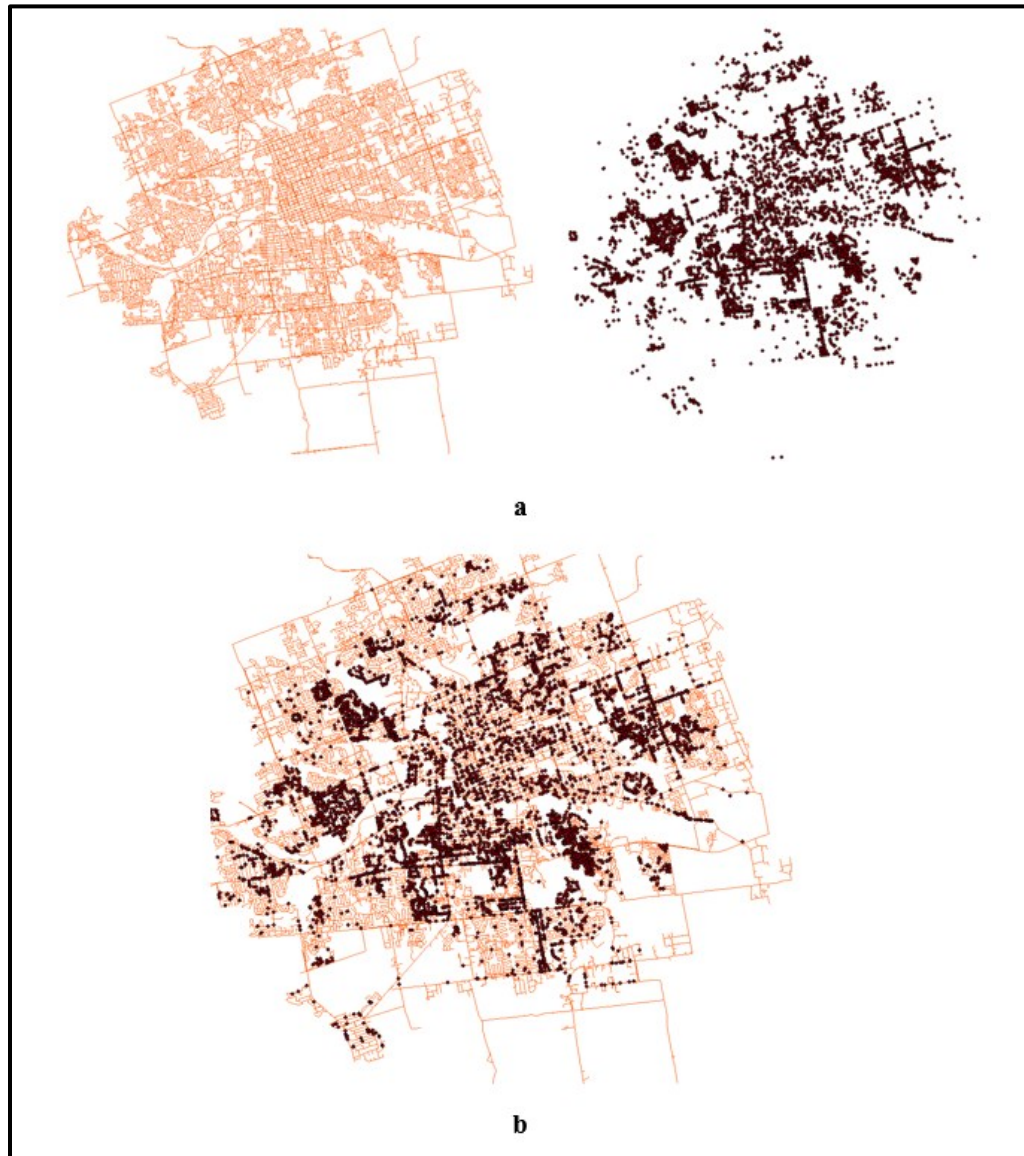


Figure 3-10: GIS Shapefiles for Water Pipe segments and Previous Breaks (London, Ontario)

Analyzing the obtained failure dataset reveals more than 3,900 breaks distributed across the London WDN. The earliest break incident dated back to April 1966 while the most recent incident was recorded in October 2017. It shall be noted that the City of London provided this dataset in November 2017. The available wealth of breakage history is flawlessly sufficient to calibrate a performance model that forecasts future breakage trends and suggests appropriate strategies for enhancement and restoration based on resilience objectives.

Table 3-3 illustrates an example of the collected failure history dataset. For each pipe segment, the previous number of failures and their data of occurrence were provided. Besides, the type of failure, nature of the break, was also provided. Dates of previous failures were utilized in calculating the inter-failure times as previously mentioned.

Table 3-3: Sample of Water Pipe Segment’s Failure History

Pipe ID	NOPB*	Break No.	Date	Nature of Break
2491	1	1	9/10/1976	Circumferential
16558	2	1	2/14/2002	Circumferential
		2	1/14/2009	Circumferential
15341	3	1	3/9/1992	Blowout
		2	2/2/2007	Longitudinal
		3	3/3/2014	Circumferential

* NOPB = Number of previous breaks.

Water pipes were then clustered into homogeneous cohorts based on their size and material type. This step was performed to cluster the segments that are likely to share similar deterioration behavior in the same cluster. Five main groups resulted from this clustering namely: segments that are made of cast iron, CI and of a diameter less than or equal to 150mm; segments that are made of CI and of diameter more than 150mm; segments that are made of ductile iron, DI and of diameter less than or equal to 150mm; segments that are made of DI and of diameter more than 150mm, and others. The “others” group contains pipelines of any sizes that are made of polyvinyl chloride.

Weibull distribution function (WDF), along with some other distributions, were then employed to model the reliability and deterioration of water mains. Weibull distribution was chosen because it is a stochastic statistical failure prediction model based on historical failure data. Unlike Markov-based models in which deterioration is predicted solely based on the immediate previous condition state, WDF can leverage the entire failure history of pipe segments in deterioration and reliability

predicting. Most of the previously developed deterioration models assumed a constant failure rate of water pipes. In this work, Weibull distribution functions were used to fit the time-to-failure data allowing for distinct failure rates for different phases of the water segment's life. The main advantage of this approach is the ability to model the failure behavior of water segments more realistically since failure rates are not constant along the service life of water segments. Weibull distribution was also chosen as it can be related to several other probability distributions such as exponential, and others. This offers more flexibility in estimating the accurate deterioration behavior of pipe segments.

Reliability is estimated for pipe segments in a dynamic fashion. Survival analysis was performed to obtain the distribution parameters for each transition state utilizing the maximum likelihood method. A state is defined here as the order of a break, and the time between states is the time elapsed between the n^{th} break and the $(n+1)^{\text{th}}$ break. For instance, the first transition time is the time to the first failure calculated from the installation date. The second transition time is the time to the second failure measured from the date of the first failure, and so on. The deterioration was evinced by a decreasing mean time to failure as the break order increases reflecting a more deteriorated segment. Different distributions were considered to fit the inter-failure time data, including both 2-parameter or 3-parameter Weibull distributions, exponential distribution, and normal distribution, among others. The data fitting was done using Matlab. The quality of each distribution fit was tested via the Anderson-Darling statistical test. Anderson-Darling statistic measures how well the data follow a specific distribution and is used to compare the fits of several distributions to determine the best one. The hypotheses for the Anderson-Darling test are

H_0 : The data follow a specified distribution, or

H_1 : The data do not follow a specified distribution

Three main measures are commonly used in this type of curve fitting, as shown below:

- Anderson-Darling statistic (AD): A Lower AD value indicates a better fit. Nevertheless, to compare the suitability of different distributions to fit the data, p-value should be assessed.
- P-value: A higher p-value indicates a better fit. A low p-value (e.g., < 0.05) indicates that the data do not follow that distribution, and other distribution shall be tested. It should be noted that the p-value cannot be calculated for 3-parameters distributions.
- LRT P, P-value for the likelihood-ratio test: A lower value indicates significant improvement realized by adding the third parameter over the 2-Parameter version.

Once the appropriate distribution parameters are computed for a cohort of water pipe segments, the reliability function of this cohort can be calculated as given by Equation 2.20. Finally, deterioration curves were established for each cohort of segments by incrementally increasing the age in Equation 2.20. It is worth mentioning that the computed reliability is a time-based one and depends on the break order. As such, if a water pipeline experiences its n^{th} break, its reliability along the subsequent years will be calculated using the reliability function of the $(n+1)^{\text{th}}$ break.

In addition, when a pipe segment is subjected to a specific intervention action, its reliability is updated according to the type of this intervention. To achieve that, previous intervention actions applied to various segments in London WDN along with their dates of occurrence were gathered. Table 3-4 shows an example of information obtained from the maintenance reports. This set included information about previous intervention rehabilitation and actions that were applied to different water pipe segments in the London WDN. For each pipe segment, the number, date, and intervention action type were provided. This information is vital in determining the realized improvement and expected deterioration behavior after specific intervention actions are taken. These two pieces of information will be utilized as inputs in the resilience enhancement model and

resilience-based restoration model to calculate the resilience improvement objectives, as will be illustrated in the subsequent sections.

Table 3-4: Sample of Water Pipe Segment’s Intervention Actions History

Pipe ID	Date	Intervention Type
2206	5/15/2006	Cement mortar
10787	6/15/2000	Cement mortar
16564	7/25/2016	Aqua pipe CIPP
8936	11/23/2010	Nordi tube CIPP

3.2.2 Redundancy

Redundancy is the extent to which a system is capable of satisfying functional requirements if significant degradation occurs (Tierney and Bruneau 2007). Several authors have employed metrics from graph theory to quantify the redundancy and connectivity of WDNs (Yazdani and Jeffrey 2011; Yazdani and Jeffrey 2012; Torres et al. 2017). In graph theory, a network is presented as a mathematical graph $G = (V, E)$ where V = the set of graph nodes with n elements; and E = the set of graph edges with m elements. Each edge of G = represented by a pair of nodes (i, j) where $i \neq j$. The size of G = the number n of vertices in V , and the order of G = the number of m edges in E (Yazdani and Jeffrey 2011; Yazdani and Jeffrey 2012). An adjacency matrix $A = [a_{ij}]$ is a non-negative $n \times n$ matrix that describes the graph G . In A , $a_{ij} = 1$ if (i, j) is an edge in G and 0 otherwise.

Three different parameters, reported in the literature, were studied to analyze their applicability and limitations in quantifying redundancy of WDNs. These metrics are link density, clustering coefficient, and meshed-ness. Link density is an important measure related to the overall structure of the network. It can be calculated as the ratio between the total and the maximum possible number of links in a network (Yazdani and Jeffrey 2011; Yazdani and Jeffrey 2012). Link density is used to indicate the sparseness or dense connectivity of network layout, yet it only

captures very general information regarding the structure of WDNs. Extending the analysis to include other structural properties such as the number of cycles and loops in a network is needed. The clustering coefficient measures the ratio between total triangles and the total connected, closed, triples in a network. Because the majority of looped structures in WDNs are non-triangular, quadrilateral, it is difficult to utilize this metric to measure redundancy in such networks (Yazdani and Jeffrey 2011). Meshed-ness is a more relevant metric in this respect that can be used to estimate the intensity of any loops in planar graphs such as WDNs. It may be regarded as a surrogate measure of path redundancy in a network. Meshed-ness is calculated as the ratio of the total number to the maximum number of independent loops in a planar graph Euler's formula, as shown in Equation 3.6 (Yazdani and Jeffrey 2011):

$$R_m = \frac{m-n-1}{2n-5} \quad (3.6)$$

Where R_m = meshed-ness coefficient, n is the total number of nodes, and m is the total number of links in a graph G . R_m can vary from zero in tree structures to one in maximal, complete, planar graphs. The value of this coefficient is increased by installing new pipe segments at selected locations across the network. Duplicating critical segments or those supplying water to sensitive facilities may be the ideal option to increase the network redundancy, especially in conditions of limited resources and funds scarcity.

3.2.3 Resilience Metric

The proposed resilience metric was finally formulated as a weighted sum of the robustness and redundancy coefficients that were discussed above, as shown in Equation 3.7:

$$\mathcal{R} = w_1 \times \frac{\sum_{i=1}^P R_i \times C_i}{\sum_{i=1}^P C_i} + w_2 \times \frac{m-n-1}{2n-5} \quad (3.7)$$

where \mathcal{R} is the resilience metric, R_i is the reliability of water pipe segment i , C_i is the criticality index of water pipe segment i , P is the total number of pipe segments, n is the network size, m is

the network order when presented as graph G , w_1 and w_2 are relative weights of importance. The lower bound of the resilience metric is 0, which is realized when R_i is 0 for all pipe segments in a fully damaged network, and no water is being delivered to customers. The theoretical upper bound is 1 and might be realized when R_i is 1 for all pipe segments, and the network is a complete planner graph. In reality, these two cases are not likely to exist, and the expected value of the resilience metric is always less than 1.

As it can be observed from Equation 3.7, this metric is not based on a specific hazard. Instead, it can be used to assess the resilience of WDNs based on the failure mode, the impacts of different hazards on the water network. As mentioned earlier, this effort is focusing only on structural impacts such as pipe breaks and leaks. These structural failures can result from different hazardous events such as earthquakes, target attacks, and accidents. The proposed metric can be used to assess the resilience of WDNs against all these types of hazards in a single analysis that investigates the number of pipes broken and the corresponding loss on resilience.

By including the criticality of pipe segments in the proposed formulation, different social, economic, and environmental consequences of pipe segments failure are considered. These all are essential dimensions of resilience that still need to be addressed (Assad et al. 2019). The reliability estimation model in this formulation can stochastically estimate the deterioration of each pipe segment utilizing its previous failure history and other characteristics such as material type, diameter, and failure order. In this model, each time a pipe segment fails or breaks, its reliability and expected deterioration over the subsequent years are estimated using a new deterioration curve, as previously explained. This approach provides a more accurate estimation of water pipe deterioration, which is reflected by the increased failure rate over time and decreased mean time to failure. A precise estimate of pipes' deteriorations is an essential cornerstone in making

decisions regarding resilience enhancement actions during the operation and management phase. Such decisions can be obtained by optimizing a resilience metric that explicitly accounts for these factors.

In short, this metric represents a measure of the structural performance of WDNs in resilience applications. This metric can be used to compare the preparedness level and the ability of different networks to withstand disruptions and continue functioning under stressing hazardous events. It can also be utilized to investigate the gradual increase in resilience during the recovery process, as will be shown in subsequent sections. The proposed metric was applied to assess the resilience of an actual WDN in the City of London, Ontario, referred here as LWDN. Robustness and redundancy of the network were first estimated before being integrated into the multi-attribute metric to quantify the network resilience. Also, the reduction in resilience due to aging and deterioration was calculated. This application concluded with a two-tier evaluation of the proposed metric in different resilience applications, as described below.

To evaluate the usefulness of utilizing the proposed metric in resilience enhancement applications, an optimization model was formulated to determine the optimal strategy for enhancing the resilience of LWDN. The objective of the optimization was to maximize the resilience of LWDN subject to a budget constraint. The resilience of LWDN could be enhanced by increasing its robustness and redundancy. Two main enhancement actions were considered in this framework: replacement of deteriorated pipe segments and installing new ones. Replacement of deteriorated segments improves the network robustness while installing new segments adds redundancy to the network and improves its robustness. The objective of this optimization framework is to maximize the resilience metric, which is given in Equation 3.7. The budget constraint of the possible enhancement actions is given in Equation 3.8:

$$C_T = \sum_{i=1}^{N_r} C_i + \sum_{j=1}^{N_j} C_j \leq B_E \quad (3.8)$$

Where C_T = total resilience enhancement cost; N_r = number of pipe segments that need to be replaced; C_i = cost of replacing pipe segment i and it is a function of its length and diameter; N_j = number of newly installed pipe segments; C_j = cost of adding pipe segment j to the network and it is a function of its length and diameter; B_E = available budget for resilience enhancement actions.

As a means of validation, the estimated resilience level of LWDN was compared to a resilience level obtained by another resilience metric developed by Farahmandfar et al. (2016). This metric is similar to the proposed one in integrating robustness and redundancy in resilience estimation. The metric is formulated as the sum of reliabilities of the connected pipelines each multiplied by its nodal demand in a modified form of the original nodal degree formulation as given by Equation 3.9 (Farahmandfar et al. 2016):

$$R = \frac{\sum_{i=1}^{N_n} \{ [\sum_{j=1}^{N_i} (1 - P_{fj})] \times Q_i \}}{4 \times \sum_{i=1}^{N_n} Q_i} \quad (3.9)$$

Where N_n = total number of nodes, N_i = total number of links connected to node i , P_{fj} = failure probability of link j , and Q_i = demand of node i .

A hydraulic model was then simulated to assess the suitability of utilizing the developed metric during the WDNs restoration phase. The performance of the proposed metric was evaluated and compared to serviceability index SI , a frequently used surrogate measure of hydraulic reliability in resilience applications of WDNs (Yoo et al. 2014). The hydraulic simulation model was built and run on the WaterGEMS software package. A topological map of LWDN was exported from the Arc-GIS shapefiles and fed into WaterGEMS software. Nodes' coordinates, pipes' lengths, diameters, and roughness coefficients were directly extracted from the available layers in the shapefiles. A Google application programming interface (API) was used to access

Google Earth® from which the user could determine the elevation of any location in the network. Nodes' elevations and estimated nodal demands were then assigned. The model was run, and data regarding the service pressure at each junction were collected. A disrupted scenario was then analyzed by modeling breaks in some selected pipe segments. In this analysis, a pipe break was modeled by changing its status to “closed” and evenly distributing a discharge flow to the end nodes as additional demands (Farahmandfar and Piratla 2017b). **Error! Reference source not found.** illustrates a sample of the approach followed in simulating breaks of water pipe segments and discharge distribution. Discharge flows were calculated using Equations (3.10) (Farahmandfar and Piratla 2017b; Tabesh et al. 2009):

$$Q_j = 84.04 \times C_d \times A_j \times P_j^{0.5} \quad (3.10)$$

Where Q_j = discharge from the orifice pipe j ; C_d = discharge coefficient (taken as 0.8 in this study); A_j = the total cross-sectional area of pipe j ; P_j = average pressure of ends nodes of pipe j .

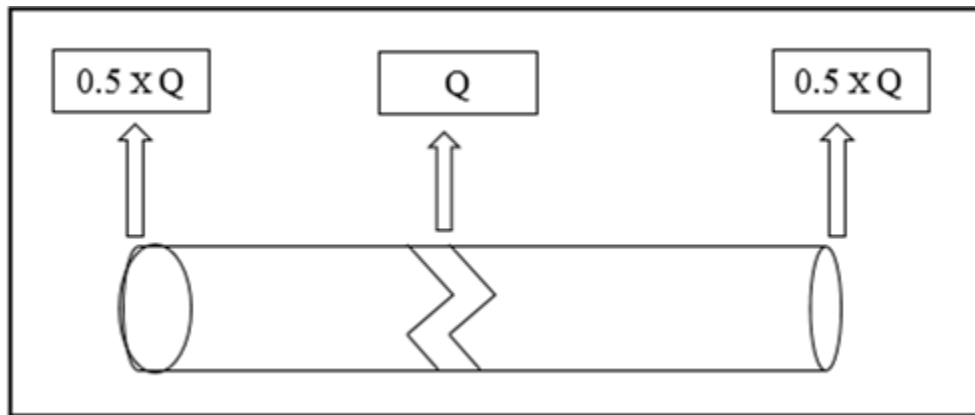


Figure 3-11: Simulation Approach for the Impact of Pipe Damages

There are two main types of hydraulic analysis methods of water systems: demand-driven analysis (DDA) and pressure-driven analysis (PDA) (Yoo et al. 2014). DDA is more suitable for analysis under normal conditions as they assume that demands at junctions are always satisfied, which might result in unrealistic negative pressure values (Yoo et al. 2014). PDA, on the other hand, is preferred when analyzing abnormal conditions as they assume that the demand is a

function of the pressure, and thus, unrealistic values can be avoided. However, PDA application requires assuming a head-outflow relationship (HOR) for each network as there is no such universally accepted relationship (Yoo et al. 2014). In this simulation, quasi-PDA was employed to deal with negative pressure that might occur during the disrupted state of the network based on the same methodology followed by Yoo et al. (2014). In this approach, whenever a negative pressure was encountered at a node, the demand at that node was set to zero and the simulation was repeated. If negative pressure reoccurred, the calculated pressure was assumed zero.

Serviceability index of the system SI was used to estimate the reliability of the network based on Equations (3.11) and (3.12) (Yoo et al. 2014):

$$SI = \frac{\sum_{i=1}^n Q_{avl,i}}{\sum_{i=1}^n Q_{req,i}} \quad (3.11)$$

$$Q_{avl,i} = \begin{cases} 0, & \text{when } P_i \leq 0 \\ Q_{new,i} \times \sqrt{\frac{P_i}{P_{min}}}, & \text{when } 0 \leq P_i \leq P_{min} \\ Q_{new,i}, & \text{when } P_i \geq P_{min} \end{cases} \quad (3.12)$$

Where $Q_{avl,i}$ = available demand at node i ; $Q_{req,i}$ = required demand at node i ; $Q_{new,i}$ = updated nodal demand after considering the disrupted state and dealing with the negative pressure at node i ; P_i = nodal pressure at node i ; P_{min} = allowable minimum nodal pressure head (taken as 15 m); n = number of nodes. Due to the new disrupted state, the minimum pressure would be available at some of the nodes only. For those nodes, the available demand would be the same as the new demand value. Results are compared to those obtained by the developed metric, and conclusions were drawn accordingly.

3.3 Resilience-based Restoration Model

In the previous section, robustness and redundancy of water networks were integrated to develop a multi-attribute metric for evaluating resilience of WDNs. In this section, two more

qualities of resilience, rapidity and resourcefulness, are included along with the developed resilience metric to formulate a resilience-based restoration model. The optimization-based restoration model aims at prioritizing and scheduling restoration actions of WDNs. The model takes into consideration efficient resource allocation by minimizing both the time and cost of recovery and maximizing resilience. To achieve these objectives, the model takes three sets of inputs, as shown in Figure 3-12. These inputs represent the results of three sub-models: resilience assessment sub-model, restoration sub-model, and crew relocation sub-model.

The resilience assessment sub-model was explained in detail in the previous section. Restoration and crew relocation sub-models determine feasible recovery methods for each pipe segment and the time and cost of the crew's relocation, respectively. The output of this model is an optimal restoration plan that comprises two main components: 1) a prioritized sequence of water segments to be repaired, and 2) an optimal repair method for each. Additionally, a time schedule is generated to visualize the restoration activities and the overall restoration process. Details of the developed methodology are described in the subsequent subsections.

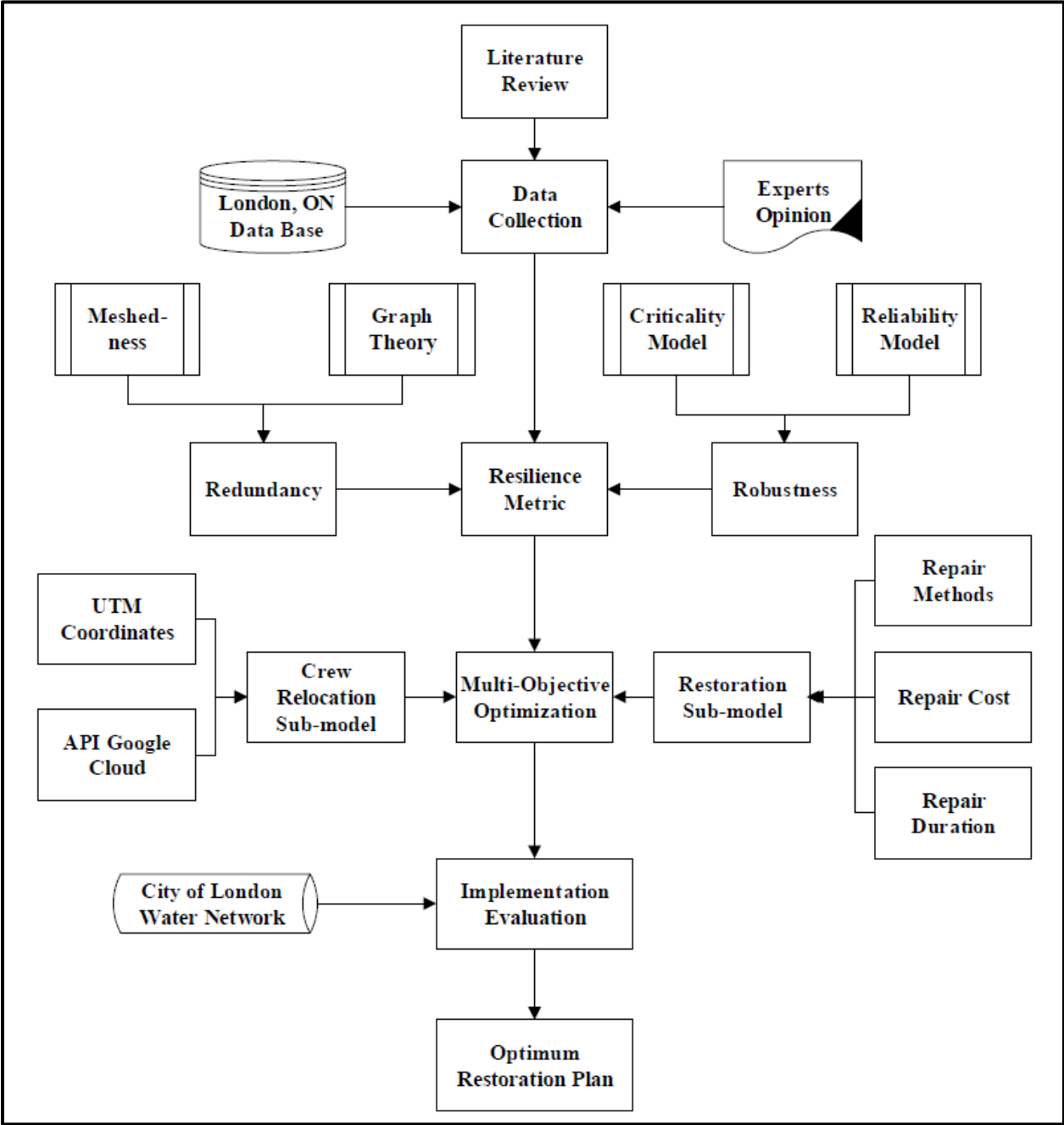


Figure 3-12: Restoration Model Methodology framework (Assad et al. 2020)

3.3.1 Crew Relocation Sub-model

Restoration crews spend time while traveling from one location to another to restore failed segments across the network. As these times and associated costs can significantly increase the time and cost of the recovery process, especially in sparse networks, they need to be considered in

developing optimum restoration plans. This sub-model was developed to accurately estimate the times and costs associated with the crew's relocation. Coordinates of pipe segments were extracted from ArcGIS (ESRI, 2011) layers to create an origin-destination matrix from which the relocation time and cost can be determined. A Google application programming interface (API) was utilized to access Google Maps from which the distance and travel time between any two locations were determined. Utilizing the abilities of Google Maps, API allowed for site routing and finding the shortest distance between the locations of failed segments. Additionally, travel times reported in Google Maps were adjusted to account for traffic conditions, which is crucial in dense urban cities and after massive disruptions. Relocation costs were then computed by multiplying the hourly rate of restoration crews by the relocation time. The final output of this model is the relocation time and cost between the locations of each pair of failed segments' locations.

3.3.2 Restoration Sub-model

Various repair methods can be utilized to restore a broken water segment. This model evaluates different alternatives for restoring failed segments and selects suitable methods based on a set of predefined criteria. The factors considered in this selection process include the pipe size, material type, location and accessibility, soil type under which the pipe is buried, the previous number of breaks, and defect characteristics. The repair methods considered in this study are mechanical clamps, pipe bursting (PB), pipe splitting (PS), and open-cut-method (OCM). Brief descriptions of these methods, along with their applicability, were provided in Chapter 2. This sub-model considers the criteria mentioned above in selecting the possible restoration methods for each pipe segment. For example, small breaks, or leaks, can be repaired using mechanical clamps and couplings while PB, splitting, and OCM are used to replace segments of bigger break sizes. A pipe

segment might be nominated for replacement even if the break size is small when the total number of breaks reaches a certain threshold set by the municipality.

The restoration time and cost were calculated based on the type of the repair method, diameter, and length of the pipe segment. Unit costs and times of the considered methods were gathered from different consultants and contractors in Canada. Resilience improvement realized from restoring a particular pipe segment depends on whether it was repaired or replaced. The theoretical value of the reliability of newly replaced segments shall be 1.0. However, this value is usually reduced to account for mistakes and other factors that compromise the installation quality. Each City can define this value based on the qualifications of the executing crews, or contractors in case of outsourcing. This value is fed as an input that reflects the skills and qualifications of the restoring crews. In this model, replacing a pipe segment was assumed to increase its reliability to a value of 0.95. On the other hand, when a pipe segment of a specific failure order was repaired, its reliability along subsequent years was calculated utilizing the survivability function of the successive failure order, as demonstrated in the previous section and in Assad et al. (2019). The final output of this model is the time, cost, and resilience improvement of all possible restoration options for each failed pipe segment.

3.3.3 Optimization Framework

The base of the formulated optimization in this study is a combination of the traditional knapsack and traveling salesman optimization problems (Lawler et al. 1985; Pisinger and Toth 1998). The proposed model aims at optimizing three conflicting objectives: 1) minimizing restoration cost; 2) minimizing restoration time; 3) and maximizing resilience level after adopting all restoration actions as shown in Equations 3.13 - 3.16.

Minimize

$$R.C. + z = \sum_{i \in P} \sum_{j \in C} \sum_{k \in M} (x_{j,k}^i \times RC_{j,k}^i) + \sum_{t \in T} \sum_{j \in C} \sum_{i \in P} \sum_{l \in P} (x_j^{i,t} \times x_j^{l,t+1}) * LC_{i,l} + z \quad (3.13)$$

Where $R.C.$ is restoration cost; $x_{j,k}^i$ is a decision variable that takes a value of 1 when pipe segment (i) is restored by crew (j) using repair method (k) and 0 otherwise; $RC_{j,k}^i$ is the cost of restoring pipe segment (i) by crew (j) using restoration method (k); $LC_{i,l}$ is relocation cost between sites at which pipe segments (i) and (l) are located respectively; $x_j^{i,t}$ is decision variable that takes a value of 1 when pipe segment (i) is restored by crew (j) during restoration time step (t); C ; P ; M ; and T is sets of the available number of crews, failed pipe segments, repair methods, and restoration time steps, respectively. A restoration time step represents the order at which a particular segment is restored. Parameter (z) represents the penalty amount resulted from violating the budget constraint. This vale represents the extra costs associated with the restoration activities. As such, it is calculated as the multiplication of the unit cost of restoration methods times the lengths of the restored segments.

$$\text{Minimize } R.T = \max_{j \in C} T.R.T_j \quad (3.14)$$

$$T.R.T_j = \sum_{i \in P} \sum_{k \in M} (x_{j,k}^i \times RT_{j,k}^i) + \sum_{t \in T} \sum_{i \in P} \sum_{l \in P} (x_j^{i,t} \times x_j^{l,t+1}) * LT_{i,l} \quad (3.15)$$

Where $R.T$ is the time of the restoration process; $T.R.T_j$ is total restoration time for crew (j); $RT_{j,k}^i$ is the time needed for restoring water pipe (i) by crew (j) using restoration method (k); $LT_{i,l}$ is relocation time between locations at which pipe segments (i) and (l) are located, respectively.

$$\text{Maximize } T.R.I. = \sum_{i \in P} \sum_{j \in C} \sum_{k \in M} (x_{j,k}^i \times \mathcal{R}I_{j,k}^i) \quad (3.16)$$

Where $T.R.I.$ is total resilience improvement realized after restoring all failed segments, $\mathcal{R}I_{j,k}^i$ is resilience improvement resulting from restoring pipe segment (i) by crew (j) using method (k).

A set of constraints was then added to represent the operational and managerial restrictions that control the optimization search process. Firstly, a constraint was added to guarantee that restoration costs would not exceed a specific allocated recovery budget, Equation 3.17. The budget constraint was considered as a soft constraint that might be violated by some solutions. However, such solutions would incur a penalty (z) in the objective function, as shown in Equation 3.13. In addition, a constraint is added in Equation 3.18 to assure that no segment will be left unrestored. It limits the number of visits for each segment to exactly 1. Another constraint was also added to avoid assigning the same crew to more than one location at the same time step, Equation 3.19. The constraint shown in Equation 3.20 allows the user to specify a minimum resilience level that shall be achieved upon accomplishing all restoration actions.

Subject to

$$Total\ Costs - z \leq B_{Total} \quad (3.17)$$

$$V_i = \{1\} \quad (3.18)$$

$$L_{it} = \{1\} \quad (3.19)$$

$$\mathfrak{R}_F \geq \mathfrak{R}_{Threshold} \quad (3.20)$$

$$x_{j,k}^i, x_j^{i,t}, x_j^{l,t+1} = \{0,1\} \quad (3.21)$$

$$z \geq 0 \quad (3.22)$$

$$\forall i \in P, j \in C, k \in M, l \in P / \{i\}, t \in T$$

Where B_{Total} is the total restoration budget; V_i is the number of visits for segment (i); L_{jt} is the number of pipe locations that can be visited by crew (j) in a time step (t). $\mathfrak{R}_{Threshold}$ is a benchmark value for network resilience at the recovered state as set by the decision-maker; and \mathfrak{R}_F = the final resilience value. Resilience threshold value represents the minimum resilience level

that a City aims to satisfy based on the importance of the considered sub-network, resilience loss, and the available budget and resources.

Weighted some method was employed to solve the multi-objective optimization problem described above. In this approach, the objectives are aggregated into a single weighted objective function, as shown in Equation 3.23.

$$\text{Minimize } Z = \alpha_1 TRC + \alpha_2 RT + \alpha_3 TRI \quad (3.23)$$

The weights here represent the relative importance of each objective. This approach is usually referred to as a prior preference approach. As with most methods that involve objective function weights, inputs from users are needed to reflect their preferences. These preferences can be exploited in two ways. Firstly, the decision-maker may directly assign the weights of each objective before the problem is solved. This allows the user to get a single solution. Alternatively, decision-makers may not be quite decisive about a specific set of relative weights, and they may wish to investigate a possible trade-off between the considered objectives. In such cases, ranges of possible weights for each objective would be sought from the decision-makers. The problem would be iteratively solved for several times, specified by the user, while systematically altering the set of relative weights according to those ranges. This analysis yields several solutions from which users choose the one that best matches their preferences. Finally, should decision-makers desire to investigate the full search space, the single objective formulation in Equation 3.23 can be further enhanced using dynamic weights, as shown in Equation 3.24 - 3.25. These dynamic weights are randomly generated to obtain an optimum Pareto frontier for the considered optimization problem.

$$\text{Minimize } F(x) = \sum_{i=1}^n \alpha_i f_i(x) \quad (3.24)$$

$$\alpha_i = \frac{\mu_i}{\sum_{i=1}^n \mu_i} \quad (3.25)$$

Where n = total number of objective value (in this case 3); α_i = relative weight; and $\sum_{i=1}^n \mu_i = 1$.

The search space for this problem is significant. The number of possible solutions equals the factorial of the number of failed segments multiplied by the possible restoration methods raised to the number of failed segments. For example, if the number of failed segments is 15, and there are two different restoration methods to restore each segment, the search space will then be 4.28×10^{16} ($15! \times 2^{15}$). Factorial operator is considered to represent each distinct sequence of repairing the failed segments. Several algorithms that are commonly used in asset management and resilience applications were investigated to identify the best performing algorithm to be used in solving the formulated restoration optimization problem. These algorithms are Genetic Algorithm (GA), Ant Colony Optimization (ACO), and Tabu Search (TS). A brief description of each can be found in Chapter 2.

3.3.4 Deterministic Versus Stochastic optimization

As previously mentioned, the model asks the users to provide three sets of inputs regarding the considered repair methods. These inputs are the unit cost, time, and resilience improvement of each repair method. In case the values of these parameters are known to decision-makers with reasonable certainty, they can be directly assigned. For example, the case when a municipality calls for estimates about the unit time and cost of specific repair methods from contractors along with their professional profiles to choose one of them. The problem, in this case, would be solved deterministically. In many cases, however, estimates about these parameters are rather uncertain, which is the case when decision-makers plan for long-term resilience. Also, hazardous events are usually accompanied by severe disruptions to supply chains, which may further increase the uncertainties in the time and cost of delivery. Estimates about costs, durations, and resilience improvements are thus subjected to change in such cases due to several factors such as material availability, skills of restoration crews, surrounding conditions, and other risks.

In order to provide decision-makers with a comprehensive analysis that includes the worst and best possible estimates regarding the restoration objectives, the optimization problem would be stochastically solved. In this approach, the optimization objective is modified such that the mean of the original objective function is minimized. In this type of optimization, a predefined number of trials, sets of distinct values of the decision variables, are generated, and the simulation runs several iterations for each specific trial. In each iteration, the probability distribution functions of the uncertain variables are sampled, and the objective function is computed.

In this analysis, minimum, maximum, and average values of the gathered restoration costs and durations were assumed to be the limits and most probable estimates that were fed to the Monte Carlo simulation. PERT distribution was selected as the type of probability distribution to sample the associated uncertainties. Different than triangular distribution, PERT distribution places more emphasis on the most probable estimate, which is usually more-well known than the extreme values. This suits the case of utility managers who consistently respond to segments' failures and, consequently, accumulate historical experience allowing them to better estimate the most probable values compared to the limit values. Besides, PERT distribution has a smoother shape compared to the angular shape of the triangular distribution, which offers a better fit for the subjective estimates of the limit values (Law et al. 2000). Upon completing the iterations, the result of the trial is the statistic of the objective function of interest. This value is then used by the optimization algorithm to guide generating new better trial solutions until some termination criterion is met. Figure 3-13 depicts the steps of stochastic optimization, as followed in this research.

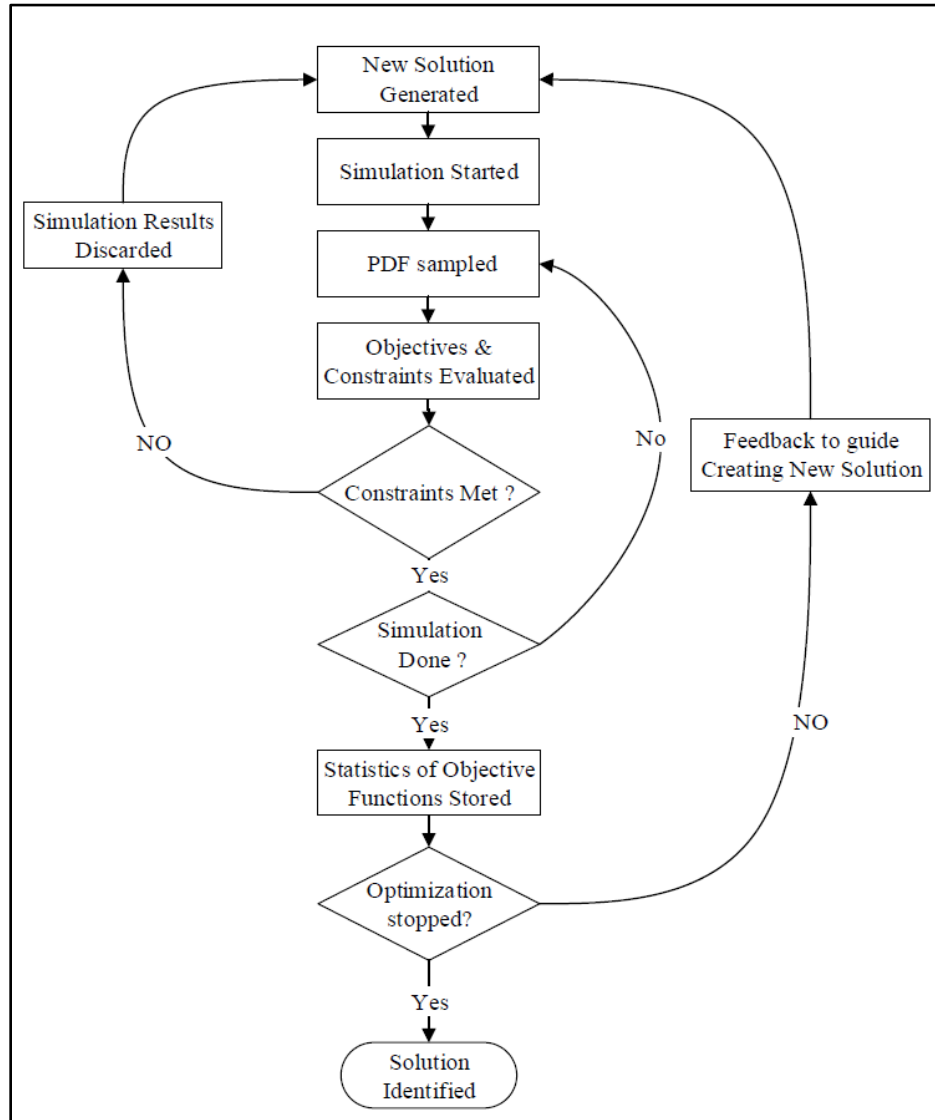


Figure 3-13: Procedure for stochastic optimization

To evaluate the performance of the developed optimization model, the obtained results were compared to a restoration plan suggested by the City of London. Differences between the City’s approach and the framework developed in this section were then highlighted and discussed. These variations resulted in enhanced values for the considered objective functions. Several sensitivity analyses were then conducted to determine the input variables whose impacts on the mean values of the objective functions are the highest.

3.4 Resilience Enhancement Model

In this section, a newly developed model for resilience enhancement planning of WDNs is presented. The objective is to develop an optimization model for determining and scheduling resilience enhancement actions of WDNs. The model integrates sustainability objectives by minimizing both the cost and carbon emissions of the resilience enhancement intervention actions. The output of this model is an optimal intervention action for each segment. Additionally, a schedule is generated to visualize the rehabilitation work packages and the overall enhancement process.

Obtaining an optimal resilience enhancement plan encompasses two main phases: 1) determining optimal enhancement actions, and 2) scheduling these actions. In the first phase, segments selected for enhancement along with the enhancement actions and their timings are determined. The second phase aims at clustering the resulted actions into work packages based on specific commonalities before scheduling them. In this model, resilience absorptive capacity is the resilience objective that is aimed to be improved. As previously mentioned, absorptive capacity is the ability of WDNs to withstand disruptions without significant degradation. It can be boosted through protective mitigation measures that enhance the current strength of WDNs. These enhancement measures play an essential role in shortening the time of recovery following disruptive events. In addition, life cycle cost and carbon emissions associated with various enhancement actions are considered to account for the sustainability aspects of WDNs. The developed method encompasses three main sub-models in addition to utilizing the previously developed resilience metric, as shown in Figure 3-14. Details of each sub-model are presented subsequently along with a description of underlying derivations and mathematical formulations.

Figure 3-14 depicts the components of the proposed framework and the relation between its sub-models.

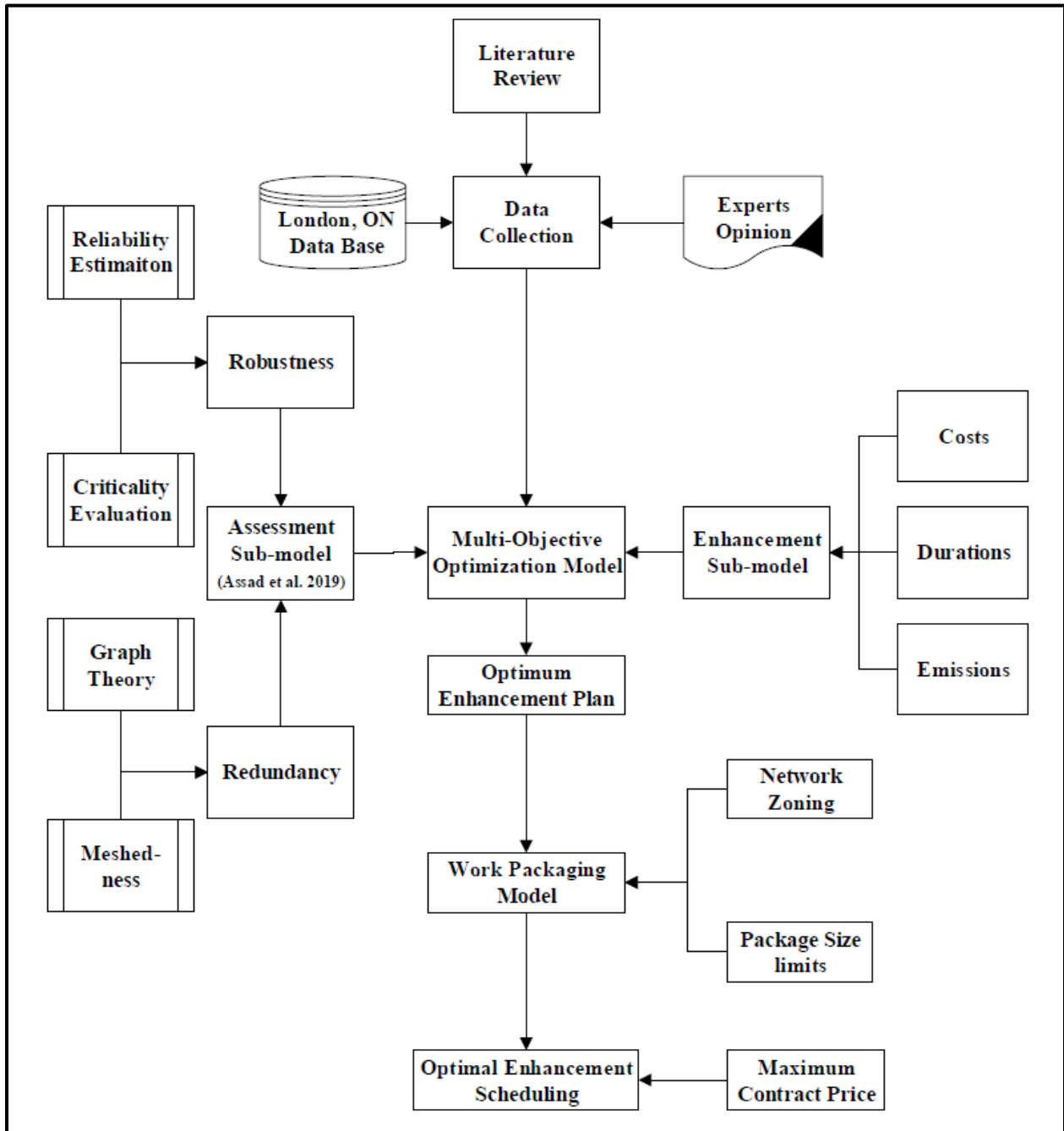


Figure 3-14: Resilience Enhancement Model Methodology framework

The model focused on enhancing resilience of water segments by improving their robustness. Rehabilitation of deteriorated segments can increase the reliability and robustness of

water networks. The innovative feature of utilizing the previously developed metric is the ability to dynamically update reliability of segments, and thus network resilience, based on their age, the previous number of failures, and intervention actions they may undergo based on the type of such actions. For example, replacing a pipe segment can increase its reliability to a value of 1.0. In practice, this value is usually less than the theoretical value of 1.0 to account for factors that compromise the installation quality. Also, the segment's reliability along the subsequent years is calculated based the deterioration curve of newly installed segments that share the same size and material cohort. Similarly, major and minor actions increase the current reliability level of a segment and change its deterioration behavior along the following years. Resilience improvement realized due to major and minor interventions were assumed to be 0.5 and 0.25, respectively. These estimated are based on the leveraged maintenance reports and the updated behavior reported. Successive deterioration of these segments was elicited based on the deterioration curves of segments that were subjected to similar intervention actions and share the same characteristics. More details about the dynamic calculation and update of segments' reliabilities and deteriorations can be found at (Assad et al. 2019).

3.4.1 Enhancement Sub-model

This sub-model investigated various types of interventions, along with their associated costs, durations, and carbon emissions. Four different intervention alternatives were considered, namely: do nothing; minor intervention; major intervention; and full replacement. Epoxy lining, Cured in Place Pipe (CIPP), and Pipe Bursting (PB) are the considered intervention actions associated with minor, major, and full replacement alternatives, respectively. A brief description of each considered enhancement method is shown in Chapter 2. It shall be noted that other methods can be included based on the preference of the responsible municipality. Costs and duration of

enhancement methods were calculated based on the method type and the segment size. Unit costs and times of the considered methods were gathered from different consultants and contractors in Canada.

Carbon emissions were then calculated for each enhancement method utilizing a calculator tool that was initially developed by the North American Society of Trenchless Technology, NASTT, (O’Sullivan 2010). The calculator has then been updated by the British Columbia chapter, NASTT-B, and approved by the province of British Columbia, Canada (Beale et al. 2013; O’Sullivan 2010). This tool estimates the carbon emission profile associated with various pipeline replacement and renovation techniques based on the project dimensions, pipeline size, material, surface type, and other factors. The estimated emission profile considers site and transportation operations, including mobilization, excavation, disposal, backfilling, and pipe installation or rehabilitation works. For example, the estimated CO₂ emissions resulting from replacing a pipe segment of 200mm in diameter, 150m in length, and buried at 2.5m depth utilizing PB technique is 2.5 (CO₂-e tonne). Similar results were calculated for all other segments and intervention methods. These results were used as inputs to the enhancement optimization model.

3.4.2 Optimization Framework

As previously mentioned, the developed enhancement model aims at optimizing three conflicting objectives: 1) minimizing life cycle cost; 2) minimizing emissions; 3) and maximizing resilience after adopting all enhancement actions, as shown in Equations 3.26-3.28, respectively.

$$\text{Minimize } T.C. = \sum_{t \in T} \sum_{i \in P} \sum_{j \in M} \frac{1}{(1+r)^t} (x_{i,j}^t * C_{i,j}^t) \quad (3.26)$$

Where $T.C.$ is the total cost of resilience enhancement actions; $x_{i,j}^t$ is a decision variable that takes a value of 1 when pipe segment i is enhanced using repair method j during year t and 0 otherwise;

$C_{i,j}^t$ is enhancement cost of pipe segment i using method j during year t ; r = discount rate; P ; M ; and T is the number of pipe segments, enhancement methods, and years respectively.

$$\text{Minimize } T.E. = \sum_{t \in T} \sum_{i \in P} \sum_{j \in M} (x_{i,j}^t * E_{i,j}^t) \quad (3.27)$$

Where $T.E.$ is total CO₂ emissions; $E_{i,j}^t$ is CO₂ emissions resulting from the enhancement of pipe segment i using method j during year t .

$$\text{Maximize } \mathcal{R}_T = \frac{\sum_{k \in S} (\mathcal{R}_k^T \times L_k)}{\sum_{k \in S} (L_k)} \quad (3.28)$$

$$\mathcal{R}_k^t = \mathcal{R}_k^{t-1} + \mathcal{R}I_k^t - \mathcal{R}D_k^t \quad (3.29)$$

$$\mathcal{R}I_k^t = \sum_{i \in P} \sum_{j \in M} (x_{i,j}^t * \mathcal{R}I_{i,j}^t) \quad (3.30)$$

Where \mathcal{R}_T is resilience at year T , the end of the planning horizon. When several subnetworks are considered, their lengths, L_k , are used to get a weighted average resilience. \mathcal{R}_k^t is resilience level of subnetwork k at year t , $\mathcal{R}D_k^t$ is resilience deterioration of subnetwork k at year t due to aging, $\mathcal{R}I_k^t$ is resilience improvement of subnetwork k at year t due to enhancement actions, $\mathcal{R}I_{i,j}^t$ is resilience improvement resulting from the enhancement of pipe segment i using method j during year t , and S is the total number of subnetworks.

A set of constraints were added to represent the operational and managerial restrictions that control the optimization process. Firstly, a constraint was added to guarantee that annual enhancement costs would not exceed annual allocated budgets, Equation 3.31. Another constraint was also added in Equation 3.32 to assure that the minimum resilience of any subnetwork along the planning horizon would be more than a minimum threshold value. This value can be specified individually for each subnetwork based on its importance. Setting different minimum resilience threshold is a realistic and practical measure that municipalities implement to manage their vast highly deteriorated water assets. In addition, enhancement actions are usually accompanied by

significant disruption to traffic, adjacent facilities, and other infrastructure systems. Hence a special constraint was added, Equation 3.33, to limit the number of visits for each specific segment along the planning horizon to a user-defined value. This factor aims at minimizing the amount of disruptions accompanying the enhancement actions. The exact number of visits for each segment can be estimated based on its criticality and the available resources. This value was set to 1 in this analysis.

Subject to

$$\sum_{i \in P} \sum_{j \in M} (C_{i,j}^t) \leq AB_t \quad (3.31)$$

$$\min_{t \in T} (\mathcal{R}_k^t) \geq \mathcal{R}_{k,Th} \quad (3.32)$$

$$V_i \leq V_{max} \quad (3.33)$$

$$x_{i,j}^t = \{0,1\} \quad (3.34)$$

$$\forall i \in P, j \in M, k \in S, t \in T$$

Where AB_t is the annual budget allocated for enhancement actions; $\mathcal{R}_{k,Th}$ is minimum resilience threshold for each subnetwork; and V_i is the number of visits for segment i .

3.4.3 Packaging and Scheduling Sub-model

Once enhancement actions of individual segments were determined along with their implementation year, the framework proceeded with the scheduling process. A set of actions during a specific year was scheduled on two main stages: 1) Clustering the enhancement actions into work packages, and 2) Determine the optimal enhancement schedule. In the first stage, pipe segments were divided into work packages (WPs) based on their geographical location and intervention method. These WPs were formulated to facilitate monitoring and control of the enhancement process. Packages were formulated based on a set of factors such as the number of pipe segments, type of enhancement intervention, its complexity, available budget, and the number

of available contractors or in-house maintenance crews. Different clustering techniques were utilized to cluster each pipe segment in a specific group based on its geographical location. Coordinates of each segment were exploited from ArcGIS files to determine its location. K-means and K-medoids clustering algorithms were tested for clustering the selected section of London WDN. The Davies–Bouldin Index was employed to compare the clustering quality of K-means and K-medoids and select the best performing algorithm.

An optimization model was then formulated to determine the best distribution of resilience enhancement actions into work packages. The objective was to maximize the resilience improvement of each work package by adding as many enhancement actions as possible while respecting a set of constraints. This was performed by maximizing the resilience improvement of the work package that had the minimum resilience improvement, as shown in Equation 3.35. A constraint was added in Equation 3.37 to specify the minimum size of a work package. Resilience variability across packages will not be an issue as the package size is respected. Two more constraints were added in Equations 3.38 and 3.39 to determine the maximum size of work packages and to assure that each package consisted of segments that share the same enhancement method, respectively. These two constraints were defined as soft constraints to account for the exceptional solutions where segments of different enhancement methods, a hybrid work package, or more actions than the maximum size, an over-sized work package, needed to be clustered in a single work package. However, such solutions would incur a penalty (α) and (β) in the objective function, as shown in Equation 3.35. Another Constraint was included in Equation 3.40 to ensure that all segments in a work package share the same geographical zone.

$$\text{Maximize } \mathcal{R} = \min_{v \in WP} (\mathcal{R}.I_v) - \alpha - \beta \quad (3.35)$$

$$\mathcal{R}.I_v = \sum_{v \in WP} \sum_{i \in P} (y_{i,v} * \mathcal{R}.I_i) \quad (3.36)$$

Subject to

$$C_v \geq C_{min} \quad (3.37)$$

$$C_v - \alpha \leq C_{max} \quad (3.38)$$

$$MT_v - \beta = 1 \quad (3.39)$$

$$Z_v = 1 \quad (3.40)$$

$$\alpha, \beta \geq 0 \quad (3.41)$$

Where $y_{i,v}$ is a decision variable that takes a value of 1 when pipe segment i is clustered in work package v ; $\mathcal{R}.I_v$ is resilience improvement of work package v , C_v is the cost of work package v , the summation of the individual enhancements actions' costs in work package v , C_{min} and C_{max} are the minimum and maximum costs of work packages representing the minimum and maximum possible size of a work package, α, β are the penalty factors to account for increased costs and excess number of methods types in a certain work package, MT_v is the number of enhancement methods in work package v , Z_v is the number of location zones in work package v , and WP is the number of work packages.

Finally, an optimization model was formulated to schedule the resulted work packages. The inputs of this model were the work packages, their total costs and durations, available number of contractors, and maximum contract value. The objective of this scheduling model was to minimize the time of the resilience enhancement process, as shown in Equation 3.42. This objective was derived from the need to strengthen WDNs as soon as possible, so they are ready to confront future expected disruptive events with minimum performance degradation.

$$\text{Minimize } T = \max_{w \in C} (TT_w) \quad (3.42)$$

$$TT_w = \sum_{w \in C} \sum_{v \in WP} (z_{v,w} * T_v) \quad (3.43)$$

Where T is the time of resilience enhancement process; TT_w is the total time for contractor w ; T_v is the duration of work package v , the summation of the individual enhancements actions' durations in work package v ; and $z_{v,w}$ is a decision variable that takes a value of 1 when work package v is assigned to contractor w . The maximum contract price constraint was added to comply with the fair business regulations, Equation 3.44.

$$C_w \leq CP_{max} \quad (3.44)$$

Where C_w is the total cost of work packages assigned to contractor w ; and CP_{max} is the maximum allowable contract price to assure fair business practices.

3.4.4 Multi-objective Optimization

Posterior approach is followed to solve the formulated optimization problem in this section. In this approach, the whole search space is investigated so that the users get a holistic view of all possible optimal solutions. The output, in this case, is not a single solution like the case in the prior approach of solving multi-objective optimization problems. Instead, the result is a set of optimal solutions, usually called a Pareto frontier. Decision-makers, in this case, need to apply some techniques to determine the most suitable solution from the set of Pareto solutions that aligns with their preferences and constraints. Various Multi-criteria decision-making techniques are available to obtain the solution that perfectly fits the decision-makers' preferences. Determining optimal resilience enhancement plans is a strategical planning process in which decision-makers would typically prefer to investigate the full search space, or a wide portion of it, to get a comprehensive view of the possible solutions. This is unlike the situation after hazards occurrence where decision-makers would typically be interested in restoring the interrupted service as soon as possible. The speed of recovery would typically receive the most relative weight. Hence, it is more efficient to exclusively search around solutions that serve this purpose.

Two algorithms were investigated to identify the best performing one to solve the formulated problem described in this section. These algorithms were a modified version of ant colony optimization, ACO, and genetic algorithm, GA. A brief description of each was provided in Chapter 2. Hypervolume indicator was utilized to compare the performance of the investigated optimization algorithms. Hypervolume indicator is the most commonly utilized metric to compare the performance of multi-objective optimization algorithms (Zitzler et al. 2003). It measures the m-dimensional volume of the region in objective space enclosed by the obtained non-dominated solutions and a reference point. Hypervolume indicator is the only indicator that can consider accuracy, cardinality, and diversity of the optimal solution (Riquelme et al. 2015). Accuracy is a closeness measure of the obtained solutions to the true non-dominated solutions. Cardinality is the number of points in the obtained solution. Diversity refers to the spread and relative distances of the obtained solutions in the search space (Riquelme et al. 2015). Equation 3.45 is used to compute the hypervolume indicator (Nebro et al. 2013):

$$I_{HV} = \text{volume} \left(\bigcup_{i=1}^{|Q|} v_i \right) \quad (3.45)$$

Where I_{HV} is the hypervolume indicator; v_i is the hypercube of non-dominated solution i ; and Q is the set of non-dominated solutions. A higher Hypervolume indicator indicates a more considerable distance between the obtained solution and the reference point, nadir point, hence a better solution.

The result of multi-objective optimization is a set of Pareto optimal solutions. Multi-criterion decision-making (MCDM) techniques can assist in selecting the most appropriate solution among the set of Pareto solutions. In this analysis, PROMETHEE II is utilized to determine the best solution of the Pareto frontier points. The PROMETHEE method is an interactive MCDM technique that can handle quantitative as well as qualitative criteria with discrete alternatives (Brans et al. 1986). Steps of applying PROMETHEE II was detailed in Chapter 2.

The two-tier scheduling optimization model developed in this section was then applied to a larger section of London WDNs. The model started by labeling the network's different areas based on their functionality. Residential, commercial, industrial, undeveloped, and others are examples of this functionality-based distribution. Three sub-networks were then selected to cover different combinations of these areas. For each sub-network, a distinct resilience threshold was set according to the importance of the areas within each sub-network. Next, resilience enhancement actions were determined for each segment, along with their timings along the planning horizon. A base year was then selected, and intervention actions happening along this year were scheduled. The scheduling process started by clustering the resilience enhancement interventions into work packages based on their type and geographical location. These packages were then scheduled, considering the number of available contracts. The attained resilience improvement was computed along with the associated cost and carbon emissions. A comparison between the obtained results and a current in-house portfolio management practice was also carried out to evaluate the performance of the developed optimization model.

3.4.5 Redundancy Enhancement Strategy

The second way of boosting the resilience of a WDN is to increase the level of redundancy offered by this network. This can be achieved by explicitly imposing alternative paths to secure water provision around critical demand points. The core idea of resilience enhancement through redundancy improvement is to ensure that as many critical segments as possible have an alternative route to provide water for the most vital customers. This is done by duplicating these pipe segments such that the newly installed segment acts as a backup to supply water to the same customer when the original segments are damaged or unable to meet the amount of needed services. The new duplicate segment is typically sought to be stronger than the original one such that it can provide

service in case the original segment went offline. The point of installing structurally stronger segments is to minimize the probability of services interruption due to anticipated disruptions that would result in damaging the original segments. This shall act a means of enhancing the system's adaptive capacity such the pipe segments are more prepared to withstand future disruptions. The new segment can also function in parallel to the original one in case the City aims to increase the system's capacity. Examples of pipe segment Duplication projects can be found in several leading cities such as British Columbia, Canada, Tokyo, Japan, and Palmerston North, New Zealand.

Mathematically, duplicating a pipe segment is assumed to increase the number of links in the network without increasing the number of corresponding nodes. This modeling is valid since both the original and duplicate segments provide service to the same set of nodes. While the new pipe segment is actually presented in the network, no demand points are added. A separate optimization model was formulated to improve the redundancy of the selected section of the London WDN. New pipe installation and expansion strategies are usually planned separately from regular rehabilitation and replacement programs. Hence, it was also separated in this research. In addition, separating the two optimization problems is important to avoid any dual effect that might result from mixing decision variables related to redundancy and robustness enhancements. The objective function of this optimizing problem is shown in Equation 3.46:

$$\text{Maximize Red. I.} = \sum_{k=1}^s \sum_{i=1}^m RedI_{ki} * x_{ki} \quad (3.46)$$

Where Red. I. is redundancy improvement; x_{si} is a binary decision variable that takes a value of 1 when pipe segment i in sub-network k is chosen to be duplicated and 0 otherwise; $RedI_{ki}$ is the redundancy improvement of sub-network k when pipe segment i is chosen for duplication; m = the number of pipe segments candidates considered for duplication in subnetwork k ; and s is the total number of sub-networks in the considered water distribution network. A candidate

segment considered for duplication is any segment with a criticality index exceeding a certain threshold, as shown in Equation 3.47. This screening metric was added to limit candidates of segments considered for duplication to the most critical ones. The focus shall be first directed to those highly critical segments given tight budgets available. A constraint was added in Equation 3.48 to specify the set of redundancy targets for each sub-network. This constraint shall serve as a bias-metric to prioritize selecting segments from most important sub-networks according to the decision-maker perceptive. Another constraint was added in Equation 3.49 to ensure the costs of duplications actions do not exceed a specific allocated budget.

Subject to

$$Cr_i \geq Cr_{Th} \quad (3.47)$$

$$Red_k \geq Red_{k,Th} \quad (3.48)$$

$$\sum_{s \in SN} \sum_{i \in m} (C_{si}) \leq AB_t \quad (3.49)$$

$$x_{ki} = \{0,1\} \quad (3.50)$$

$$\forall i \in m, k \in s$$

Where C_{si} is the cost of duplicating pipe segment i which located in subnetwork k ; AB_t is the available budget allocated for redundancy improvement via duplication actions; and $Red_{k,Th} =$ minimum redundancy threshold for subnetwork k .

3.5 Research Limitations

The proposed methodology includes some limitations that might undermine the applicability of the proposed models. The following features these limitations:

- The impacts of hazardous events studied in this research are structural impacts exclusively.
- Water pipelines are the only components of WDNs analyzed in this research as they constitute the biggest majority of components.

- Other social factors can be considered in criticality estimation of pipe segments such as the right to water. This factor accounts for the level of accessibility of some vulnerable communities to water.
- The Meshed-ness coefficient is the only metric employed to quantify redundancy in this study. It measures the intensity of available loops in the network as a way to quantify the availability of potential alternative paths. Other metrics from graph theory can reinforce the obtained results.
- The improvements in reliability due to major and minor intervention actions were assumed due to the lack of available data. Accordingly, they were coded as user-defined values.
- Updated deterioration behavior for specific segments could not be generated due to the lack of relevant data. Updated behaviors of similar segments were employed.

3.6 Summary

The methodology adopted in this research was presented in this chapter. The topics of related literature were briefly discussed, and different sources of gathered data were briefly stated. The chapter then proceeded in describing the development of the resilience assessment, restoration, and enhancement models. Underlying concepts, assumptions, and mathematical formulations of each model were presented in detail. The core idea of the developed framework is to integrate robustness, redundancy, rapidity, and restoration in resilience-based management of WDNs. Suitability of various restoration and mitigating actions, uncertainty in the recovery process, and sustainability objectives, carbon emissions and life cycle cost, were also considered in the presented framework. Survival analysis and various MCDMs tools were employed in formulating a multi-attribute resilience assessment metric. Multi-objective optimization tools along with

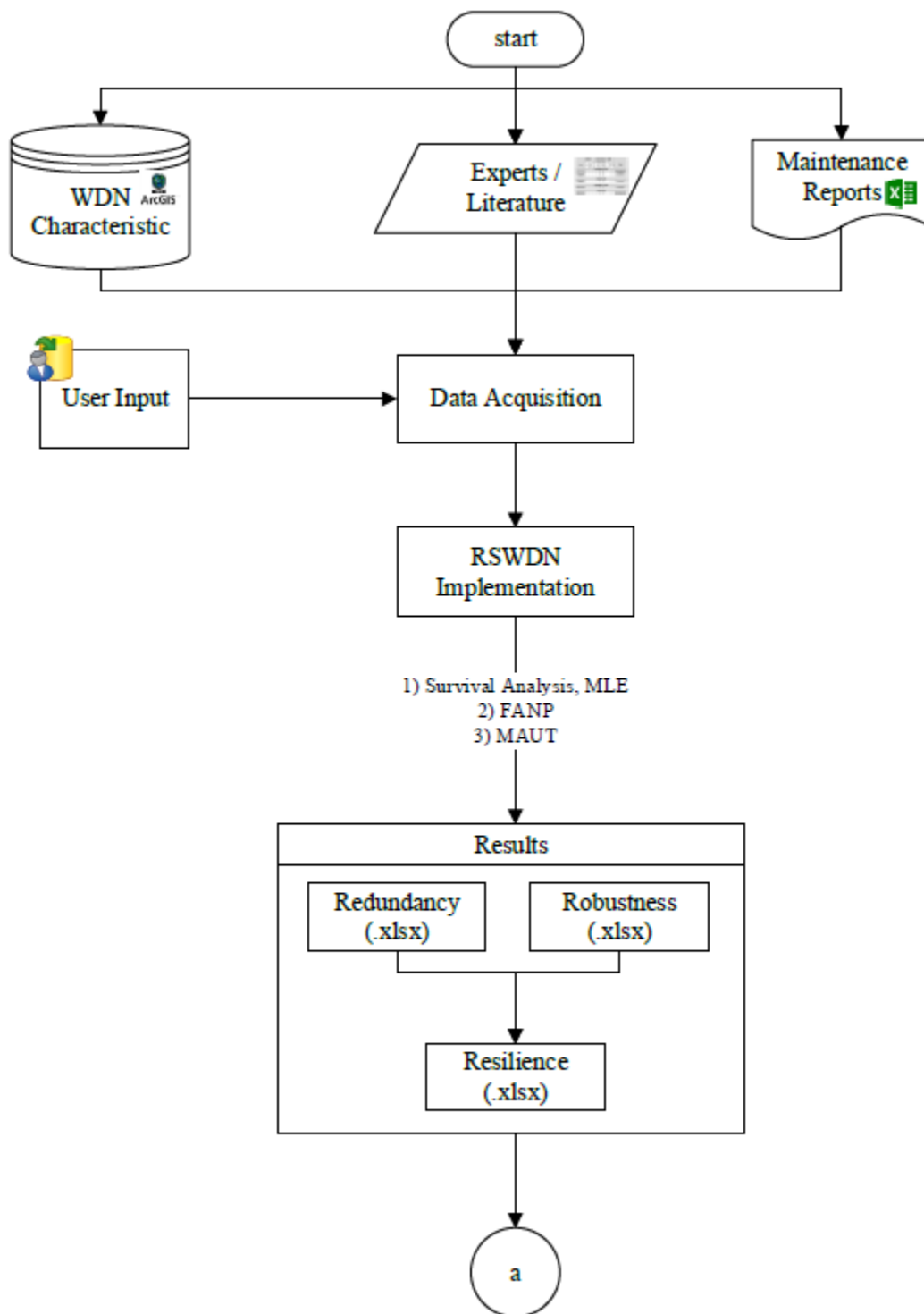
MCDM techniques, and clustering techniques were employed to ascertain the optimum resilience enhancement and restoration plans while satisfying a set of operational and managerial constraints.

Chapter 4: Developed Automated Computer Application

4.1 Overview

This chapter describes the development of an automated tool that integrates the models mentioned in Chapter 3. This tool was developed utilizing Matlab App designer® to integrate the calculations performed in Matlab scripts and Microsoft Excel sheets. This tool has three main components: (1) Resilience assessment, (2) resilience restoration, and (3) resilience enhancement. The resilience assessment module is developed using the following calculations (1) reliability assessment of water pipes segments, (2) criticality indices of water pipe segments, and (3) redundancy of the network. Resilience level of the studied network is the output of this module. The second module takes this resilience level as input, along with inputs from repair and relocation sub-models, to generate an optimal schedule of restoration activities following a hazardous scenario. Similarly, the enhancement model utilized the resilience level from the resilience assessment module and other factors to determine an optimum enhancement plan and an optimal schedule of packaged enhancement actions. Figure 4-1 shows the input and output of the developed tool, Resilient Water distribution Network (RSWDN). The following subsections illustrate a more detailed description of this tool and the navigation through different resilience modules.

In addition, this chapter presents the developed dashboard which is fully integrated within the ARC-GIS environment. The developed dashboard can be utilized to visualize the different characteristics of each segment in the network. Besides, joined filters can be applied to investigate various attributes of the pipe segment's inventory.



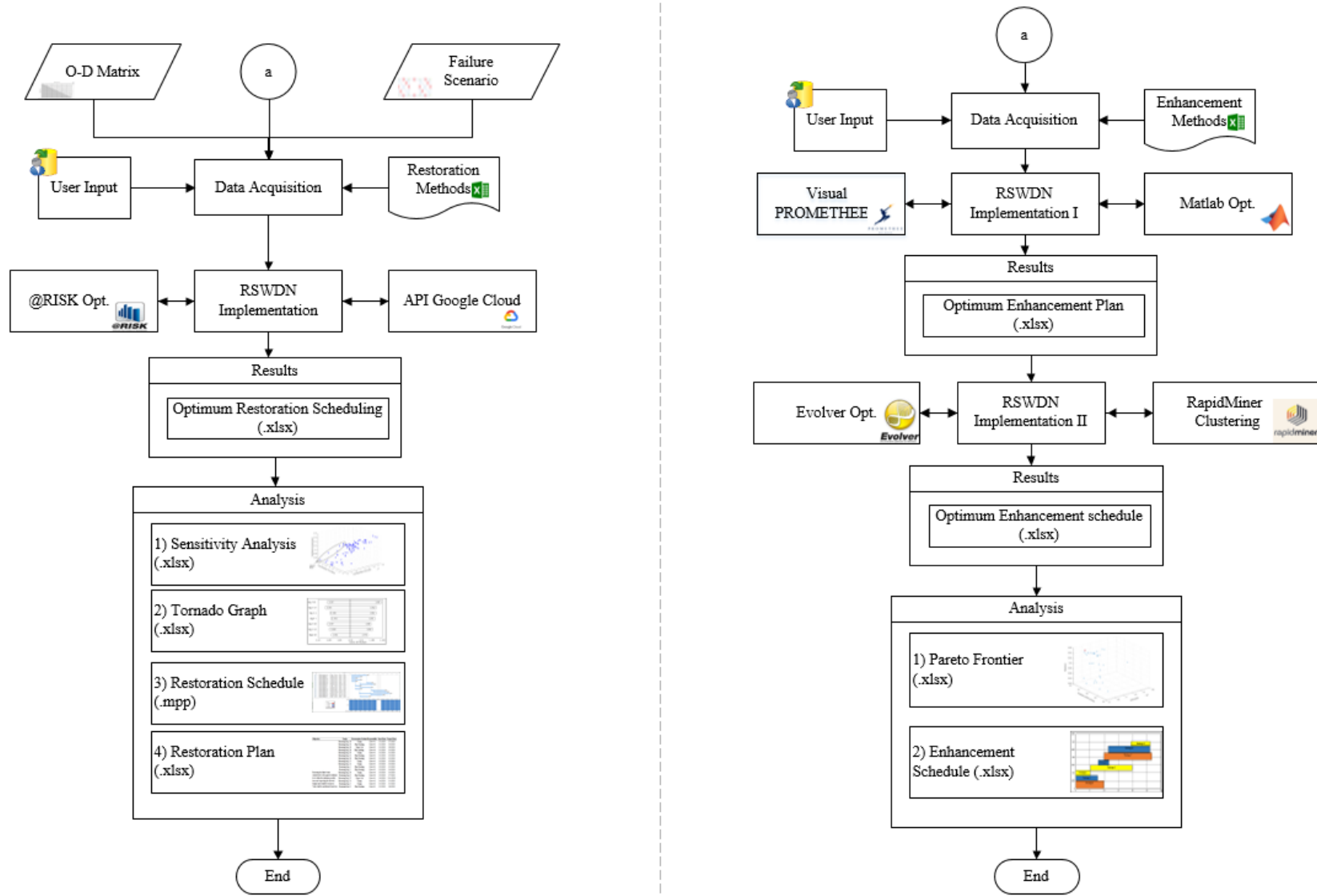


Figure 4-1: Input and Output of RSWDN

4.2 Resilience Assessment Module

Figure 4-2 shows the homepage of (RSWDN) tool, where the user chooses the type of resilience application of interest. As previously mentioned, this module integrates reliability and criticality of pipe segments to compute the network robustness. In addition, network redundancy is added to estimate the resilience level of the network. A detailed description of the developed tool to streamline these calculations is shown subsequently.



Figure 4-2: Homepage of the developed tool, RSWDN

4.2.1 Criticality computations

In order to determine the criticality index of each pipe segment, two main steps are followed. First, the weights of criticality factors are found utilizing the FANP technique. Next, the criticality index of each segment is computed based on the weights of criticality factors and the effect values

of each segment's characteristics. Figure 4-3 illustrates the set of inputs and outputs of the criticality computation module.

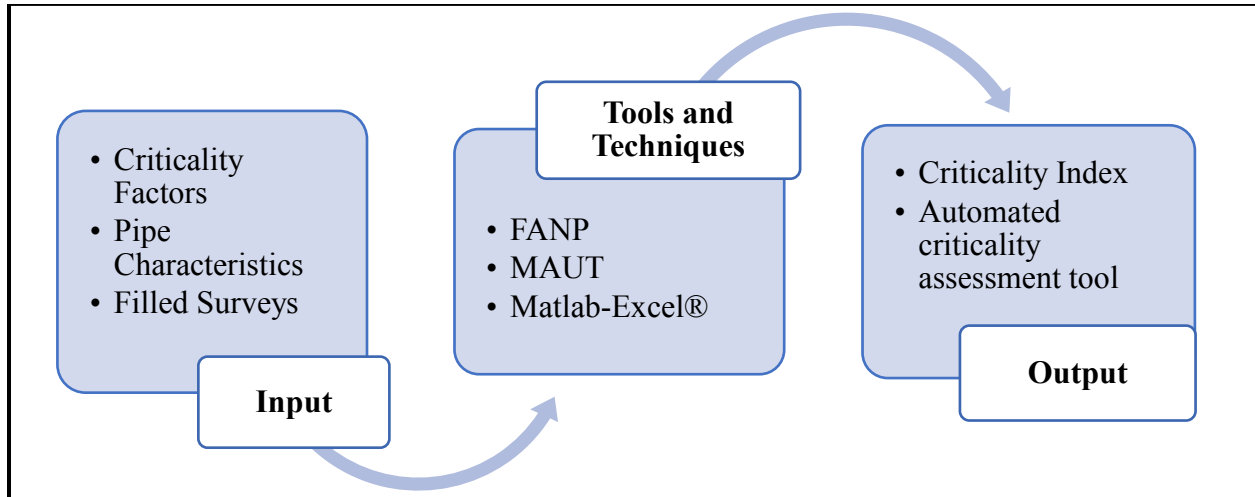


Figure 4-3: Inputs and Outputs of Criticality Computation

A Matlab-Excel interface was written to automate the calculation of criticality factors' weights. First, the survey results are filled in an excel template. The user fills the answers of each respondent, as shown in Figure 4-4. Fuzzifying scale is applied based on the collected responses. Next, the lower, most probable, and upper matrices are formulated using these data. This sheet is then fed as input to the Matlab interface, where the user specifies the sheet number. The user will need to fill to the name, number, of the sheet that contains the answers of an individual participant, as shown in Figure 4-6.

x < WATER MAINS Criticality > 1/x																	
	9	8	7	6	5	4	3	2	1	2	3	4	5	6	7	8	9
Financial	3													Environmental			
Environmental	1/3													Social			
Financial FACTORS																	
	9	8	7	6	5	4	3	2	1	2	3	4	5	6	7	8	9
Size	3													Material			
	3													Depth			
	1													Accessibility			
Material	1/3													Depth			
	1/5													Accessibility			
Depth	1/5													Accessibility			
ENVIRONMENTAL FACTORS																	
	9	8	7	6	5	4	3	2	1	2	3	4	5	6	7	8	9
Size	5													soil type			
	3													Proximity to water streams			
Soil type	1/7													Proximity to water streams			
SOCIAL FACTORS																	
	9	8	7	6	5	4	3	2	1	2	3	4	5	6	7	8	9
Density	3													Road type			
	3													Alternative route			
	3													Facility			
Traffic Disruption	1/5													Alternative route			
	1													Facility			
Alternative route	1													Facility			
ECONOMIC FACTORS																	
	9	8	7	6	5	4	3	2	1	2	3	4	5	6	7	8	9
Environmental Factors	1/3													Social Factors			
ENVIRONMENTAL FACTORS																	
	9	8	7	6	5	4	3	2	1	2	3	4	5	6	7	8	9
Financial Factors	5													Social Factors			
SOCIAL FACTORS																	
	9	8	7	6	5	4	3	2	1	2	3	4	5	6	7	8	9
Financial Factors	3													Environmental Factors			

Figure 4-4: Input Sheets for Criticality Computations

Lower				Upper			
	Financial	Environmental	Social	Financial	Environmental	Social	
Financial	1	1	1	1	2	2	
Environmental	1/2	1	1/2	1	1	1	
Social	1/2	1	1	1	2	1	
Most Probable							
	Financial	Environmental	Social	Financial	Environmental	Social	
Financial	1	1 1/2	1 1/2	1	1 1/2	1 1/2	
Environmental	2/3	1	2/3	1	1	2/3	
Social	2/3	1 1/2	1	1	1 1/2	1	

Figure 4-5: Sample of Automatically Formulated Lower, Upper and Most Probable Matrices

Once a sheet is specified, the FANP computations are performed, and the resulted unweighted, weighted, and limited matrices are automatically written in the same specified sheet. Figure 4-7 captures a sample of these matrices for one of the selected respondents.

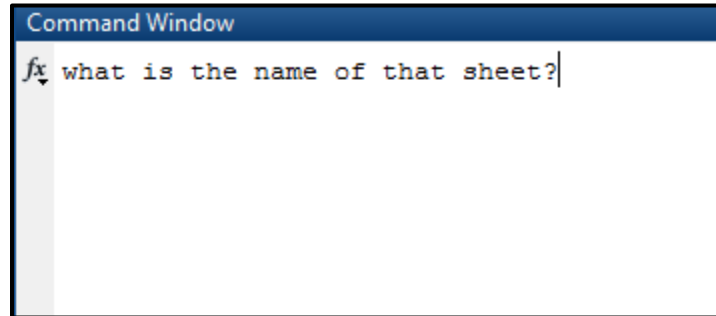


Figure 4-6: A Matlab Interface Asking the User to Specify a Sheet Contacting a Respondent's Answerers

After weights of criticality factors are determined, the user will input the characteristics of the pipe segments inventory. The Excel sheet will automatically calculate the corresponding effect value for each criticality factor possible value. These values will be aggregated with the weights to find the criticality index of each segment. As the characteristics of pipe segments are stored in ARC-GIS shapefiles, these attributes can be readily imported to an Excel sheet where the relevant calculation can be performed as need.

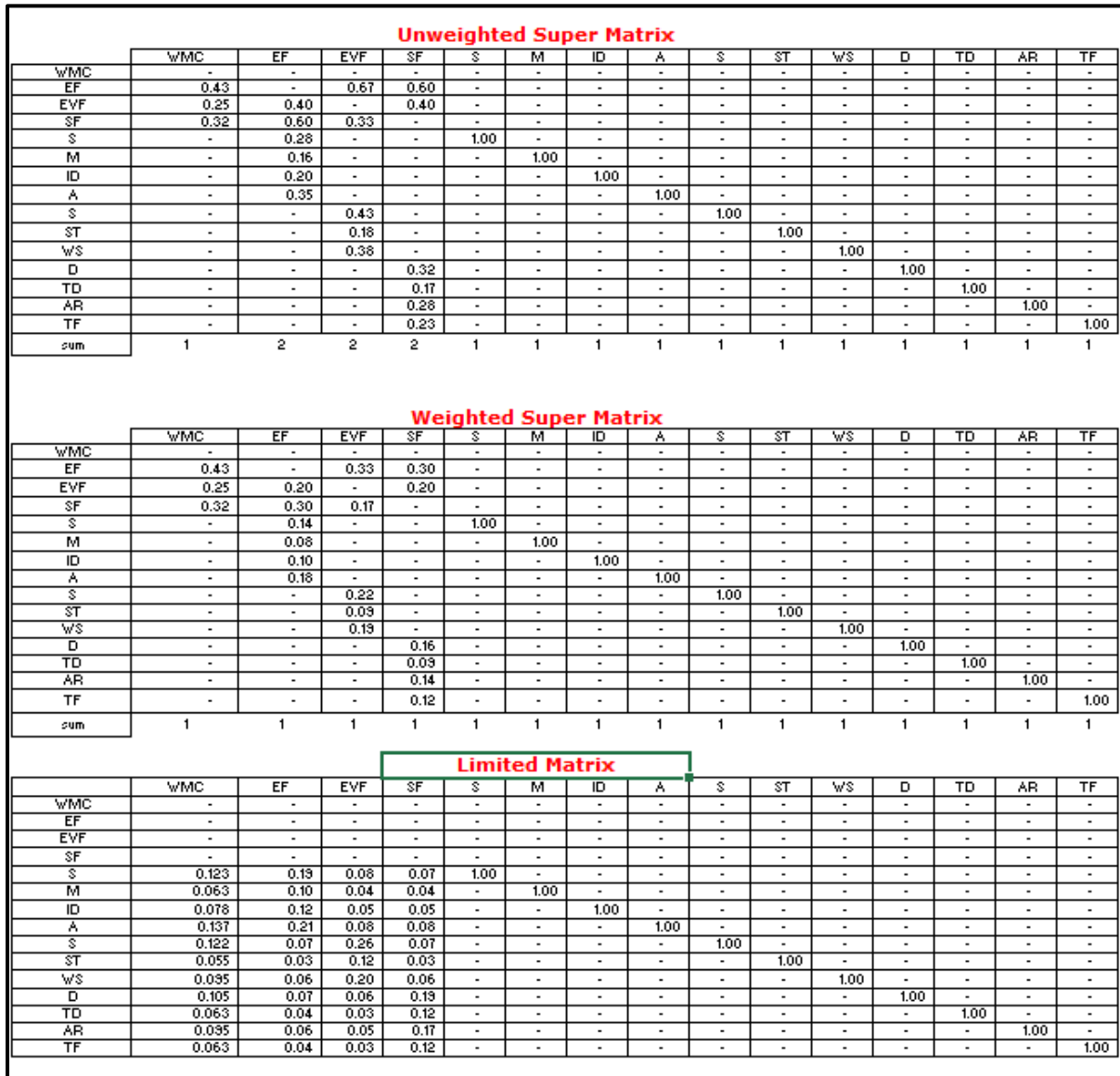


Figure 4-7: Automatically Formulated Matrices for Criticality Computations

4.2.2 Reliability computations

The first step in reliability calculation is to specify the number of previous failures and to compute the time to each failure for each homogenous cohort of pipe segments. To achieve that, two attribute tables are imported from Arc-GIS files to an Excel sheet. The first table represents the breakage dataset of pipe segments. The second table represents some main characteristics of pipe segments such as pipe ID, material type, diameter, and installation date. The output of this

model is the reliability of each pipe segment and its deterioration curve among the subsequent years. Figure 4-8 depicts the inputs and outputs of the reliability computation module.

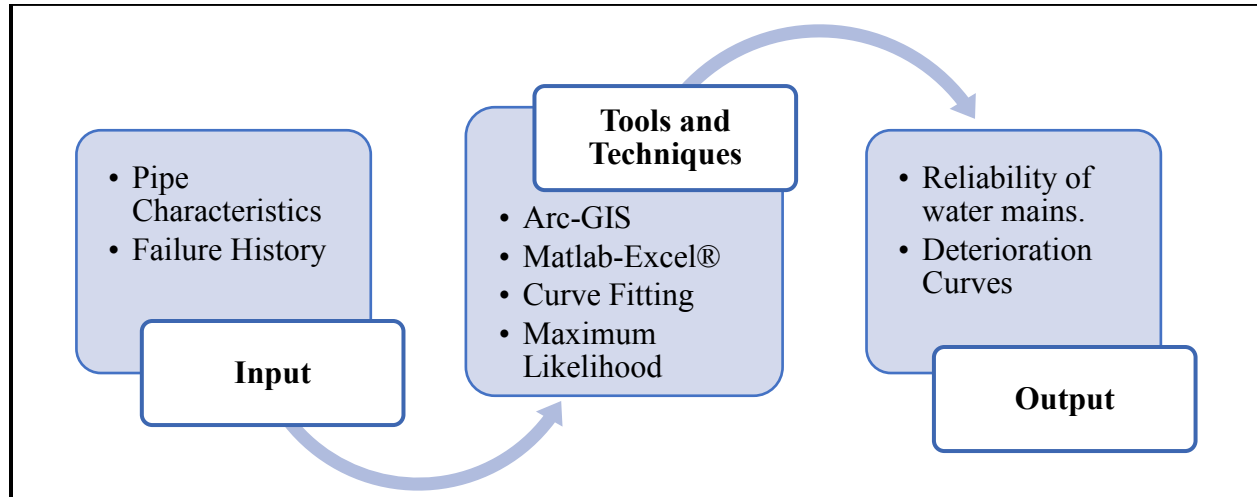


Figure 4-8: Inputs and Outputs of Reliability Computations

Figure 4-9 depicts a sample of breakage data that contains information about the break ID, breaks data, and corresponding pipe ID.

BreakDate ▾	Break ID ▾	PipeInven ▾	Break Type ▾
9/10/1976	68	L100	CIRCUMFERENTIAL
12/1/1982	124	L10006	CIRCUMFERENTIAL
12/17/1988	177	L10006	CIRCUMFERENTIAL
6/23/2015	76	L10006	BLOWOUT
10/15/1984	129	L10017	BLOWOUT
9/22/1987	111	L10018	CIRCUMFERENTIAL
1/6/1994	19	L10018	CIRCUMFERENTIAL
11/25/1977	167	L10025	CIRCUMFERENTIAL
12/2/1977	173	L10025	BLOWOUT
1/17/1988	46	L10025	MISCELLANEOUS
2/13/1994	131	L10025	JOINT
12/9/2007	164	L10025	BLOWOUT
3/15/1987	78	L10027	LONGITUDINAL

Figure 4-9: Sample of Breakage Input Data

A Matlab code is written to count the number of breaks for each pipe segment and to calculate the inter-break times as detailed in section 3.2. Figure 4-10 illustrates the result of this step.

BreakDate	Break ID	PipeInvent	# of Breaks	Break Type
9/10/1976	68	L100	1	CIRCUMFERENTIAL
12/1/1982	124	L10006	3	CIRCUMFERENTIAL
12/17/1988	177	L10006		CIRCUMFERENTIAL
6/23/2015	76	L10006		BLOWOUT
10/15/1984	129	L10017	1	BLOWOUT
9/22/1987	111	L10018	2	CIRCUMFERENTIAL
1/6/1994	19	L10018		CIRCUMFERENTIAL
11/25/1977	167	L10025	5	CIRCUMFERENTIAL
12/2/1977	173	L10025		BLOWOUT
1/17/1988	46	L10025		MISCELLANEOUS
2/13/1994	131	L10025		JOINT
12/9/2007	164	L10025		BLOWOUT
3/15/1987	78	L10027	3	LONGITUDINAL
3/10/2002	86	L10027		CIRCUMFERENTIAL
3/9/2013	68	L10027		CIRCUMFERENTIAL

Figure 4-10: Output Sample of Breaks Counting and Connecting to Pipe Segments

Another Matlab code was then written to determine the best distribution that fits the deterioration behavior of each cohort of pipe segments. A cohort of pipe segments shares the same material type and size range. This step was repeated for each break order, i.e., time to first break, time to second break, etc. This Matlab interface is integrated within an Excel environment such that an excel sheet is automatically opened when the code is run to allow the user to select the inter-failure time set of interest. Parameters of various investigated distribution fits are automatically written on the Excel sheet along with the results of the Anderson-Darling test. Figure 4-11 shows a sample of these results for a specific break order of a particular segment's cohort.

Goodness of Fit Test		
1. Normal	Mean	Std
	10.182	7.903
P-Value	0.010	
AD	0.991	
2. Weibull	Scale	Shape
	11.066	1.305
P-Value	0.170	
AD	0.534	
3. Exponential	Rate	
	10.182	
P-Value	0.279	
AD	0.689	
4. Extreme Value	Location	Scale
	14.437	8.871
P-Value	0.001	
AD	1.550	
5. LogNormal	Scale	Shape
	14.437	8.871
P-Value	0.130	
AD	0.566	

Figure 4-11: Output Sample of Inter-failure Time Fitting

Once the distribution fit is determined along with its associated parameters, the reliability and expected deterioration for each pipe segment can be estimated based on its relevant cohort, break order, and age.

4.2.3 Resilience computations

Once reliability and criticality of each pipe segment are calculated, the resilience assessment computation proceeds. Criticality and reliability values are firstly aggregated at the network level to compute the network robustness. The user is also required to specify the number of nodes and links in the selected network to facilitate the meshed-ness calculation. Network resilience is then calculated based on the computed network robustness, redundancy, and relative weight of each.

Figure 4-12 shows the window that asks the user to specify the parameters needed to calculate the network resilience. The output of this step is the resilience level for the specified network.

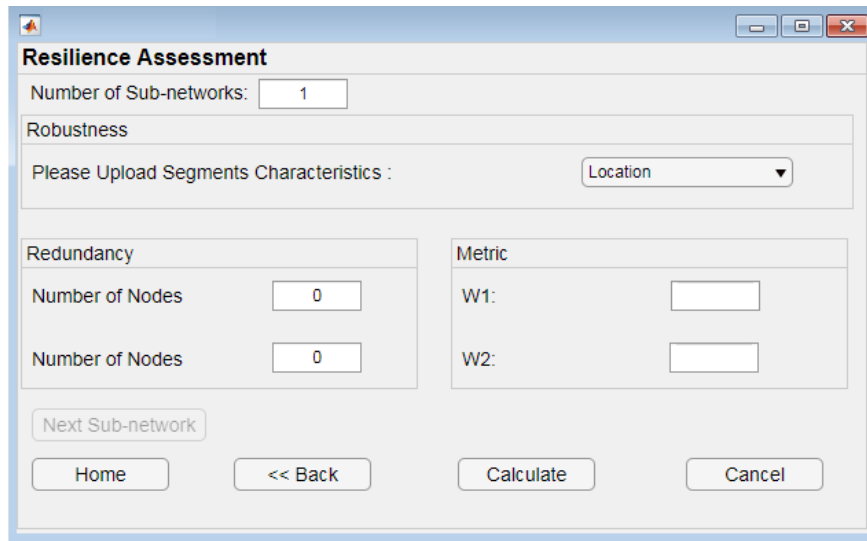


Figure 4-12: Resilience Assessment Input Window

4.3 Resilience Restoration Module

Resilience restoration module takes three sets of inputs, which represent the results of three sub-models, namely: resilience assessment model, restoration model, and relocation model. Figure 4-13 depicts the inputs and output of this restoration module. Below is a brief description of the tool that integrates the computations of this module.

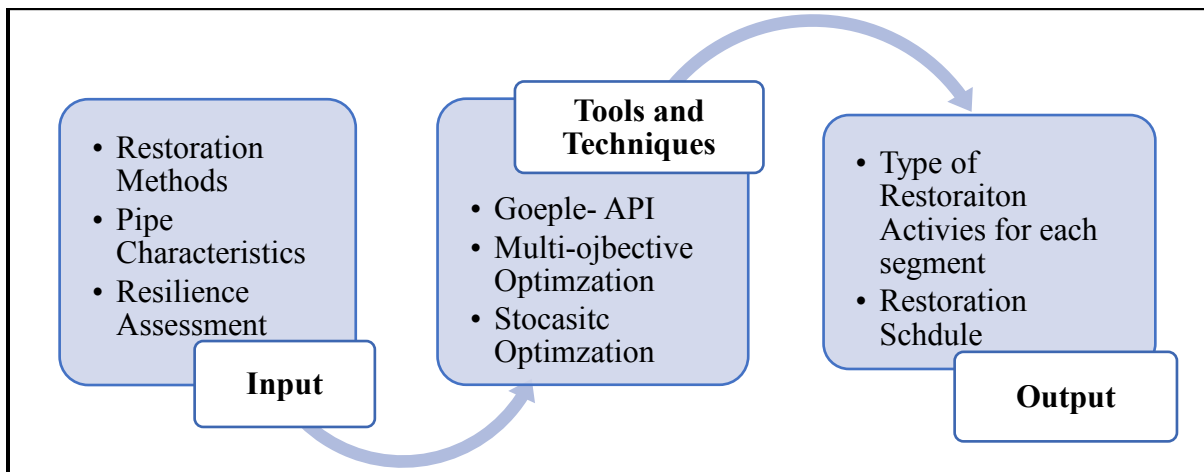


Figure 4-13: Inputs and Outputs of Resilience Restoration Module

Firstly, the user has to list the repair and replacement techniques that will be considered as decision variables in the optimization model, as shown in Figure 4-14. By default, mechanical clamp, pipe bursting, pipe splitting, and open-cut methods are included. The user can choose to disregard any of these methods or to add other new methods. In addition, the user is asked to provide the unit cost and time of each of the considered methods.

Method	Status	Unit Cost (\$/mm2/m)	Unit Cost (Day/m)
Pipe Bursting (PB)	<input type="checkbox"/>	0	0
Pipe Splitting (PS)	<input type="checkbox"/>	0	0
Mechanical Clamps	<input type="checkbox"/>	0	0
Open Cut Method (OCM)	<input type="checkbox"/>	0	0

Buttons: Add Method, Home, << Back, Next >>, Cancel

Figure 4-14: Restoration Methods Input Window

Secondly, the user is directed to upload a matrix containing the X and Y coordinates of the failed segments' locations. An origin-distention matrix, ODM, is then formulated using these coordinates. A Google API is then run to find the travel time and distance between the locations of the ODM based on routing and traffic conditions. The relocation cost is then computed by multiplying the unit rate of the repair crew by the relocation time. The results of this model are then written on an Excel sheet, as shown in Figure 4-15. Figure 4-15 shows a sample of relocation time between some of the locations of the failed segments. Similar results were obtained for relocation costs as well.

Location	1	6	10	12	17	25	33	34	42	47	53	55	58	60
1	0	5 mins	5 mins	6 mins	3 mins	3 mins	5 mins	4 mins	3 mins	5 mins	3 mins	3 mins	4 mins	5 mins
6	4 mins	0	3 mins	4 mins	7 mins	6 mins	4 mins	4 mins	4 mins	3 mins	7 mins	7 mins	4 mins	1 min
10	6 mins	2 mins	0	2 mins	7 mins	7 mins	1 min	5 mins	5 mins	4 mins	7 mins	7 mins	4 mins	3 mins
12	8 mins	5 mins	2 mins	0	8 mins	7 mins	1 min	6 mins	6 mins	6 mins	8 mins	7 mins	7 mins	5 mins
17	3 mins	5 mins	5 mins	6 mins	0	3 mins	5 mins	4 mins	3 mins	4 mins	3 mins	2 mins	3 mins	5 mins
25	3 mins	4 mins	6 mins	8 mins	4 mins	0	7 mins	6 mins	4 mins	3 mins	4 mins	4 mins	1 min	4 mins
33	7 mins	3 mins	1 min	1 min	8 mins	8 mins	0	6 mins	6 mins	5 mins	8 mins	8 mins	5 mins	3 mins
34	6 mins	3 mins	3 mins	5 mins	5 mins	5 mins	4 mins	0	4 mins	4 mins	7 mins	6 mins	5 mins	3 mins
42	4 mins	3 mins	2 mins	4 mins	3 mins	2 mins	3 mins	2 mins	0	2 mins	4 mins	3 mins	3 mins	3 mins
47	3 mins	4 mins	5 mins	7 mins	4 mins	4 mins	6 mins	5 mins	4 mins	0	4 mins	4 mins	1 min	4 mins
53	3 mins	5 mins	4 mins	6 mins	3 mins	2 mins	5 mins	4 mins	2 mins	4 mins	0	1 min	3 mins	5 mins
55	4 mins	4 mins	4 mins	6 mins	2 mins	2 mins	4 mins	4 mins	2 mins	4 mins	3 mins	0	3 mins	5 mins
58	2 mins	4 mins	5 mins	7 mins	3 mins	3 mins	6 mins	5 mins	3 mins	3 mins	3 mins	3 mins	0	4 mins
60	4 mins	1 min	3 mins	4 mins	7 mins	7 mins	4 mins	5 mins	4 mins	3 mins	7 mins	7 mins	4 mins	0

Figure 4-15: Sample of Relocation Time Results

The main piece of input to this model encompasses the pipe segments, material type, size, length, soil type, age, and the number of previous breaks. These data are utilized in specifying pipe cohort, a list of suitable restoration methods, and the deterioration curve. These data are imported to an Excel sheet as an attribute table from Arc-GIS shapefiles. The user is then asked to specify the budget constraint, minimum resilience threshold, and the maximum number of breaks after which any pipe segment shall be replaced, as shown in Figure 4-16

Figure 4-16: Resilience Restoration Input Window

The optimization will be run utilizing the Excel add-in Evolver and @Risk from Palisade Inc. Results are then shown as a restoration plan that encompasses the sequence of segments

restoration, assigned crew, and restoration method for each. This restoration plan is automatically printed on the Excel Sheet, as shown in Figure 4-17.

Task	Restoration Method	Responsible	Start Date	Target Date
Restoring Seg. 18	Clamp	Crew #1	3/1/2020	3/1/2020
Restoring Seg. 10	Pipe Bursting	Crew #2	3/1/2020	3/4/2020
Restoring Seg. 29	Open-Cut	Crew #3	3/1/2020	3/9/2020
Restoring Seg. 28	Pipe Splitting	Crew #4	3/1/2020	3/3/2020
Restoring Seg. 17	Clamp	Crew #5	3/2/2020	3/3/2020
Restoring Seg. 12	Clamp	Crew #5	3/3/2020	3/3/2020
Restoring Seg. 2	Pipe Bursting	Crew #1	3/3/2020	3/5/2020
Restoring Seg. 5	Pipe Bursting	Crew #5	3/3/2020	3/4/2020
Restoring Seg. 4	Clamp	Crew #2	3/5/2020	3/5/2020
Restoring Seg. 9	Pipe Bursting	Crew #1	3/5/2020	3/6/2020
Restoring Seg. 15	Pipe Bursting	Crew #2	3/5/2020	3/7/2020
Restoring Seg. 26	Pipe Splitting	Crew #1	3/6/2020	3/9/2020

Figure 4-17: Sample of Resilience Restoration Module Output

4.4 Resilience Enhancement Module

This resilience enhancement model aims at determining the list of optimal enhancement activities for each segment and scheduling these actions after being clustered into work packages. Figure 4-18 illustrated the list of inputs and outputs of the resilience enhancement model. A brief description of the tool that integrated these actions is presented below.

Similar to the resilience restoration module, the user is first asked to list the enhancement interventions that will be considered as decision variables in the optimization model. By default, pipe bursting, cast in place pipe, and epoxy lining are included. The user can choose to disregard any of these methods or to add other new methods. In addition, the user has to provide the unit cost and time of each of the considered methods. Also, expected the CO₂ emissions per unit length per unit area of each enhancement intervention actions are required. Figure 4-19 shows the window for defining the list of considered enhancement intervention actions.

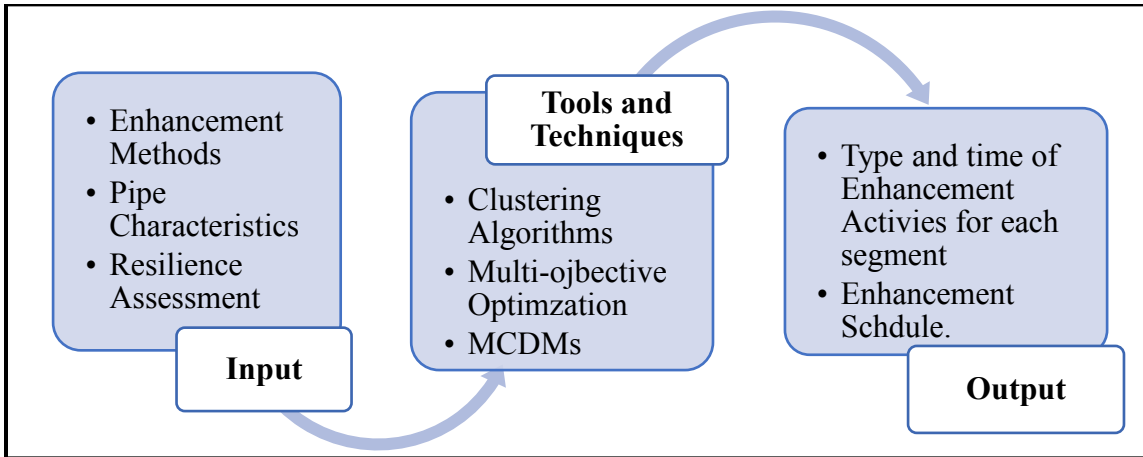


Figure 4-18: Inputs and Outputs of Resilience Restoration Module

The screenshot shows the 'Enhancement Methods' input window. It contains a table for selecting methods, with columns for Method, Status, Type, Unit Cost (\$/mm2/m), Unit Cost (Day/m), and Average Unit CO2 (CO2-e tonne/mm2/m). The methods listed are Epoxy Lining (EL), Cast in Place Pipe (CIPP), and Pipe Bursting (PB). Each method has a status checkbox, a type dropdown menu (set to 'Minor'), and three input fields for cost and CO2 values, all currently set to 0. There are also buttons for 'Add Method', 'Home', '<< Back', 'Next >>', and 'Cancel'.

Method	Status	Type	Unit Cost (\$/mm2/m)	Unit Cost (Day/m)	Average Unit CO2 (CO2-e tonne/mm2/m)
Epoxy Lining (EL)	<input type="checkbox"/>	Minor	0	0	0
Cast in Place Pipe (CIPP)	<input type="checkbox"/>	Minor	0	0	0
Pipe Bursting (PB)	<input type="checkbox"/>	Minor	0	0	0

Figure 4-19: Enhancement Methods Input Window

Each intervention action will result in different improvement and deterioration behavior. If segment replacement is chosen, the reliability values of the segment along the subsequent five years are derived utilizing the deterioration curve that represents the time to the first failure of the cohort to which this segment belongs. Similarly, minor and major interventions will change the deterioration behavior of pipe segments to ones that had the same number of previous failures and experienced similar intervention actions. However, minor and major actions would typically result in an immediate performance improvement that can be specified by the user.

The second set of input is the list of pipe segment’s characteristics for each sub-network. In this input, the user will provide information about the pipe segments such as their size, length, and material type, number of previous breaks, reliability, and criticality. The current reliability curve, distribution parameters, is required to determine the reliability improvement realized by each intervention action, as explained above. These inputs can be imported from an excel sheet, as shown in Figure 4-20. The user is then required to specify the current redundancy components of each considered sub-network. Relative weights of resilience metric components can be changed when filling the data of the first sub-network. Finally, the overall resilience level is calculated as a weighted average of individual sub-networks resilience values, with the sub-network lengths used as weights. The weighted resilience is then normalized by the total length of the considered networks. The resilience level of each network, along with the overall resilience level, will then be printed on the Excel Sheet. A minimum resilience threshold needs to be determined for each sub-network. Also, the annual and total available budgets as well as the interest discount rate along the considered planning horizon need to be identified, as shown in Figure 4-21.

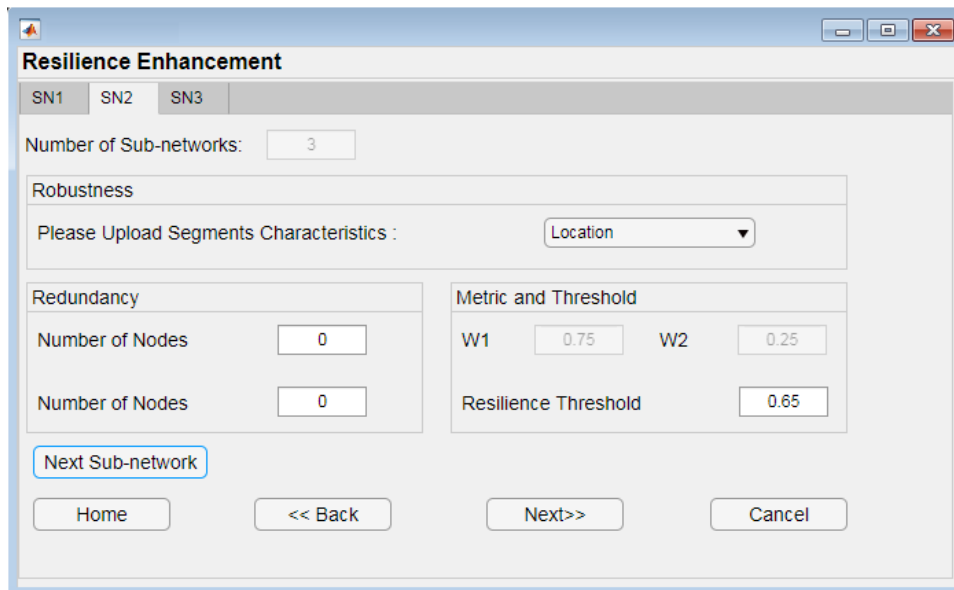


Figure 4-20: Resilience Enhancement Input Window

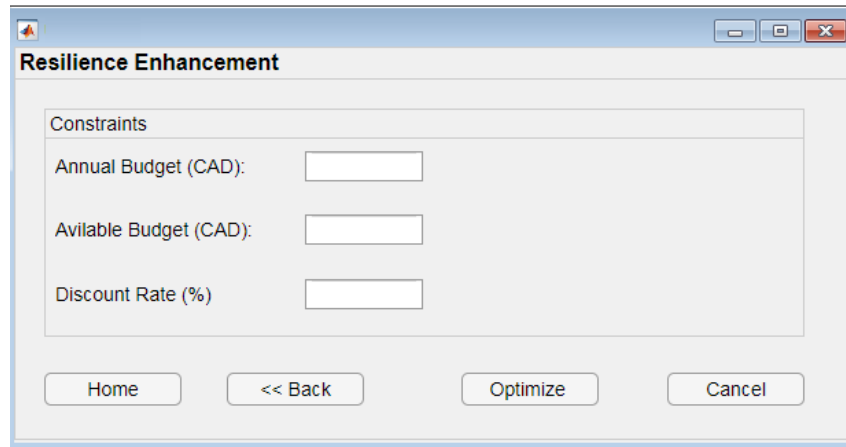


Figure 4-21: Resilience Enhancement Constraints Input Window

The optimization will then run within the Matlab environment, and the results of this phase will be imported to an Excel sheet. The result of this phase represents a set of optimal resilience enhancement plans, as suggested by the optimization algorithm. Shannon Entropy calculation will then proceed within the same Excel Sheet to determine the weights of each objective, as shown in Figure 4-22. These weights and the obtained solutions are then exported to the Visual PROMETHEE software package (Maier et al. 2003) to determine the optimal solution from the set of candidate Pareto.

The X and Y coordinates of each pipe segment are required to cluster the networks into a set of zones based on their geographical location. This clustering is performed utilizing the RapidMiner platform and is not automated within this tool. Hence, the user would have to provide this clustering result as an input for the packaging and scheduling step. In this step, the intervention actions of a specific year, or years, are fed as inputs along with their durations, costs, and resilience improvements. Type of each intervention and zone at which corresponding segment is located are also required, as shown in Figure 4-23.

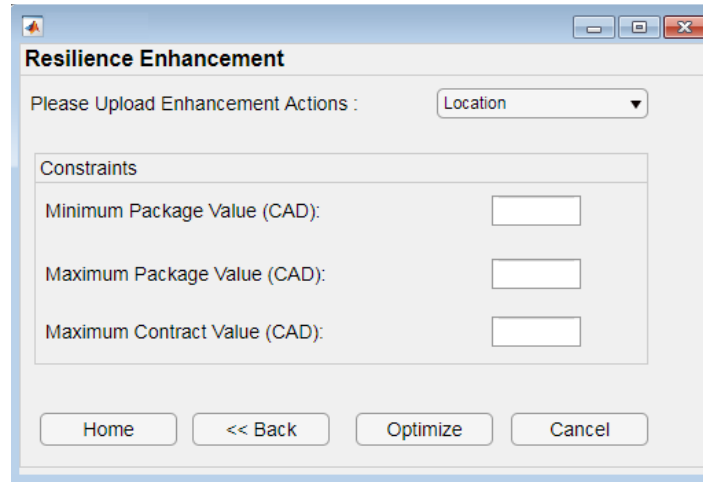
Solution	Cost	Resilience	CO2 Emissions
1	1637403.716	0.6442767	133
2	1628295.874	0.6443397	139.2
3	1626081.3	0.643672	138
4	1815164.379	0.6457779	136.1
5	1624256.558	0.64358	137.5
6	1666685.979	0.6453535	134.8
7	1657574.319	0.6456883	136.1
8	1707167.562	0.6455424	134.8
9	1615887.42	0.6432448	137.7
10	1692530.644	0.6451408	134.5
11	1652363.552	0.6450683	135.7
12	1655642.674	0.6455384	136.1
13	1610153.645	0.6430659	136
14	1623311.991	0.6434227	137.2
15	1651539.108	0.6448892	134.1
16	1655060.249	0.6452683	134.9
17	1634179.569	0.6442086	133.8
18	1605534.99	0.6429193	135.7
19	1650666.624	0.6447305	132.7
20	1638139.775	0.6443904	133.3
Weights	51.23%	30.25%	18.52%

Figure 4-22: Sample of Resilience Enhancement Output - Phase I

Action No.	Res Impr	Cost	Time	Method	Zone
1	0.00064	5,713.7154	0.4612	CIPP	1
2	0.00068	2,501.8103	0.2019	CIPP	1
3	0.00100	11,667.3612	0.7384	PB	1
4	0.00034	2,995.9592	0.4513	EL	2
5	0.00024	2,781.2499	0.2245	CIPP	1
6	0.00036	2,771.1436	0.4174	EL	2
7	0.00072	7,318.6175	0.5907	CIPP	1
8	0.00043	13,545.6194	0.7289	CIPP	1
9	0.00089	23,830.4393	1.2824	CIPP	2
10	0.00089	14,073.9935	0.5680	CIPP	1
11	0.00051	6,746.5260	1.0163	EL	2
12	0.00035	4,460.0388	0.6718	EL	1
13	0.00060	5,466.2754	0.8234	EL	1
14	0.00043	12,797.7269	1.9278	EL	1
15	0.00053	5,070.7619	0.7638	EL	2
16	0.00061	7,282.7244	1.0970	EL	2

Figure 4-23: Sample of Inputs to the Packaging and Scheduling Step

The user is then asked to specify the minimum and maximum values of each package along with the maximum contract value as shown detailed in section 3.4 as shown in



The image shows a software dialog box titled "Resilience Enhancement". At the top, it says "Please Upload Enhancement Actions :" followed by a dropdown menu currently set to "Location". Below this is a section titled "Constraints" which contains three input fields: "Minimum Package Value (CAD):", "Maximum Package Value (CAD):", and "Maximum Contract Value (CAD):". At the bottom of the dialog are four buttons: "Home", "<< Back", "Optimize", and "Cancel".

Figure 4-24: Packaging Constraints Input Window

Evolver, adds-in solver, is utilized to run the packaging and scheduling optimization. The output of this model, which consists of two components, is finally presented on the same Excel sheet. The first component includes the list of intervention actions of pipe segments that achieves the optimal values according to the considered constraints. The second component represents the packaging and scheduling results of the enhancement intervention actions. Intervention actions are clustered such that those sharing similar intervention type and geographical zone are clustered into one package while respecting the maximum package size.

4.5 Dashboard

This section presents the concept and main features of the developed dashboard that integrates the results of the developed resilience modules. The dashboard facilitates visualization of the main characteristics of pipe segments along with the results of the previously developed modules in a single platform. The main purpose of this visualization is to support timely decisions regarding resilience enhancement and restoration activates. The dashboard is designed and fully

integrated within Arc-GIS environment. It is also available as a Webpage application that can be accessed online without the need to install the Arc-Map software package. Distinct levels of access can be granted for different users to visualize, update, and even modify the developed dashboard based on their organizational role.

Figure 4-25 depicts the main components of the developed dashboard. Characteristics of pipe segments encompasses information regarding segments sizes, material types, breakage history, and external condition. These information were imported from attribute tables available at the different shapefiles provided by the City of London, Ontario. Next, the results of the previously developed resilience modules are imported from their excel sheets to the main layer dedicated for establishing this dashboard. Arc-Pro was utilized to publish this layer along with tis features as a web map. The last step involved creating the different widgets by selecting specific pairs, or more, of variables whose relationship need to be assessed and visualized. Current widgets can be modified and new ones can be created based on user's input. Various levels of filtering and dynamic relationship were designed as will be shown subsequently. Figure 4-26 depicts the homepage of the developed dashboard.

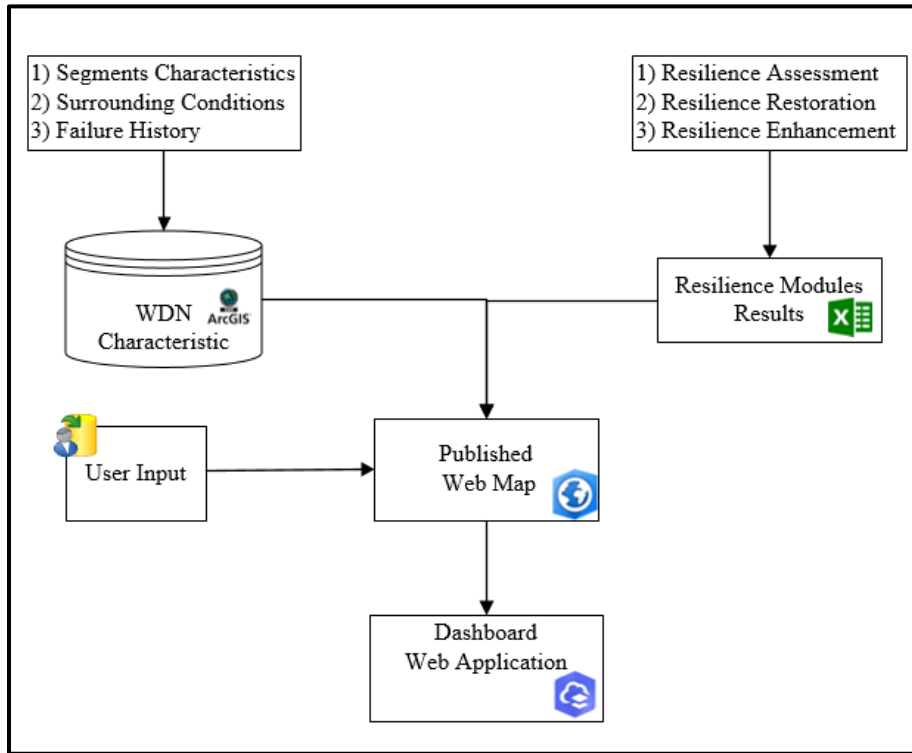


Figure 4-25: Dashboard Components



Figure 4-26: Homepage View of London WDN Dashboard

In Figure 4-26, the top right filter is used to select the specific sub-network of the entire considered section of the London WDN. These sections were generated based on land use, population density, tax base, and other factors, as illustrated in section 3.4. Once a particular network is chosen, all the widgets are updated to reflect the data of the selected network. These widgets include the distribution of the segments' sizes, ages, and material types. Also, the average age of the selected segments is shown. Results of the reliability calculation are transferred into a condition rating scheme that consists of four degrees, namely: very poor, poor, good, and very good. These rankings are shown on the condition widgets, which specifies the number of pipe segments in each condition rating. The results of the resilience enhancement module are also shown in this dashboard. A special widget is created to show the number and individual pipe segments for each resilience enhancement action along each year of the planning horizon. Finally, the resilience assessment widget is used to show the results of resilience metric components, namely: redundancy, robustness, and resilience for each sub-network. Figure 4-27 shows a different view of the developed dashboard at which sub-network 2 is chosen. It can be observed that all distribution widgets and measures are updated to reflect the data of the selected network. For example, the average age of the pipe segments in sub-network 2 is around 37 years, and the replacement value is around CAD 21.6 million. Size, material, age distribution, condition, and resilience enhancement actions are also updated, as shown in Figure 4-27.



Figure 4-27: Sub-network 2 View of London WDN Dashboard

All the created widgets are dynamically connected to facilitate deriving whatever needed metric by the decision-makers. For example, Figure 4-28 and Figure 4-29 show the updated views when segments in poor and good conditions are selected, respectively. The age, size, material, and resilience enhancement widgets are automatically updated. As expected, the average age is bigger for segments that are in poor conditions. Besides, most of the enhancement actions for such segments are either major actions or full replacement, unlike those in good conditions where minor enhancement actions are the dominant options are depicted in Figure 4-27 and Figure 4-28. Relationships between the age and condition, age and resilience enhancement actions, and resilience enhancement actions and condition can be readily validated utilizing this dynamic tool.



Figure 4-28: Segments in Poor Condition View of London WDN Dashboard



Figure 4-29: Segments in Good Condition View of London WDN Dashboard

Breakage data are also innovatively presented in this dashboard. Two main views are created for this purpose. The first one is a heat map of breaks along the selected section of London WDN. This heat map is essential in identifying critical sections of the network that experienced

more frequent series of breakage incidents. Efforts are then paid to study and analyze the internal and external factors that contribute to such failure increase. For example, Figure 4-30 shows the heat map of the previous break incidents in the considered section of the London water network. It can be observed from Figure 4-30 that specific segments experienced a higher breakage rate as indicated by bigger and darker bubbles. Asset managers can then derive a relationship between this increase in breaks from one side and the characteristics of those segments and the surrounding conditions such as traffic volume from the other side.

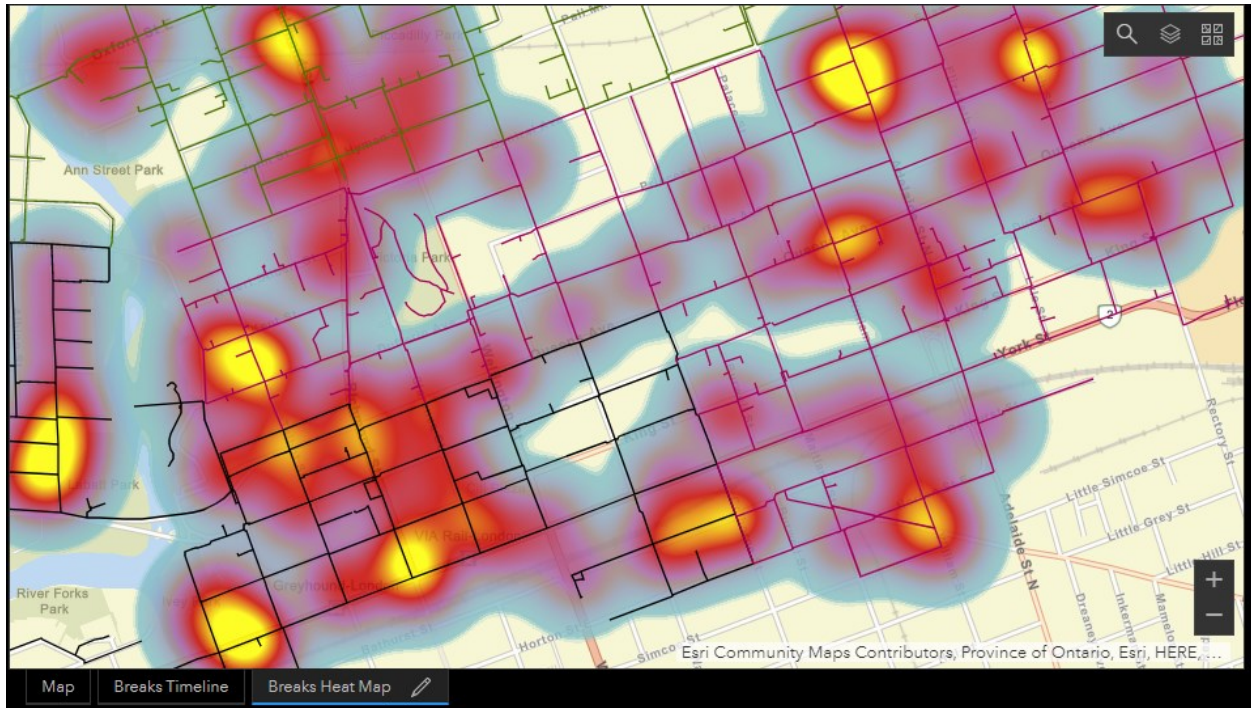


Figure 4-30: Breaks Heat Map of London WDN

In addition, a breakage timeline is also developed such that it dynamically shows the occurrence of segments' breaks along their service lives since installation until 2017, the data at which these data were collected. This timeline is vital in understanding how breaks propagated in the past and how certain existing breaks may contribute to the formation of new ones in the future. Figure 4-31 illustrates a sample of this created timeline for the considered section of London WDN

for the period from December 1973 until December 2017. Breaks are consecutively shown in this view, bright red bubbles, as the time elapses during the selected period.

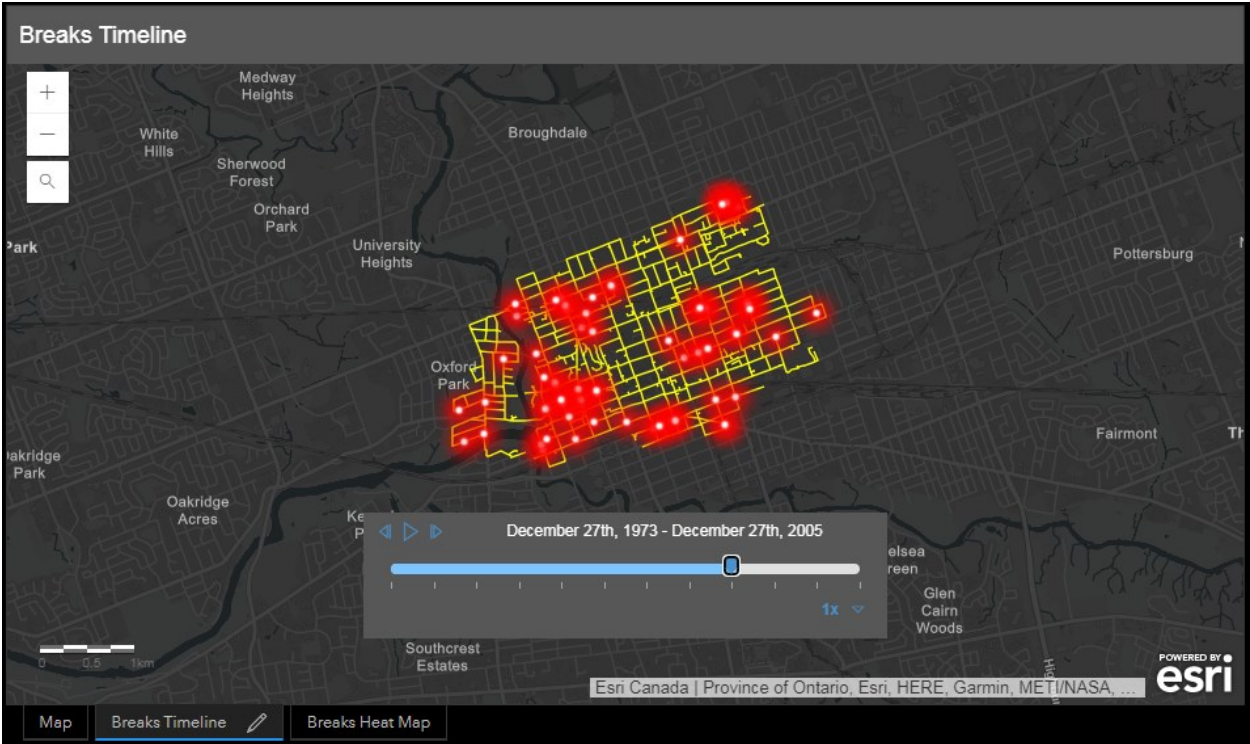


Figure 4-31: Breaks Timeline of London WDN

4.6 Summary

This chapter introduced a graphical user interface that integrates various components of the developed resilience-based WDNs management methodology. Several feature windows of the inputs and outputs as well as the fields of user-defined variables were shown. This integration tool was coded in Matlab® to integrate a set of Matlab codes and Excel Sheets. Finally, the results of applying the developed modules on London WDN were integrated and visualized utilizing a specially developed dashboard that is fully integrated within Arc-GIS environment.

Chapter 5: Testing and Validation

5.1 Overview

In this chapter, the application of different developed models on real WDNs is presented. To demonstrate the robustness and validity of the developed models, their performance was evaluated through different case studies. The implementation phase encompasses applying three main models, along with their various components. Firstly, the resilience assessment model is applied to evaluate the resilience level of a section in London's water distribution network. Then, a random failure scenario is assumed, leading to multiple breaks and leaks along with the network. Users can specify the intensity of assumed scenarios by changing the number of expected breaks and leaks in the network. Different recovery strategies are then investigated through a multi-objective restoration model. Finally, the resilience level of a larger section of London's water distribution network is enhanced through a multi-objective resilience enhancement model. The considered section was bigger in the third case study to demonstrate various capabilities and features of the resilience enhancement model.

Figure 5-1 depicts the steps for the application and validation of the developed models. In Figure 5-1, the performance of the newly developed metric was assessed by comparing with two previously developed resilience metrics. One topology-based and one hydraulic-based metric were utilized for this purpose. The resilience-based restoration model was verified on two steps: first, the best performing optimization algorithm was selected, then the obtained restoration strategy was compared to a plan suggested by the City of London. Similarly, different optimization algorithms were investigated to pick the best performing one to solve the resilience enhancement model. Subsequently, the attained enhancement plan was compared to a plan generated utilizing existing management portfolio practice.

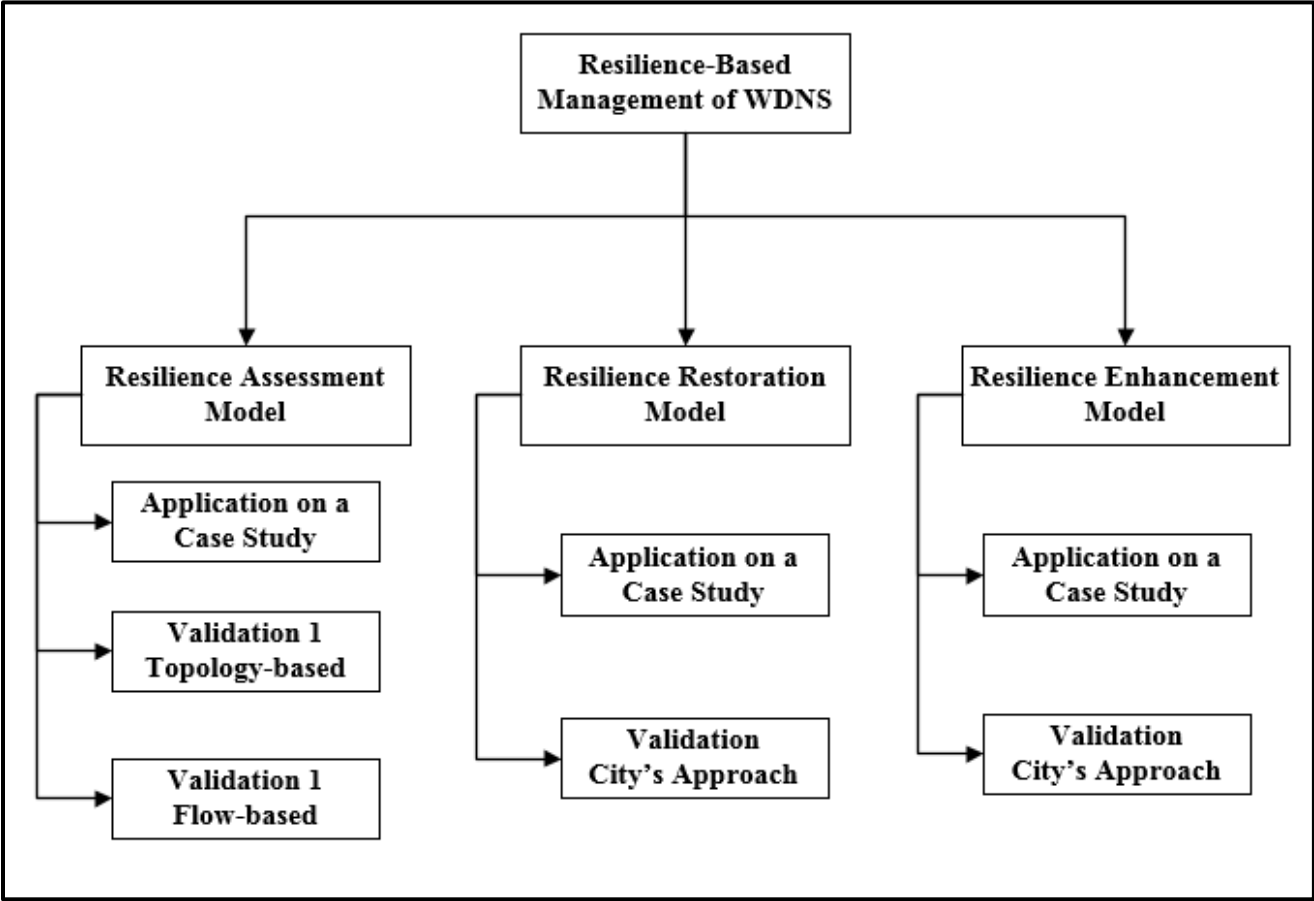


Figure 5-1: Developed Models’ Application and Validation

The City of London was incorporated in 1855 and rapidly established itself as a business hub in southern Ontario. The City of London owns a water main network in excess of 1,500 Km with a replacement value of more than \$2.7B (SOI 2013). The total number of pipe segments in the network is more than 24,000, with some installed as far back as 1900 and are still active until today. Table 5-1 shows a sample for the data found in the GIS shapefiles regarding the characteristics of the pipe. As shown in Table 5-1, data such as the segment’s length, diameter, material type, year of installation, start, and end nodes are available. In addition, details about the status of each segment, whether active or abandoned, are found.

Table 5-1: Sample Pipelines Characteristics in GIS Shapefiles (London, Ontario)

Pipe ID	Nominal Size (mm)	Length (m)	Start Node	End Node	Installation Date	Material	Status
549	100	186.771	N10743	N10742	1/1/1986	DI	Abandoned
682	200	227.442	N11911	N14895	1/1/1985	DI	Abandoned
2038	300	232.8505	N4143	N5109	1/1/1979	CI	Active
2085	100	98.3560	N11152	N11296	1/1/1973	CI	Active
2105	200	73.9638	N4144	N4143	1/1/1988	DI	Active
2163	200	64.889	N11172	N11152	1/1/1966	CI	Active
2183	200	55.4926	N11316	N10805	1/1/1988	DI	Active

Pipe segments of the London water distribution network are composed of different material types such as cast iron (CI), ductile iron (DI), Polyvinyl chloride (PVC copper), copper, concrete, and others. Figure 5-2 shows a distribution of pipe segments in London WDNs based on their material type. It can be observed from Figure 5-2 that PVC is the most available material in the network, followed by CI and DI pipes. The “others” category in Figure 5-2 includes pipe segments that are made of material types such as copper, steel, galvanized steel, Polyethylene. These pipe segments represent a tiny portion of the total pipe segments in London WDN.

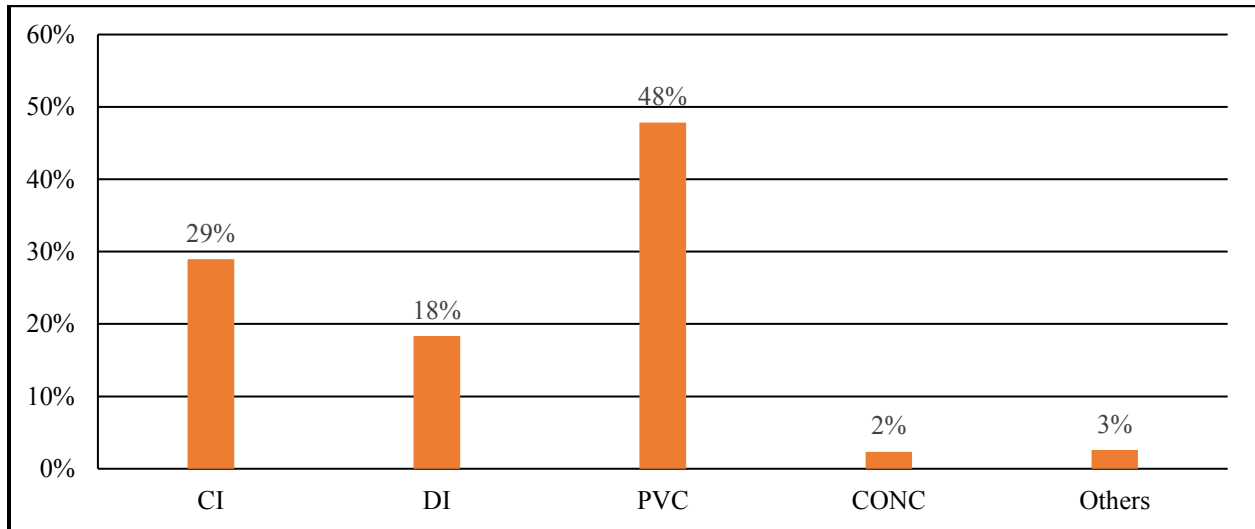


Figure 5-2: Distribution of Pipes' Material in Collected Data

On the other hand, Figure 5-3 depicts the distribution of pipe segments in the City of London according to their size. London WDN encompasses a broad spectrum of pipe sizes that

ranges from 40 mm in diameter to 1350 mm in diameter. Large diameter pipes are only needed for transmission of water from the source to the distribution pipes. Most of the pipe segments in this water network are of 150 mm to 250mm in diameter. These categories constitute the vast majority of available sizes, as evidenced in Figure 5-3.

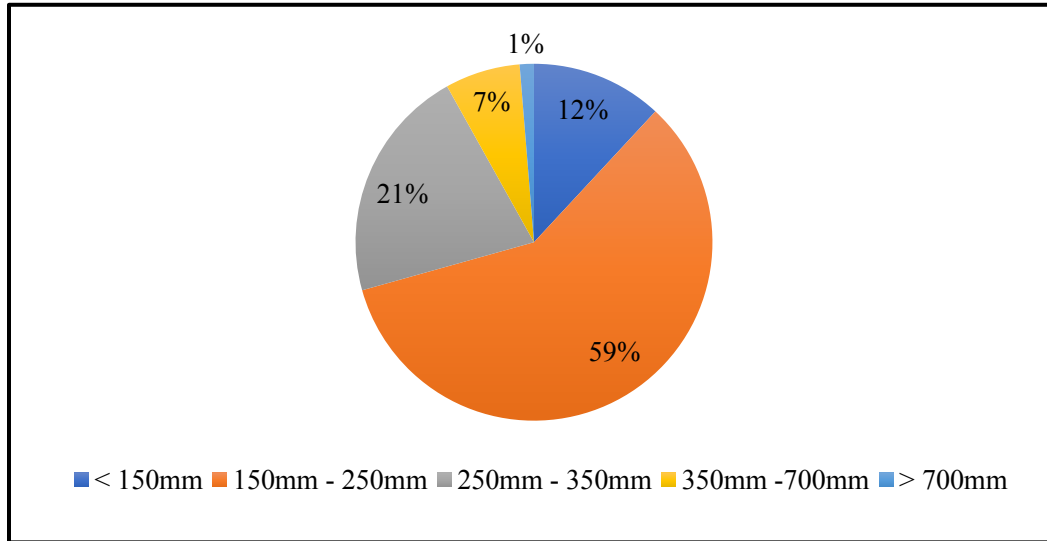


Figure 5-3: Distribution of Pipes’ Diameters in Collected Data

Another set of information regarding external surrounding conditions of water pipe segments was also extracted from GIS shapefiles. These conditions are expressed by some socioeconomic parameters associated with each water pipe segment. Table 5-2 illustrates a sample of these data which includes information about the street's types, soil types, and serviced facilities of various water segments. The main soil types available in the City of London are sand, clay, Alluvium, and sand gravel. Water segments in the City of London are buried under different types of streets. According to the road class, size, and number of lanes, the volume of traffic could be either low, medium, or high. Water segments secure the provision of water for various types of facilities. These facilities could be either residential, the most common type, commercial, industrial, or parks. These parameters are vital in estimating the criticality associate with each pipe segment.

Table 5-2: Sample Pipelines Surrounding Conditions in GIS Shapefiles (London, Ontario)

Pipe ID	Soil Type	Traffic Volume	Type of Facility
549	Sand	Residential	Low
682	Sand	Industrial	Low
2038	Sand	Commercial	High
2085	Clay	Residential	High
2105	Alluvium	Commercial	High
2163	Sand	Residential	Low
2183	Clay	Residential	Low

Finally, geographical features were also available in GIS shapefiles. In this type of data, connectivity options, coordinates, elevations could be retrieved. Figure 5-4 depicts a view of the water distribution network in the City of London. Coordinates of the start, mid, and end nodes of each pipe segment can be viewed. In addition, the elevation of any selected point can also be computed. This information is essential in calculating the relocation time and cost across failed segments' locations in the resilience-based restoration model and in calibrating the hydraulic model for the verification purposes. This map can also be superimposed with other maps from Google Earth for the City of London to locate water streams and other types of adjacent structures. Such information will be utilized in the criticality estimation model.

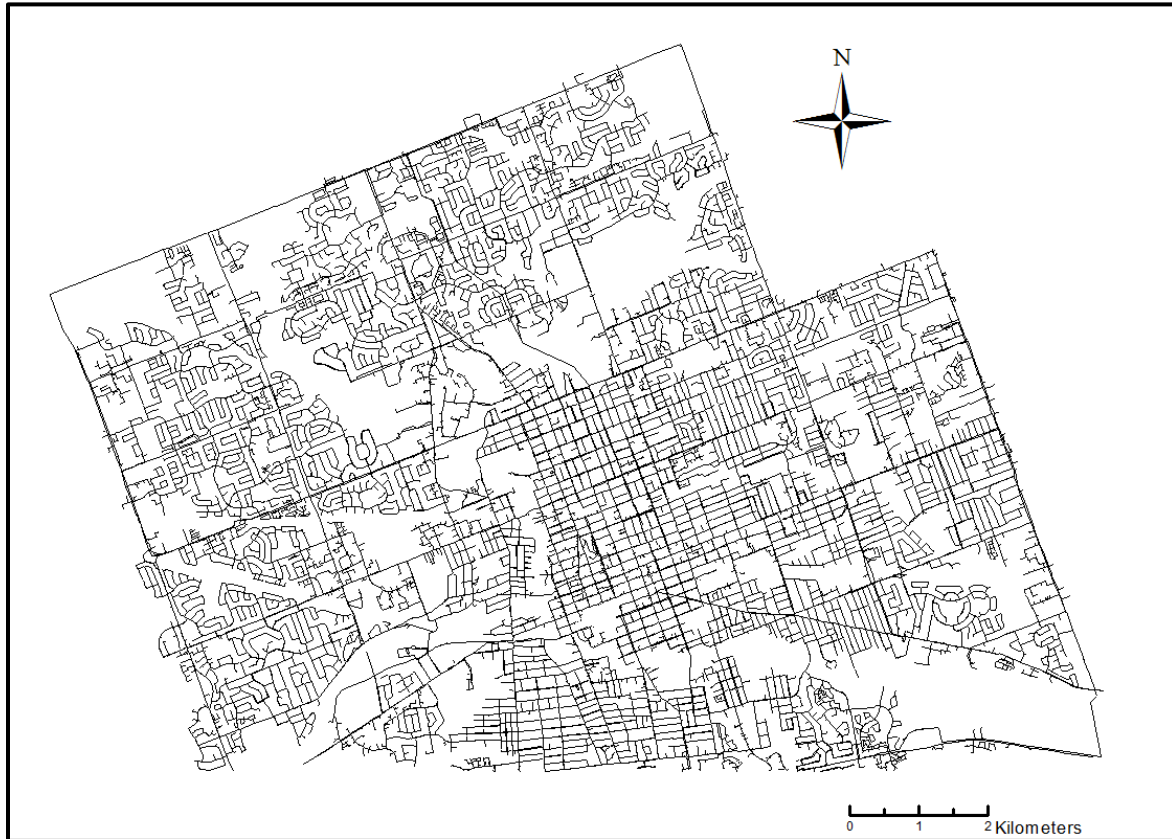


Figure 5-4: Water Distribution Network (London, Ontario)

5.2 Resilience Assessment Model

As previously discussed in section 3.2, the developed metric for assessing resilience of WDNs integrates two main qualities of the network: robustness and redundancy. This section starts with an illustration of utilizing the proposed metric in assessing resilience of WDNs following the steps detailed in section 3.2. Next, a two-tier validation process is illustrated to demonstrate the practicality of the developed metric. In this validation, the utilization of the proposed metric in two other resilience applications is briefly tested in this section. More complex formulations of such applications are presented in subsequent sections. In the first application, an optimization model was formulated to determine the optimal resilience enhancement plan. The objective of this

optimization framework was to assess the usefulness of utilizing the developed metric in improving the current resilience level. Subsequently, the developed metric was utilized in evaluating different restoration strategies after assuming a specific resilience loss scenario. This evaluation aimed to select the most effective restoration strategy that minimizes the time of service disruption after a hazard occurrence. The analysis here focuses on the impacts of the hazard on the network rather than the hazard itself. This three-level application demonstrates the practicality and usefulness of integrating the proposed metric in operation and management programs of WDNs both before and after disruption events. Obtained results were compared to values obtained by previous resilience metrics to highlight the main differences and improvements offered by the proposed metric. In the second sub-section, the obtained results were compared to values obtained by previous resilience metrics to highlight the main differences and improvements offered by the proposed metric.

The developed metric was utilized to assess the resilience of a real-life water network that serves a specific area in the City of London, Ontario. The selected subnetwork serves a specific region in the heart of London downtown. This sub-network is composed of 186 pipe segments that amount approximately 13.1 km of length and has 143 demand nodes. Figure 5-5 shows the layout of the selected sub-network, referred here as LWDN, which is carefully selected to provide water to a wide spectrum of diverse customers. LWDN is located in a condensed area that serves various residential, commercial, and institutional buildings. LWDN is mainly composed of cast iron (CI) and Polyvinyl chloride (PVC) pipes with diameters ranging from 40mm to 450mm. The distributions of pipe material and size for the LWDN are illustrated in Figure 5-6.

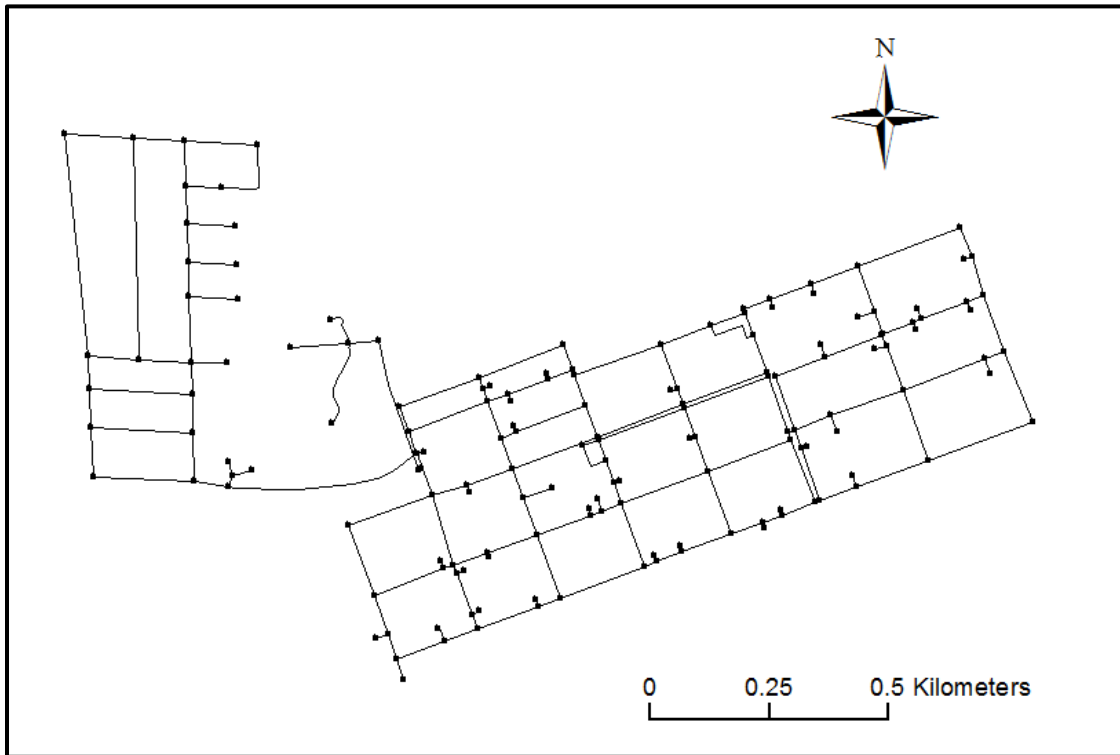


Figure 5-5: A layout of London Water Distribution Network, LWDN (Assad et al. 2019)

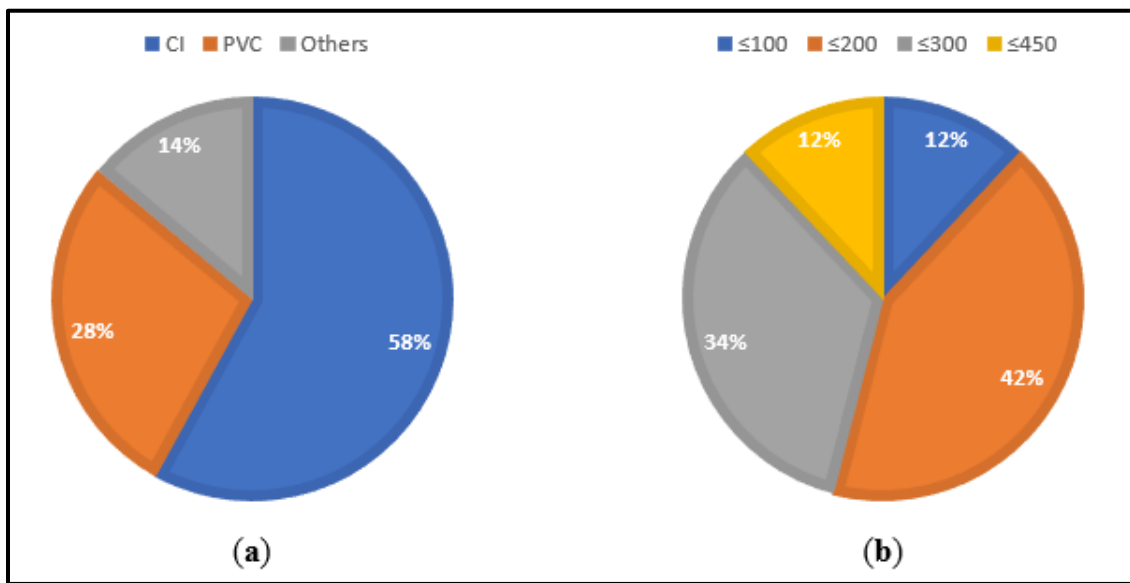


Figure 5-6: Characterization through Distribution of Pipe: (a) Material; (b) Diameter (mm) of the Selected Network for Resilience Assessment Model (Assad et al. 2019)

The first part of this section shows sample calculations to obtain criticality and reliability of a selected pipe segment. Subsequently, the results of all pipe segments in LWDN are integrated to

compute the robustness of the network. Redundancy is then added to estimate the resilience level of LWDN. Data needed for the criticality calculations were gathered from two primary sources GIS shapefiles and Experts' opinions. Characteristics of pipe segments were extracted from the shapefiles. Experts were asked to rank the relative importance of criticality factors. The FANP procedure then started by applying Chang's fuzzifying scale to construct the upper and lower matrices. Table 5-3 to Table 5-9 show the fuzzified pairwise comparison of the main factors and sub-factors. Each cell has three values representing the lower, most probable, and upper values obtained as a result of applying the fuzzifying scale.

Table 5-3: Main Factors Pairwise Comparison With respect to Main Goal for (Lower, Most Probable, Upper)

Factor	Financial	Environmental	Social
Financial	(1,1,1)	(1,1 1/2,2)	(1,1 1/2,2)
Environmental	(1/2,2/3,1)	(1,1,1)	(1/2,2/3,1)
Social	(1/2,2/3,1)	(1,1 1/2 ,2)	(1,1,1)

Table 5-4: Financial Sub-Factors Pairwise Comparison (Lower, Most Probable, Upper)

Factor	Size	Material	Depth	Accessibility
Size	(1,1,1)	(1 1/2,2,2 1/2)	(1,1 1/2,2)	(1/2,1,1 1/2)
Material	(2/5,1/2,2/3)	(1,1,1)	(1/2,2/3,1)	(2/5,1/2,2/3)
Depth	(1/2,2/3,1)	(1,1 1/2,2)	(1,1 ,1)	(2/5,1/2,2/3)
Accessibility	(2/3,1,2)	(1 1/2,2,2 1/2)	(1 1/2,2,2 1/2)	(1,1,1)

Table 5-5: Environmental Sub-Factors Pairwise Comparison (Lower, Most Probable, Upper)

Factor	Size	Soil type	Proximity to water streams
Size	(1,1,1)	(1 1/2,2,2 1/2)	(1,1 1/2,2)
Soil type	(2/5, 1/2,2/3)	(1,1,1)	(2/5,1/2,2/3)
Proximity to water streams	(1/2, 2/3,1)	(1 1/2,2,2 1/2)	(1,1,1)

Table 5-6: Social Sub-Factors Pairwise Comparison (Lower, Most Probable, Upper)

Factor	Population Density	Traffic Disruption	Alternative route	Serviced Facility
Population Density	(1,1,1)	(1,1 1/2,2)	(1,1 1/2,2)	(1,1 1/2,2)
Traffic Disruption	(1/2,2/3,1)	(1,1,1)	(2/5,1/2,2/3)	(1,1 1/2,2)
Alternative route	(1/2,2/3,1)	(1 1/2,2,2 1/2)	(1,1,1)	(1/2,1,1 1/2)
Serviced Facility	(1/2,2/3,1)	(1/2,2/3,1)	(2/3,1,2)	(1,1,1)

Table 5-7: Pairwise Comparison between Environmental and Social (Lower, Most Probable, Upper)

Factor	Environmental Factors	Social Factors
Environmental Factors	(1,1,1)	(1/2,2/3,1)
Social Factors	(1,1 1/2,2)	(1,1,1)

Table 5-8: Pairwise Comparison between Financial and Social (Lower, Most Probable, Upper)

Factor	Financial Factors	Social Factors
Financial Factors	(1,1,1)	(1 1/2,2,2 1/2)
Social Factors	(2/5,1/2,2/3)	(1,1,1)

Table 5-9: Pairwise Comparison between Financial and Environmental (Lower, Most Probable, Upper)

Factor	Financial Factors	Environmental Factors
Financial Factors	(1,1,1)	(1,1 1/2,2)
Environmental Factors	(1/2, 2/3,1)	(1,1,1)

The lower, upper, and most probable pairwise comparison matrices were then used as inputs to generate the unweighted supermatrix, Table 5-10. A Matlab code was written specifically for this purpose. Weighted supermatrix, shown in Table 5-11, is then established by normalizing each cell by the summation of the column in which it is located. The last step was to obtain the limited matrix, Table 5-12, by multiplying the weighted supermatrix by itself several times until convergence. The multiplication was done using a Matlab environment where the weighted matrix was multiplied by itself around 1075 times before convergence.

Table 5-10: Unweighted Super Matrix (Assad et al. 2019)

	WMC¹	EF²	EVF³	SF⁴	S⁵	M⁶	ID⁷	A⁸	S	ST⁹	WS¹⁰	D¹¹	TD¹²	AR¹³	TF¹⁴
WMC	0	0	0	0	0	0	0	0	0	0	0	0	0	0	0
EF	0.425	0	0.667	0.60	0	0	0	0	0	0	0	0	0	0	0
EVF	0.253	0.40	0	0.40	0	0	0	0	0	0	0	0	0	0	0
SF	0.322	0.60	0.333	0	0	0	0	0	0	0	0	0	0	0	0
S	0	0.319	0	0	1.0	0	0	0	0	0	0	0	0	0	0
M	0	0.171	0	0	0	1.0	0	0	0	0	0	0	0	0	0
ID	0	0.196	0	0	0	0	1.0	0	0	0	0	0	0	0	0
A	0	0.314	0	0	0	0	0	1.0	0	0	0	0	0	0	0
S	0	0	0.523	0	0	0	0	0	1.0	0	0	0	0	0	0
ST	0	0	0.277	0	0	0	0	0	0	1.0	0	0	0	0	0
WS	0	0	0.200	0	0	0	0	0	0	0	1.0	0	0	0	0
D	0	0	0	0.317	0	0	0	0	0	0	0	1.0	0	0	0
TD	0	0	0	0.171	0	0	0	0	0	0	0	0	1.0	0	0
AR	0	0	0	0.235	0	0	0	0	0	0	0	0	0	1.0	0
TF	0	0	0	0.277	0	0	0	0	0	0	0	0	0	0	1.0

¹ Water mains criticality, ² Economic factors, ³ Environmental factors, ⁴ Social factors, ⁵ Pipeline size, ⁶ Pipeline material, ⁷ Installation depth, ⁸ Accessibility, ⁹ Soil type, ¹⁰ Proximity to water streams, ¹¹ Population Density, ¹² Traffic Disruption, ¹³ Alternative route, ¹⁴ Type of Facility.

Table 5-11: Weighted Super Matrix (Assad et al. 2019)

	WMC¹	EF²	EVF³	SF⁴	S⁵	M⁶	ID⁷	A⁸	S	ST⁹	WS¹⁰	D¹¹	TD¹²	AR¹³	TF¹⁴
WMC	0	0	0	0	0	0	0	0	0	0	0	0	0	0	0
EF	0.425	0	0.333	0.300	0	0	0	0	0	0	0	0	0	0	0
EVF	0.253	0.200	0	0.200	0	0	0	0	0	0	0	0	0	0	0
SF	0.322	0.300	0.167	0	0	0	0	0	0	0	0	0	0	0	0
S	0	0.160	0	0	1.0	0	0	0	0	0	0	0	0	0	0
M	0	0.085	0	0	0	1.0	0	0	0	0	0	0	0	0	0
ID	0	0.098	0	0	0	0	1.0	0	0	0	0	0	0	0	0
A	0	0.157	0	0	0	0	0	1.0	0	0	0	0	0	0	0
S	0	0	0.261	0	0	0	0	0	1.0	0	0	0	0	0	0
ST	0	0	0.139	0	0	0	0	0	0	1.0	0	0	0	0	0
WS	0	0	0.100	0	0	0	0	0	0	0	1.0	0	0	0	0
D	0	0	0	0.159	0	0	0	0	0	0	0	1.0	0	0	0
TD	0	0	0	0.086	0	0	0	0	0	0	0	0	1.0	0	0
AR	0	0	0	0.117	0	0	0	0	0	0	0	0	0	1.0	0
TF	0	0	0	0.138	0	0	0	0	0	0	0	0	0	0	1.0

¹ Water mains criticality, ² Economic factors, ³ Environmental factors, ⁴ Social factors, ⁵ Pipeline size, ⁶ Pipeline material, ⁷ Installation depth, ⁸ Accessibility, ⁹ Soil type, ¹⁰ Proximity to water streams, ¹¹ Population Density, ¹² Traffic Disruption, ¹³ Alternative route, ¹⁴ Type of Facility.

Table 5-12: Limited Matrix (Assad et al. 2019)

	WMC¹	EF²	EVF³	SF⁴	S⁵	M⁶	ID⁷	A⁸	S	ST⁹	WS¹⁰	D¹¹	TD¹²	AR¹³	TF¹⁴
WMC	0	0	0	0	0	0	0	0	0	0	0	0	0	0	0
EF	0	0	0	0	0	0	0	0	0	0	0	0	0	0	0
EVF	0	0	0	0	0	0	0	0	0	0	0	0	0	0	0
SF	0	0	0	0	0	0	0	0	0	0	0	0	0	0	0
S	0.128	0.198	0.078	0.075	1.0	0	0	0	0	0	0	0	0	0	0
M	0.068	0.106	0.042	0.040	0	1.0	0	0	0	0	0	0	0	0	0
ID	0.079	0.121	0.048	0.046	0	0	1.0	0	0	0	0	0	0	0	0
A	0.126	0.195	0.077	0.074	0	0	0	1.0	0	0	0	0	0	0	0
S	0.142	0.087	0.305	0.087	0	0	0	0	1.0	0	0	0	0	0	0
ST	0.075	0.046	0.162	0.046	0	0	0	0	0	1.0	0	0	0	0	0
WS	0.054	0.033	0.117	0.033	0	0	0	0	0	0	1.0	0	0	0	0
D	0.104	0.068	0.054	0.190	0	0	0	0	0	0	0	1.0	0	0	0
TD	0.056	0.037	0.029	0.102	0	0	0	0	0	0	0	0	1.0	0	0
AR	0.077	0.050	0.040	0.140	0	0	0	0	0	0	0	0	0	1.0	0
TF	0.090	0.059	0.047	0.166	0	0	0	0	0	0	0	0	0	0	1.0

¹ Water mains criticality, ² Economic factors, ³ Environmental factors, ⁴ Social factors, ⁵ Pipeline size, ⁶ Pipeline material, ⁷ Installation depth, ⁸ Accessibility, ⁹ Soil type, ¹⁰ Proximity to water streams, ¹¹ Population Density, ¹² Traffic Disruption, ¹³ Alternative route, ¹⁴ Type of Facility.

The first column in the limited matrix represents the global weights of importance for each sub-factor. Table 5-13 shows that the most influential factor in estimating criticality of a pipe segment is its size, followed by its accessibility level, population density, and the type of facility it serves, respectively.

Table 5-13: Global Weights of Criticality Factors (Assad et al. 2019)

Criticality Factor	Weight
Size	0.2703
Accessibility	0.1261
Population Density	0.1036
Type of Facility	0.0904
Depth	0.0786
Alternative route	0.0767
Soil type	0.0754
Material	0.0685
Traffic Disruption	0.0559
Proximity to water streams	0.0544

A particular pipe segment was chosen to estimate its criticality for demonstration purposes. This pipe segment was made of ductile iron and had a diameter of 150mm. The characteristics and effect values are shown in Table 5-14. Criticality index of this pipe segment was found to be 0.41 using Equation 3.4. As mentioned earlier, the effect values for each criticality factor were obtained from experts working in the WDN in different cities and municipalities across Canada and the US.

Reliability computations started next by leveraging the previous failure history of pipe segments in calculating the times between breaks for each break order, transition state. Curve fitting techniques were then applied utilizing the maxim likelihood method to obtain the parameters of the best distribution. These parameters were then used to estimate the reliability of pipe segments and generate their deterioration curves. A distinct deterioration curve associated with each break order was derived. This step was repeated for each cluster of homogenous pipe segments, as stated in

section 3.2. Pipes were clustered into cohorts according to their size and material type to acquire a more accurate estimation of their reliability and deterioration behavior.

Table 5-14: Criticality Computation for a Pipe Segment in LWDN (Assad et al. 2019)

Critical Factor	Actual Value	Assigned Value
Size	150 mm	3
Material	Ductile Iron	5
Depth	1.6 m	1
Accessibility	Low	10
Soil type	Sand	10
Proximity to water streams	No	1
Population Density	Low	3
Traffic Disruption	Low	3
Alternative route	Yes	1
Type of serviced facility	Residential	3

Table 5-15 illustrates a sample of the obtained parameters of Weibull distribution for the group of pipelines that are made of cast iron and of a nominal size that is less than 150mm, (CI <150mm). In this case, a 3-parameter Weibull distribution yielded a better fitting for data related to the time to the first failure and for subsequent failures. This is evidenced by the results of the Anderson-Darling (AD) test in which the p-value of 3-parameter Weibull distributions are higher, which represents a better fit.

Table 5-15: Parameters of the Weibull Fitting for Each State (CI<150mm) (Assad et al. 2019)

State	Shape Parameter β	Scale Parameter η	Location Parameter γ
Time to 1 st failure	2.461	62.642	-1.655
Time to 2 nd failure	2.221	59.168	-0.214
Time to 3 rd failure	2.101	56.249	-0.798
Time to 4 th failure	1.756	42.579	-0.430

Table 5-16 illustrated the results of the Anderson-Darling (AD) test for some of the considered distributions. As previously mentioned, several distribution functions were tested to select the best distribution that fits the inter-failure time data.

Table 5-16: Goodness of Fitting the Time to 1st Failure Data (CI<150mm)

State	2-Parameter Weibull	3-Parameter Weibull	Normal	Exponential
AD Statistics	0.396	0.360	0.991	0.689
P-Value	0.250	0.466	0.111	0.273

Values of the shape parameter in each of the previous Weibull distributions were more than one. These values correspond to an increasing failure rate over time, deteriorating reliability. This phase is known as the wear-out phase or end-life failures, which reflects aged pipe segments. The reliability curve for this cohort (CI <150mm) is shown in Figure 5-7. The red "dots" represent the reliability values every ten years. The age of the selected pipe segment in criticality calculation was 31 years.

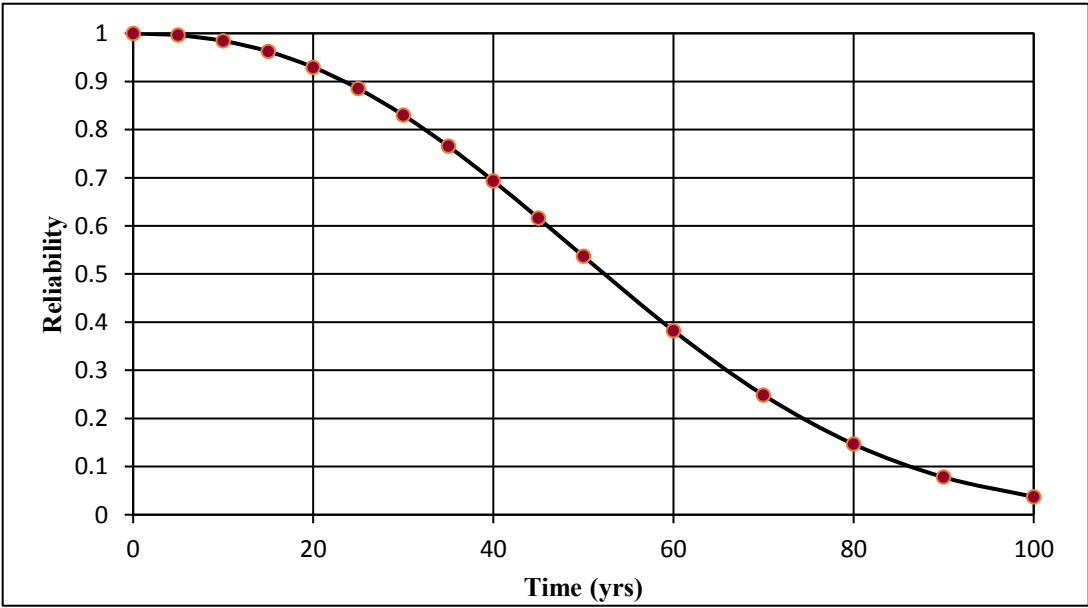


Figure 5-7. Reliability, Survival, Behavior for the Cohort (CI <150mm) (Assad et al. 2019)

Substituting the shape and scale parameters from Table 5-15 in Equation 3.7, the reliability of this specific segment over the following five years is depicted in Table 5-17. Reliability is continuously decreasing under the assumption that no maintenance or repair actions are considered for this pipe segment during the planning horizon of the next five years. It is also worth mentioning that this pipe segment will reach a reliability level of 0.751 in five years from today, not the year since it was initially installed. The overall robustness of the network was then computed by aggregating the reliabilities of all pipe segments and normalizing the summation over the sum of criticalities, as previously mentioned.

Table 5-17: Reliability Computations for a Pipe Segment in LWDN (Assad et al. 2019)

Year	Age	Reliability (t)
0	31	0.818
1	32	0.805
2	33	0.792
3	34	0.779
4	35	0.765
5	36	0.751

The Meshed-ness coefficient was then calculated to estimate the redundancy of the network. In LWDN, the numbers of links and nodes are 186 and 143, respectively. Using Equation 3.6, the meshed-ness coefficient (R_m) for LWDN was found to be 15.30%. This value indicates a low redundancy level evidenced by the scattered structure of the network, as can be observed in Figure 5-5. This was also due to the existence of a large number of dead-end nodes in the network, almost 25% of the nodes. Dead-end nodes are those connected to dead-end links that are not part of any loop. This represents an exception to the usual rule, where each node is connected to at least 2-3 links, because only one link is connected to a node, Figure 5-5. The result of such configuration is

an increase in the number of nodes, without a proportional increase in the number of connected links (Assad et al. 2019).

The resilience of LWDN was found to be 0.467, which is a low resilience level. Besides its structure, which offers little redundancy, this might be related to other factors such as the aging of this network. Table 5-18 shows a continuous decrease in the resilience of LWDN, mainly due to aging and deterioration when no enhancements actions are considered. As this metric measures the preparedness of LWDN to withstand disruptions and to continue supplying water to customers, such decrease compromises the network's ability to withstand these disruptions and contributes to extending the periods of service interruptions. This is due to the increased risk of pipe segments failure, especially the most deteriorated ones. For example, a failure of the two most deteriorated segments during a hazard event might cost between \$142,600 and \$166,200 in both direct and indirect costs, respectively, due to service interruption and other factors. To mitigate these risks, the City of London is expected to take several actions to increase this resilience level up to a certain acceptable level. Acceptable levels are defined by the end users, accounting for criticality of the considered sub-network, initial resilience loss, and the available budget and resources. Such actions may include a broad spectrum of alternatives for repairing and replacing deteriorated pipe segments in addition to the possibility of installing new segments to increase the network's redundancy. It shall be noted that these estimates are based on the local context of the City of London and the set of contractors/suppliers the City is committed with. The bottom line is that aging and deterioration are contributing to decreasing resilience and increasing the risk of failure. Those risks might be reduced by establishing efficient resilience enhancement programs, as will be demonstrated below.

Table 5-18: Resilience of LWDN along the Next Five Years (Assad et al. 2019)

Year	Resilience (t)
0	0.467
1	0.460
2	0.453
3	0.446
4	0.439
5	0.432

The relative weights of robustness and redundancy that were used in estimating resilience are 75% and 25%, respectively. These weights can be changed based on the preference of decision-makers that manage the operation and maintenance of the network. Figure 5-8 shows the results of sensitivity analysis in which the weights of robustness in Equation 3.7, and accordingly weights of redundancy, were changed from 100% to 0%. This verification is aimed to provide decision-makers with a full analysis to illustrate the impact of the relative weights of importance on the resilience level computations. The resilience increases with the increase of robustness's weight because the robustness level of the considered network is higher than its redundancy level.

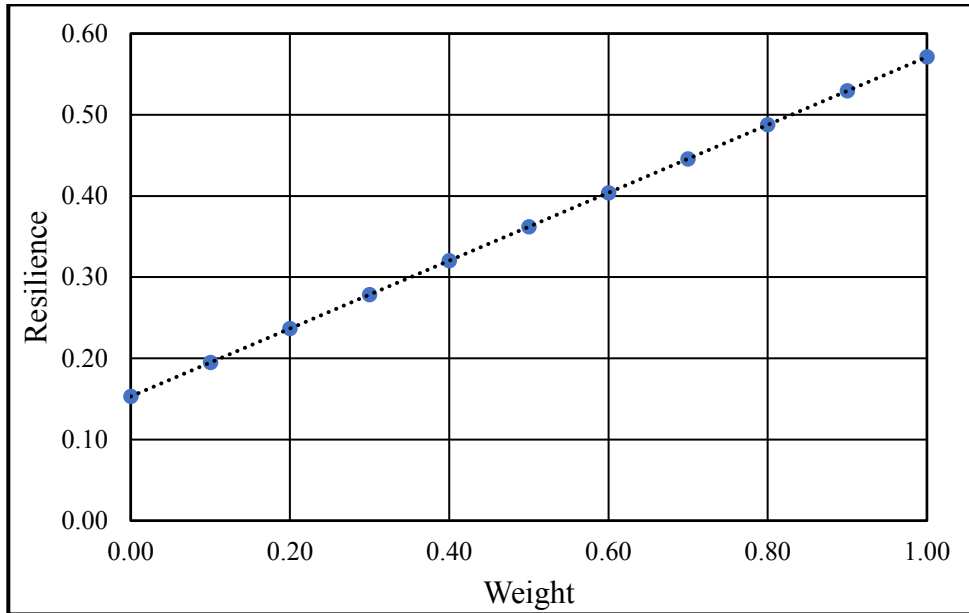


Figure 5-8: Effect of Changing Robustness's Weight on Resilience (Assad et al. 2019)

Next, an optimization model to maximize the resilience of LWDN subject to a budget constraint was formulated. Decision variables included replacement of deteriorated pipe segments and installing new ones. Replacement of deteriorated segments improves the network robustness while installing new segments adds redundancy to the network and improves its robustness. All pipe segments in LWDN, 186 segments, were considered for replacement. Besides, the nodes of newly installed segments include the set of nodes that were connected to one link only. When a pipe segment was chosen for replacement, the replacing segment was assumed to be of the same diameter as the original one. Also, when a pipe segment was newly installed, its diameter was assumed to be equal to the maximum diameter of segments connected to any of its end nodes. Lengths of newly installed segments were found by measuring the distance between each two end nodes using the features of Arc-GIS. The reliability of new pipe segments was assumed to be 0.99. This value should be theoretically one; however, it was reduced to account for installation mistakes and other flaws

that could occur in reality and compromise the theoretical value. Pipe bursting technique was used for replacement, and horizontal directional drilling technique was utilized for new installations.

This study employed genetic algorithm, GA, to determine the optimal, or near-optimal, resilience enhancement plan. Figure 5-9 shows the convergence of the optimization model for a sample budgetary constraint of \$500,000, in which the y-axis represents the resilience of LWDN, and the x-axis represents the number of generations after which the model would converge. An optimum value of 0.564 was obtained after 2,200 generations, following which no improvement was observed. The optimization algorithm was run on an 8GB RAM, 3.60 GHz i7 core CPU, and Windows 7 with a 64-bit operating system. The optimization model run time was 42 seconds. It was found that replacement actions constituted about 77%, \$384,500, of the total resilience enhancement budget. This could be explained by the existence of multiple deteriorated, aged, pipe segments in this subnetwork. Replacing such severely deteriorated segments would significantly increase the resilience of LWDN with a relatively cheaper cost than installing new segments; thus, such solutions were selected.

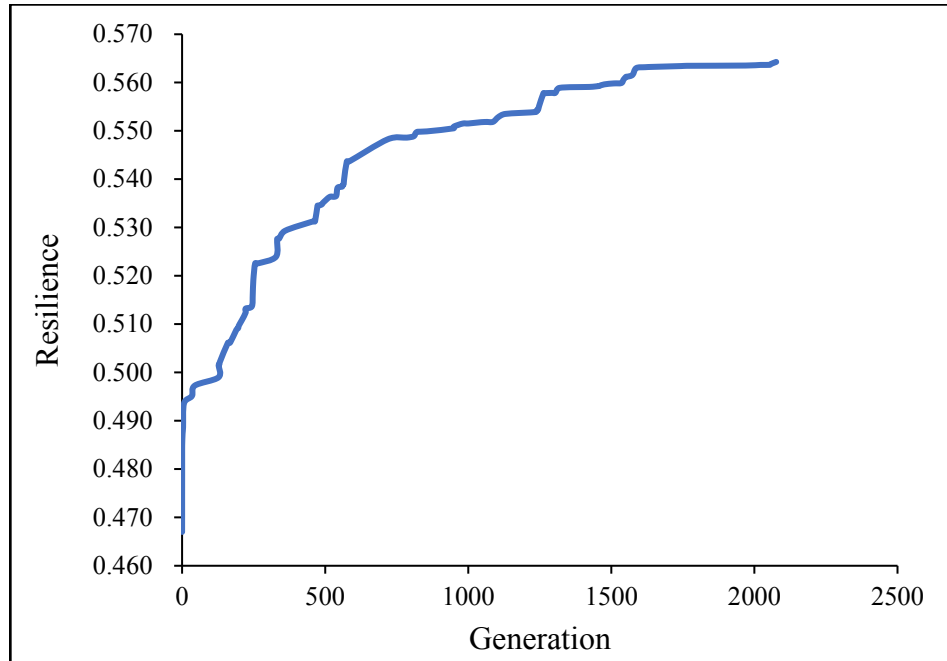


Figure 5-9: Convergence of the Genetic Algorithm Optimization Model (Assad et al. 2019)

Resilience enhancement budgets ranging between \$200,000 and \$1 million, with an increment of \$200,000, were then considered to be the budget constraint of the optimization model. Figure 5-10 depicts a trade-off between the resilience of LWDN and the costs of resilience enhancement. It can be observed from Figure 5-10 that resilience of LWDN could be increased to 0.564, by 21%, with a \$500,000 investment. Also, it can be increased to a value of 0.599, by 28%, with a \$1 million investment in resilience enhancement actions. It is observed that the amount of resilience increase tends to decrease after increasing the investment budget over \$2,000,000. This could be related to the reduced number of possible segments candidates that can be enhanced. It is worth mentioning that to increase the practicality of installing new pipe segments as a way to enhance resilience, these new installations shall be integrated within long-term capital planning.

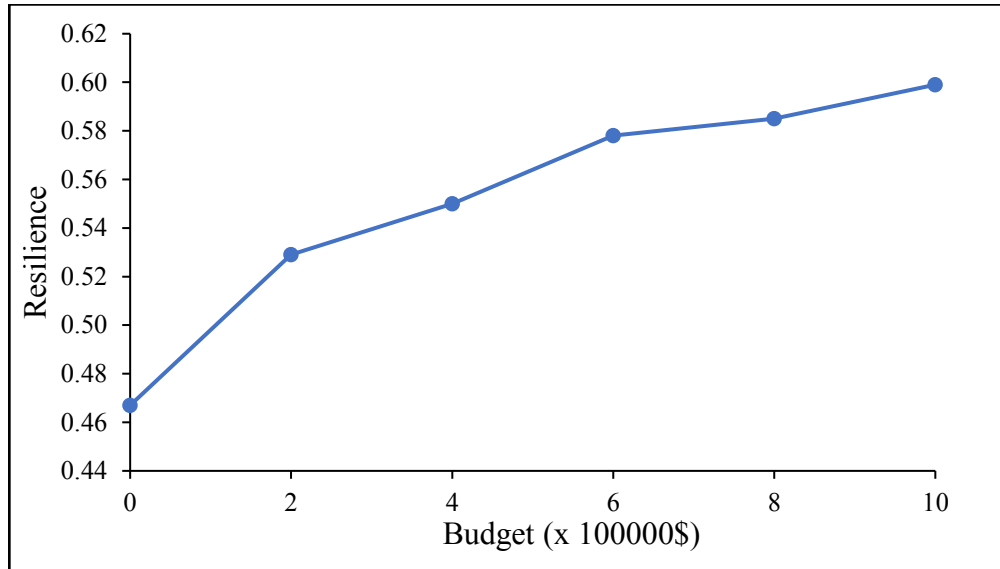


Figure 5-10: Resilience Versus Cost Trade-Off for LWDN (Assad et al. 2019)

Finally, to demonstrate the practicality of using the proposed metric during the restoration phase, a simple scenario is discussed below. Assuming a disruption event that caused a certain number of segments to fail. The failed pipe segments were randomly chosen to depict the case of natural disruptions such as earthquakes. The initial resilience level of 0.467 was used as a reference value, which represented the undisrupted state of LWDN. A disruption event that caused a failure of nine randomly chosen segments was assumed. When a pipe segment fails, its reliability, probability of survival, is reduced to zero in Equation 3.7, and the resilience metric is recalculated. As a result, the resilience of LWDN had decreased around 5% to a value of 0.443. It was then required to investigate three possible recovery strategies. Each pipe segment required a different restoration period based on its size, material type, and external conditions. Pipe bursting technology was considered to replace the failed pipe segments. The initial set-up time for the repair team was neglected in this illustration. The relocation time was also ignored in this example, i.e., time spent when the repair crew moved from one segment to another was not considered. Each restoration strategy specified the sequence, order, in which pipe segments would be restored. The first strategy was to restore the failed segments

based on their criticality in descending order. The second one was to repair the failed segments based on their age from the oldest to the newest pipe segment. The last strategy was to fix the failed segments based on the realized increase in resilience metric such that those segments that yield the most significant improvement are fixed first. The first two strategies are employed here for comparison because they are commonly utilized in several cities across Canada. Yet, it shall be noted that the resilience-based strategy already accounts for both the ageing effect and the criticality simultaneously. Table 5-19 describes the state of LWDN after each time step following the first restoration strategy.

Table 5-19: LWDN Behavior Following Restoration Strategy 1 (Assad et al. 2019)

Pipe Segment	Status										
	t_0	t_d	t_1	t_2	t_3	t_4	t_5	t_6	t_7	t_8	t_9
34	1	0	1	1	1	1	1	1	1	1	1
148	1	0	0	0	1	1	1	1	1	1	1
76	1	0	0	1	1	1	1	1	1	1	1
161	1	0	0	0	0	1	1	1	1	1	1
56	1	0	0	0	0	0	1	1	1	1	1
42	1	0	0	0	0	0	0	0	1	1	1
130	1	0	0	0	0	0	0	0	0	0	1
185	1	0	0	0	0	0	0	1	1	1	1
1	1	0	0	0	0	0	0	0	0	1	1

At t_d , time of disruption, a disruption occurred, which caused a sudden resilience drop (in this specific case $t_o=t_d$). This drop is indicated by a status value of 0 for the failed pipe segments. Pipe segments were then sequentially restored, indicated by a value of 1, from time steps t_1 through t_f , the time step at which restoration actions were accomplished. The increase in resilience over time following restoration strategy 1 is depicted in Table 5-20. Similar computations were attained for restoring strategies 2 and 3. Figure 5-11 illustrates three distinct resilience restoration behaviors for

LWDN. For example, the resilience of LWDN reached a level of 97% of its original value after 16 days following strategy 3 and reached the same level after 31 and 20 days following strategy 1 and strategy 2, respectively. In general, the third strategy was the fastest in restoring LWDN to its original state. It is worth mentioning that this example is simplified to illustrate the applicability of the proposed resilience metric. However, the distinct behaviors of each strategy imply the importance of developing more reliable methods to determine the best restoration plan. Optimization and other multi-criteria decisions making tools can be utilized to achieve this purpose, as will be shown in the following section.

Table 5-20: Resilience Computations for Strategy 1 (Assad et al. 2019)

Time (days)	Resilience	Resilience (%)
0	0.467	100.00
0	0.443	94.84
7	0.443	94.89
20	0.445	95.37
23	0.447	95.89
27	0.449	96.13
31	0.452	96.82
32	0.456	97.63
36	0.459	98.46
41	0.463	99.18
53	0.467	100.00

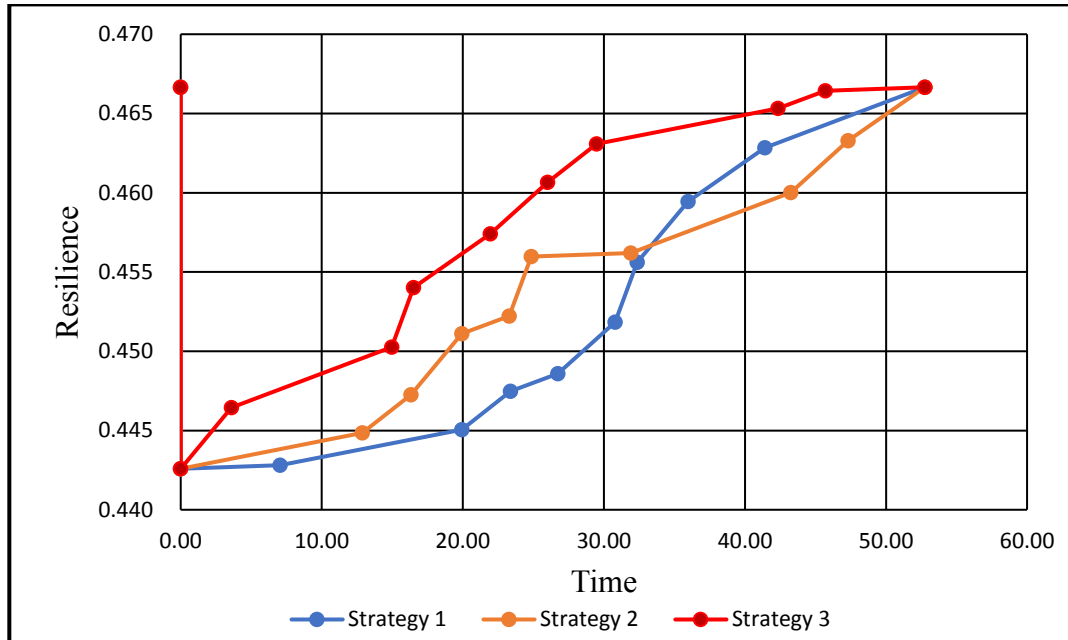


Figure 5-11: Comparison of Three Resilience Restoring Strategies Based on the Proposed Metric (Assad et al. 2019)

Resilience Metric Validation

This section proceeds with an evaluation of utilizing the proposed metric in the three resilience applications that were described previously. Firstly, the obtained resilience results of LWDN under different states were compared to those found by a previously developed metric in the literature. Secondly, a hydraulic model was simulated to evaluate the same restoration strategies investigated in the previously described failure scenario. Results were compared to those obtained by the proposed metric, and main differences were discussed.

Firstly, the estimated resilience level of LWDN was compared to a resilience level obtained by another resilience metric developed by Farahmandfar et al. (2016) as a means of validation. The resilience level of LWDN using that metric was found to be 0.454 compared to a level of 0.467, as found using the developed metric in this research. The concept of resilience is still emerging and being investigated both in academia and in practice. The City of London does not have an estimation

of the resilience level of their network yet. Thus, it is not possible to judge which metric is overestimating the resilience level or which metric is outperforming in terms of resilience evaluation. However, the resilience levels of LWDN as obtained by these metrics are quite comparable with the proposed metric yielding a higher, less than 3% increase, resilience level. These results shall serve a way of validating the viability of the proposed metric in the resilience assessment application of WDNs.

Additionally, resilience levels attained by the two metrics during the different disrupted and enhanced states were compared. This was done to investigate the consistency in the differences between the obtained results and to highlight the main improvements offered by the newly developed metric. When the same resilience enhancement actions were applied, the resilience of LWDN, using the metric developed by Farahmandfar et al. (2016), had increased by 19% to a value of 0.540. This was comparable to an increase of 21% obtained using the developed metric. The difference between the resilience levels of LWDN under the enhanced state, as obtained by the two metrics, was around 4%. The original resilience level of LWDN, 0.454, was then used as a reference value, and the same failure scenario was assumed, a failure of the same nine pipe segments. The resilience of LWDN, using the metric developed by Farahmandfar et al. (2016), decreased 4% to a value of 0.435. This was also comparable to the result obtained by the proposed metric, where a reduction of 5% was encountered. The difference between resilience levels of LWDN under the disrupted state was less than 2%. Generally, it was observed that the proposed metric estimated a higher resilience level, which can be referred to the difference between the two metrics in quantifying robustness and redundancy.

While in their metric, Farahmandfar et al. (2016) depended solely on the nodal degree, the developed metric in this study considered both the number of nodes and links in determining the

number of loops in a network, Equation 3.6. Additionally, Farahmandfar et al. (2016) utilized nodal demand as a weighting factor, multiplied by the sum of reliabilities, to highlight the nodes of higher demand. However, the demand can be zero for some nodes based on the network structure. Hence, reliabilities of the segments connected to such nodes would not be counted in resilience estimation. This was avoided in the developed metric, where criticality of each segment was used as a weighting factor instead of nodal demand (Assad et al. 2019). As such, the developed metric offers an advantage in ability to account for the structural performance of water pipe segments more accurately. Decisions related to enhancement and restoration based on this metric shall yield a better performance for the considered objectives such as the total time and cost. In addition, the developed metric can be easily integrated within the City's management tools.

Secondly, to verify the suitability of utilizing the developed metric in restoration applications, a hydraulic model was simulated. The previously mentioned failure scenario was simulated on WaterGEMS software utilizing the failure mechanism mentioned in section 3.2. Table 5-21 depicts a sample of the hydraulic simulation results both before and after the disruption. Nodes elevation and demand data were assigned before running the simulation and obtaining the pressure requirements. Subsequently, the failures scenarios were simulated as described above, and the new pressure information along with the satisfied demand was observed.

Table 5-21: Sample of Hydraulic Simulation Results both before and after Disruption

Node ID	Elevation (m)	Demand (L/day)	Hydraulic Grade* (m)	Pressure* (bars)	Hydraulic Grade** (m)	Pressure** (bars)	Demand Available (L/day)
Node 28	248.65	15,000	286.21	3.68	257.08	0.83	11,157
Node 227	234.27	20,000	264.94	3.01	256.59	2.19	20,000
Node 362	248.14	24,000	286.16	3.73	257.38	0.91	18,693
Node 353	247.91	62,000	286.16	3.75	257.64	0.95	49,340
Node 352	248.43	20,000	286.18	3.7	257.9	0.93	15,748

* Base Values.

** Values at the disrupted state.

The network was then restored three times based on the same restoration strategies considered earlier in the previous sub-section. In each time, pipe segments were gradually reopened, the assigned flow discharge was removed, and the serviceability index (*SI*) index was iteratively computed. Figure 5-12 shows three different restoration behaviors of *SI* from a value of 0.835 to the original value. Restoration strategy 3 yielded the fastest rate at which *SI* was recovered, as shown in Figure 5-12. This strategy suggests restoring the failed segments based on the improvement in the proposed resilience metric. These results were obtained without running any optimization model. Running such models shall establish the most optimum restoration strategy.

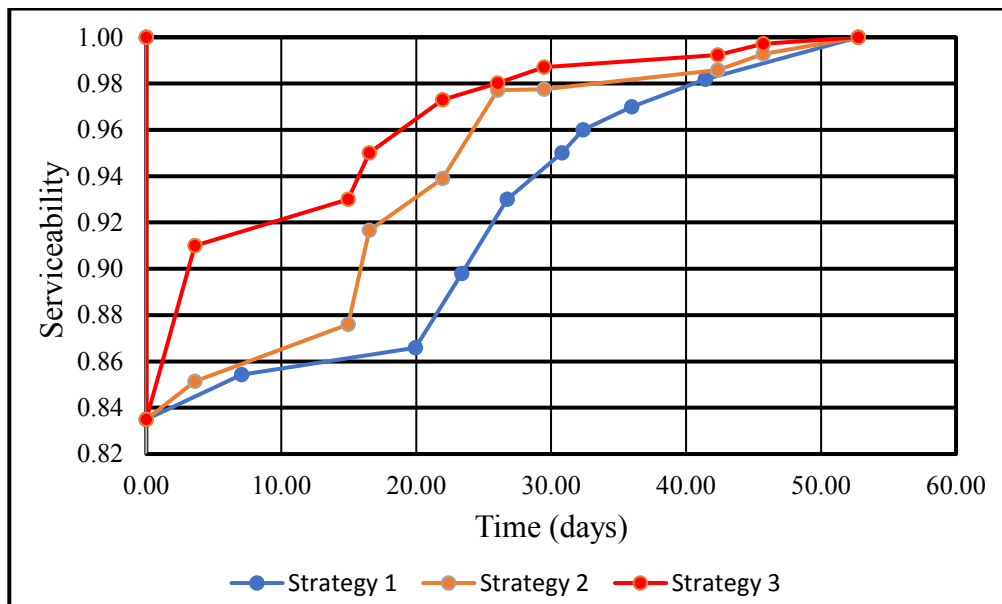


Figure 5-12: Comparison of Three Resilience Restoring Strategies Based on Serviceability (Assad et al. 2019)

In addition, Figure 5-11 and Figure 5-12 show different relative behavior for strategy 1 and strategy 2 toward the last three restoration actions, which might need further investigation. However, as the primary objective after a service interruption is to restore the system rapidly, the developed

metric had shown similar results to those obtained by *SI* in this regard, the fastest recovery. This shows the potentiality of using the proposed metric as a proxy indicator for *SI*. Using the proposed metric requires much less computational time in investigating and selecting the best restoration strategy during the recovery phase. In a real application, this can be assured through an optimization model that determines the fastest restoration plan. Such optimization models can be formulated to search over all possible restoration strategies in terms of the order and method of restoring each failed segment. This way, decision-makers can be more confident about their decisions, since all possible strategies have been considered. The formulation and solution of such a holistic optimization model are presented in the following section.

5.3 Resilience-Based Restoration Model

As previously mentioned in section 3.3, the resilience-based restoration model integrates the results of the resilience assessment model, along with the restoration and crew relocation sub-models, to achieve the most rapid recovery. In this section, the application of this restoration optimization model on a case study is presented. Various optimization algorithms were investigated to select the best performing one. Results obtained were also compared with a heuristics approach followed by municipalities in Canada to restore WDNs that are subjected to multiple simultaneous failures.

Resilience Metric Application

The restoration model was applied on the same section of London WDN for which the resilience level was evaluated in section 5.1. To demonstrate the practicality of the developed model, a disruption scenario that caused a failure of 30 pipe segments in the form of small and big breaks was assumed. These failures were assumed at different location across the network. It was assumed that five repair crews would be available to respond to this event. Table 5-22 illustrates a sample of

the input data to the restoration optimization model. All the data in Table 5-22 were extracted from the database provided by the City of London, Ontario.

Table 5-22: Sample of Input Data Used in the Restoration Optimization Model (Assad et al. 2020)

Pipe ID	X (Easting)	Y (Northing)	R _i	C _i	Diameter (mm)	Length (m)	Soil Type	NOPB*	Age	Material	Break Type
1	480,086	4,758,960	0.375	0.402	150	116.38	Sand	0	28	CI	Small
2	479,268	4,758,590	0.383	0.394	450	107.55	Clay	4	19	CI	Small
3	478,790	4,759,090	0.695	0.321	150	82.97	Sand	1	21	CI	Big
4	478,850	4,759,650	0.769	0.333	200	152.92	Clay	0	17	PVC	Small
5	479,833	4,759,070	0.514	0.368	250	64.58	Clay	1	25	CI	Big
—	—	—	—	—	—	—	—	—	—	—	—
30	479,790	4,758,790	0.446	0.422	450	57.06	Sand	0	30	CI	small

*NOPB = Number of previous Breaks

As previously mentioned, several restoration techniques were considered in this model. Several factors were taken into account in specifying the set of possible restoration methods for each segment. For example, open-cut and splitting methods are the possible options for replacing pipe segments that are made of ductile iron since they do not fracture using regular pipe bursting. Also, the existing of rocks, densely compacted soils, or expansive soils represents unfavorable conditions for PB. Costs and durations of the considered restoration methods were gathered from various contractors across Canada.

Inputs from various contractors and consultants in the field operation and management of WDNs in Canada were consulted to determine the unit costs and required durations of various rehabilitation methods. These data are needed for applying this resilience-based restoration model and the resilience enhancement model explained in the subsequent section. Table 5-23 depicts the unit costs and durations of considered restoration and enhancement methods. These estimates represent the average values of the collected responses. It shall be noted that the main contribution of this research study is not to collect data regarding the costs and duration of different rehabilitation

techniques. As such, these estimated costs and durations are fed as inputs to the model, where decision-makers can either use them or specify different values according to their preferences. In addition, the same gathered values related to unit costs and durations are utilized during the validation of the developed models.

Table 5-23: Summary of Rehabilitation Methods

Intervention Action	Intervention Type	Unit Cost (CAD/mm ² /m)	Unit time (days/m)
Mechanical Clamps / Couplings	Repair	8,000*	8.00**
Epoxy lining (EL)	Renewal (minor)	66.39***	0.01000
Cured in Place Pipe (CIPP)	Renewal (major)	2.04	0.01615
Pipe Bursting (PB)/ Splitting	Replacement (Trenchless)	3.02	0.02019
Open-Cut Method (OCM)	Replacement	5.43	0.08833

* This estimate is an average lump sum value in CAD.

** This estimate is an average total duration in hours not days.

*** Cost is in CAD/m.

Deterministic Analysis

Next, the multi-objective optimization problem was solved deterministically as per Equation 3.23. In this analysis, the relative weights for the cost, time, and resilience objectives were suggested as 0.3, 0.5, and 0.2, respectively. Genetic algorithm (GA), ant colony optimization (ACO), and Tabu search (TS) were tested to determine their respective capabilities in achieving a near-optimal solution of the three considered objectives. Table 5-24 presents the results obtained from solving the problem using those three algorithms. It was observed that the three algorithms were able to provide similar solutions in terms of restoration cost and resilience improvement. However, there were some variations when it comes to the restoration time. GA provided a 12% and 14% shorter restoration time than ACO and TS, respectively. This comparison indicates that GA is the most suitable algorithm to get the optimum values of the formulated problem. It is also suggested to be the

algorithm employed for solving this restoration problem even if the number or individual failed segments change.

Table 5-24: Comparison of Optimization Results Using GA, ACO, and TS (Assad et al. 2020)

Criterion	GA	ACO	TS
Time (days)	13.9	15.8	16.2
Cost (x10 ³ CAD)	1,557	1,557	1,557
Resilience Improvement	0.106	0.106	0.106

While the time objective would typically pose the most significant concern in restoration applications, there are cases where the fund and other resources could be scarce. In others, achieving a certain level of resilience after accomplishing the recovery process might be required. For both cases, decision-makers will aim to define a range of possible weights for each objective instead of assigning a specific value. The problem would then be iteratively solved several times to investigate the part of the Pareto front enclosed within the defined ranges. This would yield a set of various near-optimal solutions from which decision-makers can choose the one that best matches their preferences. For illustration purposes, it was assumed that the range of weights for the time objective is (0.3-0.5) and for the cost objective (0.1-0.4). The range of weights for resilience objective was calculated as the complement of the corresponding values to 1. The problem was then solved using several combinations of the possible weights between these ranges (15 sets). Table 5-25 shows a sample of the different runs of the multi-objective optimization problem that were solved using different combinations of weights.

Table 5-25: Different Optimal Solution Sets Resulting from Different Iterations (Assad et al. 2020)

Iteration	W ₁	W ₂	W ₃	Cost (x10 ³ CAD)	Time (days)	Resilience Improvement	Weighted Objective Function
1	0.3	0.3	0.4	1,588	14.45	0.110	0.471
2	0.4	0.3	0.3	1,557	14.26	0.106	0.734
3	0.1	0.5	0.4	1,587	14.30	0.110	0.435
4	0.4	0.4	0.2	1,557	13.84	0.106	0.965
5	0.3	0.5	0.2	1,557	13.86	0.106	0.949
—	—	—	—	—	—	—	—

15	0.2	0.5	0.3	1,557	14.26	0.106	0.707
----	-----	-----	-----	-------	-------	-------	-------

Note: The bold row represents the combination of weights that was assumed in solving the optimization problem.

The optimization problems were run on an 8GB RAM, 3.60 GHz i7 core CPU, and Windows 7 with a 64-bit operating system. The computational time of the different optimization runs ranged between 125 s and 179 s. This performance allows utility managers to obtain real-time near-optimal restoration plans to respond to different hazard events. The realized saving in computational time is around 80% compared to running hydraulic simulation. The benefit in computational time is expected to increase as the size and complexity of WDSs increase.

The model allows the user to investigate a larger portion of the search space utilizing randomly generated dynamic weights of the objectives, as illustrated in section 3.3. It is worth mentioning that this case is rarely needed in practice, where decision-makers would typically know ahead of time the relative importance of restoration objectives. However, it is provided here to complete the theoretical analysis. The different solution sets resulted from 100 runs of solving the optimization problem in Equation 3.15 with randomly generated weights is shown in Figure 5-13.

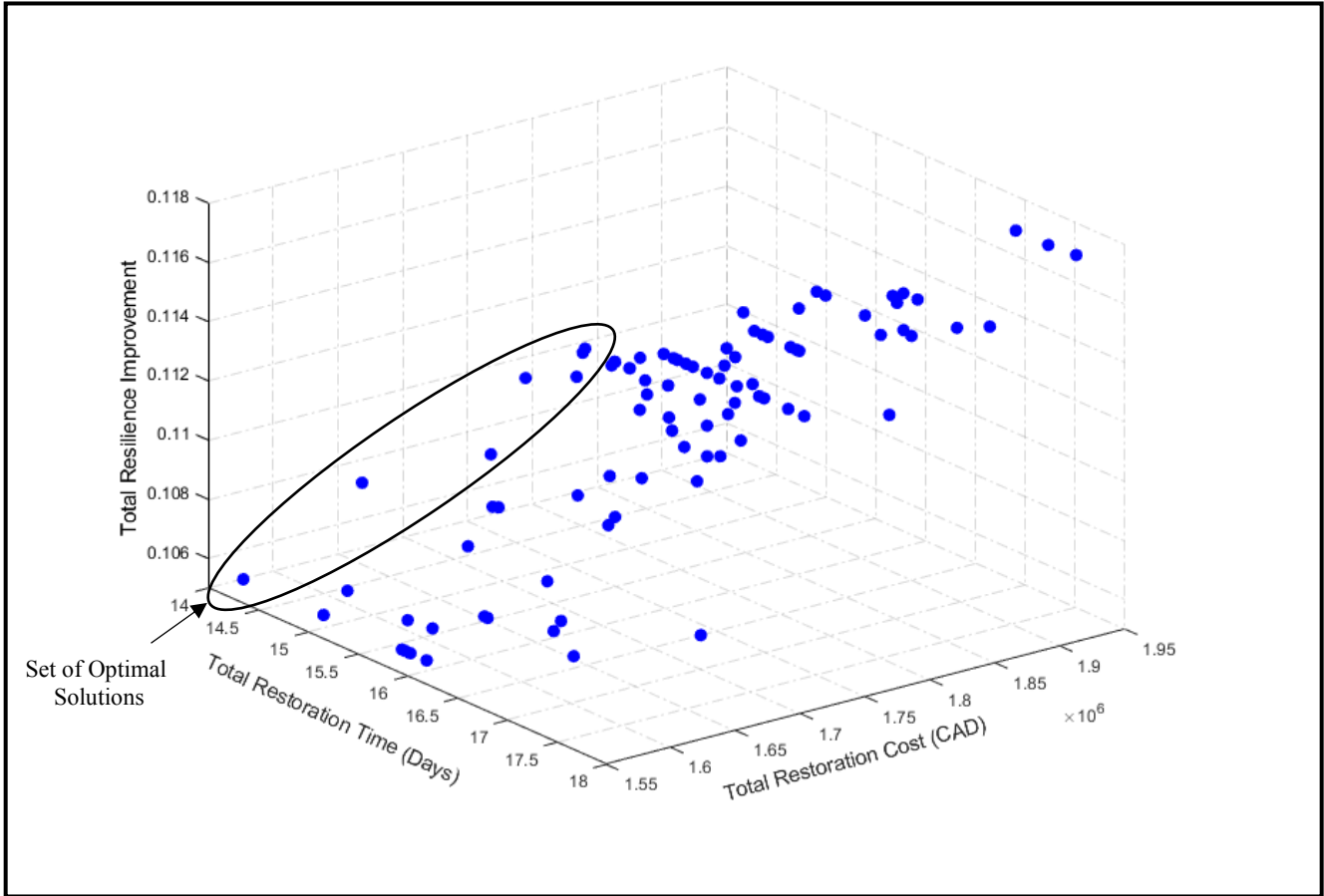


Figure 5-13: Optimal Solution Sets Generated from Running Optimization Model

The solution resulting from the optimization model was then used to create a restoration work plan and a restoration schedule. A typical restoration work schedule encompasses the sequence of segments restoration, the methods of restoration, start and end dates, and the crew assignment. Also, restoration activities assigned to each crew were connected, assuming a finish-to-start logical relationship to generate the restoration schedule. Lag times between successive activities were introduced to capture the relocation time between the locations of failed segments across the network. Detailing the steps of each restoration method is beyond the scope of this work. Readers can refer to (Yazdekhashti et al. 2014; Weaver and Woodcock 2014; Simicevic and Sterling 2001) for more about major activities and best practices regarding the various possible restoration methods. Figure 5-14

and Table 5-26 depict a restoration schedule and restoration work plan for one solution of the optimization model.

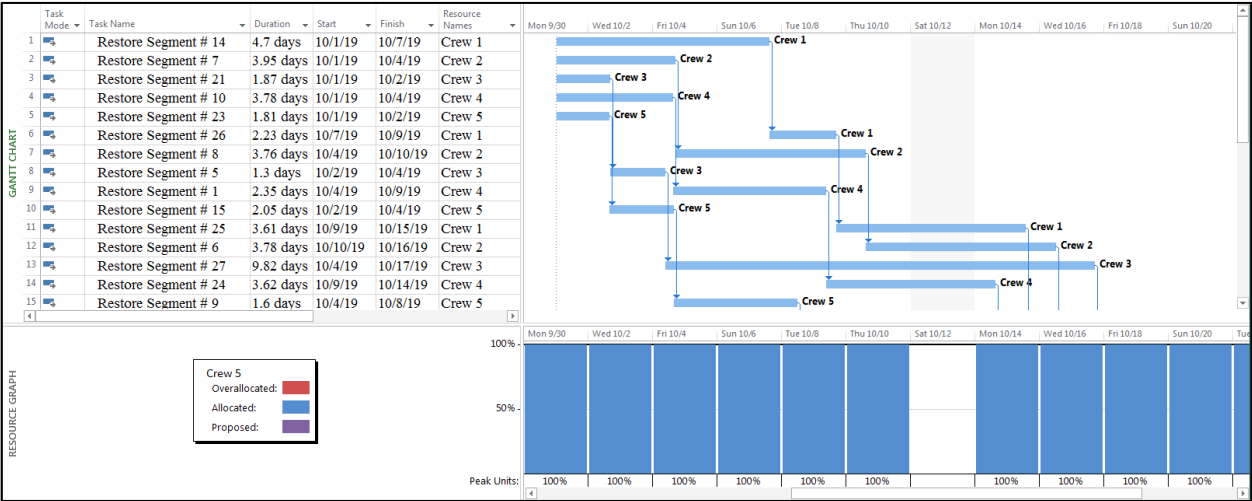


Figure 5-14: Restoration Schedule Based on a Sample Output of the Restoration Model

Stochastic Analysis

When decision-makers cannot make certain estimates about the unit time, cost, and resilience improvement of the various considered repair methods, stochastic optimization can be utilized to provide a range of expected values of the considered objectives. Decision-makers would be asked to provide some minimum, maximum, and most probable estimates about the uncertain values. these values were then fed to the Monte Carlo simulation. Stochastic optimization was then run as per the steps explained in section 3.3.

Table 5-26: Restoration Schedule Based on a Sample Output of the Restoration Model (Assad et al. 2020)

Objective	Tasks	Restoration Method	Responsible	Start Date	Target Date
Restoring the failed water subnetwork to the agreed resilience level within the minimum possible time and respecting the allowed budget and available resources. Tasks shall be performed based on the listed sequence and specified restoration method.	Restoring Seg. 18	Clamp	Crew #1	3/1/2020	3/1/2020
	Restoring Seg. 10	Pipe Bursting	Crew #2	3/1/2020	3/4/2020
	Restoring Seg. 29	Open-Cut	Crew #3	3/1/2020	3/9/2020
	Restoring Seg. 28	Pipe Splitting	Crew #4	3/1/2020	3/3/2020
	Restoring Seg. 30	Clamp	Crew #5	3/1/2020	3/1/2020
	Restoring Seg. 21	Pipe Bursting	Crew #1	3/1/2020	3/3/2020
	Restoring Seg. 19	Pipe Bursting	Crew #5	3/1/2020	3/2/2020
	Restoring Seg. 17	Clamp	Crew #5	3/2/2020	3/3/2020
	Restoring Seg. 12	Clamp	Crew #5	3/3/2020	3/3/2020
	Restoring Seg. 2	Pipe Bursting	Crew #1	3/3/2020	3/5/2020
	Restoring Seg. 5	Pipe Bursting	Crew #5	3/3/2020	3/4/2020
	Restoring Seg. 20	Clamp	Crew #4	3/3/2020	3/3/2020
	Restoring Seg. 8	Pipe Bursting	Crew #4	3/3/2020	3/7/2020
	Restoring Seg. 27	Open-Cut	Crew #5	3/4/2020	3/14/2020
	Restoring Seg. 13	Clamp	Crew #2	3/4/2020	3/5/2020
	Restoring Seg. 4	Clamp	Crew #2	3/5/2020	3/5/2020
	Restoring Seg. 9	Pipe Bursting	Crew #1	3/5/2020	3/6/2020
	Restoring Seg. 15	Pipe Bursting	Crew #2	3/5/2020	3/7/2020
	Restoring Seg. 26	Pipe Splitting	Crew #1	3/6/2020	3/9/2020
	Restoring Seg. 24	Pipe Bursting	Crew #2	3/7/2020	3/11/2020
	Restoring Seg. 11	Clamp	Crew #4	3/7/2020	3/7/2020
	Restoring Seg. 14	Pipe Bursting	Crew #4	3/7/2020	3/12/2020
	Restoring Seg. 6	Pipe Splitting	Crew #1	3/9/2020	3/13/2020
Restoring Seg. 22	Clamp	Crew #3	3/9/2020	3/10/2020	
Restoring Seg. 16	Pipe Bursting	Crew #3	3/10/2020	3/12/2020	
Restoring Seg. 3	Clamp	Crew #2	3/11/2020	3/11/2020	
Restoring Seg. 25	Pipe Splitting	Crew #3	3/12/2020	3/16/2020	
Restoring Seg. 7	Pipe Bursting	Crew #4	3/12/2020	3/16/2020	
Restoring Seg. 1	Clamp	Crew #3	3/16/2020	3/16/2020	
Restoring Seg. 23	Pipe Splitting	Crew #3	3/16/2020	3/18/2020	

Figure 5-15 illustrates the probability distribution functions associated with the cost and time of fixing pipe segment #1 using pipe bursting technique. The minimum and maximum costs associated with resorting this segment utilizing PB are 34,500 CAD and 41,160 CAD, respectively. [Figure 5-15(a)] shows that in 95% of the simulated runs, the cost of this restoration activity would approximately range between CAD 35,900 and CAD 41,800. Additionally, [Figure 5-15(b)] shows that there is a 0.95 probability of accomplishing this restoration action between 2.2 days and 2.6

days. Similar distributions were sampled to model uncertainties associated with the time, cost, and resilience improvement of all possible restoration methods for each pipe segment.

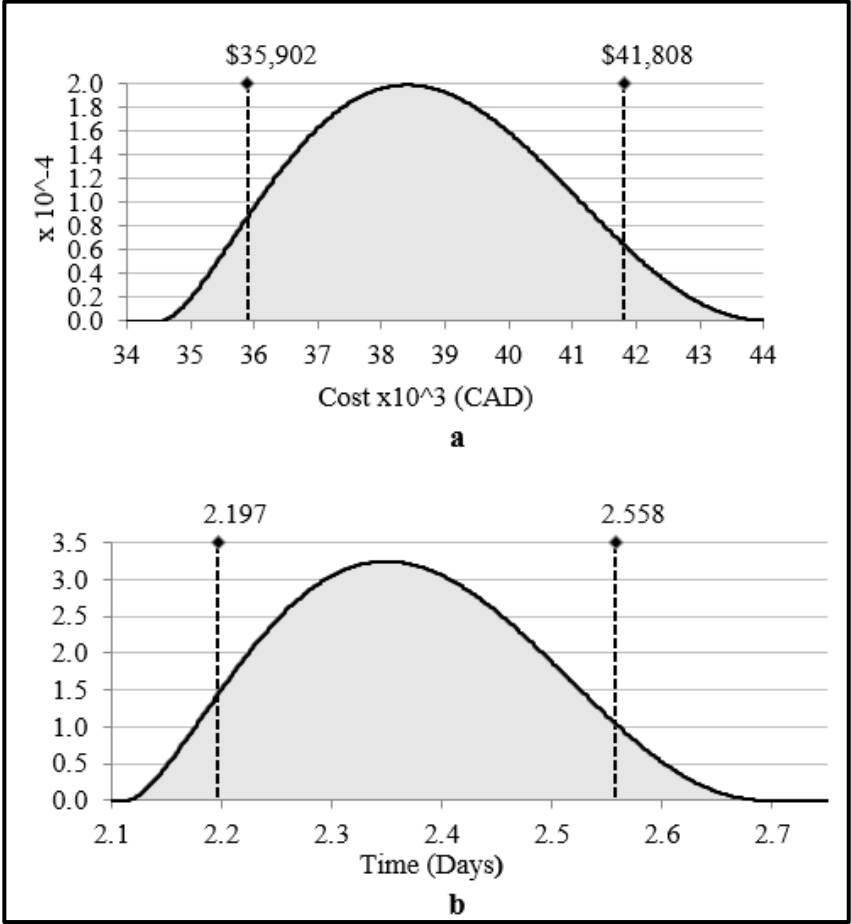
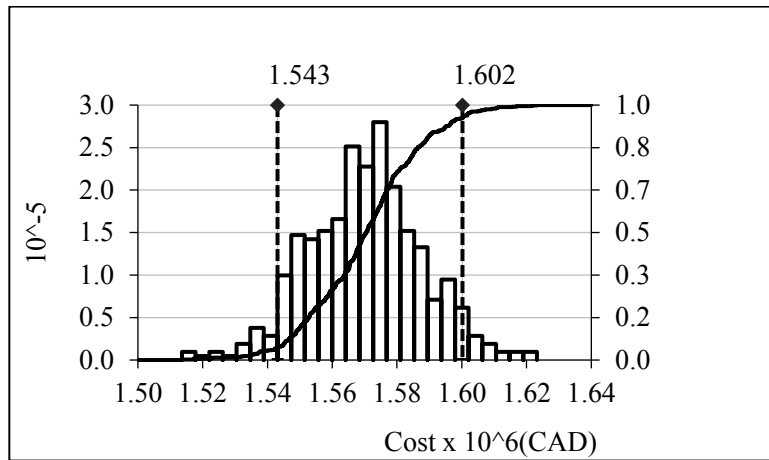


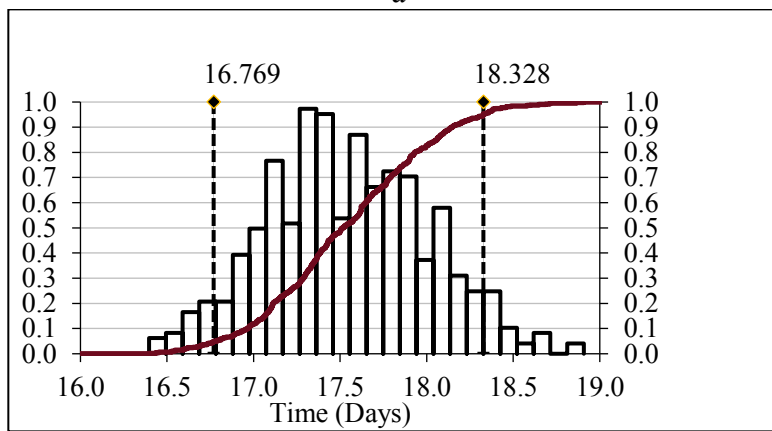
Figure 5-15: Sample of Input Probability Distributions (a) Cost (b) Time

Figure 5-16 illustrates the probability density functions and the cumulative distribution functions for the total cost, time, and resilience improvement of the restoration plan obtained using GA algorithm. [Figure 5-16(a)] shows that the minimum and maximum values of the total restoration cost were CAD 1.513 million and CAD 1.623 million, respectively. Similarly, the minimum and maximum total restoration durations were 16.40 days and 18.91 days, respectively [Figure 5-16(b)], and the minimum and maximum resilience improvement were 0.1058 and 0.1070, respectively [Figure 5-16(c)]. This variation range reflects the level of confidence in the skills of the restoration

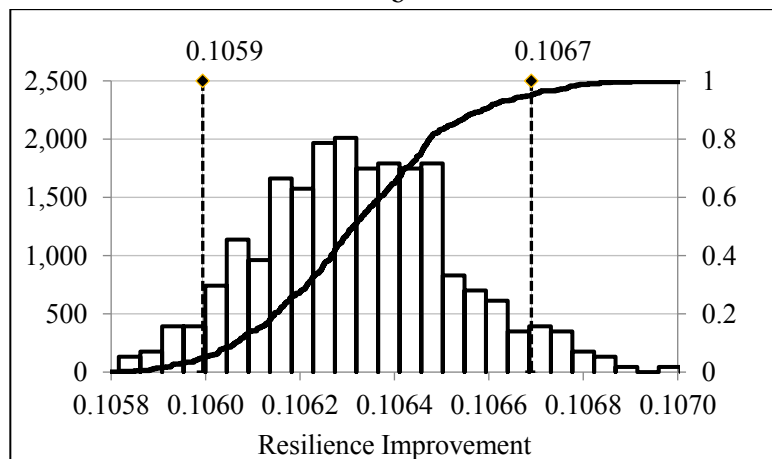
crews. The mean values of the restoration cost, time, and resilience improvement were CAD 1,570 million, 17.54 days, and 0.106, respectively.



a



b



c

Figure 5-16: Distributions of the Optimal Solution Resulting from Stochastic Optimization (a) Cost (b) Time (c) Resilience Improvement (Assad et al. 2020)

Table 5-27 depicts a comparison between the results of the deterministic and stochastic solutions of the formulated problem. As evidenced by the observable variations, utility managers shall consider utilizing a stochastic approach in cases when the input estimates are highly uncertain. In stochastic analysis, different statistics can be optimized instead of the mean of the original objective such as the 95th percentile. However, when decision-makers have reasonable certainty about the used estimates, deterministic approach is preferred due to the significant decrease in the computational time and effort. It is worth mentioning that the objective functions need to be normalized before the optimization is run to avoid any bias due to the distinct performance range of each objective.

Table 5-27: Comparison between Deterministic and Stochastic Solutions of the Restoration Optimization Model (Assad et al. 2020)

Criterion	Deterministic Results	Stochastic Results (Mean Values)
Time (days)	13.86	17.54
Cost ($\times 10^3$ CAD)	1,557	1,570
Resilience Improvement	0.106	0.106
Computational Time (min.)	2.1 – 3.0	10.5 - 14.1

Restoration Model Validation

To evaluate the performance of the developed optimization model, the obtained results were compared to a restoration plan suggested by the City of London. Municipalities in Canada develop in-house heuristics to guide investment planning and obtain such restoration plans. The total restoration time, cost, and resilience improvement resulting from the City’s plan were calculated. The suggested optimization model resulted in a significant improvement over the City’s plan concerning the restoration time and cost, as shown in Table 5-28. The obtained restoration plan by the optimization model was around 13 days shorter and CAD 63,000 less expensive. The realized improvement in network resilience, as suggested by the optimization model, was around 4% more

than its corresponding value following the City’s approach. The two plans were mainly different in the sequence of restoring the failed segments and in the individual segments that were suggested to be replaced despite having a small break because of exceeding a certain number of breaks. This policy is followed to avoid significant decrease in performance capacity of water segments. While respecting the available budget, the segment that was selected for replacement by the optimization model is more critical, and thus resulted in a more significant resilience improvement, than the corresponding segment suggested based on the City’s plan. This is because the criticality of each segment is explicitly considered in the utilized resilience metric, as shown in Equation 3.7 (Assad et al. 2020).

Table 5-28: Comparison between City’s Approach and Suggested Optimization Model (Assad et al. 2020)

Criterion	Optimization Model	City’s Approach	Enhancement
Time (days)	13.86	26.95	48.5%
Cost (x10 ³ CAD)	1,557	1,620	3.9%
Resilience Improvement	0.1056	0.1018	3.7%

Several sensitivity analyses were then conducted to determine the input variables whose impacts on the mean values of the objective functions were the highest. Figure 5-17 depicts a tornado graph showing the sensitivities of total restoration cost to different inputs. Restoring pipe segments #10 and #27 were found to impact the restoration cost the most. Segments 10 and 27 are two of the largest segments in this studied network with diameters of 450mm and 300mm, respectively. Additionally, the restoration methods suggested for these two segments were pipe bursting and open-cut-method. Similar analyses were performed to highlight critical segments based on restoration time and resilience improvement. This kind of analysis is essential to determine the crucial segments whose restoration needs to be carefully reviewed and monitored.

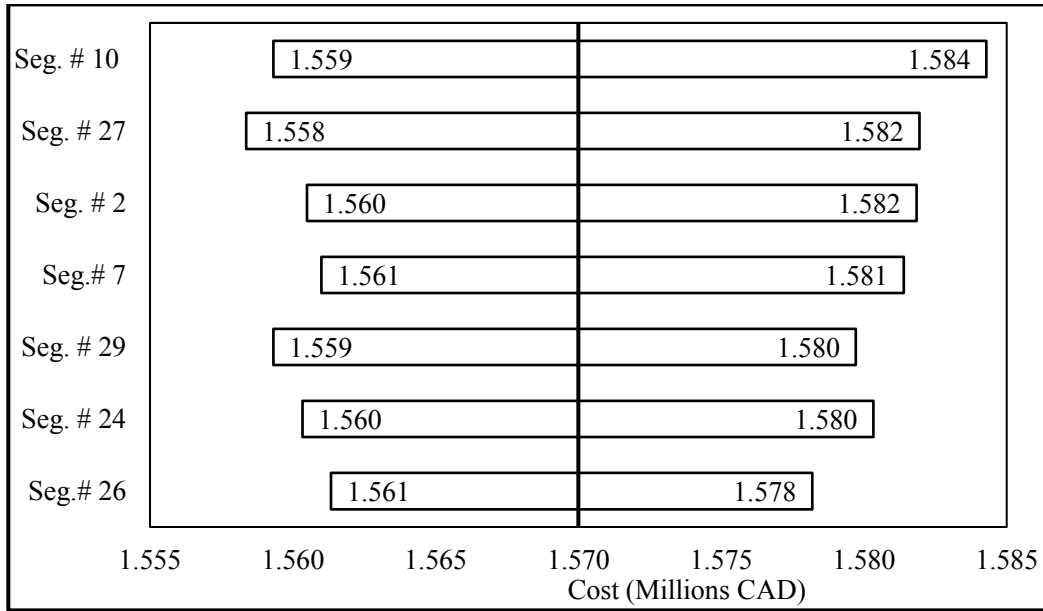


Figure 5-17: Tornado Graph Ranking Inputs by Effect on the Mean of the Restoration Cost (Assad et al. 2020)

5.4 Resilience Enhancement Model

As previously mentioned in section 3.4, the resilience enhancement model is the last model developed in this dissertation. This model aims to increase the strength of WDNs to withstand future disruptions without significant performance loss. This model integrates resilience and sustainability objectives to determine the optimum resilience enhancement plan of WDNs. This section illustrates the application of this enhancement optimization model. Similar to the restoration model, various optimization algorithms were investigated to select the best performing one. In addition, obtained results were also compared against a heuristics approach followed by municipalities in Canada to evaluate the robustness of the developed optimization model.

The developed model was applied on a section of the water network in London, Ontario. The selected section is composed of 369 pipe segments of diameters ranging between 40mm and 450 mm that amount approximately to 34 km of length. The material types available are cast iron (CI), ductile iron (DI), and PVC. The selected section consists of three sub-networks covering a wide variation in

land use, serviced facilities, and road types, as shown in Figure 5-18 and Figure 5-19. Figure 5-18 shows the overall water network in the City of London with the land use zones superimposed. Figure 5-19 depicts three sub-networks that form the selected case study of this section. Each network is assumed to have a different minimum accepted resilience threshold reflecting its importance to the decision-makers, as previously explained in section 3.4. It is observable that the section of London WDN selected to implement the enhancement level is bigger than the section that was selected to implement the previously developed model. This is because the resilience enhancement model explicitly accounts for different land use. Also, the nature of this model requires considering a larger portion of the network to capture situations similar to those that municipalities deal with on a daily basis. Municipalities are typically responsible for managing and sustaining a large inventory of water assets. Given the limited resources and scarce funds, they will have to develop prioritization models to assess the urgency of the rehabilitation needs of these assets. As such, this model is applied to a bigger section of the London water network that covers segments in various zones of the network. Each zone represents a particular land use and relative importance compared to other zones in the selected case study. It is also remarkable that Figure 5-18 includes multiple distinct residential zones. That is true because these zones are different in several attributes such as the population size and tax base. This zoning can also be useful to highlight areas that are more prone to certain types of hazards such as seismic prone locations or floods prone locations. These zones would then receive a higher priority in resilience enhancement decisions.

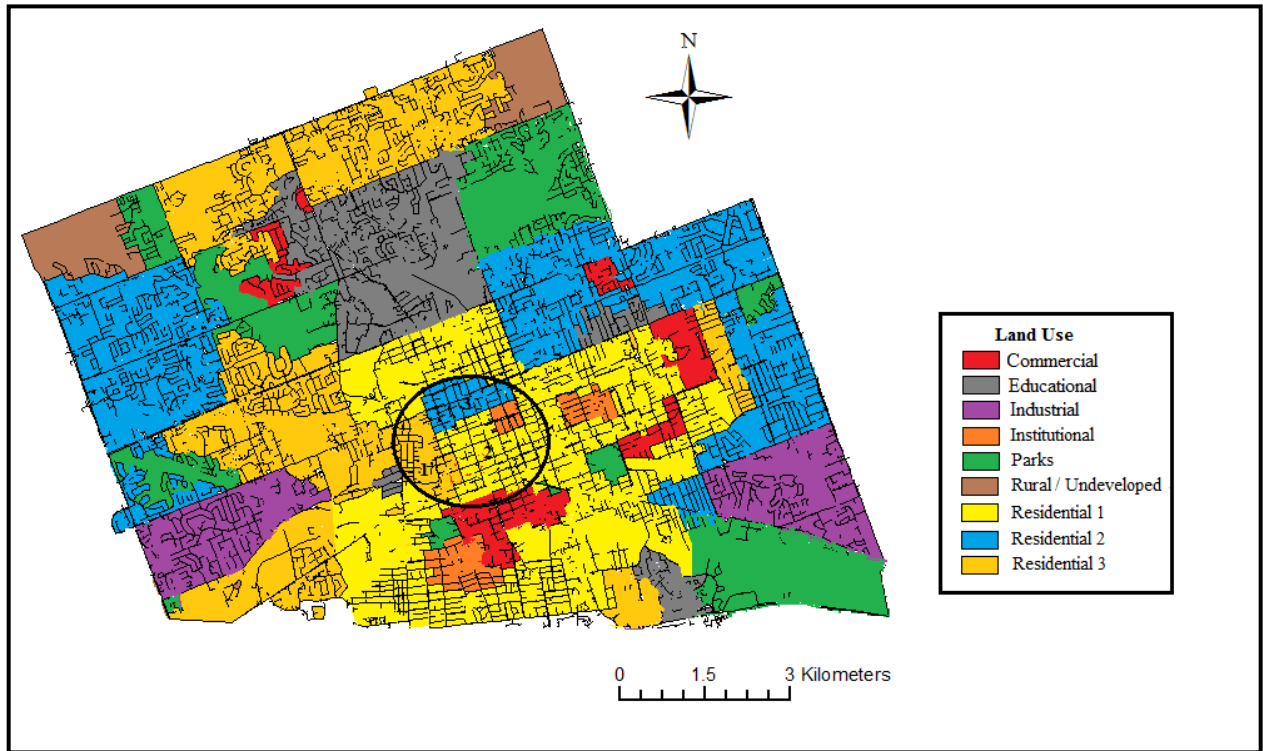


Figure 5-18: Layout of the Water Network in the City of London, Ontario

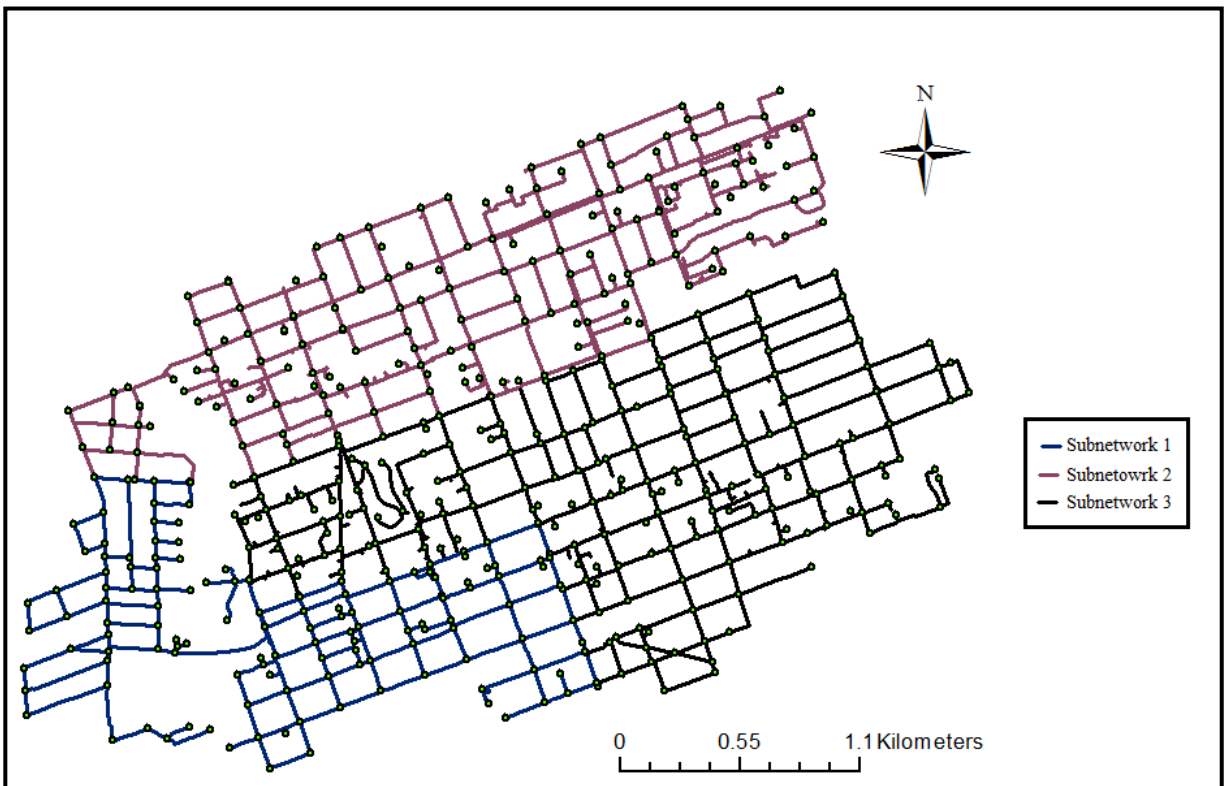


Figure 5-19: Layout of the Selected Sub-networks

Enhancement Actions Determination

The resilience enhancement optimization problem was formulated, as described in section 3.4. Two main set of inputs were used in calculating the objectives of this optimization. The first set of inputs represents the results of the resilience assessment model. The resilience metric introduced in section 5.2 was utilized to evaluate the resilience level of the selected section of the London WDN. The second set of inputs represents the cost, resilience improvement, and carbon emissions associated with each of the considered resilience enhancement actions. Costs and resilience improvements are calculated as detailed in section 3.4. Carbon emissions were also calculated utilizing the North American Society of Trenchless Technology calculator, as mentioned in section 3.4. Figure 5-20 depicts a sample of the carbon emissions results associated with PB and CIPP techniques that were calculated utilizing this NASTT calculator. These emissions were calculated considering a pipe segment that was made of cast iron and of 200mm in diameter. The 150m in length segment was buried at a depth of 2.5m. Dump location was assumed to be 10m away from the segment's location. This information is important in calculating the CO₂ emissions associated with open- cut method for comparison analysis. Emissions associated with the Open Cut method was also added to highlight the realized reductions in carbon emissions when utilizing trenchless technologies.

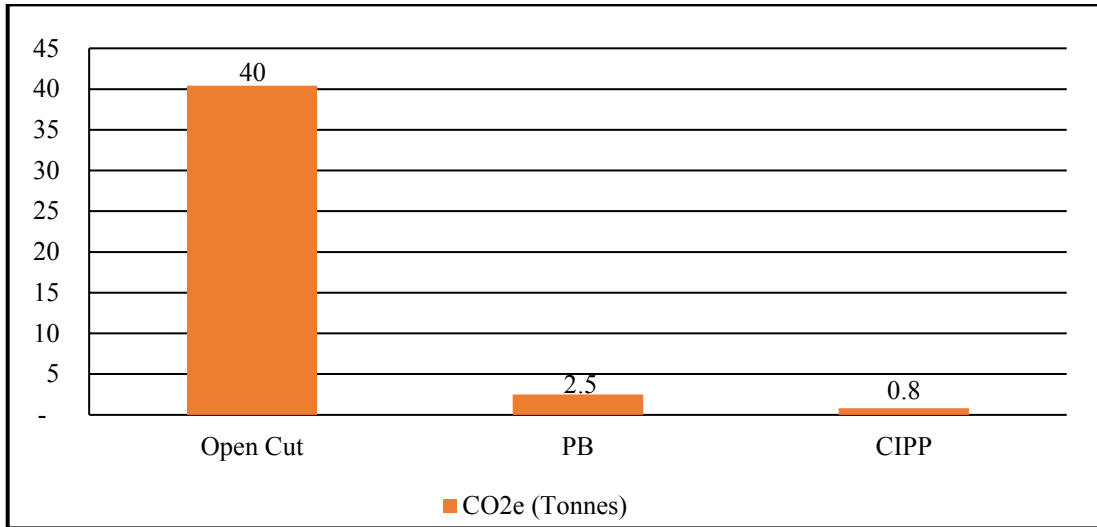


Figure 5-20: Variation of Carbon Emissions Associated with Various Rehabilitation Techniques

In this work, the formulated multi-objective optimization problem was solved using a modified version of ant colony optimization (ACO) and genetic algorithm (GA) to determine their respective capabilities in achieving a near-optimal solution for the considered problem. Theoretical concepts and underlying mathematical computations of the modified ACO and GA were detailed in section 2.8. Each algorithm was run several times with distinct initialization to provide a fair comparison between the optimization algorithms and to assure the consistency of the obtained results. To provide a meaningful basis of comparison, the number of iterations was assumed 200, and the population size is assumed 150 for the considered optimization algorithms. Table 5-29 illustrates the comparison results between the modified ACO and GA based on the outputs of ten runs.

The modified ACO achieved the best values for the cost, resilience, and emissions objectives. Similarly, the worst values for the cost, resilience, and emissions objectives obtained by the modified ACO were better than those obtained by GA. The modified ACO had a lower standard deviation regarding all the considered objective functions, indicating higher stability of the algorithm. It also had a larger hypervolume indicator (78.79%) than GA. On the other hand, GA had a longer computational time (8.11 min) than the modified ACO (5.38 min). All optimization runs were

performed on an 8GB 343 RAM, 3.60 GHz i7 core CPU, and Windows 7 with a 64-bit operating system. It can be observed from Table 5-29 that the range of resilience variation is less than the ranges of other objectives. This is due to the size of the considered network, 370 segments, and the minimum resilience threshold constraints. The dual effect of these factors limits the solution engine in certain preferred area of the search space.

Table 5-29: Comparison between Results of the Modified ACO and GA

	Objective function	Modified ACO	GA
Minimum	Cost (million CAD)	1.6055	1.7148
	Resilience	0.6429	0.6128
	Emissions (CO ₂ -e tonne)	132.70	135.10
Maximum	Cost (Million CAD)	1.8152	2.2827
	Resilience	0.6458	0.6228
	Emissions	139.20	140.40
Mean	Cost (million CAD)	1.6547	2.0621
	Resilience	0.6447	0.6159
	Emissions (CO ₂ -e tonne)	135.13	137.34
Standard deviation	Cost (million)	0.0376	0.1652
	Resilience	0.0008	0.0032
	Emissions (CO ₂ -e tonne)	1.50	3.06
Hypervolume indicator (HV)		78.79%	60.43%
Computational time (min)		5.38	8.11

Note: The bold values represent the best values corresponding to each performance metric

Next, a two-tailed student’s t-test was performed to statistically evaluate the significance level of the optimal solutions. The student’s t-test investigated the null hypothesis (H₀) that assumed no

significant difference between the optimal solutions obtained from the optimization algorithms. The alternative hypothesis (H_1) implied that there was a significant difference between the obtained optimal solutions. The P-value needs to be less than the significance level ($\alpha = 0.05$), to reject the null hypothesis in favor of the alternative hypothesis. Before running the t-test, a condition that the data are coming from approximately normal distributions needs to be satisfied. This is the case in our example since the sample size is large (>30), according to the central limit theory. The t-test performed in this analysis assumed unequal variances of the population of the data since such equality was not possible to be proved. The computed P-value was found to be 9.505×10^{-6} , which indicates that the performance of the modified ACO was on average statistically significantly better than GA. From the previous analysis, the modified ACO was recommended to solve the formulated problem in this paper.

The model then proceeded with the MCDM process to determine the best solution among the Pareto frontier points obtained from the multi-objective optimization. First, the Shannon entropy method was exploited to compute the weights of the objective functions. The weights of the cost, resilience, and emissions attributes were 51.36%, 29.28%, and 19.36%, respectively, as shown in Table 5-30.

Table 5-30: Calculation of Objectives’ Weights based on Shannon Entropy

Criterion	Cost	Resilience	Emissions
Entropy value (e_j)	0.273	0.5856	0.726
Variation coefficient (d_j)	0.727	0.4144	0.274
Weight (w_j)	51.36%	29.28%	19.36%

Once the objectives’ weights were found, PROMETHEE II was utilized to determine the best solution based on the steps explained in section 2.7. Figure 5-21 depicts a sample of the Pareto frontier points obtained by the modified ACO algorithm for one of the runs with the selected optimal

solution highlighted in red. Table 5-31 illustrates some of these candidate solutions along with their ranking based on the net outranking flow, as calculated by Equation 2.18.

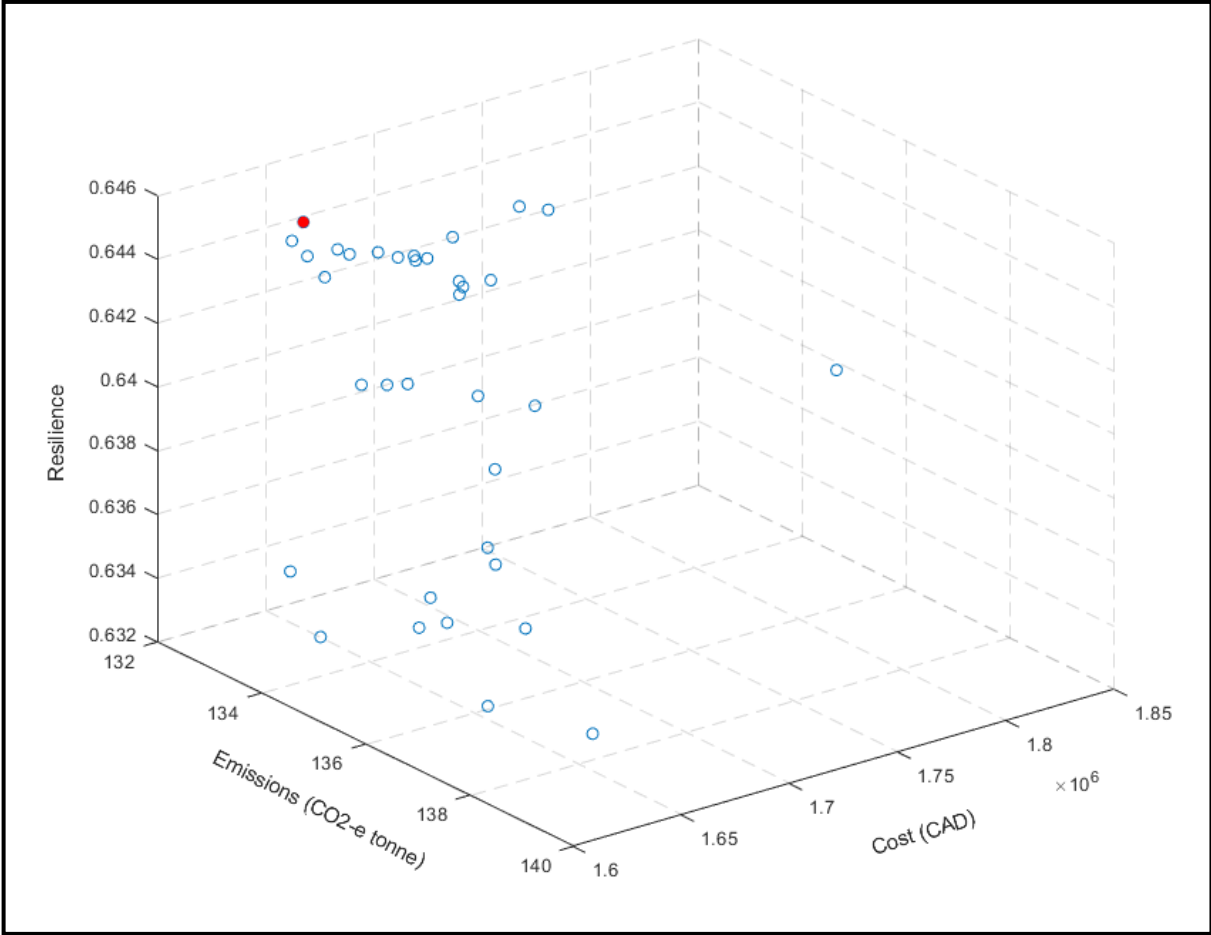


Figure 5-21. Pareto Frontier Points of the Modified ACO Algorithm

Table 5-31: Different Optimal Solution Resulting from the Modified ACO

Solution	Cost (x10 ⁶ CAD)	Resilience	Emissions (CO ₂ -e tonne)	ϕ (a)	Rank
1	1.637	0.6443	133.0	0.1227	9
2	1.628	0.6443	139.2	-0.1219	25
3	1.626	0.6437	138.0	-0.2164	32
:	:	:	:	:	:
19	1.651	0.6447	132.7	0.1707	1
:	:	:	:	:	:
35	1.657	0.6456	134.9	0.1334	6

Note: The bold row represents the selected optimal solution for the optimization problem.

Solution number 19 in Table 5-31, involved interventions actions for 57%, a total of 211, of the pipe segments in the considered sub-networks to achieve the reported objective values while satisfying the set of defined constraints. Figure 5-22 illustrates the distribution of these segments based on their sub-network, diameter, and age. It can be observed from Figure 5-22 that most of the selected segments for enhancements were in subnetwork 3. This is due to the fact that this subnetwork had the most deteriorated segments, as evidenced by the average age of its segments. The average ages of the segments in subnetworks 1, 2, and 3 were 31, 37, and 50 years, respectively. The attained resilience improvement with CAD 1.65 million investment represented a 20% increase in resilience compared to the case where no enhancement actions were taken over the five subsequent years.

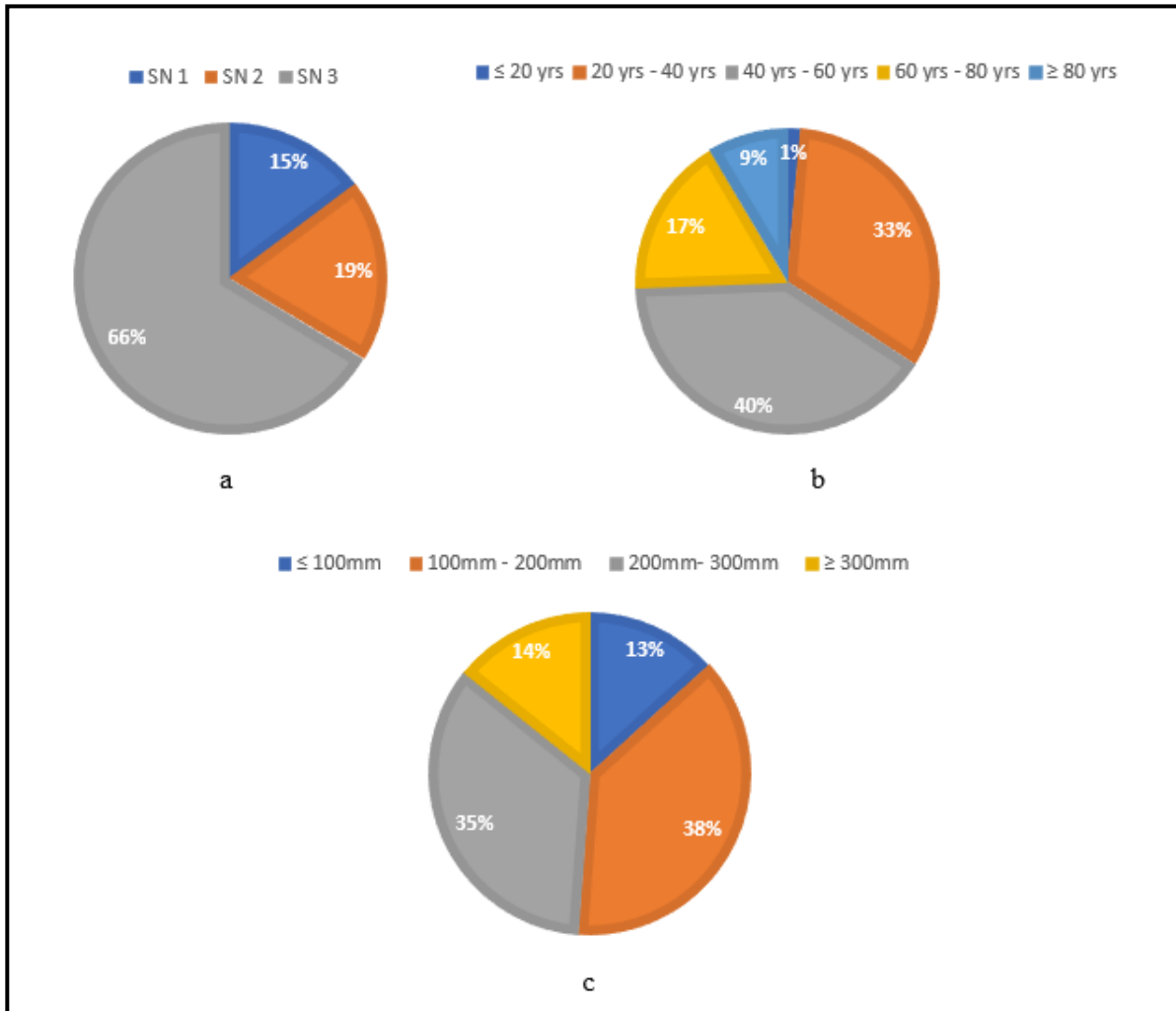


Figure 5-22: Distribution of Rehabilitated Segments Based On a) sub-network; b) age; and c) size.

Enhancement Actions Packaging and Scheduling

Next, resilience enhancement actions of year one were selected to be scheduled. The first step was to cluster them into work packages based on the intervention method and geographical location. The area of the considered networks has been divided into two zones to speed up the travel time. Both K-means and K-medoids clustering techniques were tested to cluster the pipe segments into two groups based on their geographical locations. K-means yielded a lower Davies–Bouldin index, 0.850, than K-medoids. Thus, K-means was selected for the geographical clustering. RapidMiner 7.5 is the platform that is used to perform the clustering algorithms (Mierswa et al. 2006). Figure 5-23

depicts the interface of the RapidMiner Platform, where the clustering techniques were performed and tested.

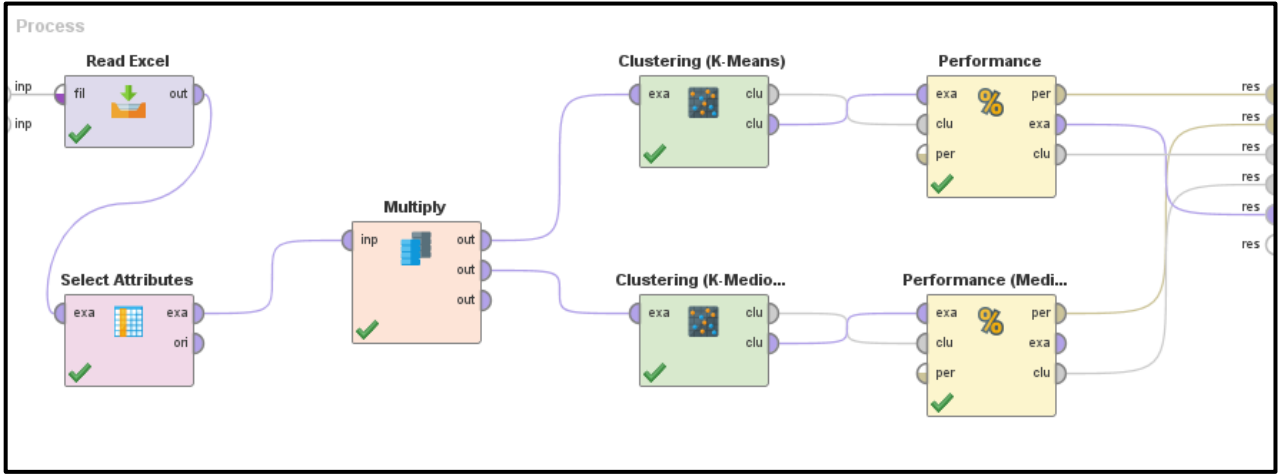


Figure 5-23: Interface of the Clustering Algorithms Utilizing RapidMiner Platform

Enhancement actions were then clustered into work packages as per Equation 3.35. Table 5-32 illustrates the output of this clustering process. It shows nine packages, each composed of segments that share the same geographical zone and intervention method except for package two, which was a mixed one. These work packages were then scheduled, assuming three contractors will perform enhancements actions along three time steps. A time step represents the order at which a work package is being performed. The scheduling process aims at minimizing the cumulative time of the resilience enhancement process while satisfying the maximum contract price of each contractor.

Table 5-32: Packaging and Scheduling of Enhancement Actions of Year 1

Package No.	Cost (x10 ³ CAD)	Resilience	Time (day)	Enhancement Action	Time Step	Contractor
1	99.42	0.0035	7.03	PB	1	C1
2	76.93	0.0036	5.26	PB & CIPP	1	C2
3	89.92	0.0055	9.74	CIPP	1	C3
4	93.11	0.0036	4.46	CIPP	2	C1
5	87.20	0.0027	6.33	CIPP	3	C1
6	48.92	0.0038	14.74	EL	2	C2
7	56.36	0.0050	16.98	EL	2	C3

8	49.12	0.0047	14.80	EL	3	C2
---	-------	--------	-------	----	---	----

Figure 5-24 depicts the incremental increase of resilience with time. According to this plan, it was possible to achieve a total of 0.034 resilience enhancement resulting from the first year’s actions during 26.72 days. The assignments of contractors among the different time steps are also shown in Table 5-32. The total price values for contractors 1, 2, and 3 were CAD 241,649, CAD 213,057, and CAD 146,284, respectively.

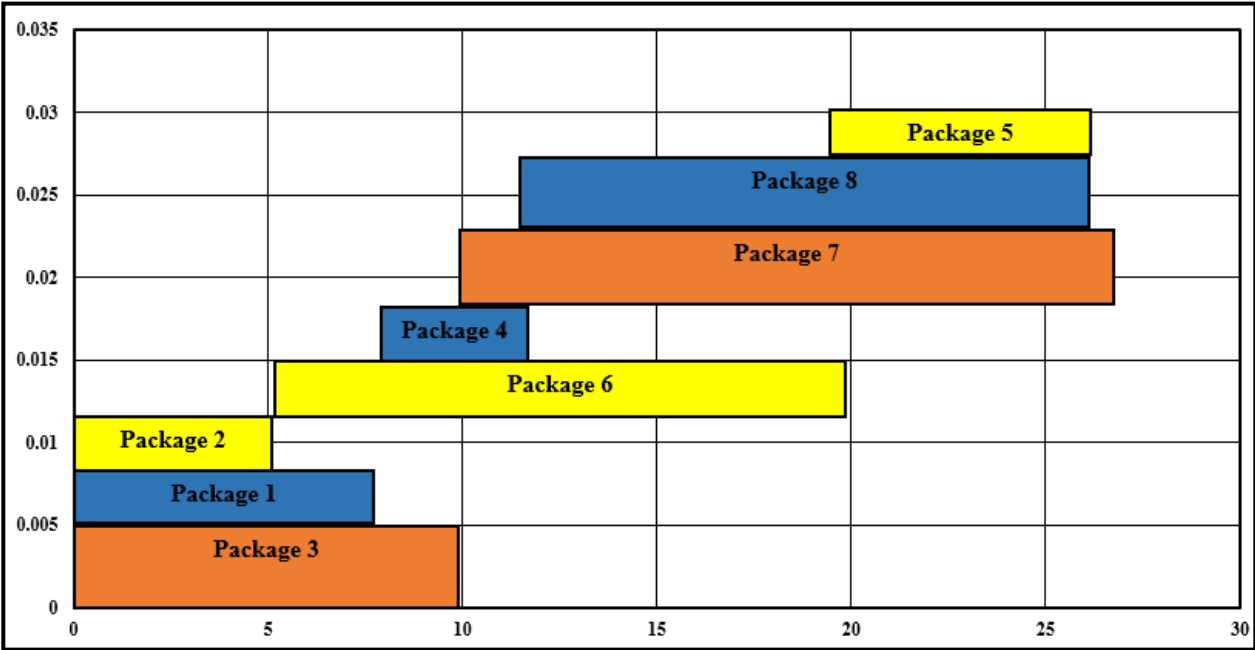


Figure 5-24: Optimum Scheduling Results

Redundancy Enhancement Strategy

As previously stated, a separate optimization model was formulated to improve the redundancy of the selected section of the London WDN. This is achieved by duplicating some of the most critical segments in each sub-network.

By applying the proposed model, it was possible to increase the redundancy level of sub-networks 1, 2, and 3 by 21%, 18%, and 23%, respectively, as shown in Table 5-33. Resilience

enhancement percentages resulting from this redundancy improvement are also shown in Table 5-33.

These results were obtained after substantiating the new redundancy values in Equation 3.7.

Table 5-33: Results of Resilience Enhancement due to Redundancy Improvement

Sub-network	Original Redundancy	Updated Redundancy	Redundancy Improvement	Resilience Enhancement
1	0.15	0.18	20.6%	5.2%
2	0.16	0.19	18.1%	4.5%
3	0.18	0.22	23.2%	5.8%

Enhancement Model Validation

A comparison between the obtained results of the resilience enhancement optimization model and an in-house portfolio management plan suggested by the City of London was then performed to evaluate the performance of the developed optimization model. Table 5-34 shows that the developed model resulted in a 32% cost savings, a 6% increase in resilience improvement, and a 6% carbon emissions reduction. The two plans were different in the selection criteria of individual segments to be enhanced. While the City’s approach focused on the age and reliability of segments, the developed method integrated the criticality of segments in the selection process. Thus, asserting more weights to select the most critical segments. In addition, the dynamic nature of reliability computation yielded a more accurate deterioration estimation of various segments. Table 5-34 shows the comparison results, excluding resilience enhancement due to redundancy improvement. Currently, network expansion strategies are handled at a different level of management for which relevant data for comparison and validation purposes could not be retrieved.

Table 5-34: Comparison between City’s Approach and Suggested Optimization Model

Criterion	Optimization Model	City’s Approach	Enhancement
Cost (x10 ⁶ CAD)	1.651	2.440	32.35%
Resilience	0.6447	0.6083	5.99%
Emissions (CO ₂ -e tonne)	132.7	141.2	6.02%

5.5 Summary

In this chapter, the implementation of the developed models was presented. Actual data from real water networks were used to demonstrate the efficiency and practicality of the developed models. The proposed resilience metric was validated by comparing its results with the results of flow-based and topological-based metrics. The results obtained assured the usefulness of utilizing this metric in various resilience applications of WDNs. A section of London WDN was leveraged as a case study, and a failure scenario was assumed to apply the resilience-based restoration model. Different algorithms were tested to select the best performing one to solve the formulated optimization problem. In addition, the generated restoration schedule was compared to a suggested schedule by the City of London. The comparison showed that the developed model would result in considerable cost-savings if employed instead of the currently utilized heuristics. Similarly, the resilience enhancement optimization model was applied and evaluated utilizing a real water network. A modified version of ACO optimization was compared to the performance of GA to solve the formulated optimization model. It was found that the performance of the modified ACO is better than that of the GA and of the results optioned by current portfolio management practices. Several strategies could be elicited from the results of the developed models. Firstly, segments of bigger sizes that secure the provision of water to bigger population are the most critical ones. Their performance shall be restored at the earliest and constantly enhanced. Secondly, when planning for enhancement actions, intervention type and geographical location shall be utilized as the basis of clustering to facilitate efficient resource utilization and scheduling. Thirdly, when selecting the set of enhancement actions, suitability of various methods to the existing pipe segment shall be assessed. Finally, relocation time and cost shall be accurately estimated to capture the routing and traffic conditions during widespread hazardous events.

Chapter 6: Conclusions and Recommendations

6.1 Summary

A newly developed holistic resilience-based asset management model for WDNs is developed. This model encompasses three main steps to systematically integrate resilience in sustainable performance management of WDNs. Firstly, robustness and redundancy were integrated to assess the current network resilience level. Network redundancy was estimated by employing graph theory and complex network indicators. The core idea behind this step is to measure the extent to which alternative paths can be secured to supply water in case of structural damage of some components. Network robustness was measured as a function of various segments reliabilities. A real-life network was utilized to demonstrate the practicality of the proposed metric in various resilience applications. Results were compared to flow-based and topological-based metrics as a means of validation. It was also shown that the proposed metric could be used as a proxy indicator for the serviceability index in resilience restoration application without the need to run extended hydraulic simulations.

The second step is to develop a resilience-driven restoration model of WDNs. Because this study aims to propose a general methodology framework, disruption scenarios on WDS were simulated by randomly assuming a certain number of broken pipe segments, neglecting the dependence of the failure probability on disasters. This model accounts for the time and cost that crews spend in relocating from one location to another across the network. The restoration process was formulated as a multi-objective optimization problem that aims at minimizing the time and cost of recovery and maximizing the resilience improvement. As this model aims to plan for future expected hazardous scenarios, accurate estimates about specific optimization parameters may not be known with an acceptable confidence level. As such, stochastic optimization was utilized to account

for these uncertainties. The restoration model resulted in 4% cost savings, 48% duration reduction, and 4% resilience improvement when compared to a plan suggested by the City of London.

Subsequently, a two-tier resilience enhancement model was developed. In the first phase, a multi-objective optimization framework is formulated to maximize the resilience level of WDNs while minimizing the life cycle cost of enhancement actions and the associated carbon emissions. A dynamic reliability estimation model was utilized to determine the resilience improvement and the updated deterioration behavior after implementing various sets of intervention actions. The resilience enhancement plan resulting from this phase consists of optimum resilience actions along with their timing along the planning horizon. These actions were then clustered into work packages based on the intervention type and geographical location. Next, an optimization-based scheduling model was formulated to determine the optimum sequence of resilience enhancement work packages. A resilience improvement of 20% was attained with CAD 1.65 million investment in enhancement actions over the planning horizon of five years. Resilience enhancement model resulted in a 32% cost saving, a 6% increase in resilience improvement, and a 6% reduction in carbon emissions when compared to a portfolio management approach that is commonly followed by several cities in Canada.

Finally, an automated computer application was developed to integrate the previously developed models. The application was programmed and fully compatible with Microsoft Excel[®] and Matlab[®] environments. Options to specify, add, and change any user-defined values or relevant constraints were also added. Results of these models were presented as Excel spreadsheets and on a specially developed dashboard that is fully integrated with Arc-GIS.

6.2 Recommendation and Future Work

Several interesting topics relevant to this study could be researched in the future. Some of these promising suggestions are extensions that may enrich and enhance current research. Others represent major and fundamental reinforcement to extend the applicability and efficacy of the developed models. Recommended future topics are listed subsequently:

- Including other assets of WDNs such as pumps, valves, and other accessories. Robustness of each segment can be modified to consider the reliability and criticality of other components. Additionally, availability of alternative components can be studied to quantify the network's redundancy.
- Utilizing other metrics to quantify redundancy of water segments. Beside the meshed-ness coefficient, other graph theory and complex graph metrics can be utilized to measure the redundancy level of water networks.
- Reformulating the criticality model such that the segment's criticality is dynamically updated once pipe segments are replaced with a segment of another size or material type.
- Including other failure modes of WDNs such as hydraulic failures and failures related to water quality. This will require calibrating and running hydraulic simulation models. For example, adding the service pressure to the formulation can help in obtaining an accurate estimation of hydraulic performance loss.
- Refining the resilience enhancement analysis to include more sustainability objectives other than carbon emissions such as energy requirements. Energy needed for different pumping operational conditions can be calculated utilizing a hydraulic simulation model.

References

- Abdullah, L., Chan, W., & Afshari, A. (2019). Application of PROMETHEE method for green supplier selection: A comparative result based on preference functions. *Journal of Industrial Engineering International*, 15(2), 271-285.
- Adams, T. M., Bekkem, K. R., & Toledo-Duran, E. J. (2012). Freight resilience measures. *Journal of Transportation Engineering*, 138(11), 1403-1409.
- Akyene, T. (2012). Cell phone evaluation base on entropy and TOPSIS. *Interdisciplinary Journal of Research in Business*, 1(12), 9-15.
- Alan Atalah. (2009). *Pipe bursting* (2nd Ed.). Irving, TX: Plastics Pipe Institute. Retrieved from http://www.knovel.com/web/portal/browse/display?_EXT_KNOVEL_DISPLAY_bookid=5198
- Almoghathawi, Y., Barker, K., & Albert, L. A. (2019). Resilience-driven restoration model for interdependent infrastructure networks. *Reliability Engineering & System Safety*, 185, 12-23.
- Archetti, F., Candelieri, A., & Soldi, D. (2015). Network analysis for resilience evaluation in water distribution networks. *Environmental Engineering and Management Journal*, 14(6), 1261-1270.
- ASCE. (2017). *2017 infrastructure report card*. USA: American Society of Civil Engineers. Retrieved from <https://www.infrastructurereportcard.org/>
- Assad, A., Moselhi, O., & Zayed, T. (2019). A new metric for assessing resilience of water distribution networks. *Water*, 11(8), 1701.
- Assad, A., Moselhi, O., & Zayed, T. (2020). Resilience-driven multiobjective restoration planning for water distribution networks. *Journal of Performance of Constructed Facilities*, 34(4), 04020072.
- Ayyub, B. M. (2014). Systems resilience for multihazard environments: Definition, metrics, and valuation for decision making. *Risk Analysis*, 34(2), 340-355.
- Bałut, A., Brodziak, R., Bylka, J., & Zakrzewski, P. (2019). Ranking approach to scheduling repairs of a water distribution system for the post-disaster response and restoration service. *Water*, 11(8), 1591.
- Baños, R., Reca, J., Martínez, J., Gil, C., & Márquez, A. L. (2011). Resilience indexes for water distribution network design: A performance analysis under demand uncertainty. *Water Resources Management*, 25(10), 2351-2366.

- Barker, K., Ramirez-Marquez, J. E., & Rocco, C. M. (2013). Resilience-based network component importance measures. *Reliability Engineering & System Safety*, 117, 89-97.
- Baroud, H., Barker, K., & Ramirez-Marquez, J. E. (2014). Importance measures for inland waterway network resilience. *Transportation Research Part E: Logistics and Transportation Review*, 62, 55-67.
- Basu, S. (2012). Tabu search implementation on traveling salesman problem and its variations: A literature survey. *American Journal of Operations Research*, 2(2), 163.
- Beale, D. J., Marlow, D. R., & Cook, S. (2013). Estimating the cost and carbon impact of a long term water main rehabilitation strategy. *Water Resources Management*, 27(11), 3899-3910.
- Bentley Systems Incorporated. *WaterGEMS v8Users Manual 2006*, Haestad Methods Solution Center, Watertown, NY, USA.
- Bocchini, P., Frangopol, D. M., Ummenhofer, T., & Zinke, T. (2013). Resilience and sustainability of civil infrastructure: Toward a unified approach. *Journal of Infrastructure Systems*, 20(2), 04014004.
- Brandão, J. (2009). A deterministic tabu search algorithm for the fleet size and mix vehicle routing problem. *European Journal of Operational Research*, 195(3), 716-728.
- Brans, J., Vincke, P., & Mareschal, B. (1986). How to select and how to rank projects: The PROMETHEE method. *European Journal of Operational Research*, 24(2), 228-238.
- Brashear, J. P., & Jones, J. W. (2008). Risk analysis and management for critical asset protection (RAMCAP plus). *Wiley Handbook of Science and Technology for Homeland Security*.
- Bruneau, M., Chang, S. E., Eguchi, R. T., Lee, G. C., O'Rourke, T. D., Reinhorn, A. M. . . . Von Winterfeldt, D. (2003). A framework to quantitatively assess and enhance the seismic resilience of communities. *Earthquake Spectra*, 19(4), 733-752.
- Chang, S. E., & Shinozuka, M. (2004). Measuring improvements in the disaster resilience of communities. *Earthquake Spectra*, 20(3), 739-755.
- Cheng, C., Yang, K., & Hwang, C. (1999). Evaluating attack helicopters by AHP based on linguistic variable weight. *European Journal of Operational Research*, 116(2), 423-435.
- Choi, Y. H., & Kim, J. H. (2019). Development of multi-objective optimal redundant design approach for multiple pipe failure in water distribution system. *Water*, 11(3), 553.
- Cimellaro, G. P., Tinebra, A., Renschler, C., & Fragiadakis, M. (2015). New resilience index for urban water distribution networks. *Journal of Structural Engineering*, 142(8), C4015014.

- Cimellaro, G. P., Tinebra, A., Renschler, C., & Fragiadakis, M. (2015). New resilience index for urban water distribution networks. *Journal of Structural Engineering*, 142(8), C4015014.
- Cimorelli, L., Morlando, F., Cozzolino, L., D'Aniello, A., & Pianese, D. (2018). Comparison among resilience and entropy index in the optimal rehabilitation of water distribution networks under limited-budgets *Water Resources Management*, 32(12), 3997-4011.
- CIRC. (2019). *Monitoring the state of Canada's core public infrastructure: The Canadian infrastructure report card 2019*. Canada: The Canadian Infrastructure Report Card.
- Collins, P. A., & Baggett, R. K. (2009). *Homeland security and critical infrastructure protection*. Westport, Conn: Praeger Security International.
- Creaco, E., Franchini, M., & Todini, E. (2016). Generalized resilience and failure indices for use with pressure-driven modeling and leakage. *Journal of Water Resources Planning and Management*, 142(8), 04016019.
- Cromwell, J. E. (2002). *Costs of infrastructure failure*. American Water Works Association.
- Cutter, S. L., Ahearn, J. A., Amadei, B., Crawford, P., Eide, E. A., Galloway, G. E., . . . Schoch-Spana, M. (2013). Disaster resilience: A national imperative. *Environment: Science and Policy for Sustainable Development*, 55(2), 25-29.
- Cutter, S. L., Barnes, L., Berry, M., Burton, C., Evans, E., Tate, E., & Webb, J. (2008). A place-based model for understanding community resilience to natural disasters. *Global Environmental Change*, 18(4), 598-606.
- Da Conceicao Cunha, M., & Ribeiro, L. (2004). Tabu search algorithms for water network optimization. *European Journal of Operational Research*, 157(3), 746-758.
- Davies, D. L., & Bouldin, D. W. (1979). A cluster separation measure. *IEEE Transactions on Pattern Analysis and Machine Intelligence*, (2), 224-227.
- Dessavre, D. G., Ramirez-Marquez, J. E., & Barker, K. (2016). Multidimensional approach to complex system resilience analysis. *Reliability Engineering & System Safety*, 149, 34-43.
- Di Nardo, A., Di Natale, M., Giudicianni, C., Greco, R., & Santonastaso, G. F. (2018). Complex network and fractal theory for the assessment of water distribution network resilience to pipe failures. *Water Science and Technology: Water Supply*, 18(3), 767-777.
- Dorigo, M., Birattari, M., & Stutzle, T. (2006). Ant colony optimization. *IEEE Computational Intelligence Magazine*, 1(4), 28-39.
- Dorigo, M., & Gambardella, L. M. (1997). Ant colonies for the travelling salesman problem. *Biosystems*, 43(2), 73-81.

- Dorigo, M., Maniezzo, V., & Colormi, A. (1996). Ant system: Optimization by a colony of cooperating agents. *IEEE Transactions on Systems, Man, and Cybernetics, Part B: Cybernetics*, 26(1), 29-41.
- El Chanati, H. (2014). *Performance assessment of water network infrastructure*. Doctoral dissertation, Concordia University, Montreal, QC, Canada.
- El-Abbasy, M. S., El Chanati, H., Mosleh, F., Senouci, A., Zayed, T., & Al-Derham, H. (2016). Integrated performance assessment model for water distribution networks. *Structure and Infrastructure Engineering*, 12(11), 1505-20. doi:10.1080/15732479.2016.1144620
- Elbeltagi, E., Hegazy, T., & Grierson, D. (2005). Comparison among five evolutionary-based optimization algorithms. *Advanced Engineering Informatics*, 19(1), 43-53.
- El-Ghandour, H. A., & Elbeltagi, E. (2017). Comparison of five evolutionary algorithms for optimization of water distribution networks. *Journal of Computing in Civil Engineering*, 32(1), 04017066. Doi: 10.1061/ (ASCE) CP.1943-5487.0000717
- ESRI (2011). "ArcGIS Desktop: Release 10". Redlands, CA: *Environmental Systems Research Institute*, 437, 438.
- Etaati, L., Sadi-Nezhad, S., & Moghadam-Abyaneh, P. M. (2011). Fuzzy analytical network process: An overview on methods. *American Journal of Scientific Research*, 41, 101-114.
- Exler, O., & Schittkowski, K. (2007). A trust region SQP algorithm for mixed-integer nonlinear programming. *Optimization Letters*, 1(3), 269-280.
- Farahmandfar, Z., & Piratla, K. R. (2017a). Comparative evaluation of topological and flow-based seismic resilience metrics for rehabilitation of water pipeline systems. *Journal of Pipeline Systems Engineering and Practice*, 9(1), 04017027.
- Farahmandfar, Z., & Piratla, K. R. (2017b). Resilience-based water main rehabilitation planning in a multi-hazard context. *Journal of Water Supply: Research and Technology-Aqua*, 66(8), 651-664.
- Farahmandfar, Z., Piratla, K. R., & Andrus, R. D. (2016). Resilience evaluation of water supply networks against seismic hazards. *Journal of Pipeline Systems Engineering and Practice*, 8(1), 04016014.
- Fiksel J, Goodman I, Hecht A. (2014). Resilience: Navigating a sustainable future. *Solutions*, 5(5), 38-47.
- Fisher, R. E., Bassett, G. W., Buehring, W. A., Collins, M. J., Dickinson, D. C., Eaton, L. K., ... & Millier, D. J. (2010). *Constructing a resilience index for the enhanced critical infrastructure*

- protection program* (No. ANL/DIS-10-9). Argonne National Lab. (ANL), Argonne, IL (United States). Decision and Information Sciences.
- Gay Alanis, L. F. (2013). *Development of a resilience assessment methodology for networked infrastructure systems using stochastic simulation, with application to water distribution systems*. Doctoral dissertation, Virginia Tech, Virginia, USA.
- Gheisi, A., & Naser, G. (2014). A surrogate measure for multi-component failure based reliability analysis of water distribution systems. *Procedia Engineering*, 89, 333-338.
- Glover, F. (1997). Tabu search and adaptive memory programming—advances, applications and challenges. *Interfaces in computer science and operations research* (pp. 1-75). Springer, Boston, MA, USA.
- He, X., & Yuan, Y. (2019). A framework of identifying critical water distribution pipelines from recovery resilience. *Water Resources Management*, 33(11), 3691-3706.
- Henry, D., & Ramirez-Marquez, J. E. (2012). Generic metrics and quantitative approaches for system resilience as a function of time. *Reliability Engineering & System Safety*, 99, 114-122.
- Herrera, M., Abraham, E., & Stoianov, I. (2016). A graph-theoretic framework for assessing the resilience of sectorised water distribution networks. *Water Resources Management*, 30(5), 1685-1699.
- Holland, J. H. (1975). Adaptation in natural and artificial systems. An introductory analysis with application to biology, control, and artificial intelligence. *Ann Arbor, MI: University of Michigan Press*. 439-444.
- Hosseini, S., Barker, K., & Ramirez-Marquez, J. E. (2016). A review of definitions and measures of system resilience. *Reliability Engineering & System Safety*, 145, 47-61. doi:10.1016/j.ress.2015.08.006
- InfraGuide. (2004). Managing infrastructure assets. *Decision making and investment planning (DMIP) best practice*.
- Işıklar, G., & Büyüközkan, G. (2007). Using a multi-criteria decision making approach to evaluate mobile phone alternatives. *Computer Standards & Interfaces*, 29(2), 265-274.
- Jain, A. K. (2010). Data clustering: 50 years beyond K-means. *Pattern Recognition Letters*, 31(8), 651-666.
- Jardine, A. K., & Tsang, A. H. (2013). *Maintenance, replacement, and reliability: Theory and applications*. Florida: Taylor and Francis Group.

- Jayaram, N., & Srinivasan, K. (2008). Performance-based optimal design and rehabilitation of water distribution networks using life cycle costing. *Water Resources Research*, 44(1)
- Kiriş, Ş. (2013). Multi-criteria inventory classification by using a fuzzy analytic network process (ANP) approach. *Informatica*, 24(2), 199-217.
- Kleinbaum, D. G., & Klein, M. (2010). *Survival analysis*. New York, USA. Springer.
- Klise, K. A., Murray, R., & Walker, L. T. N. (2015). *Systems measures of water distribution system resilience* (No. SAND2015-20746R). Sandia National Lab. (SNL-NM), Albuquerque, NM (United States).
- Laucelli, D., & Giustolisi, O. (2015). Vulnerability assessment of water distribution networks under seismic actions. *Journal of Water Resources Planning and Management*, 141(6), 04014082.
- Law, A. M., Kelton, W. D., & Kelton, W. D. (2000). *Simulation modeling and analysis* (Vol. 3). New York: McGraw-Hill.
- Lawler, E. L., Lenstra, J. K., Rinnooy Kan, A. H., & Shmoys, D. B. (1985). *The traveling salesman problem; a guided tour of combinatorial optimization* John Wiley & sons.
- Lee, M. C. (2010). The analytic hierarchy and the network process in multicriteria decision making: Performance evaluation and selecting key performance indicators based on ANP model. *Convergence and Hybrid Information Technologies*, 426.
- Liu, H., Savić, D. A., Kapelan, Z., Creaco, E., & Yuan, Y. (2017). Reliability surrogate measures for water distribution system design: Comparative analysis. *Journal of Water Resources Planning and Management*, 143(2), 04016072.
- Liu, W., Song, Z., Ouyang, M., & Li, J. (2020). Recovery-based seismic resilience enhancement strategies of water distribution networks. *Reliability Engineering & System Safety*. 107088.
- Luna, R., Balakrishnan, N., & Dagli, C. H. (2011). Postearthquake recovery of a water distribution system: Discrete event simulation using colored petri nets. *Journal of Infrastructure Systems*, 17(1), 25-34.
- Mahmoud, H. A., Kapelan, Z., & Savić, D. (2018). Real-time operational response methodology for reducing failure impacts in water distribution systems. *Journal of Water Resources Planning and Management*, 144(7), 04018029.
- Mareschal, B., & De Smet, Y. (2009). Visual Promethee: Developments of the PROMTHEE & GAIA multicriteria decision aid methods. *In the Proceedings of the IEEE 2009 International Conference on Industrial Engineering and Engineering Management* (pp 1646-1649), Hong Kong.

- Maier, H. R., Simpson, A. R., Zecchin, A. C., Foong, W. K., Phang, K. Y., Seah, H. Y., & Tan, C. L. (2003). Ant colony optimization for design of water distribution systems. *Journal of Water Resources Planning and Management*, 129(3), 200-209.
- Meirelles, G., Brentan, B., Izquierdo, J., Ramos, H., & Luvizotto, E. (2018). Trunk network rehabilitation for resilience improvement and energy recovery in water distribution networks. *Water*, 10(6), 693.
- Meng, F., Fu, G., Farmani, R., Sweetapple, C., & Butler, D. (2018). Topological attributes of network resilience: A study in water distribution systems. *Water Research*, 143, 376-386.
- Mierswa, I., Wurst, M., Klinkenberg, R., Scholz, M., & Euler, T. (2006). Yale: Rapid prototyping for complex data mining tasks. In *Proceedings of the 12th ACM SIGKDD international conference on Knowledge discovery and data mining* (pp. 935-940).
- Mohammed, A. U. (2016). *Integrated reliability assessment of water distribution networks*. Doctoral dissertation, Concordia University, Montreal, QC, Canada.
- Moursi. (2016). *Priority assessment model for water distribution networks*. Doctoral dissertation, Concordia University, Montreal, QC, Canada.
- Murthy, D. P., Rausand, M., & Østerås, T. (2008). *Product reliability: Specification and performance* Springer Science & Business Media.
- Nebro, A. J., Durillo, J. J., & Coello, C. A. C. (2013). (2013). Analysis of leader selection strategies in a multi-objective particle swarm optimizer. Paper presented at the *2013 IEEE Congress on Evolutionary Computation*, 3153-3160.
- Nicholson, C. D., Barker, K., & Ramirez-Marquez, J. E. (2015). Vulnerability analysis for resilience-based network preparedness. *Reliab Eng Syst Saf*, (145), 62–73.
- Nunoo, C. N. (2001). *Optimization of pavement maintenance and rehabilitation programming using shuffled complex evolution algorithm*. Florida International University.
- O'Sullivan D (2010). Reduce your carbon footprint using trenchless. *No Dig Show 2010*, Chicago, Illinois, USA, North American Society for Trenchless Technology.
- Ouyang, M., Duenas-Osorio, L., & Min, X. (2012). A three-stage resilience analysis framework for urban infrastructure systems. *Structural Safety*, 36, 23-31.
- Pant, R., Barker, K., Ramirez-Marquez, J. E., & Rocco, C. M. (2014). Stochastic measures of resilience and their application to container terminals. *Computers & Industrial Engineering*, 70, 183-194.

- Pisinger, D., & Toth, P. (1998). Knapsack problems. *Handbook of combinatorial optimization* (pp. 299-428). Boston, MA, USA: Springer.
- Polat, G. (2016). Subcontractor selection using the integration of the AHP and PROMETHEE methods. *Journal of Civil Engineering and Management*, 22(8), 1042-1054.
- Prasad, T. D., & Park, N. (2004). Multiobjective genetic algorithms for design of water distribution networks. *Journal of Water Resources Planning and Management*, 130(1), 73-82.
- Riquelme, N., Von Lücken, C., & Baran, B. (2015, October). Performance metrics in multi-objective optimization. In *2015 Latin American Computing Conference (CLEI)* (pp. 1-11). IEEE.
- Rose, A. (2007). Economic resilience to natural and man-made disasters: Multidisciplinary origins and contextual dimensions. *Environmental Hazards*, 7(4), 383-398.
- Saaty, T. L. (2007). The analytic hierarchy and analytic network measurement processes: Applications to decisions under risk. *European Journal of Pure and Applied Mathematics*, 1(1), 122-196.
- Sahani, R., & Bhuyan, P. K. (2017). Pedestrian level of service criteria for urban off-street facilities in mid-sized cities. *Transport*, 32(2), 221-232.
- Sahebjamnia, N., Torabi, S. A., & Mansouri, S. A. (2015). Integrated business continuity and disaster recovery planning: Towards organizational resilience. *European Journal of Operational Research*, 242(1), 261-273.
- Salman, A. (2011). *Reliability-based management of water distribution networks*. Doctoral dissertation, Concordia University, Montreal, QC, Canada.
- Sawant, K. B. (2015). Efficient determination of clusters in K-mean algorithm using neighborhood distance. *The International Journal of Emerging Engineering Research and Technology*, 3(1), 22-27.
- Schlüter, M., Egea, J. A., & Banga, J. R. (2009). Extended ant colony optimization for non-convex mixed integer nonlinear programming. *Computers & Operations Research*, 36(7), 2217-2229.
- Schlüter, M., Gerdts, M., & Rückmann, J. (2012). A numerical study of MIDACO on 100 MINLP benchmarks. *Optimization*, 61(7), 873-900.
- Shahata, K. F. (2013). *Decision-support framework for integrated asset management of major municipal infrastructure*. Doctoral dissertation, Concordia University, Montreal, QC, Canada.
- Shannon, C. E. (1948). A mathematical theory of communication. *The Bell System Technical Journal*, 27(3), 379-423.

- Shuang, Q., Liu, H. J., & Porse, E. (2019). Review of the quantitative resilience methods in water distribution networks. *Water*, 11(6), 1189.
- Simicevic, J., & Sterling, R. L. (2001). Guidelines for pipe bursting. *US Army Corps of Engineers, Vicksburg, Miss. TTC technical report*, (2001.02).
- Soldi, D., Candelieri, A., & Archetti, F. (2015). Resilience and vulnerability in urban water distribution networks through network theory and hydraulic simulation. *Procedia Engineering*, 119, 1259-1268.
- Srichetta, P., & Thurachon, W. (2012). Applying fuzzy analytic hierarchy process to evaluate and select product of notebook computers. *International Journal of Modeling and Optimization*, 2(2), 168.
- Suribabu, C. R. (2017). Resilience-based optimal design of water distribution network. *Applied Water Science*, 7(7), 4055-4066.
- Suribabu, C. R., Prashanth, K., Vignesh Kumar, S., & Ganesh, N. S. (2016). Resilience enhancement methods for water distribution networks. *Jordan Journal of Civil Engineering*, 10(2).
- Tabesh, M., Yekta, A. A., & Burrows, R. (2009). An integrated model to evaluate losses in water distribution systems. *Water Resources Management*, 23(3), 477-492.
- Tierney, K., & Bruneau, M. (2007). Conceptualizing and measuring resilience: A key to disaster loss reduction. *TR News*, (250)
- Todini, E. (2000). Looped water distribution networks design using a resilience index based heuristic approach. *Urban Water*, 2(2), 115-122.
- Torres, J. M., Duenas-Osorio, L., Li, Q., & Yazdani, A. (2017). Exploring topological effects on water distribution system performance using graph theory and statistical models. *Journal of Water Resources Planning and Management*, 143(1), 04016068.
- Vanier, D. J., & Rahman, S. (2004). *A primer on municipal infrastructure asset management*. University of British Columbia, Vancouver: NRC.
- Verma, A. K., Ajit, S., & Karanki, D. R. (2010). *Reliability and safety engineering* (Vol. 43, pp. 373-392). London: Springer.
- Vugrin, E. D., Warren, D. E., & Ehlen, M. A. (2011). A resilience assessment framework for infrastructure and economic systems: Quantitative and qualitative resilience analysis of petrochemical supply chains to a hurricane. *Process Safety Progress*, 30(3), 280-290.

- Wang, S., Hong, L., & Chen, X. (2012). Vulnerability analysis of interdependent infrastructure systems: A methodological framework. *Physica A: Statistical Mechanics and its Applications*, 391(11), 3323-3335.
- Weaver, T., & Woodcock, M. E. (2014) Pipe bursting water lines with confidence. *North American Society for Trenchless Technology (NASTT) NASTT's 2014 no-Dig Show*, Orlando, Florida, USA.
- Wei, J. Y., Sun, A. F., & Wang, C. H. (2010, January). The application of fuzzy-ANP in the selection of supplier in supply chain management. In *2010 International Conference on Logistics Systems and Intelligent Management (ICLSIM)* (Vol. 3, pp. 1357-1360). IEEE.
- Yazdani, A., Otoo, R. A., & Jeffrey, P. (2011). Resilience enhancing expansion strategies for water distribution systems: A network theory approach. *Environmental Modelling & Software*, 26(12), 1574-1582.
- Yazdani, A., & Jeffrey, P. (2011). Complex network analysis of water distribution systems. *Chaos: An Interdisciplinary Journal of Nonlinear Science*, 21(1), 016111-10.
- Yazdani, A., & Jeffrey, P. (2012). Water distribution system vulnerability analysis using weighted and directed network models. *Water Resources Research*, 48(6)
- Yazdekhesti, S., Piratla, K. R., Khan, A., & Atamturktur, S. Analysis of factors influencing the selection of water main rehabilitation methods. Paper presented at the *North American Society for Trenchless Technology (NASTT)*.
- Yoo, D. G., Kang, D., Jun, H., & Kim, J. H. (2014). Rehabilitation priority determination of water pipes based on hydraulic importance. *Water*, 6(12), 3864-3887.
- Zadeh, L. A. (1965). Information and control. *Fuzzy Sets*, 8(3), 338-353.
- Zarghami, S. A., Gunawan, I., & Schultmann, F. (2018). Integrating entropy theory and cospanning tree technique for redundancy analysis of water distribution networks. *Reliability Engineering & System Safety*, 176, 102-112.
- Zhao, X., Cai, H., Chen, Z., Gong, H., & Feng, Q. (2016). Assessing urban lifeline systems immediately after seismic disaster based on emergency resilience. *Structure and Infrastructure Engineering*, 12(12), 1634-1649.
- Zhao, X., Chen, Z., & Gong, H. (2015). Effects comparison of different resilience enhancing strategies for municipal water distribution network: A multidimensional approach. *Mathematical Problems in Engineering*, 2015.

- Zhuang, B., Lansey, K., & Kang, D. (2013). Resilience/availability analysis of municipal water distribution system incorporating adaptive pump operation. *Journal of Hydraulic Engineering*, 139(5), 527-537.
- Zitzler, E., Thiele, L., Laumanns, M., Fonseca, C. M., & Da Fonseca, V. G. (2003). Performance assessment of multiobjective optimizers: An analysis and review. *IEEE Transactions on Evolutionary Computation*, 7(2), 117-132.